Natural Hazards (2005) 36: 1–4

Preface

In recent years flooding and the risk associated have been rising with increased frequency in many European countries. Major floods have occurred in a wider part of Europe in recent years including the 1997 flood in Odra, 1998 and 2000 floods in the UK and most destructive flood in Central Europe in summer 2002 causing serious damages and vast economic consequences. Flood risk and vulnerability is increasing due to changes in rainfall pattern, increased frequency of extreme events, land-cover changes and development into flood-prone areas as a result of socio-economic demand. In addition change in climate is causing significant impact on the hydrological system and increasing the risk and vulnerability to flooding. Human lives, property, environment and socio-economics are at increasing risk due to flooding.

River flooding has been recognised as a major natural hazard in many European countries after the recent catastrophic floods. Important lessons have been learned from recent floods and flood management has begun to focus on the practical problems, dilemmas and challenges at European scale. Basin-wide co-operation in large transnational river catchments can help to adopt sustainable flood management strategies e.g., land use regulations, upstream control/regulations etc. Risk based forecasting and dissemination tools would provide effective protection from flooding. Development of efficient operational flood warning system (with the ability to provide timely warnings to properties and lives at risk of imminent flooding) would reduce the loss of life and property due to major floods. Efficient flood warning system would be a vital part in flood risk management in areas with extensive development on the natural flood plain. Flood simulation is a major strategic planning tool for effective reduction of risk and damage due to flooding. However, there are uncertainties inherent in such prediction of flooding. Probabilistic analysis and uncertainty will play a major part in the decision-making process of determining the flood risk. Adopting flood defence measures at catchment, regional and national scales can improve the flood risk management. Integrated planning and management will enhance the effectiveness of flood defence infrastructure with other possible measures.

Publication of this special issue will be a timely and topical contribution that will aid in the development and implementation of new technologies/strategies to reduce the risk and vulnerability due to flooding. The combination of the papers will provide opportunities for interaction between engineers, scientists, economists, planners, regulators and decision-makers. It will also open areas/issues where further research is needed.

The guest editors would like to thank Dr. T. S. Murty, one of the Editors of *Natural Hazards* journal and former President of the International Society for the Prevention and Mitigation of Natural Hazards, for inviting us to edit this special issue on *Flooding in Europe: Risks and Challenges*. The guest editors have a particular interest on flooding and flood risk assessment. There has been very positive response from potential contributors throughout Europe. This has given the opportunity to edit a double issue of the journal. The script for a companion book volume tentatively entitled *Flooding in Europe: Challenges, Developments in Flood Risk Management* is presently under preparation and its publication is anticipated for early next year (in the book series Advances in Natural and Technological Hazards Research). Many thanks are due to all the contributors to the special issue. Fifteen peer-reviewed articles have been selected for publication in this special issue. These articles contribute to the following general themes: *flood risk management, operational flood forecasting, extreme events, climate change, flood protection, importance of collaboration, modelling, dealing with uncertainty and case studies of flooding*. The articles have been subdivided into four sections: the importance of collaboration, consequences of flooding, models of flooding, case studies of flood risk and flooding. First two sections contain two articles each; the third section contains three articles and eight articles in the last section. The authors come from different European countries e.g., Belgium, Czech Republic, Germany, United Kingdom, Italy, Poland and the Netherlands. Each paper was subjected to rigorous scientific review by at least two referees. The guest editors would like to thank all the very experienced reviewers for their contribution in the review process to raise the technical quality of this special issue.

We would like to thank many individuals/organisations for their interest and co-operation for this special edition. Special thanks are due to Ms. Kirsten Overmann, technical advisor, European Water Association for her kind help and co-operation in circulating the call for papers. We would also like to thank Drs. Petra van Steenbergen, senior publishing editor of Geosciences, Kluwer and Mrs. Mieke van der Fluit, assistant to the senior publishing editor for their assistance throughout the publication process.

Finally the guest editors wish to express their deep appreciation and gratitude to Mr. Steve Wheatley, Regional Flood Defence Manager, Anglian Region, Environment Agency, UK for his endless help, moral support, encouragement and assistance throughout the process of publishing this special issue. We gratefully acknowledge the support of Mr. Wheatley for the success of publishing this special issue *Flooding in Europe: Risks and Challenges*. We would also like to acknowledge the support of the Environment Agency in general and in particular the Flood Defence of the Anglian Region, Environ-

ment Agency. Thanks are also due to Mrs. Jean Dalton, secretary, Flood Defence for her secretarial help.

SELINA BEGUM
Environment Agency, Kingfisher House, Goldhay Way, Orton Goldhay, Peterborough, PE2 5ZR, UK
E-mail: selina_begum@hotmail.com

PIETER VAN GELDER
Delft University, Faculty of Civil Engineering, Stevinweg 1, 2628 CN Delft, The Netherlands
E-mail: P.vanGelder@ct.tudelft.nl

Acknowledgement of Reviewers

The guest editors of the Special Issue *Flooding in Europe: Risks and Challenges* acknowledge the colleagues listed below for their excellent review of the contributions. Referees have a critical role in maintaining the quality of the publication and we are grateful for their efforts.

Dr. Erica Dalziell, University of Canterbury, Christchurch, New Zealand; Dr. Paul Sayers, HR Wallingford, Wallingford, Oxford, UK; Prof. Dr. Ives Zech, Catholic University of Louvain, Belgium; Prof. Dr. Jim Hall, University of Bristol, Bristol, UK; Miss Ana Lisa Vetere, European Commission, IPSC, Italy; Prof. Dr. Andrew Black,University of Dundee, Dundee, Scotland, UK; Dr. Bruno Merz, Division of Geomechanics and Geotechnology, Germany; Dr. Yusuf Kaya, Babtie Group, Glasgow, Scotland, UK; Prof. Dr. Edmund Penning-Rowsell, Middlesex University, London, UK; Dr. Laurens Bouwer, Vrije University, Amsterdam, The Netherlands; Prof. Dr. Paul Bates, University of Bristol, Bristol, UK; Prof. Dr. Alan Ervine, University of Glasgow, Glasgow, Scotland, UK; Dr. D. Han, University of Bristol, Bristol, UK; Dr. Keming Hu, Black & Veatch Consulting Ltd., Surrey, UK; Fabrizio Fenicia, Delft University of Technology, The Netherlands; Prof. Dr. Dominic Reeve, University of Plymouth, Plymouth, UK; Prof. Dr. Huib de Vriend, Delft University of Technology, The Netherlands; Mr. Cees-Jan van Westen, Rijkswaterstaat, Delft, The Netherlands; Prof. Dr. Huub Savenije HHG, Delft University of Technology, The Netherlands; Dr. Herbert Berger, Rijkswaterstaat, Lelystad, The Netherlands; Dr. A. De Roo, DG Joint Research Center, European Commission, Ispra, Italy; Dr. Daniel Gellens, KMI, Brussels, Belgium; Prof. Dr. H. D van Schalkwyk, University of Orange Free State, Bloemfontein, South Africa; Prof. Dr. P. Burlando, ETH Zurich, Switzerland; Prof. Dr. Han Vrijling, Delft University of Technology, The Netherlands; Prof. Dr. B. Petry, IHE, Delft, The Netherlands; Prof. Dr. Ton Vrouwenvelder, Delft University of Technology, The Netherlands; Dr. H.J.J. Stolwijk, CPB, Den Haag, The Netherlands; Prof. Dr. Jan van Noortwijk, Delft University of Technology, The Netherlands.

Natural Hazards (2005) 36: 5–24

Interregional and Transnational Co-operation in River Basins – Chances to Improve Flood Risk Management?

BIRGIT HAUPTER[1,★], PETER HEILAND[2] and JÜRGEN NEUMÜLLER[3]

[1]*Technische Universität Darmstadt, Fachgebiet Umwelt- und Raumplanung, Petersenstr. 13, 64287 Darmstadt, Germany;* [2]*INFRASTRUKTUR & UMWELT, Professor Böhm und Partner, Julius-Reiber-Str. 17, 64293 Darmstadt, Germany;* [3]*INFRASTRUKTUR & UMWELT, Professor Böhm und Partner, Kurfürstenstraße 15, 14467 Potsdam, Germany (E-mail: juergen.neumueller@iu-info.de)*

(Received: 18 November 2003; accepted: 30 June 2004)

Abstract. In European river basins many flood management and protection measures are planned. However, the realisation of effective but space consuming measures such as retention areas and dike relocation mostly lags far behind time schedules. The development and set-up of an interregional and transnational basin-wide co-operation structure ("flood management alliance") is substantial to realise catchment oriented flood management. In particular, this co-operation structure must involve spatial planning. The interregional and transnational co-operation structure establishes the framework for the joint accomplishment of instruments for flood risk management which is basin-wide agreed on. One of these instruments comprises financial compensations between downstream and upstream regions which shall improve the acceptance and the realisation of measures which bear disadvantages for the regions where measures are located. Existing and planned basin-wide co-operations in large transnational European river catchments demonstrate reasonable developments towards these goals. However, further efforts have to be made to exploit the chances interregional co-operation offers for improved flood risk management.

Key words: spatial planning, flood management, interregional co-operation, burden sharing, risk management

Abbreviations: AER – Assembly of European Regions; ELLA – Transnational project; ELBE – LABE Flood Management Measure by Transnational Spatial Planning (INTERREG IIIB-project); ESDP – European Spatial Development Perspective; EU – European Union; ICPE – International Commission for the Protection of the Elbe/Labe; ICPO – International Commission for the Protecting of the Oder; ICPOAP – International Commission for the Protection of the Odra River against Pollution; ICPR – International Commission for the Protection of the Rhine; IKSO – Internationale Kommission zum Schutz der Oder (International Commission for the Protection of the Oder); INTERREG – European Community initiative which aims to stimulate interregional co-operation in the EU. It is financed under the

★ Author for correspondence. Phone: +49-6151-163148; Fax: +49-6151-163739; E-mail: b.haupter@iwar.tu-darmstadt.de

European Regional Development Fund (ERDF); IRMA – INTERREG IIC Rhine Meuse Activities (1998–2001); MKOO – International Commission for the Protection of the Odra River against Pollution (Polish Abbreviation); MKRO – Ministerkonferenz für Raumordnung; NGO – Non-Government Organisations; NRW – North Rhine – Westphalia; SPONGE – Scientific Programme ON GEnerating sustainable flood control (INTERREG IIC-project); UN – United Nations

1. Preface

To meet the future demands for sustainability all approaches of spatial and environmental planning can no longer be seen as separated in different spatial units which are not linked to each other. The transboundary impact of natural hazards and the internationalisation of political solutions call for transnational co-operation in planning and regulation. Interregional and transnational co-operation of all different actors involved and on different levels have become more and more substantial. This is politically and scientifically required (see EU, 1995; MKRO, 2000; UN, 2000). Thus, approaches have to be adapted to reflect current regional and national needs so as to promote voluntary co-operation amongst actors in order to force co-operation where necessary. Furthermore, incentives should be created to raise the willingness to co-operate amongst stakeholders.

The EU Water Framework Directive (WFD) provides a good starting point for catchment wide policy, but it falls short in addressing spatial planning and flood issues. It is important that basin wide co-operation in river basin management and flood prevention has to become common practice, which must be facilitated by EU policy.

This article tries to summarise the demand on the different co-operation styles for spatial planning oriented flood management in large river basins. It gives examples of the state of art for the Rhine, Oder and Elbe basins. The focus is laid on flood risk management strategies for entire large river basins.

The scientific basis for this publication are various EU-funded research projects (e.g. INTERREG, IRMA, SPONGE) and practical implementation projects (e.g. OderRegio, ELLA) that have been worked out by the authors.

2. Needs for Co-operation

As a transnational framework for interregional co-operation, binding agreements exist at the transnational level between the countries involved regarding water management targets and flood protection along the large European rivers e.g. Rhine, Elbe, Oder or Danube. They are laid down in action plans on flood defence of the transnational river commissions (e.g. for the Rhine: ICPR, 1998). The outreach and impact at regional and local level, as well as local acceptance, is considered inadequate. However, the implementation of the strategic plans is the responsibility of local and regional

authorities. Thus, it is difficult to meet the goals of the action plans on flood defence in many cases (e.g. ICPR, 2001). A concrete transnational and cross-regional working level must be created to be responsible for the control of land use with regard to regional flood protection considerations and to make economical solutions possible. Such structures dealing with tasks of spatial planning have proved very successful in many cases and responsibilities other than flood management like waste management in interregional frameworks. The urgent tasks in preventive flood management that especially call for excellent co-operation structures are e.g.:

- Working out and agreeing on visions and strategies for transnational river basins, including measures, budgets, timeframes.
- Production and continuous agreement procedure on a catchment area-wide, cross-regional, spatial planning action program for all fields of action in spatial planning to implement the action plans on flood defence.
- Extension of the action plans including concrete regional planning.
- Adaptation of flood-relevant contents of the action plans in the individual regional plans as well as their communication with the municipalities.
- Creation of incentives and increase of acceptance in reclaiming large retention areas and burden sharing agreements.
- Creating a framework for negotiations to address upstream–downstream relations.
- Increase public awareness.
- Monitoring of processes and achievements of regional planning in all preventive flood management efforts.

Different styles of co-operation can be distinguished: vertical (i.e. EU-Nations-Regions-Cities), horizontal (i.e. cross-boundary) and interdisciplinary. Vertical co-operation is ruled by legislation and functions more or less effectively. It is not the focus of this article since it is not the major concern of voluntary steps. On the other hand, forced horizontal co-operation is strictly limited by the independence of nations, regions and municipalities in Europe. Therefore, this kind of co-operation is an excellent field to be improved by applying voluntary principles. However, in all cases different actors will have to work together closely on solutions for flood risk management. The so called interdisciplinary co-operation is already well accepted and not subject to far reaching disputes. Even more it is the fundamental for all co-operation initiatives.

3. Concept for Improved Co-operation

3.1. LEVELS OF CO-OPERATION

Due to their competence and practical possibilities, the co-operation levels within a catchment area each have specific tasks (see Figure 1):

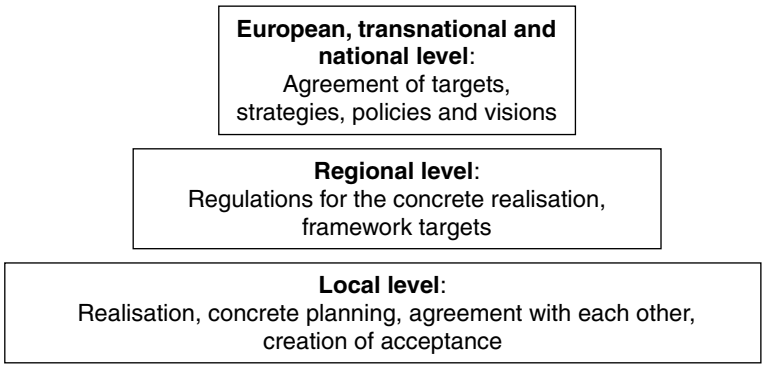

Figure 1. Scheme of levels and competencies of spatial planning.

Within the framework of the EU and with regard to the catchment area-wide water management, transboundary co-operations gain in importance. The national level is important for (international) co-operation, since here, legitimised democratically, perspectives and strategies for the spatial development are defined. The limited number of partners at this level within transnational river basins represents a comparatively favourable condition for agreements between the partners. However, this level does not achieve concrete planning and mostly has no direct influence or control on land use decision.

According to the Assembly of European Regions "Declaration on Regionalism in Europe", an European region is defined as "... the territorial body of public law established at the level immediately below that of the State and endowed with political self-government. The region shall be recognised in the national constitution or in legislation which guarantees its autonomy, identity, powers and organisational structures." (AER, 2001). The regional level is in most European countries a democratically legitimised authority with extensive authority for regional planning. Thereby, it can make direct obligations for spatial use. Although this level is not responsible for concrete land use decisions, distinct possibilities exist to direct the municipalities regarding regional requirements. As a rule, the number of regions in transnational river catchment areas is too large for the creation of a genuine working group in the context of a co-operation stucture. A further subdivision into clusters is necessary (see below).

In most European countries the local level is decisive for concrete land use decisions, and partly also for building permits. It is shown that local spatial planning instruments exist and can successfully be used according to the criteria of flood damage prevention if the public and political awareness is sufficient (see e.g. Böhm *et al.*, 1999, 2001). However, both the very large number and the locally very different needs and threats to flooding are insufficient conditions for homogeneous river basin related flood

management in spatial planning on the municipal level. Co-operation on this level is more driven by local interests than an integrated approach aimed at mutual support for catchment wide improvements in spatial planning. Due to the conditions named above the municipal level is not suitable as decisive framework for the development of common approaches and for the negotiation of measures or mutual compensation.

From the characterisations of levels it can be concluded that

- the transnational and national level is suitable for giving targeted performance specifications but that these bodies are not suitable for further concrete realisation,
- the local level has competence only for areas which are too small to permit a successful river basin-wide agreement process.

Therefore, it is the regional level which is deemed most suitable for the tasks at hand. The co-operation structure developed is based on a voluntary union of regional government units. In almost all European countries, they fulfil a series of criteria which are required for the desired co-operation partners:

- they are small enough and they are in close contact with the population,
- they have got competencies for spatial planning at the regional level and direct the municipal planning (exception: e.g. France),
- they have got responsibility for regional water management with competence in flood protection (exception: e.g. the Netherlands).

Thus, the interregional co-operation (''Flood risk management alliance'') for preventive flood management should be an institutionalised co-operation with participants (authorities, organisations, public) from planning fields above the local and below the national level in (transnational) river catchment areas. The goal of the co-operation is the reduction of the flood risk and the assistance in the realisation of flood protection goals set in overall strategies, perspectives or action plans.

3.2. ACTORS FOR CO-OPERATION

According to the approach developed the basic members of the co-operation ''Flood risk management alliance'' are spatial planning authorities of the regions in the river catchment. They are the ''key actors'' for the preparation of long term strategies and the implementation of flood protection regional planning. Other partners within the co-operation are representatives of the

- regional water management administrations,
- other expert regional administration bodies such as nature conservation or waterways,
- superposed spatial management authorities,

- non-government organisations (NGO),
- municipalities.

As described above, the co-operation area should include the complete river catchment area, i.e. both the area along the main river itself as well as on the tributaries and their catchment areas.

3.3. OPERATING AND PROMOTING ASPECTS OF CO-OPERATION

Due to the large volume of potential co-operation partners, it is obvious that smaller sub-units (''clusters'') must be formed to produce concrete results and to negotiate co-operation benefits. A clear clustering following the similarity principle is recommended (example for the Rhine catchment see Figure 3):

- regions directly along the main river (''1st level regions''),
- regions aside the main tributaries (''2nd level regions''),
- other regions in the river catchment area (''3rd level regions'').

One requirement for any successful co-operation is the development of trust and the building up of partner relationships. As a basic structure for the intended co-operations this clustering would bind the participating partners together in working groups.

The co-operation structure developed foresees the foundation of a union on the basis of a contract, with a public legal body designating the tasks, financing, structure and work programme for the first two years. A central office, as well as regular meetings of the participating groups with permanent designated representatives of the above mentioned regions, are necessary (see Figure 2). The concept envisages an overall working group, as well as areal and expert subject clusters and a central co-operation management office.

Numerous criteria must be observed in the choice of a suitable legal form, e.g. the possibility of making contracts, national differences in the planning and legal systems, trustworthy regional co-operation forms, take-over of sovereign rights (see Spannowsky, 1999, p. 17), as well as necessary or existing international agreements.

Experiences have shown that one of the most important operational aspects of co-operations is the necessity to set up a central operating office and a co-operation management, which is available to carry out the detailed structuring of the on-going workload and, which is responsible for the scientific and technical processing of questions which arise.

3.4. SUPPORT BY ECONOMIC INCENTIVES AND FINANCIAL COMPENSATION

The task of preventive flood protection presents a classical upstream–downstream problem scenario. The benefits, costs and other burdens of preventive actions to lower the discharge peaks are in different geographical locations and, as a rule, also affect different interest and actor groups.

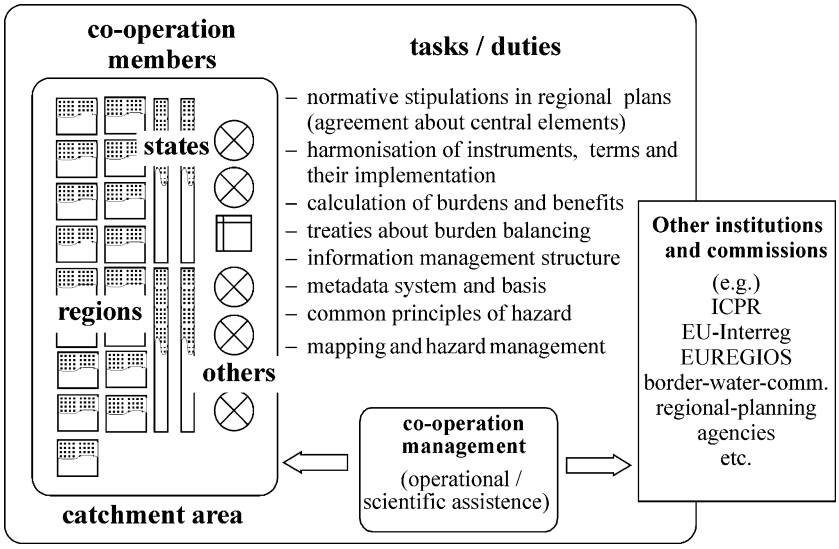

Figure 2. The recommended "Flood Risk Management Alliance" in spatial planning (Böhm *et al*., 2001)

The current principles of financing flood protection measures by the countries themselves do not provide for any compensating effects between diverging costs and benefits in transnational river basins and do not include the use of incentives.

Financial compensation as an equalisation payment for direct or indirect costs can be made either as a legal obligatory payment or as a voluntary performance. Incentives, in contrast to financial compensatory performance or payments in kind, are not designed to directly compensate for costs which can be defined in money terms but they are rather an offer designed to increase the acceptance of (usually indirect) burdens. The nature of the offer must not necessarily be directly connected to the cause of the burdens which have occurred. The volume of the incentive – in contrast to compensation – cannot be calculated with a neutral formula. As a rule, it is the result of negotiations. Agreements involving the provision of incentives are not based on legal regulations but they are agreed in an informal manner.

Economic incentives and financial compensations should

- strengthen the principle of the "causer pays" for future uses in flood plains,
- create incentives for local/regional measures by providing compensation for disadvantages,
- be based on the interconnections between measures and effects, including cost sharing,

- create the acceptance for a higher level of transparent negotiations and processes.

The calculation of the compensation offer to internalise external benefits follows the principle (see Table I):

$$\text{Compensation offer} = \text{benefits}_{\text{extern}} - \text{costs}_{\text{extern}} - \text{benefits}_{\text{intern}}$$

The decisive factor is the willingness of the downstream areas to actually offer and pay some of their potential savings to the upstream areas – and on the other side – the willingness of the upstream regions to accept disadvantages for their land use in the meadow lands (effective only in large scale) by getting paid for their burdens.

Particularly on this point there is much room for negotiation because the potential savings only represent a part of the overall costs. The definition of a reducing factor is important to accomplish agreement. This represents the willingness of downstream regions to pay for the reductions of potential damage by upstream measures. Examples show that the sums offered are much lower than the theoretically calculable value of the expected damage reduction. All in all, the principle of burden sharing between the beneficiaries and those affected represents a necessary further development in financing practice which – in view of the large financing volumes – in the long term, cannot be oriented towards subsidising funds alone.

To succeed in the approach to support regulatory water management and spatial planning instruments by economic instruments, which can encourage the initiative of upstream regions, it is necessary to:

Table I. Calculation of the compensation offer from benefits and costs (Böhm *et al.*, 2001)

Benefits for downstream actors (= extern benefits)	
+	• Reduction of damage potential (municipalities / private / companies / agriculture) • Saved costs for maintenance (dikes e.g.)
Costs for the measure at the place of construction (= external costs)	
–	• Acquisition of land • Costs for planning and constructions • Landscape and renaturalisation • Compensation for farmers or affected infrastructure
Indirect benefits at the place of the construction (if possible for calculation) (= intern benefit)	
–	• Revitalisation of meadow lands • Improvement of the tourism and recreation qualities / Promotion for regions
= (result:) Compensation offer of downstream region and responsibles to affect local actors (if positive)	

- develop an integrated co-operation of responsible actors both of regional spatial planning and water management (see above),
- reduce still existing reservations between actors from upstream/downstream and the views of "do not believe in upstream measures, better help yourself ",
- evaluate the limits of the willingness to pay for risk reduction and to accept measures in relation to the compensation offers,
- calculate (theoretical) compensation offers for single measures,
- start negotiations (by an institutional co-operation; neutral mediators),
- examine and, where appropriate, change international law to reduce the problems of interregional transnational agreements.

4. Present State and Visions in Large European River Basins

4.1. CO-OPERATION IN THE RHINE CATCHMENT

In the past, in the Rhine catchment area different co-operation forms between participants of spatial planning and other partners have developed. However, preventive flood management plays, in most institutionalised transnational co-operations, which are rather spatial planning or regional planning orientated, no or only a temporary, rather coincidental role. Three co-operations exist, in which flood protection is the only goal or one of the most important (see Figure 3).

In the Rhine catchment, at transnational level, some decades of successful international efforts have led to an institutional co-operation (International Commission for the Protection of the Rhine – ICPR) which has set ambitious goals for preventive flood protection agreed upon by the national governments (Action plan for the Rhine: ICPR, 1998). Members of the commission are high-ranking officials of the member states from the national and regional water management authorities as well as individual representatives of national planning authorities. Representatives of regional spatial planning are not appointed to the ICPR-commission. Because of the missing regional representation negotiations on compensation offers and incentives between regions cannot take place.[1]

Activities primarily focus on the main river course. Execution instruments, besides international-law self obligations (international contracts) do not exist. Therefore, the implementation of suitable measures is again dependent on the national and regional levels of water management and spatial planning. Accordingly, the results vary compared to the aims of the action plan. Most intermediate objectives of the action plan were reached until the year

[1]Even though the Upper Rhine contract obliges these regions to compensate for lost retention areas – following the causer-must-pay principle – it does not provide for compensation offers, including benefits of downstream regions and burdens of upstream regions.

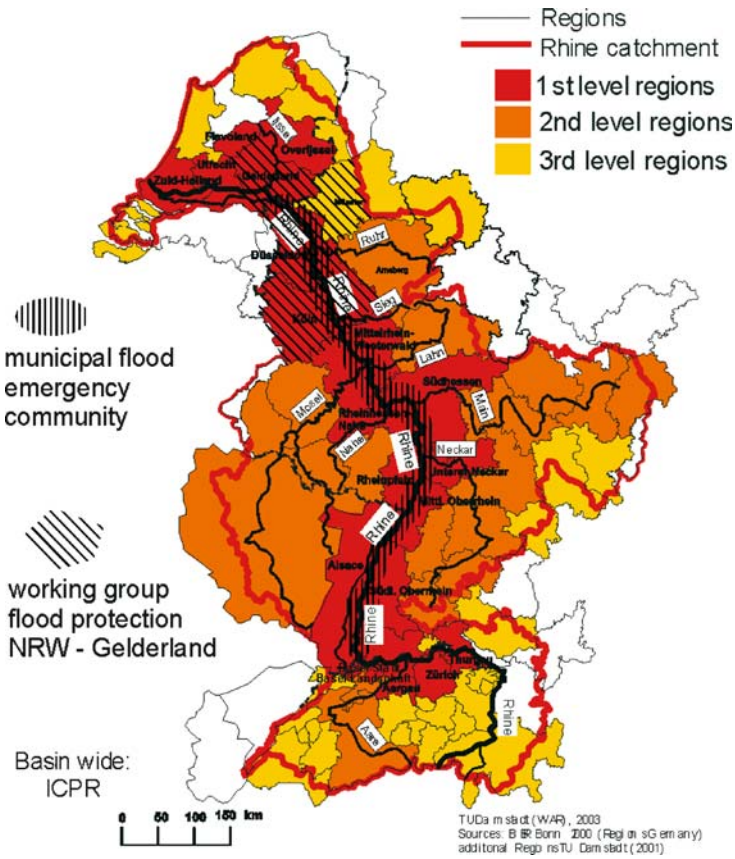

Figure 3. Rhine catchment: recommended *versus* existing co-operation structures with an orientation towards spatial planning and flood risk management.

2000, but the goal to not increase damage potential was missed (ICPR, 2001, p. 4). Thus, an effective land use control in risk areas (behind the dykes) cannot be carried out by the ICPR. However, the ICPR can be evaluated as an important framework for future development of co-operation in spatial planning in the Rhine basin.

The German–Dutch working group for flood protection (North Rhine-Westphalia/Germany and Gelderland/The Netherlands) was established at Ministerial level after the extreme flood of 1995. Concrete binding agreements are not the original goal of the working group, which was not legitimised for that. Among others, the main objectives are mutual information with informal coordination of projects and planning standards of protection, as well as developing the simulation programs (German–Dutch working group flood protection, 1997, p. 5; van de Nes, 1999, p. 72). The extension of

co-operation by further entry of other regions from the Rhine catchment area is desired (Kamminga, 1999, p. 6).

The *Hochwassernotgemeinschaft Rhein e.V.* (Rhine Flood Emergency Community) is a transnational union at municipal level comprising municipalities along the entire river. The emergency community works as an interest agency for municipalities. For example, it may try to increase the acceptance for upstream measures. The emergency community is a good example of the co-operation of upstream and downstream actors. It is an important functioning structure for flood protection on the Rhine. However, it only has a small influence on interregional planning processes and does not have a mandate for negotiations nor authority for flood protection planning. Furthermore, it does not cover the whole river catchment.

Apart from the co-operations acting on the transnational scale, various co-operations for flood risk management exist within national boundaries. Examples are the regional clusters defined in the Netherlands within the framework of the IRMA programme (IRMA, 2000; van Venetie, 2000) or the ministerial working group for flood danger mapping in Baden-Württemberg (Germany). However, these co-operations are limited to national boundaries and have no legal or formal structure. Furthermore, they do not fulfil the requirements of the long-term interregional approach as described above.

From a different angle, the impacts of the European Union Regional Development programmes (IRMA 1998–2001, INTERREG IIIB 2000 – 2006) will now be addressed. These programmes are distinctly designed to integrate spatial planning and flood protection. However, long-term strategies cannot be carried out as their promoting impact is limited in time. These financial subsidies could support long-term strategies through better co-ordination amongst actors. There is a need to better integrate local and regional decision-makers into the programmes, at they have the mandate of making land use decisions.

Up to date, a deficit of the co-operation structures in the Rhine catchment is recognised by the fact that there is no concrete interregional working level responsible for integrating those responsible for regional land use management into the whole river catchment area. So far the option of partly financing the development of such structures by Community Initiatives has not been seized. As a rule, partners of INTERREG IIIB flood management projects in the Rhine basin are water management authorities and other organisations, but up to date no project aims at integrating all relevant regions within the Rhine catchment.

In programmes such as IRMA, 78% of all funding was directed to regions in the lowland valley which obviously is the most affected region. However, in future, in the interest of all actors, larger parts of funding must be transferred to the central and upper catchment regions. In the Rhine basin, more than 80% of

the necessary expenses for flood protection measures will have to be spent in the upper and middle Rhine regions by 2020 (ICPR, 1998). To achieve this, self-reliance will not be enough, if no additional measures support such efforts. Either legally binding conditions or incentives could be used. Here, it becomes clear that interregional transaction could help.

In addition the linking of action plan targets and action priorities with the necessary financing is required, in the interest of all regions in the catchment area. Thus, upstream regions and those which benefit of upstream measures have to be linked by future financing strategies.

4.2. THE ODER CATCHMENT – CO-OPERATION

Over the past decades and centuries, extreme flood events have often occurred in the Oder valley causing considerable damage. The most recent event, i.e. the summer floods of 1997, is still fresh in memory. The flooding and dam breaches caused enormous material damage – particularly in the Republic of Poland and the Czech Republic – and unfortunately in these countries there was loss of life as well (Bronstert *et al.*, 1999; IKSO, 1999).

The ''OderRegio Project – Transnational Conception for Preventive Flood Protection in the Oder Catchment Area'' has devoted itself to the task of achieving an integrated flood protection. The target of the project was to develop methods and priority actions in spatial planning for flood prevention in the Oder catchment area (Böhm and Neumüller, 2000; Neumüller and Böhm, 2000; INFRASTRUKTUR & UMWELT *et al.*, 2001).

The necessity of taking the complete river basin area into consideration is self-evident. The extreme flooding in 1997 showed that floods do not stop at national borders and that there are very important relationships between downstream and upstream areas. Flood protection on the Oder is thus a transnational task for the countries where this river flows i.e. the Czech Republic, the Republic of Poland and the Federal Republic of Germany. The international commission for the protection of the Oder is working on a transnational action plan to outline a framework for water management tasks.

To meet this international challenge of integrating spatial planning and water management, in order to carry out the OderRegio project, the most important water management and spatial planning actors from national and regional levels from all three countries agreed to work together in a co-operative process. In a working group accompanying the project, more than 30 actors were involved. Here, intermediate results of fact finding and of potential and effect analysis were presented and discussed. Enormous benefits for the realisation of the OderRegio project were achieved through the active contributory work and co-operation of the participants, the inclusion of their expertise and local knowledge provided. National investment programs such

as the Polish ''Program for the Oder – 2006'' were also integrated into the project (Zaleski, 2000).

The result has been the successful production of a ''Conception for Preventive Flood Protection'', which has been transnationally agreed on. In this conception, general principles and targets of preventive flood protection are formulated. Moreover, on the basis of the analyses carried out, concrete action recommendations for partial areas were made.

So far the following results have been achieved:

(a) A robust working structure has been created,
  - which is formed by representatives from national and regional level administrations from Germany, Poland and the Czech Republic,
  - in which both the spatial planning and regional planning, as well as water management are represented,
  - which guarantees agreement with the work of legitimate initiatives such as the ''Stettiner Initiative'' and the International Commission for the Protection of the Odra River against Pollution (ICPOAP, German – IKSO, Polish – MKOO).

(b) General fundamental principals and targets of spatial planning for preventive flood protection in the catchment area of the Oder have been defined and agreed on.

(c) These fundamental principles and targets were concretised for individual partial areas (areas of action) and corresponding action requirements were named.

(d) The results have been included in the consultations of the ''Stettiner Initiative'' (signature of a declaration by the responsible ministers for spatial planning from the Czech Republic, the Republic of Poland and the Federal Republic of Germany on 29th June 2001) and in studies for the draft ''Action Program Floods'' of IKSO (compare IKSO, 2001).

Thus, the OderRegio project provides an important contribution to a trinationally agreed and integrated action program for preventive flood protection in the Oder catchment area. However, until now the agreements do not affect the planning at regional and local level. To include the regional level, basin-wide, into the implementation, a second project phase OderRegio part-financed by INTERREG IIIB programme was set up to be executed from 2003 until 2006.

4.3. DEVELOPMENTS IN THE ELBE RIVER BASIN

The flood events in the Elbe catchment of 2002 showed, dramatically, that flood prevention and common management approaches have to be improved, in particular regarding long term spatial planning. Like in other river basins,

an action plan for flood defence was drafted in summer 2002 by the International Commission on the protection of the Elbe (ICPE) but had to be revised after the flood. The revised version was agreed on at the end of 2003.

The Elbe basin is characterised by a very heterogeneous structure of authorities, commissions, working groups and planning groups of all different groups of actors, at all levels, transnational, national, regional, local. Driven by this, the idea was created to develop the INTERREG III B project ELLA (''Elbe-Labe flood management measures by transnational spatial planning'').

The extraordinary challenge of the ELLA project is the transnational co-operation of nearly all regional spatial planning authorities in the Elbe basin. This unique comprehensive partnership covers almost the whole catchment area of the Elbe. Thus, the aims of EU water policies and the EU spatial planning perspective can be obtained under this INTERREG III B project. National and regional partners that are responsible for spatial planning, water management and agriculture assure that the far reaching integrated transnational approach will be implemented in many different regions at the same time.

The added value of the INTERREG ELLA project is that none of the regions would be able to achieve as extensive improvements in risk prevention as they do in the common INTERREG approach. Especially in view of the enlargement of the EU in 2004, an important brick for an adjustment of the planning strategies and policies in the field of risk prevention in the Czech Republic, Germany, Poland, Hungary and Austria will be delivered in ELLA. For positive development of economically disadvantaged risk areas, information on risk, improvements of safety standards and adapted land use planning will be achieved.

The intended ELLA-results are:

- Production of transnational strategic planning maps for the entire river basin.
- Exemplary improved regional plans, regional strategies, etc., following the transnational needs.
- An efficient transregional network of authorities regarding spatial planning and flood management.
- A transnational strategy for burden sharing incentives (compensation funds, negotiations).
- Risk maps ('Atlas'), agreement on retention measures, land use options (e.g. agriculture, forestry).

The ELLA project was granted by the Programme secretariat at begin of 2004 and will run until summer 2006. An important milestone will be May 2004 when the new EU member states Poland, Czech Republic and Hungary can apply for their own EU INTERREG subsidies. This could accelerate the project and, even more, the co-operation process itself. It is foreseen to

evaluate the role of funds, with view to the willingness to co-operate in the river basin. Results can be expected in 2006.

In the first period, the co-operation will be based on a voluntary working basis ruled by a joint convention, which will direct the co-operation processes and which is for the time being, necessary for the INTERREG project according to the EU regulations. But for the time being it is not planned to build up a new co-operation institution. Experience and accompanying evaluation will grade clearly the strength and weakness of the voluntary approach. Conclusions will lead to continuation or changes. This will be in 2006/2007.

5. Conclusions

Activities of spatial planning are necessary contributions to all flood risk management approaches since land use regulations are an important component of risk mitigation. Decisions on land use options in river valleys with dense population usually follow many competing stakes of different actors and are affected by local and economical interests. Preventive measures with precautionary effects for other (downstream) regions suffer from missing acceptance, information and incentives. Thus, river basin wide co-operation can support the progress towards sustainable flood management strategies.

The status of the three compared approaches on co-operation in the three river basins of the Rhine, the Oder and the Elbe are too different to draw final conclusions yet. While the co-operation within the Rhine catchment has grown over nearly two decades, the Oder basin co-operation on concrete questions of flood management started only five years ago. In the Elbe basin the building-up of structures has begun and is not yet finished. However, in all basins important lessons have been learned which can be summarised as ''interim conclusions'' in the most cases. Table II gives an overview about characteristics and differences between the co-operation structures and results.

Especially until today, the starting phases have been evaluated by comparing the three basins. From this comparison, crucial criteria for the starting phase can be deduced.

5.1. INITIATION

The initiation process is the first important step towards the establishment of co-operation structures. In all cases, it has been initiated by stakeholders or regional planning authorities (in the Elbe basin accompanied by a national authority) who are situated in the downstream areas of the river basins. This seems logical since downstream regions aim at benefits from co-operations more than upstream regions. In the Oder and the Elbe basin, it was possible to start the coordination and co-operation through continuous intensive contacts and negotiations about possible benefits. The important lesson

learned is that without great efforts of downstream actors, a robust basis for effective co-operation structures cannot be developed eventhough the request of European policies like the ESDP.

Table II. Comparison of co-operation structures in the Rhine, Oder and Elbe basins

Criteria/requirements	Rhine	Oder	Elbe
Co-operation structure			
Co-operation levels	National or local level	National, regional (local levels planned)	National, regional
Spatial coverage	Basin wide only in water management	Basin wide	Basin wide
Working clusters	Partly for defined tasks, e.g. risk mapping along the main river	Aimed at until 2006	Aimed at until 2006
Members with responsibility for spatial planning	Only sporadic integration, mostly national level	At national and partly regional level regional level aimed at in 2006 (exemplary)	Aimed at on national and regional level until 2006 (partly)
Basin wide co-operation structure	Institution ICPR for water management; regional spatial planning not included	Institution ICPO for water management; regional spatial planning not included Spatial planning: Joint INTERREG-project	Institution ICPE for water management; regional spatial planning not included Spatial planning: Joint INTERREG-project
Level of institutionalisation	ICPR: contract between river basin states	ICPO contract between river basin states. INTERREG: Joint convention of partners (voluntary)	ICPE contract between river basin states. INTERREG: Joint convention of partners (voluntary)
Initiator	Different stake-holders in water quality debate (farmers, fishery)	Regional partner	National and regional partners

Table II. Continued

Tasks and goals			
Harmonisation of instruments, terms and their implementation	Mainly for the main river course, not the whole catchment, strategies at national level, no concrete implementation on regional level	Focus is on implementation; enquiry on legal harmonisation possibilities.	Comparison, joint conclusions for the river basin; enquiry on legal harmonisation possibilities.
Calculation of burdens and benefits	No	No	Aim
Basis for upstream–downstream negotiations	No, except 'causer must pay principle' (Upper Rhine)	Negotiations on precautionary measures; incentives or compensation not foreseen yet	Not clear enough yet
Hazard information base	Existing for most part of the basin; for main tributaries until 2010	Very general for the Oder; planned for the rest of the basin.	Not existing; planned for parts of the Elbe river by 2006

5.2. IMPORTANCE OF MUTUAL CONFIDENCE AND SLOWLY GROWING NETWORKS

It is decisive for the success of a co-operation to follow significant steps in the right order together with all partners at the right pace. Clear structures are needed from the coordination phase onwards. All three examples have underlined exisiting earlier experiences of regional and interregional co-operations, that much time is needed before first benefits of the co-operation can be expected. In the Rhine basin the co-operation in flood management issues is based on earlier networks of water management authorities and spatial planning authorities that have grown over years. The International commission for the protection of the Rhine is an example of effective co-operation over the decades, even if the real benefits for water quality were only experienced after 20 years. The examples of co-operation also confirm that 'natural' steps have to be made in the right order and that speeding up the development phase is not sensible for enhancing the quality of the co-operation. The steps are (according to Frey, 2001, p. 4):

- (no co-operation),
- information,

- consultation,
- co-ordination,
- co-operation,
- integration.

There is also evidence in the examples that at least two stages are necessary in building up the co-operations: the first one should aim only at an agreement on goals and strategies. The second should only focus on concrete measures.

5.3. RANGE OF AUTONOMY

The co-operations in the Oder and the Elbe basins are based on voluntary networks with a very wide range of autonomy. The joint work follows a framework of funding programmes for and joint conventions about the co-operation. However, further regulations or policies do not limit the autonomy of the single partners. The importance of this framework for the effectiveness of the co-operations cannot be proved yet. But it can be stated that the start of the co-operations with transnational networks in Germany, Poland, and Czech Republic etc. would not have been possible if a transfer of planning responsibility would have been an obligatory part of the joint conventions. Another criterion is the autonomy of the co-operation structure against other national authorities. This cannot clearly be rated for Oder and Elbe. But for the Rhine, Durth (1996, p. 202) attributes the great successes of the ICPR in water pollution reduction to the fact that the ICPR had a considerable autonomous range of action at its disposal and also used this. This means that the co-operation and its central office can only act on the instruction of its members through their representatives in the plenary session. The decisions are made by the representatives in the plenary session. At the same time, however, the members themselves must be obliged in the co-operation agreement to fulfil and/or abide by these decisions.

The overall perspective of interregional and transnational co-operation in the evaluated river basins demonstrates reasonable developments for positive long term improvements. To overcome the bottlenecks described in this article, dedicated promoters, sufficient flow of information and the political will to collaborate even if local concessions have to be made, are essential. It is a slow but gradual process, which hopefully continues even without great flood disasters to remind of its need.

Acknowledgements

The research was part financed by IRMA within the SPONGE project and co-financed by Darmstadt University of Technology, University of Berne, the Swiss Federal Office for Education and Science and the Forest Department of

the State of Berne. OderRegio was part financed by the EU Interreg II C programme and co-financed by regional and national authorities in the Oder basin in Poland, Germany and the Czech Republic.

References

AER (Assembly of European Regions): 2001, *Working programme*, Linz.

Böhm, H. R., and Neumüller, J.: 2000, Transnationale Konzeption zur raum-ordnerischen Hochwasservorsorge im Einzugsgebiet der Oder, In: Senatsverwaltung für Stadtentwicklung des Landes Berlin/Ministerium für Landwirtschaft, Umweltschutz und Raumordnung Brandenburg (ed.), *Europäische Zusammenarbeit durch transnationale Projekte zur Raum-entwicklung in Mittel- und Osteuropa am 3. Juli 2000*, Berlin.

Böhm, H. R., Heiland, P., Dapp, K., and Haupter, B.: 1999, *Anforderungen des vorsorgenden Hochwasserschutzes an Raumordnung, Landes-/Regionalplanung, Stadtplanung und die Umweltfachplanungen – Empfehlungen für die Weiterentwicklung*, Umweltbundesamt (UBA) Texte 45/99, Berlin. http://www.umweltbundesamt.de/rup/45-99/45-99.html.

Böhm H. R., Heiland, P., Dapp, K., and Haupter, B.: 2001, Spatial planning and supporting instruments for preventive flood management, In: Netherland Centre of Riverstudies (ed.), *IRMA-SPONGE – Towards sustainable flood risk management in the Rhine and Meuse river basins*, NCR-Publication 18-2002.

Bronstert, A., Ghazi, A., Hladny, J., Kundzewicz, Z., and Menzel, L.: 1999, *Proceedings of the European Expert Meeting on the Oder Flood 1997*, Potsdam.

Budapest initiative: 2002, *Budapest initiative on strengthening international cooperation on sustainable flood management: Joint Statement by the Heads of Delegations 1.12.2002.*

Deutsch-Niederlandische Arbeitsgruppe Hochwasserschutz (German-Dutch working Group): 1997, Gemeinsame Erklarung fur die Zusammenarbeit im nachhaltigen Hochwasserschutz der Provinz Gelderland, Rijkswaterstaat und dem Ministerium fur Umwelt, Raumordnung und Landwirtschaft des Landes Nordrhein-Westfalen, Arnheim.

Dieperink, C.: 2000, The cleanup of the Rhine as a successful international effort, In: Technical University of Berlin (ed.*), International Water Cources- Potential für Conflicts and Prospects for Co-operation. Proceedings of the International Conference 27.10.2000*, Berlin.

Durth, R.: 1996, *Grenzüberschreitende Umweltprobleme und regionale Integration*, Baden-Baden.

Enderlein, R. E.: 2000, The role international water law in forstering co-operation: The European experience, In: Technical University of Berlin (ed.): *International Water Cources – Potential for Conflicts and Prospects for Co-operation*, Proceedings of the International Conference 27.10.2000, Berlin.

Enderlein, R. E.: 2001, International agreements: A platform for hydrological co-operation in Europe; In: Deutsches Nationalkommitee für das Internationale Hydrologische Programm (IHP) der UNESCO und das Operationelle Hydrologische Programm (OHP) der WMO (ed.), *Hydrological Challenges in Transboundary Resources Management*; IHP/OHP-Berichte Sonderheft 12, Koblenz, pp. 351–361.

ESDP: 1999, *European Spatial Development Perspective*, Potsdam.

EU: 1995, *Unterrichtung durch das Europäische Parlament: Entschließung zu den Überschwemmungen in Europa*, Bonn.

Frey, Rene L.: 1999, Grenzuberschreitende Kooperation zur Starkung der Wettbewerbsfahigkeit von stadtischen Regionen, Presentation and Manuscript, 53. Deutsche Geographentag October 3, 2001, Leipzig.

ICPE (International Commission for the Protection of the Elbe/Labe): 2002, *Action Plan on Flood Defence – draft*, Magdeburg.

ICPR (International Commission for the protection of the Rhine): 1998, Aktionsplan Hochwasser, Koblenz.

ICPR (International Commission for the protection of the Rhine): 2001, *Umsetzung des Aktionsplans Hochwasser bis 2000*, Koblenz.

IKSO (International Commission for the protection of the Oder): 1999, *Das Oderhochwasser 1997*, Wroclaw.

INFRASTRUKTUR & UMWELT, Ruiz Rodriguez + Zeisler, Technische Universität Darmstadt: 2001, *Transnationale Konzeption zur raumordnerischen Hochwasservorsorge im Einzugsgebiet der Oder, Endbericht*, Darmstadt/Potsdam/Wiesbaden.

IRMA: 2000, *Cluster approach to regional water management in the Netherlands*, The Hague, fact sheet 8.

Kamminga, J.: 1999, Nordrhein-Westfalen und Gelderland, Gute Nachbarn!, In: Provincie Gelderland (ed.), *Hochwasserkonferenz Rheineinzugsgebiet – Hoogwaterconferentie Stroomgebied van de Rijn*, Arnhem, pp. 6–9.

MKRO (Ministerkonferenz für Raumordnung): 2000, *Vorbeugender Hochwasserschutz durch die Raumordnung (Handlungsempfehlungen der MKRO zum vorbeugenden Hochwasserschutz)*.

Neumüller, J., and Böhm, H. R.: 2000, Transnational Conception for River Flood Prevention Through Spatial Planning, In: Potsdam Institute for Climate Impact Research (ed.), *European Conference on Advances in Flood Research*, Potsdam, PIK Report No. 65.

Spannowsky, W.: 1999, *Verwirklichung von Raumordnungsplänen durch vertragliche Vereinbarungen, Endbericht*, Selbstverlag des Bundesamtes für Bauwesen und Raumordnung, Bonn.

United Nations: 2000, *Guidelines on sustainable flood prevention/Leitlinien für nachhaltige Hochwasservorsorge*, Geneva, meeting document MP.WAT/2000/7.

Van de Nes, T.: 1999, Arbeitsprogramm 1997–2001: Für mehr Sicherheit bei Hochwasser, In: Provincie Gelderland (ed.), *Hochwasserkonferenz Rheineinzugsgebiet – Hoogwaterconferentie Stroomgebied van de Rijn*, Arnhem, pp. 72–77.

Van Venetie, R.: 2000, *Clusterapproach in the Netherlands*; Presentation on the IRMA Conference 16.5.2000 in Bonn.

Zaleski, J.: 2000, Programm für die Oder 2006, In: Senatsverwaltung für Stadtentwicklung des Landes Berlin/Ministerium für Landwirtschaft, Umweltschutz und Raumordnung Brandenburg (ed.), *Europäische Zusammenarbeit durch transnationale Projekte zur Raumentwicklung in Mittel- und Osteuropa*, Berlin.

Natural Hazards (2005) 36: 25–42

Flood Forecasting and Warning at the River Basin and at the European Scale

MICHA WERNER[1,*], PAOLO REGGIANI[1], AD DE ROO[2], PAUL BATES[3] and ERIC SPROKKEREEF[4]

[1]*Delft Hydraulics, P.O. Box 177, 2600 MH Delft, The Netherlands;* [2]*Institute of Environment and Sustainability, European Union Joint Research Centre, T.P. 263, 21020 Ispra (VA), Italy;* [3]*School of Geographical Sciences, University of Bristol, University Road, Bristol BS8 1SS, UK;* [4]*Institute for Inland Water Management and Waste Water Treatment (RIZA), Gildemeesterplein 1, 6826 LL Arnhem, The Netherlands*

(Received: 7 November 2003; accepted: 30 June 2004)

Abstract. Application of recent advances in numerical weather prediction (NWP) has the potential of allowing delivery of flood warning to extend well beyond the typical lead times of operational flood warning at the river basin scale. A prototype system, a European Flood Forecasting System (EFFS) developed to deliver such pre-warnings, aiming at providing a pre-warning at lead times of between 5 and 10 days is described. Considerable uncertainty in the weather forecast at these lead times, however, means that resulting forecasts must be treated probabilistically, and although probabilistic forecasts may be easy to disseminate, these are difficult to understand. This paper explores the structure of operational flood warning, and shows that integration in the flood warning process is required if the pre-warning is to fulfil its potential. A simple method of summarising the information in the pre-warning is presented, and the system in hindcast mode is shown to give clear indication of an upcoming major event in the Rhine basin up to 10 days before the actual event. Finally recommendations on the use of data assimilation to embed the EFFS system within an operational environment are given.

Key words: flood forecasting, data assimilation, pre-warning, ensemble forecasting

1. Introduction

Recent flood events in Europe, including the 1993 and 1995 events in the Rhine and Meuse basins, the summer floods of 1997 and 2002 in the Oder, Elbe and Danube basins and the UK floods of 2000/2001 have raised interest in the provision of flood warning in an effort to reduce losses of property and life due to large floods (De Roo *et al.*, 2003). While some of the attention is in part political (Penning-Rowsell *et al.*, 2000) and will probably diminish with time, the potential of flood warning systems to reduce the negative impacts of floods is broadly accepted (e.g., Krzysztofowicz *et al.*, 1992; Parker and Fordham, 1996; Haggett, 1998; Penning-Rowsell *et al.*, 2000).

* Author for correspondence. E-mail: micha.werner@wldelft.nl

The ability to provide timely warnings to properties and lives at risk of imminent flooding so that simple yet effective measures can be taken is a main objective of the development of operational flood warning (Carpenter *et al.*, 1999), providing a cost effective way of reducing flood risk. This can help reduce investment in more traditional engineering flood control measures such as raising dykes and building flood control dams (Krzysztofowicz *et al.*, 1992). The effect of greater flood awareness and preparedness was clearly shown in the Meuse basin, where losses in the Netherlands due to the 1993 flood greatly exceeded those in the 1995 event, despite the fact that the two events were comparable in magnitude. The reduction was partly attributed to the provision of an early warning and subsequent response (Wind *et al.*, 1999).

A number of operational flood warning systems are in use both in Europe (e.g., Parker and Fordham, 1996; Bürgi, 2002, Sprokkereef, 2001) and overseas (e.g., Du Plessis, 2002; Grijsen *et al.*, 1992; Burnash, 1995). Most systems rely on detection of floods through hydro-meteorological observation networks, and while the use of observations is a primary element of a flood warning system (Haggett, 1998), more state-of-the art systems incorporate also a (model based) flood forecasting system (Parker and Fordham, 1996). Flood forecasting systems typically use hydrological models to predict short term flood evolution due to a combination of recent and forecast precipitation with the objective of increasing the lead time with which warnings can be delivered. Lead time in the context used here defines how much warning can reliably be given of imminent flooding. The lead time at which effective warning can be delivered is clearly dependent on the lag times between precipitation falling and the flood peak reaching the point of interest. Warning lead times therefore vary greatly even in a single basin, where for example in the Rhine catchment warning lead times in the upper basin may only be of the order of 24 h (Bürgi, 2002) while in the lower basin forecasts at lead times of up to 4 days can be provided using only hydro-meteorological observations and a rainfall-runoff and routing model (Sprokkereef, 2001).

Extension of lead time has the obvious advantage that this gives more time to raise awareness for an oncoming flood, thus allowing for measures to be implemented to reduce potential flood damage. Recent developments in meteorological forecasting and the ability to link these with forecasting systems offers the potential of increasing forecasting lead time beyond the short range currently provided by observational networks or operational forecasts to the order of 5–10 days. An EU supported research project, a European Flood Forecasting System (EFFS) has recently been undertaken to this effect (De Roo *et al.*, 2003).

This paper explores the structure and application of the established practice of flood forecasting as a part of flood warning on the operational

river basin scale. The proposed structure of the Pan-European pre-warning system as envisaged in the EFFS project (De Roo *et al.*, 2003) is described, and the potential role of the pre-warning system described as an integrated part of the flood warning process is explored.

2. Operational Flood Warning at the River Basin Scale

2.1. FLOOD FORECASTING IN THE FLOOD WARNING PROCESS

Operational flood warning systems are relatively widespread, and there are probably as many different approaches as there are systems. These flood warning systems are typically tailor made to the location(s) for which the warnings are to be provided, ranging from fast responding local warning systems in the headwaters of a river (e.g., Krzysztofowicz et al., 1992) or urban areas (e.g., Koussis et al., 2003), to flood warning systems for lower reaches of large river basins (e.g., Sprokkereef, 2001) or for all rivers in an administrative region (e.g., Moore and Jones, 1998). Despite this apparent variety of approaches, a general description of the ideal flood warning scheme can be characterised in four important steps depicted in Figure 1 (Parker and Fordham, 1996; Haggett, 1998).

Detection. In the detection stage real-time data on processes that could generate a flood event are monitored. This includes hydrological and meteorological information often gathered through telemetry systems, climate stations, weather radar etc.

Forecasting. In the forecasting stage predictions are made of the levels and flows, as well as the time of occurrence of a forthcoming flood event. Typically this involves the use of hydrological models, driven using both the real-time data gathered in the detection phase and forecasts of meteorological conditions such as rainfall and temperature. These are often obtained through external meteorological forecasts.

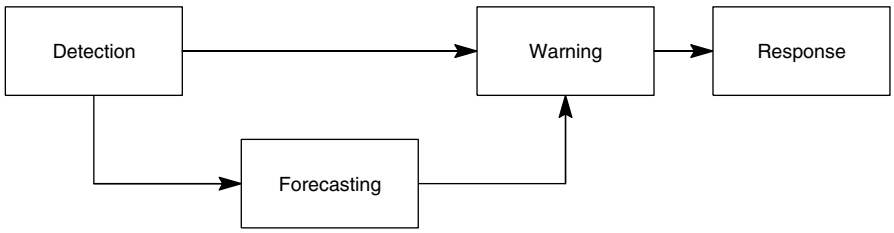

Figure 1. Steps in the flood warning process.

Warning. The warning stage is key to the success of operational flood warning. Using information derived from the detection and forecasting stages, the decision to warn appropriate authorities and/or properties at risk must be taken. The warning must be such that this gives an unambiguous message on the imminent flood potential.

Response. Response to flood warnings issued is vital for achieving the aims of operational flood warning. If the objective is to reduce damage through flood preparedness, an appropriate response by relevant authorities and affected persons must be taken following a warning to realise this.

Although flood forecasting takes a prominent position in these four steps, the most basic forecasting systems do not include an explicit forecasting step and issue flood warnings on the basis of observations such as gauged rainfall and flows, combined with the judgement and experience of the forecasters (Cluckie, 2000). Of the four elements the most important in attaining the objectives of flood warning are the last two. In an evaluation of operational flood warning schemes across Europe (Parker and Fordham, 1996), most of the criteria introduced in assessing the matureness of flood warning systems relate to the dissemination of flood warnings and the organisational embedding of the systems. Failure of flood warnings to reach the public (Penning-Rowsell *et al*., 2000), or a large number of warnings issued to the public that prove to be false due to low accuracy forecasts (Krzysztofowicz *et al*., 1992) will lead to performance deterioration of the service as a whole. Despite this, most attention from hydrologists is traditionally targeted at the flood forecasting step. Technological advances have led to the development of more complicated flood forecasting systems, utilising a range of hydrological methods. Examples include transfer function or statistical type models (Wilke, 1998; Young, 2003; Laio *et al*., 2003), lumped conceptual hydrological models (Grijsen *et al*., 1992; Moore and Jones, 1998; Bürgi, 2002) and hydrodynamic modelling codes. (Grijsen *et al*., 1992; Sprokkereef, 2001) Existing flood warning systems are often in a state of migration, with simple statistical methods being replaced with the more complex models (Wilke, 1998). The advantage of more complex methods is that this allows lead times of forecasts to be extended, thus increasing the usefulness of the flood warning system. Extension of the lead time, however, implies that the fluvial forecast relies more and more on prediction of future rainfall, rather than downstream propagation of water already in the river system. These predictions become less and less certain as lead times increase. Some methods in providing precipitation predictions are through standard scenarios (Grijsen *et al*, 1992) short term statistical extrapolation based on observations (Toth *et al*., 2000), propagation of radar images (Cluckie, 2000) or through quantitative precipitation prediction from meteorological forecasting agencies (Collier and Krzysztofowicz, 2000).

2.2. FLOOD FORECASTING AND DATA ASSIMILATION

Common to the use of models in a flood forecasting context is that in contrast to the use of models in calibration, particular attention must be paid to use in real-time. Obviously the models are required to function in a real-time environment which adds requirements to computational performance and robustness (Moore and Jones, 1998). More importantly, however, it cannot be assumed that a model that has been optimally calibrated to a historical dataset performs equally well when set in a forecasting environment (Young, 2003). The reason for this is that errors made by a model in an n step ahead forecast may be very different from errors made by a model viewed over a calibration period where deviations between modelled output and observations are minimised over the whole period. In short-term forecasting these short term deviations must be taken explicitly into account through some sort of feedback mechanism (Refsgaard, 1997). Commonly referred to as data assimilation or updating, this feedback mechanism combines model results and observations and is considered a fundamental element of a forecasting system (Grijsen *et al.*, 1992; Kachroo, 1992; Madsen *et al.*, 2000). In principle there are four main approaches in data assimilation (WMO, 1992; Refsgaard, 1997); (i) input correction, (ii) state updating, (iii) parameter updating, and (iv) output updating or error correction. Of these the last technique is perhaps the most simple and widely employed (Moore and Jones, 1998). State updating, typically implemented through a Kalman Filtering approach has also been applied widely (Grijsen *et al.*, 1992; Young, 2003), while input updating is used in only selected systems (Bürgi, 2002). Parameter updating is typically not considered philosophically viable when using conceptual or physical modelling (Kachroo, 1992), though for data driven modelling approaches such as neural networks or transfer functions it may be a good option (Young, 2003).

The importance of data assimilation in forecasting is shown in Figure 2. The forecast is shown for the station of Lobith on the Rhine river at the Dutch/German border. The results are from a re-analysis run of the 1995 flood event using observed rather than forecast precipitation. Rainfall-runoff modelling is through the HBV conceptual model (Bergström, 1995), with runoff from main tributaries routed through to the main Rhine river. The SOBEK hydrodynamic model (Delft Hydraulics, 2004) is applied for the Rhine from the upstream station at Maxau to Lobith, a distance of some 500 km, with an estimated travel time of flood peaks in the reach in the order of 4 days. Extreme floods at Lobith, however, generally do not originate in the basin upstream of Maxau (mainly Switzerland), but rather in the uplands of the middle Rhine along the Neckar, Main and Mosel tributaries. These tributaries flow into the Rhine at travel times from Lobith of between 2 and $3\frac{1}{2}$ days (Disse and Engel, 2001). Simulation results show the models tend to

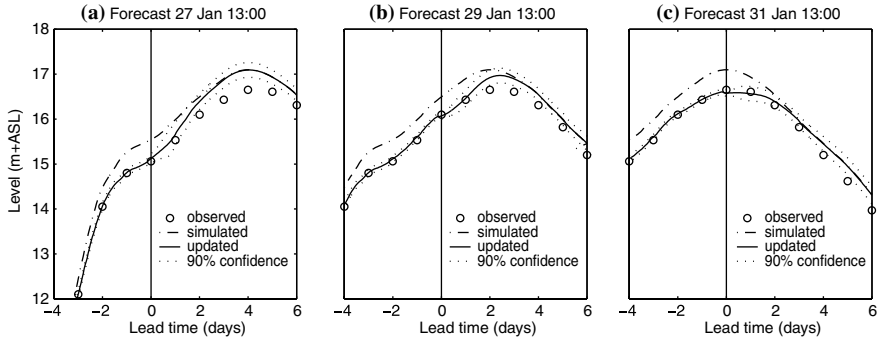

Figure 2. Forecast levels at Lobith with and without Kalman filtering applied in hydrodynamic model.

overestimate runoff and as a consequence levels at Lobith quite significantly. The consequence of such overestimation may be a high rate of false warnings being issued. The extended Kalman filter option available in the SOBEK model is configured using on-line observations from eight gauges upstream of and including Lobith. Particularly for the first day in the forecast updated water levels show a clear improvement compared to simulation results. The effect of updating starts to diminish, however, and after 4 days the simulated and updated results are identical. These 4 days comply more or less with the lag time of flood waves in the reach considered. The Kalman filter additionally outputs the uncertainty in the updated level, and the 90% confidence envelope is shown. Further updating is possible using more of the available gauges in the reach as well as other updating methods such as error correction applied to inflows at tributaries. Although this will help improve forecast results for lag times between zero and 4 days, little improvement will be achieved beyond that as a consequence of the typical lag times in the system. For the operational forecasting system of the Rhine at Lobith this is, however, sufficient as currently the requirement for reliable flood warning delivery is set at 3 days, with an extension to 4 days foreseen in the near future (Sprokkereef, 2001).

3. Flood Forecasting at the European Scale

A recent research initiative, a European Flood Forecasting System (EFFS, as described fully in De Roo *et al.*, 2003) has focused on a methodology to utilise recent advances in numerical weather prediction (NWP) in flood forecasting.

The aim was to develop a prototype pan-EFFS using both global and downscaled regional numerical weather predictions, and use these to drive high-resolution scale (1 or 5 km grid scale) water balance and rainfall-runoff

models. Due to its use of NWP, forecast lead times can be increased to well beyond the characteristic time of concentration of even the larger European basins, with the system targeting delivery of pre-warnings at lead times in the order of five–ten days. For selected reaches the system accommodates an inundation modelling system allowing advance prediction of inundated extent. This prototype is potentially a front runner of an operational system that will act predominantly as a pre-warning system to operational flood forecasters, allowing implementation of flood damage alleviation measures such as drawing down flood control reservoirs, stockpiling emergency supplies and placing key personnel on alert. Medium-range weather forecasts are considered both as deterministic forecasts and as probabilistic ensemble forecasts. Using the probabilistic ensemble weather forecast, fluvial forecasts generated by the EFFS system are equally considered more as probabilistic than deterministic (De Roo *et al.*, 2003).

3.1. GLOBAL NWP MODELS

Large scale meteorological forecasts for the EFFS system are derived from the European Centre for Medium Range Weather Forecasting (ECMWF) Ensemble Prediction System (EPS). Forecasts of up to 10 days ahead are produced using the EPS (Buizza and Hollingsworth, 2002) for both the Northern and Southern hemispheres. Each ensemble forecast contains a deterministic control run and a 50 member ensemble run where the initial state for each member is perturbed using a singular vector analysis technique that tries to identify unstable regions of the atmosphere by calculating where small initial uncertainties would affect the 48 hour forecast most rapidly (Buizza and Palmer, 1995). Each ensemble member is assumed to have the same *a priori* likelihood. Relevant variables such as precipitation, temperature, wind etc. are retrieved from these ensemble forecasts every 6 h at a horizontal resolution of around 80 km across the European continent for use in the EFFS hydrological forecast runs.

Besides the global ensemble predictions of the ECMWF, global weather predictions are also used in the EFFS system from the German Weather Service. This global model, DWD-GME produces forecasts of the same relevant variables for up to 156 h ahead with a 6 h time step (Majewski *et al.*, 2002).

3.2. REGIONAL NWP MODELS

Meteorological services increase spatial and temporal resolution in forecasts through the use of regional NWP models nested within the global models. Two such models, the Danish Meteorological Institute High Resolution Local Area Model (DMI-HIRLAM, Sattler, 2002) and the German Weather Service "Lokal Modell" (DWD-LM, Damrath *et al.*, 2000) are applied in EFFS. These models obtain boundary conditions from the ECMWF and DWD-GME

models respectively, and while forecasting lead times are shorter, being 72 h for DMI-HIRLAM and 48 h for DWD-LM, the spatial grid resolution may be as detailed as approximately 7 km. This allows better inclusion of important features such as orography and surface type, with resulting forecasts expected to be more accurate. DWD-LM is also non-hydrostatic, and therefore likely to provide more realistic results than other local area models. Given the forecast lead times, however, these models are more relevant for use in operational flood forecasting than in the envisaged pre-warning role of the EFFS.

3.3. CATCHMENT HYDROLOGY, ROUTING AND INUNDATION MODELS

To determine runoff from NWP models, the EFFS system takes a two pronged approach. As a default the raster based LISFLOOD catchment hydrology modelling suite is used. This is a distributed hydrological model under development at the European Commission Joint Research Centre (De Roo *et al*., 2000). A full description of the model concept as used in EFFS is given in De Roo *et al*. (2003). To make forecasts the model is used in two steps. First, a water balance version of the model (LISFLOOD-WB) is run at a daily time step with observed precipitation over a long historic period of 1–5 years to establish an estimate of catchment wetness at the start of the forecasting run. Following this, the flood forecasting version (LISFLOOD-FF) is run for the forecast period at an hourly time step using the NWP derived forecasts as boundary condition. Besides this default model, available for the whole of the continent, specific rainfall-runoff models may be used for particular basins. The HBV rainfall-runoff and coupled SOBEK hydrodynamic models are, for example, used within the EFFS system for the Rhine basin, while the TOPKAPI model (Ciarapica and Todini, 2002) is applied in the Po basin. The use of different models in different basins was considered desirable as this allowed comparison of results from EFFS to existing operational software, as well as the existing models being better suited to local conditions.

As the final step the EFFS system provides an inundation model to estimate extent of inundation along selected reaches as a result of the discharge forecasts obtained from the rainfall-runoff models. This model, LISFLOOD-FP (Bates and de Roo, 2000) uses a simple one-dimensional kinematic wave model for solving main channel flow while overbank floodplain flow is resolved using a simple cell inundation approach (Cunge, 1975). Inundation cells are formed on the basis of the grid cells in the digital elevation model, typically derived through high resolution floodplain surveys such as laser altimetry (Marks and Bates, 2000).

3.4. OPERATIONAL PLATFORM

Combining the results from multiple NWP models, administering historical and forecast data and running both the default rainfall-runoff LISFLOOD

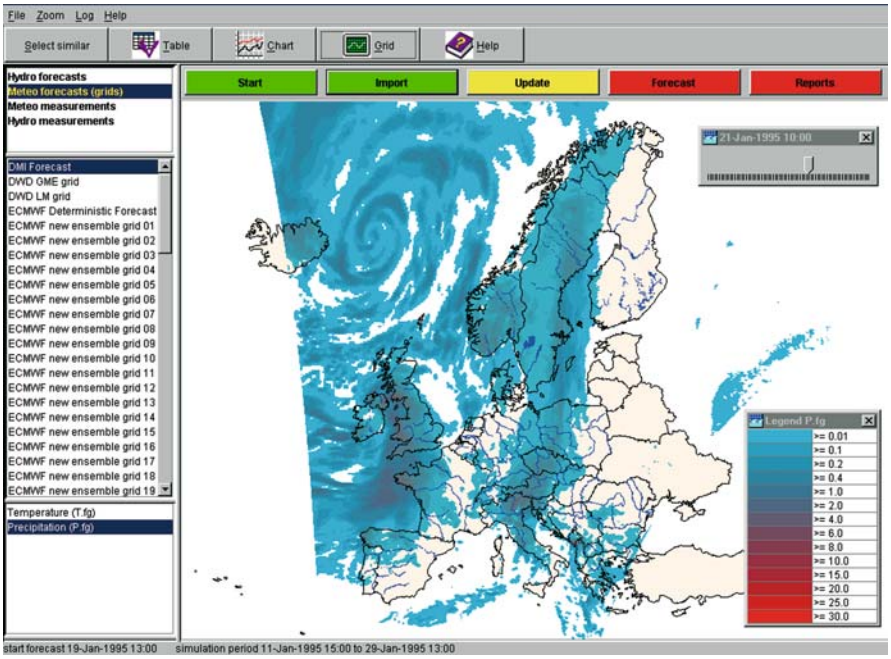

Figure 3. The user interface of the EFFS system.

modelling suite as well as various other models for specific basins requires a versatile, open interface flood forecasting system. Such a system has been developed at DELFT HYDRAULICS in conjunction with the EFFS project, allowing import of the various meteorological forecasts, processing these for use in the hydrological models and running the models. Figure 3 shows an example of the user interface, displaying the precipitation field on the 21st of January 1995 from the DMI-HIRLAM model as forecast on the 19th of January (see www.wldelft.nl/soft/fews for details on the open shell forecasting system used).

3.5. APPLICATION TO THE 1995 EVENT IN THE RHINE BASIN

An example of the use of a ten-day lead time forecast is given through a hindcast run of the January 1995 flood event in the Rhine basin. While this event was not so extreme for the upper and Alpine Rhine, melting snow and extreme precipitation on frozen soil caused one of the largest events for the middle and lower Rhine of the last century (Disse and Engel, 2001). Hindcast ensemble runs from the ECMWFS models for a sequence of days before the peak of the event arrived at the Dutch–German border gauging station of Lobith on January 31st are shown. Precipitation and temperature forecasts are used to force the HBV rainfall-runoff model of the entire Rhine basin,

which in turn inputs forecast flow into the SOBEK hydrodynamic model of the main Rhine downstream of the gauging station at Maxau, some 500 km upstream of Lobith. At Lobith a simple statistical (ARMA) error correction model is applied to correct forecast flows. Note that the meteorological inputs are probabilistic as given by the EPS ensemble forecast, while the rainfall-runoff and routing models are here considered to be deterministic.

Figure 4a shows the results of the ensemble run for the 20th January (grey lines) as well as the observed flows (black line), 11 days before the actual peak. The ensemble results clearly show that a significant flood event is evolving, but the spread of results is such that the results are difficult to interpret. Two days later the ensemble spread shows a slightly higher certainty of an event in the order of 11,000–12,000 m^3/s peaking around January 31st (actual peak was just under 12,000 m^3/s). Again two days later, but still a week ahead of the actual peak, there is no doubting of the severity of the upcoming event. By the 26th the spread in the ensemble forecast is already

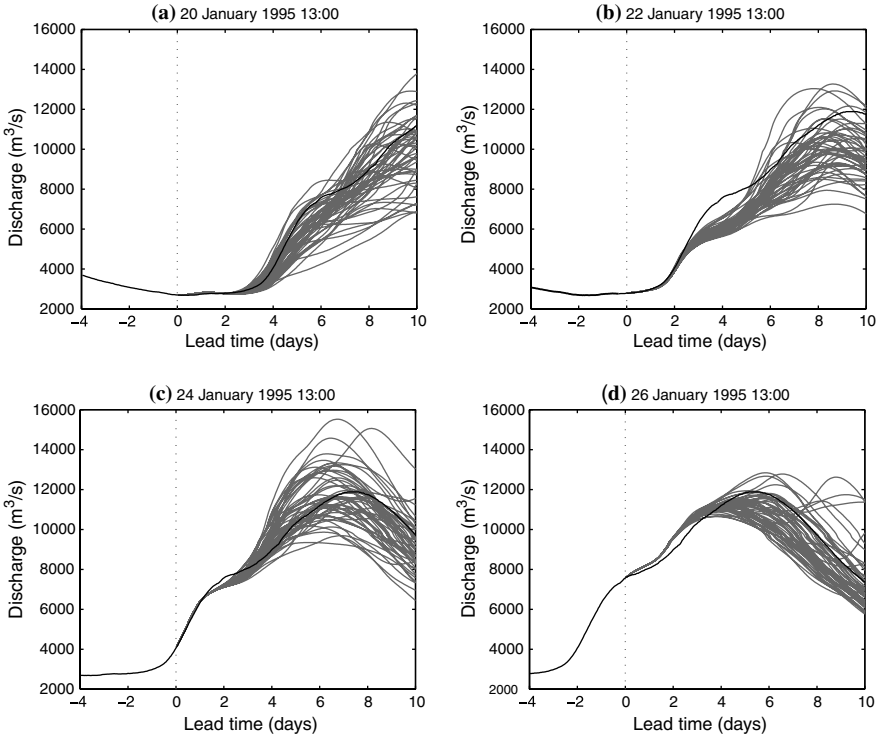

Figure 4. Ensemble forecasts at Lobith issued at 2 day intervals starting 20 January 1995 at 13:00. Grey lines are the results of ensemble runs. The black line is the observed discharge, with results prior to time 0 being the same as the observed due to error correction.

reducing, and lead times are such that more accurate predictions can be derived using higher resolution meteorological forecasts and data assimilation such as in the operational forecast results shown in Figure 2.

Ensemble forecasts as shown in Figure 4 are difficult to interpret and the quantitative nature of the ensemble may be misleading. As all the ensemble members have the same prior likelihood it is impossible to assign uncertainties to the forecast. Instead the ensemble forecast is to be seen as a probabilistic forecast, and one approach in presenting this is to interpret the ensemble as quartiles (De Roo *et al.*, 2003). While this summarises the spread of the ensemble forecast to an extent, procedures to use these as a pre-warning to operational forecasting are unclear. A simpler, alternative representation is to group the ensemble predictions in classes of severity at incremental lead times.

An example is given in Figure 5, where the shades of grey indicate the maximum severity at discrete lead times. Runs falling into classes of increasing discharge are given using darker greys (colours can be equally used), while the percentage of runs in each class determines the height of the class in the figure. This gives a powerful visual interpretation showing that for the forecast on the 20th indications of the upcoming event were clear with some uncertainty as to the severity (large gradient of gray scale). Two days

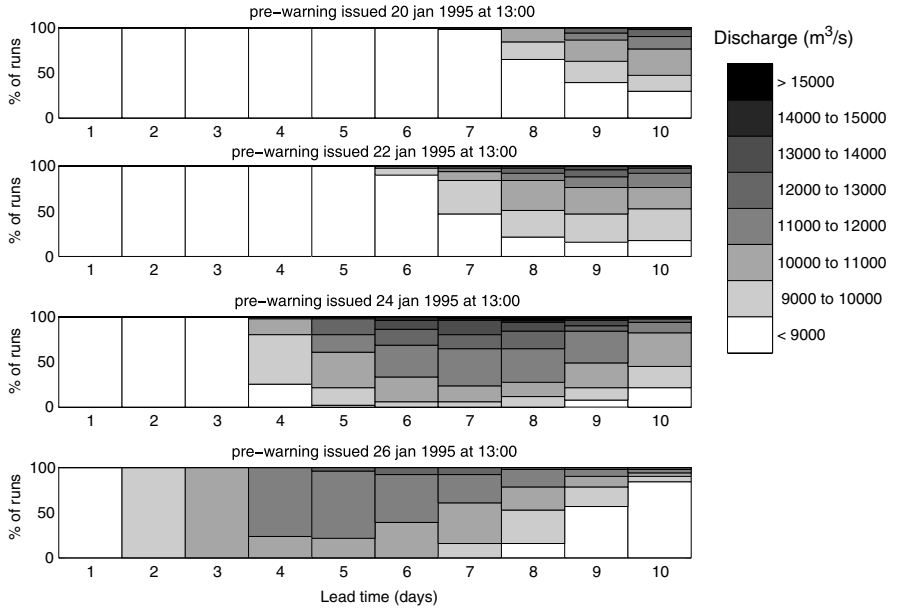

Figure 5. Pre-warning for discharge at Lobith issued at two day intervals starting 20 January 1995 at 13:00.

later there is no doubt that a large event is imminent, but uncertainty is still large. On the 24th the full scale of the event is clear, and the timing of the peak of the flood accurate when compared to observations. The magnitude of the event is still unclear, but by the 26th this uncertainty has clearly diminished with almost all ensemble runs falling in a single class. By this time, the flood event will also be picked up by the 4 day lead time operational forecast, which through the use of higher detail numerical weather predictions (e.g., from DWD-LM and DMI-HIRLAM), combined with data assimilation in the real-time hydrological and hydraulic models can begin to give accurate predictions of the peak and timing of the event.

4. Discussion

4.1. POSITION OF PRE-WARNING IN OPERATIONAL FLOOD WARNING

The EFFS system has demonstrated the provision of a medium-range flood forecast as a pre-warning through integration of ensemble NWP and hydrological modelling at a European scale, or in some cases using hydrological models to cover a specific basin. The value of a pre-warning system is demonstrated by the lead time at which an indication of an imminent flood event for the 1995 event in the Rhine at Lobith is predicted. Similar results have been achieved for the Meuse basin using the LISFLOOD rainfall-runoff model (De Roo *et al.*, 2003). Even for highly convective extreme events in Switzerland the potential of such pre-warning is illustrated in Quiby and Schubiger (1998), where despite the fact that the NWP models had a very low skill rate in predicting exact amounts and locations of a number of convective events studied, a clear indication at a reasonable lead time of the high potential for flooding in the area was given. Pre-warning is similarly used in flashy catchments by the National Weather Service NWS in the USA, where runoff thresholds based on physical characteristics are used in conjunction with soil moisture accounting and areal rainfall data (Carpenter *et al.*, 1999). Fox and Collier (2000) similarly present a pre-warning methodology through a probabilistic estimate of medium range flood potential in a catchment. The success of any pre-warning will, however, be dependent on its integration with established flood forecasting and warning procedures. In principle, forecasting as a part of the pre-warning can be seen as the same four steps as operational forecasting (Parker and Fordham, 1996; Haggett, 1998) shown in Figure 1. Figure 6 extends Figure 1 to show the most appropriate position of the pre-warning system. The main difference with operational forecasting is that rather than target warnings at the public, pre-warnings are targeted at operational staff of the established flood forecasting system. This makes the use of probabilistic forecasts easier as these staff can be assumed to have a good understanding of floods and the problems of flood prediction. Simply

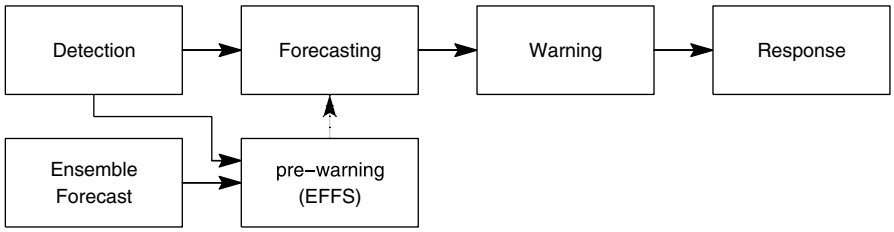

Figure 6. Integrating pre-warning in the operational flood warning process.

passing the probabilistic forecast to the public will only lead to confusion. Clear procedures will need to be established on how the pre-warnings are utilised, and these procedures can be established through, for example, levels of pre-warning based on the number of members in the ensemble forecast falling into increasing classes at incremental lead times (see Figure 5). More practical response to pre-warning could then be in three ways;

1. Once it is clear that a major event is evolving, duty staff at flood forecasting centres can start to enhance forecasting using the operational system as well as rigourous verification and validation of the data used etc. Additionally, models with a higher spatial resolution, or with a more complex representation of the physics could be used, and a rigourous evaluation of uncertainties can be done. This will ensure information is as up to date as possible well before the event actually starts.
2. Relevant authorities can be alerted to the potential threat of flooding. This can raise flood preparedness and ensure that sufficient staff are available or on alert to take action once the event actually starts.
3. Data collection can be expanded through both manual and automatic systems not in use during non-flood conditions. This may allow a larger than normal data set being applied in for example data assimilation prior to the flood event and consequently increasing the accuracy of prediction while not significantly adding to cost of data collection. Given sufficient lead time, staff at operational forecasting centres can even simply phone known contacts in the catchment and inform themselves of relevant catchment conditions often not adequately measured, such as snow cover. This will increase not only the accuracy of operational forecasts but also the confidence with which warnings are delivered.

Particular attention in the use of the probabilistic pre-warning in alerting relevant authorities should be given to the skill levels of the system. The hindcast results for the 1995 flood in the Rhine basin, as well as similar results for the same flood in the Meuse basin show that notice given using the EFFS system is adequate. As a part of future research, however, the accuracy

level of the system needs to be assessed for events just under the flood warning level, and whether ensemble forecasts would generate a high false pre-warning rate for these. Procedures in using the pre-warning must be established carefully as false flood warnings need to be avoided much the same as operational systems centres should avoid delivering false warnings to the end-users (Krzysztofowicz *et al.*, 1992; Du Plessis, 2002). A centralised service offering unreliable pre-warnings will soon be ignored or even blamed for issuing false warnings. Given the probabilistic nature of the pre-warning, the use of complex models with a high degree of detail such as the floodplain inundation models would be more logical in operational forecasting. Indeed, indicative pre-warnings such as in Figure 5 could perhaps be developed equally well using rainfall accumulations from the ensemble forecasts combined through heuristic rules or fuzzy reasoning with the soil moisture accounting in a water balance model such as LISFLOOD-WB.

4.2. DATA ASSIMILATION

The value of data assimilation in improving accuracy in the forecast is demonstrated in Figure 2 and reported by many authors (Grijsen *et al.*, 1992; Kachroo, 1992; WMO, 1992; Refsgaard, 1997; Madsen *et al.*, 2000; Young, 2003). In its current form the EFFS system does not consider any form of data assimilation. Given the lead times for which the forecasts and subsequent pre-warnings are considered, it is important to identify appropriate methods of data assimilation. Even for a relatively large basin as in the case of the Rhine, lag times of floods in the main river between the main flood generating catchments and the river mouth is in the order of two to four days (Disse and Engel, 2001), and as shown in Figure 2 the effect of data assimilation in the main river dissipates after this. Some additional improvement could be achieved through error correction on the (main) tributaries, but even this will be limited in view of the lead times considered in EFFS. While these two methods will not generally improve the forecast at lag times between five and ten days, some improvement in the first few days of the ensemble forecast will be achieved in the same way as in the deterministic operational forecast (see Figure 4). At lag times of the order of 5–10 days the main source of error in the forecast (if it can be called error in view of the spread of the ensemble forecast) is uncertainty with respect to the catchment condition. Despite the process in which the LISFLOOD-WB model is run using a long history of observed precipitation so as to provide a good initial state for the forecast model (De Roo *et al.*, 2003), it is unlikely that this will always result in the most accurate representation of antecedent moisture conditions to be used at the start of a forecast. Aubert *et al.* (2003) demonstrate that accuracy of forecasts can be significantly improved through updating the initial states of the hydrological model using observed streamflow and soil

moisture, and discuss the potential of using remotely sensed soil moisture data. Much recent research has examined updating catchment states using satellite borne sensors (a special issue of *Advances in Water Resources* was dedicated to the topic, see Troch *et al*. (2003)), but the limited penetration of the soil surface make the use of this data problematic given the current state of the art in hydrological modelling and interpretation of remotely sensed data (Loon and Troch, 2003).

5. Conclusions

In this paper, we have described the structure of a European scale flood forecasting system (EFFS) and have explored the value of this system as a pre-warning to operational flood warning at the river basin scale. The potential of the system to provide valuable information of a major flood event well in advance of the actual event and at a lead time beyond the range of the operational flood forecasting system is demonstrated in a hindcast for the 1995 flood event in the Rhine basin at the forecasting point of Lobith on the Dutch–German border. This ability to provide pre-warnings at lead times of between 5 and 10 days is possible through utilisation of medium range numerical weather predictions.

At these lead times, however, weather predictions are uncertain and this is clearly expressed in the ensemble predictions provided. The spread in the meteorological forecast ensemble is translated by the modelling system to an ensemble of hydrological flow predictions, and although this gives an impression of the spread of things to come, interpretation is difficult. To allow effective dissemination of this ensemble, an alternative to the simple display of the spread of predicted hydrographs is proposed. For each day of lead time the maximum levels for that day are grouped into bins of increasing flow and a simple yet concise warning card summarising the probabilistic ensemble results is derived. Besides clear visual interpretation, this also provides the basis for developing procedures in integrating the pre-warning into the operational flood warning process.

Analysis of the operational flood warning process shows that while the forecasting element plays an important role in the delivery of flood warning, the ensuing steps of dissemination and response are more important in delivering an effective warning. This holds equally to the delivery of a pre-warning and the procedures established based on the warning card concept presented, would need to clearly identify the response operational forecasters should take. Examples could include enhancement of forecasting and of data acquisition, the use of more detailed or physically based models, and rigourous analysis of uncertainties. This will help increase reliability of the operational forecast as well as allowing for timely alerting of relevant authorities to increase flood preparedness.

Although the preliminary development of the EFFS system has shown its potential in utilising advances in meteorological forecasting, much further work needs to be done on the real-time perspective. Data assimilation is shown to play an important role in running hydrological models in real-time within operational flood forecasting systems, and this applies also for models running in a pre-warning system. Given the lead times at which pre-warnings are targeted, widely used methods in data assimilation such as state-updating in hydrodynamic modelling and error correction in hydrological modelling, will not necessarily improve reliability of the pre-warnings due to typical lag times in most European basins being at most four to five days. The persistence of errors in initial states of the hydrological models, however, means that updating of these can potentially improve reliability at medium-range lead times as demonstrated by Aubert *et al*. (2003).

While the idea of Hahn (in Patrick, 2002), describing the future of flood forecasting as an internet based service giving fluvial forecasts with lead times of 90 days, driven through quantitative precipitation forecasts, seems a long way off, application of a pre-warning such as through the EFFS is shown to be a realistic possibility. Achievement of the potential in increasing flood preparedness and reducing losses is, however, dependent on clear procedures to integrate the pre-warning into the operational flood warning process at the basin scale.

Acknowledgements

Marc van Dijk, Albrecht Weerts and Hanneke van der Klis of Delft Hydraulics are thanked for the many discussions and for providing much of the research work for which results are briefly presented. Two anonymous referees are thanked for providing useful comments.

References

Aubert, D., Loumagne, C., and Oudin, L.: 2003, Sequential assimilation of soil moisture and streamflow data in a conceptual rainfall-runoff model. *J. Hydrol.* **280**, 145–161.

Bates, P. and de Roo, A.: 2000, A simple raster-based model for flood inundation simulation. *J. Hydrol.* **236**, 54–77.

Bergström, S.: 1995, The HBV Model. In: V. Singh (ed.), *Computer Models of Watershed Hydrology*. Water Resources Publications, New York, pp. 23–68.

Buizza, R. and Hollingsworth, A.: 2002, Storm Prediction over Europe using the ECMWF Ensemble Prediction System. *Meteorol. Appl.* **9**(3), 289–305.

Buizza, R. and Palmer, T.: 1995, The aingular vector structure of the atmospheric general circulation. *J. Atmos. Sci.* **52**, 1434–1456.

Bürgi, T.: 2002, Operational flood forecasting in mountainous areas – an interdisciplinary challenge. In: M. Spreafico and R. Weingartner (eds.), *International Conference in Flood Estimation*. Bern, CHR Report II-17, pp. 397–406.

Burnash, R.: 1995, The NWS river forecasting system – catchment modelling. In: V. Singh (ed.), *Computer Models of Watershed Hydrology*. Water Resources publication, New York, pp. 311–366.

Carpenter, T., Sperfslage, J., Georgakakos, K., Sweeney, T., and Fread, D.: 1999, National threshold runoff estimation utilizing GIS in support of operational flash flood warning systems. *J. Hydrol.* **224**, 21–44.

Ciarapica, L. and Todini, E.: 2002, TOPKAPI: A model for the representation of the rainfall-runoff process at different scales. *Hydrol. Processes* **16**, 207–229.

Cluckie, I.: 2000, Fluvial flood forecasting. *J. Chart. Inst. Water Environ. Manage.* **14**, 270–276.

Collier, C. and Krzysztofowicz, R.: 2000, Quantitative precipitation forecasting. *J. Hydrol.* **239**, 1–2.

Cunge, J.: 1975, Two dimensional modeling of floodplains. In: K. Mahmood and V. Yevjevich (eds.): *Unsteady Flow in Open Channels*, Vol. II. Water Resources Publications, P.O. Box 303, Fort Collins, Co. USA, Chapt. 17, pp. 705–762.

Damrath, U., Doms, G., Früwald, D., Heise, E. Richter, B., and Steppeler J.: 2000, Operational quantative precipitation forecasts at the German weather service. *J. Hydrol.* **239**, 260–285.

De Roo, A., Gouweleeuw, B., Thielen, J., Bartholmes, J., Bongioannini-Cerlini, P., Todini, E., Bates, P., Horritt, M., Hunter, N., Beven, K., Pappenberger, F., Heise, E., Rivin, G., Hills, M., Hollingsworth, A., Holst, B. Kwadijk, J., Reggiani, P., van Dijk, M., Sattler, K., and Sprokkereef, E.: 2003, Development of a European flood forecasting system. *Intl. J. River Basin Manage.* **1**, 49–59.

De Roo, A., Wesseling, C., and van Deursen: W.: 2000, Physically based river basin modelling within a GIS: The LISFLOOD model. *Hydrol. Processes* **14**, 1981–1992.

Delft Hydraulics: 2004, Sobek. URL: http://www.sobek.nl.

Disse, M. and Engel: H.: 2001, Flood events in the Rhine Basin: Genesis, influences and mitigation. *Nat. Hazards* **23**, 271–290.

Du Plessis, L.: 2002, A review of effective flood forecasting, warning and response system for application in South Africa. *Water SA* **28**, 129–137.

Fox, N. and Collier, C.: 2000, Estimating medium-range catchment flood potential. *J. Hydrol.* **237**, 1–16.

Grijsen, J., Snoeker, X., Vermeulen, C., el Amin Moh. Nur, M., and Mohamed, Y.: 1992, An information system for flood early warning, In: A. Saul (ed.), *Floods and Flood Management*, Kluwer Academic Publishers, pp. 263–289.

Haggett, C.: 1998, An integrated approach to flood forecasting and warning in England and Wales. *J. Chart. Inst. Water Environ. Manage.* **12**, 425–432.

Kachroo, R.: 1992, River flow forecasting. Part 1: A discussion of principles. *J. Hydrol.* **133**, 1–15.

Koussis, A., Lagouvardos, K., Mazi, K., Kotroni, V., Sitzmann, D., Lang, J., Zaiss, H., Buzzi, A., and Malguzzi, P.: 2003, Flood forecast for urban basin with integrated hydro-meteorological model. *J. Hydrol. Eng.* **8**, 1–11.

Krzysztofowicz, R., Kelly, K., and Long, D.: 1992, Reliability of Flood Warning Systems. *J. Water Resour. Plann. Manage.* **120**, 906–926.

Laio, F., Porporato, A., Revelli, R., and Ridolfi, L.: 2003, A comparison of nonlinear flood forecasting methods, *Water Resour. Res.* **39**(5), 1129. DOI:10.1029/2002WR001551.

Loon, E. v. and Troch, P.: 2003, Final Report of the DAUFIN project. Technical Report 115, Hydrology and Quantative Water Management group, Wageningen University. EU Project EVK1-CT1999-00022, ISSN 0926-230X.

Madsen, H., Butts, M., Khu, S., and Liong, S.: 2000, Data Assimilation in rainfall-runoff forecasting. In: *Proceedings of the 4th Hydroinformatics Conference*, Iowa, USA. IAHR.

Majewski, D., Liermann, D. Prohl, P., Ritter, B. Buchhold, M., Hanisch, T. Paul, G., Wergen, W., and Baumgardner, J.: 2002, The operational global Icosahedral-hexagonal gridpoint model GME: Description and high-resolution tests. *Monthly Weather Review* **130**, 319–338.

Marks, K. and Bates, P.: 2000, Integration of high-resolution topographic data with floodplain flow models. *Hydrol. Processes* **14**, 2109–2122.

Moore, R. and Jones, D.: 1998, Linking hydrological and hydrodynamic forecast models and their data. In: R. Casale, K. Havn, and P. Samuels (eds.), *RIBAMOD: River Basin Modelling, Management and Flood Mitigation, Proceedings of the First Expert Meeting*. European Community, EUR17456EN, pp. 37–56.

Parker, D. and Fordham, M.: 1996, Evaluation of flood forecasting, warning and response systems in the European Union. *Water Resour. Manage*. **10**, 279–302.

Patrick, S.: 2002, The future of flood forecasting. *Bull. Am. Meteorol. Soc*. p. 183.

Penning-Rowsell, E., Tunstall, S., Tapsell, S., and Parker, D.: 2000, The benefits of flood warnings: Real but elusive, and politically significant. *J. the Chart. Inst. Water Environ. Manage*. **14**, 7–14.

Quiby, J. and Schubiger, F.: 1998, Quality assessment of the meteorological computer forecasts for localised flash floods. In: R. Casale, G. Pedroli, and P. Samuels (eds.), *RIBAMOD: River Basin Modelling, Management and Flood Mitigation, Proceedings of the First Workshop*, European Community, EUR18019EN. pp. 73–79.

Refsgaard, J.: 1997, Validation and intercomparison of different updating procedures for real-time forecasting. *Nordic Hydrol*. **28**, 65–84.

Sattler, K.: 2002, Precipitation hindcasts of historical flood events. Technical Report 02–13, Danish Meteorological Institute.

Sprokkereef, E.: 2001, *Extension of the Flood Forecasting Model FloRIJN*. NCR Publication 12-2001, ISSN no. 1568234X.

Toth, E., Brath, A. and Montanari, A.: 2000, Comparison of short-term rainfall prediction models for real-time flood forecasting. *J. Hydrol*. **239**, 132–147.

Troch, P., Paniconi, C., and McLaughlin, D.: 2003, Catchment scale hydrological modelling and data assimilation. *Adv. Water Res*. **26**, 131–135.

Wilke, K.: 1998, State-of-the-art in flood forecasting systems and future improvements. In: K. Wilke (ed.), *RIBAMOD: River Basin Modelling, Management and Flood Mitigation, Proceedings of the First Workshop*. European Community, EUR18019EN, pp. 177–187.

Wind, H., Nierop, T., de Blois, C., and de Kok, J.: 1999, Analysis of flood damages from the 1993 and 1995 Meuse floods. *Water Resour. Res*. **35**, 3459–3465.

WMO: 1992, Simulated real-time intercomparison of hydrological models. Technical Report 38, World Meteorological Organisation, Geneva, Switzerland.

Young, P.: 2003, Advances in real-time flood forecasting. *Phil. Trans. R. Soc. Lond*. **A360**, 1433–1450.

Natural Hazards (2005) 36: 43–64

Estimating Injury and Loss of Life in Floods: A Deterministic Framework

EDMUND PENNING-ROWSELL[1,★], PETER FLOYD[2], DAVID RAMSBOTTOM[3] and SURESH SURENDRAN[4]
[1]*Flood Hazard Research Centre, Middlesex University, UK;* [2]*Risk and Policy Analysts Ltd., Norwich, UK;* [3]*HR Wallingford Ltd., Wallingford, Oxford, UK;* [4]*Environment Agency, Reading, UK*

(Received: 1 December 2003; accepted: 30 June 2004)

Abstract. This paper presents an outline methodology and an operational framework for assessing and mapping the risk of death or serious harm to people from flooding, covering death and physical injuries as a direct and immediate consequence of deep and/or fast flowing floodwaters (usually by drowning), and deaths and physical injuries associated with the flood event (but occurring in the immediate aftermath). The main factors that affect death or injury to people during floods include flow velocity, flow depth, and the degree to which people are exposed to the flood. The exposure potential is related to such factors as the ''suddenness'' of flooding (and amount of flood warning), the extent of the floodplain, people's location on the floodplain, and the character of their accommodation. In addition, risks to people are affected by social factors including their vulnerability and behaviour. A methodology is described for estimating the likely annual number of deaths/injuries. This is based on defining zones of different flood hazard and, for each zone, estimating the total number of people located there, the proportion that are likely to be exposed to a flood, and the proportion of those exposed who are likely to be injured or killed during a flood event. The results for each zone are combined to give an overall risk for each flood cell and/or community. The objective of the research reported here is to develop a method which could be applied using a map-based approach in which flood risks to people are calculated and displayed spatially for selected areas or communities. The information needed for each part of the process is described in the paper, and the further research to provide the required information is identified.

Key words: floods, loss of life, serious injury, deterministic model, case examples

1. Introduction: The Nature of Risk Assessment

The risk to life and of serious injury from floods in continental Europe is not uncommon, for example in Poland in 1997 and in the Gard *Department* in southern France in 2002. In the UK these flood impacts occur infrequently, although most major flood events such as in 1998 and autumn 2000 see some

★ Author for correspondence. E-mail: e.penning-rowsell@mdx.ac.uk

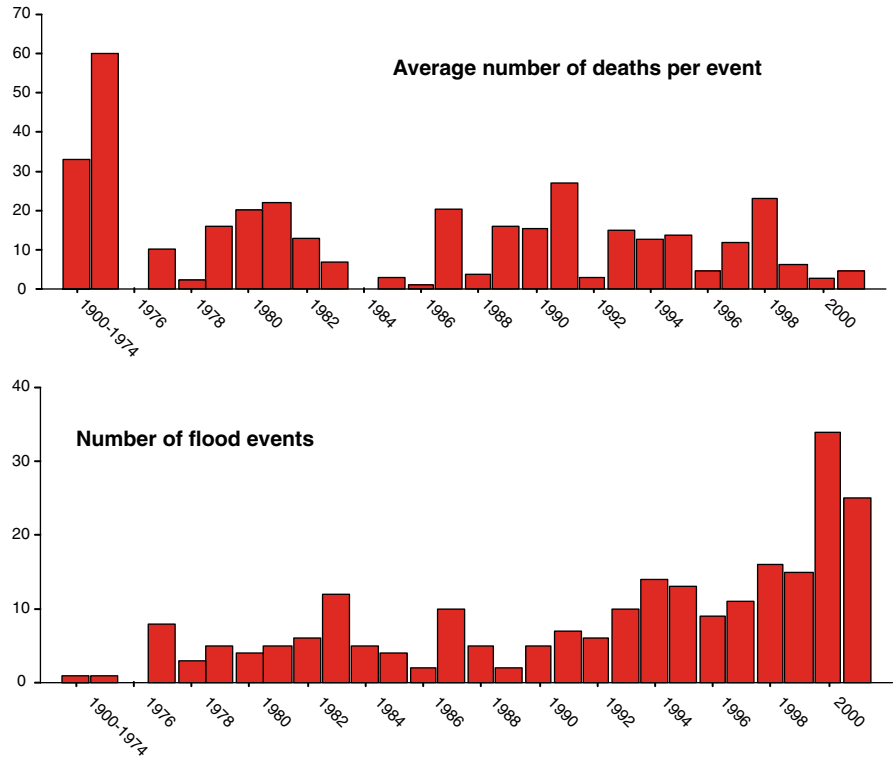

Figure 1. The number of flood events and related deaths in Europe (data for 1900–1974 are means). Source: WHO.

incidents of both. The loss of life in European floods appears generally to be falling, but nevertheless a significant risk remains (Figure 1).

Research on loss of life in floods is sparse, and has so far concentrated on small-scale experiments (Abt *et al.*, 1989) or reviews of broad scale models (Jonkman *et al.*, 2002). This paper presents an outline methodology and an operational framework for assessing and mapping the risk of death or serious harm to people from flooding at an intermediate or "community" scale. We cover death and physical injuries as a direct and immediate consequence of deep and/or fast flowing floodwaters (usually by drowning), and the risk of death and serious physical injuries associated with the flood event (but occurring in the immediate aftermath).

In so doing we recognise that risk is a complex concept, but the use of the term within the field of flood and coastal defence is commonplace. Definitions appear to be converging towards risk being a product of event probability and consequences. Thus the *Project Appraisal Guidance Series* developed by the UK Department of the Environment, Food and Rural Affairs (Defra) covers risk in *FCDPAG 4 – Approaches to Risk* (Defra, 2003a),

stating that risk depends on a combination of both the likelihood and consequences of an event.

This reflects definitions used across the risk field. For example, the Royal Society (1992) defined risk as a combination of the probability, or frequency, of occurrence of a defined hazard and the magnitude of the consequences of that occurrence. A similar definition is used by the British Standard Institution (1996). Comparable definitions have been adopted by DG SANCO (European Commission: Directorate-General for Health & Consumer Protection) for a range of risks to EU citizens (European Commission, 2000). The associated definition for "hazard" is the potential of a risk source to cause an adverse effect, and in the UK the *Departmental Guidance for Environmental Risk Assessment and Management* (DETR, 2000) uses "risk" and "hazard" in similar ways.

This convergence leads us to use the term risk here to denote the probability and severity of an adverse effect/event affecting people following exposure, under defined conditions, to a risk source. In the context of this paper the risk source is floodwater, the hazard is the potential to cause direct injuries, and the risk is the likelihood/probability[1] that such a potential is realised.

2. The Procedure of Risk Assessment

The procedure by which risk is determined is a 'risk assessment': a process of evaluating the likelihood and severity of the adverse effect/event, including identifying the attendant uncertainties. The European Commission's (2000) DG SANCO report defines a risk assessment as comprising hazard identification, hazard characterisation, exposure assessment, and risk characterisation, and we have adopted this four-step sequence (Table I). It is similar to the framework for risk assessment recommended by the DETR (2000) although the terminology differs slightly.

As far as *hazard identification* is concerned the risk source considered here is floodwater and the hazard is the potential of that floodwater to cause physical injury or death during or immediately after flooding (i.e., within days). We are concerned here with these short-term physical effects, and not the longer term physical and psychological effects analysed elsewhere (e.g., Tapsell *et al*., 2002).

The purpose of *hazard characterisation* is to evaluate the effects of being exposed to the risk source. In simple terms, the effects may be characterised by the expression:

[1]It should be noted that "likelihood" here relates to chances per year (i.e. expected frequency) whereas probability is the chance of occurrence within a specified time frame or per event.

Table I. The risk assessment framework

Risk assessment stage	Definition[a]
Hazard identification	The identification of a risk source(s) capable of causing adverse effect(s)/event(s) to humans or the environment, together with a qualitative description of the nature of these effect(s)/event(s)
Hazard characterisation	The quantitative or semi-quantitative evaluation of the nature of the adverse health effects to humans and/or the environment following exposure to a risk source(s). This must, where possible, include a dose/response assessment[b]
Exposure assessment	The quantitative or semi-quantitative evaluation of the likely exposure of humans and/or the environment to risk sources from one or more media
Risk characterisation	The quantitative or semi-quantitative estimate, including attendant uncertainties, of the probability of occurrence and severity of adverse effect(s)/event(s) in a given population under defined exposure conditions based on hazard identification, hazard characterisation and exposure assessment

[a]Definitions taken from European Commission (2000).
[b]A "dose/response assessment" examines the relationships between the scale of the exposure and the scale of the adverse effects.

$$E = f(F, L, P)$$

where E is the nature/extent of effects (on those exposed), F is the flood characteristics (depth; velocity, etc.), L is the location characteristics (inside/outside buildings; nature of housing, etc), and P is the population characteristics (age; health, etc.).

This posits that these 'dose–response' relationships are different for different groups of people (for example, those outdoors, those indoors or those in vehicles). Given such a 'dose–response' assessment, the *exposure assessment* focuses on the relationship between the presence of the floodwaters and the probability that the adverse effects are realised. For example, if people are indoors and upstairs when a flood affects a residential area, no-one will be exposed (directly) to the risk source: this step in the risk assessment examines, in effect, the conditional probabilities that someone present will be exposed to the risk source.

The final step of the risk assessment is *risk characterisation*. This combines the likelihood/probability of a flood (to produce the risk source), the probabilities that people will be exposed (based on the nature/size of population present and associated probabilities of exposure), and the probabilities that those exposed will be injured or will suffer loss of life.

3. The Determining Variables to be Considered

3.1. OVERVIEW: HAZARD IDENTIFICATION, CHARACTERISATION AND EXPOSURE

The research literature suggests that there are three broad sets of characteristics which will influence the degree of immediate harm to people in the event of a flood (see Ramsbottom, *et al.*, 2003; Jonkman *et al.*, 2002). These are the flood's characteristics (depth, velocity, etc.), the location's characteristics (inside/outside, nature of housing), and the population characteristics (age, health, etc.).

Regarding the flood, there is broad agreement that the degree of hazard is primarily associated with depth and velocity, predominantly the latter (Abt *et al.*, 1989). Table II lists other possibly relevant parameters.

At any particular time, people potentially at risk may be outdoors on foot, outdoors in a vehicle, indoors in a basement, or confined by disabilities to the ground floor, etc. The distributions of people amongst these locations (or the probabilities of particular individuals being in a particular location) will vary with nature of the area, the time of day, and the time of year, etc. For example, at night in mid-winter in a small town, people will predominantly be at home, mainly in bedrooms on the first floor. On a summer holiday saturday afternoon many people would be outdoors, in their gardens, in parks, campsites or in shopping centres.

But the usual precursors to flooding are heavy rainfall and/or storms at sea and these circumstances will affect these locational distributions. They will, for example, reduce the numbers of people outdoors on foot. Flood warnings will affect peoples' locations, as will the evacuation of exposed people in extreme cases. At one extreme, the lower stretches of large rivers can receive several days' flood warning, allowing people to be alerted and to take appropriate evasive action. At the other extreme, flooding can occur very quickly – most notably with a failure of a coastal defence – allowing no time for a flood warning and any exposure reduction measures. Significantly, at 18 UK locations flooded from rivers in 2000 surveyed in research on the health impacts of floods (Risk and Policy Analysts, 2003), nearly 70% of 655 respondents received no flood warning prior to their house being flooded.

Taking a particular flood in a defined area under specified circumstances (with its degree of flood warning, timing, etc.) will indicate the probabilities that people will be exposed to the flood. The probability that a particular individual will suffer serious short-term physical injuries will then depend, to some extent, on their personal characteristics. We would expect the very old to be more at risk and the infirm/disabled/long-term sick to be at greatest risk. Although, theoretically, a young child would be at high risk, it is very unlikely that, say, a 4-year-old would be left alone

Table II. Flood characteristics potentially relevant to loss of life and major injury (in addition to water depth and velocity)

Parameter	Comment
Speed of onset and flood warning	The speed of onset and flood warning are important factors but predominantly affect the probability that people will be exposed rather than the intrinsic hazardous properties of the floodwaters (i.e. speed and depth)
Flood duration	Within Europe, flood durations are likely to range from several hours to a few weeks. Whilst people trapped in their homes in a winter flood for several days are more likely to suffer hypothermia, duration *per se* is unlikely to be a significant factor for immediate serious injuries or worse
Debris	Fast moving floodwaters carrying debris present a greater threat (to both people and structures) than those with no debris. Sources of (large) debris include trees, cars, caravans, ice floes, etc.
Nature of floodwater	Different types of floodwater have varying degrees of damage potential. It is generally acknowledged that seawater causes more damage to buildings than river water. Sewage contamination would be expected to present an increased risk of disease. However, in terms of serious short-term physical human effects, the nature of the floodwater is unlikely to be a significant factor
Level of flood risk and presence of defences	The presence and condition of flood defences together with the past flooding record and predictions of future flooding all relate to the risk of the flood event occurring, and are therefore taken into account in the estimation of flood probability. This includes breaching of defences, where the probability of failure is equal to the probability of the event. The flood hazard is expressed in terms of velocity and depth of the resulting flood
Nature of floodplain	The depth and velocity of floodwaters will vary with distance from the source of the flooding (breach, river, overtopping, etc.) which, in turn, will depend on the nature of the floodplain (topography, presence of obstructions, etc.). As such, knowledge of the floodplain will inform the estimates of flood depth and velocity, as opposed to being a separate variable, except insofar as floodplain size affects evacuation success or otherwise

in a flood situation: their exposure is therefore related to their family or social circumstances at the time (as would be the exposure of many individuals).

More generally, the possibility that direct physical injuries will be a function of other socio-demographic factors such as income, level of education, or employment status, is unsubstantiated. They are known to influence the extent and impact of longer term physical and psychological flood effects (Tapsell *et al.*, 2002; Penning-Rowsell and Wilson, 2003) but that is not our concern here.

3.2. SINGLE FLOOD EVENT ASSESSMENTS

In this methodology, we suggest that the number of deaths and injuries for a single flood event may be estimated as follows:

$$N(I) = N \cdot X \cdot Y$$

where $N(I)$ is the number of deaths/injuries, N is the population within the floodplain, X is the proportion of the population exposed to a chance of suffering death/injury (for a given flood), and Y is the proportion of those at risk who will suffer death/injury.

To calculate $N(I)$, methods are needed to calculate X and Y, having determined the population of the floodplain area (N). Estimating the numbers of people at risk requires we estimate the degree of hazard by location within the floodplain. In essence, this will require determining the numbers of people ($N(Z)$) within different hazard zones, where the degree of hazard can be related to flood depth, velocity and debris content, and where that hazard is broadly constant across the hazard zone. The first step is therefore to define the hazard zones.

Whilst it is clear that the degree of hazard is a function of both velocity (v) and depth (d) (e.g., Abt *et al.*, 1989), and that a flood with depth but no velocity is hazardous, a flood with (virtually) no depth is not. We have used therefore the function $(v + 1.5) \times d$ for this aspect of the degree of hazard. A further factor for debris content is added to reflect the extra hazard in this respect (Table III). This expression is somewhat arbitrary, although it is based on considerable experience of flood hazard estimation. Refinement of this relationship is needed in the future, not least because it is central within this methodology to estimating the fatality rate within those injured in the extreme floods analysed here.

The numbers of people exposed is likely to depend on four factors: the existence of a flood warning, the flood's speed of onset, the nature of the area (type of housing, presence of parks, etc.), and the timing of the flood. Defence overtopping and breaching are a special case, where the speed of onset can be rapid and, whilst severe conditions may be forecast, there may be no warning of the actual flooding. Although all such factors could be calculated probabilistically, we have used a simple scoring system on a three point scale (Table IV) and again there clearly is scope for refinement of this approach.

Table III. Hypothetical example: hazard zones and the number of people at risk [variable $N(Z)$ and the derivation of the Hazard Rating]

Distance from river/ coast (m)	$N(Z)$	Typical depth, d (m)	Typical velocity, v (m/sec)	Debris factor (DF)	Hazard rating = $d(v + 1.5) + DF$
0–50	25	3	2	2 – Likely	12.5
50–100	50	2	1.8	1 – Possible	7.6
100–250	300	1	1.3	0 – Unlikely	2.8
250–500	1000	0.5	1.2	0 – Unlikely	1.35
500–1000	2500	0.1	1	0 – Unlikely	0.25

Table IV. Hypothetical example: area vulnerability's components and their scores

Parameter	1 – Low risk area	2 – Medium risk area	3 – High risk area
Flood warning[a]	Effective tried and tested flood warning and emergency plans	Flood warning system present but limited	No flood warning system
Speed of onset	Onset of flooding is very gradual (many hours)	Onset of flooding is gradual (an hour or so)	Rapid flooding
Nature of area[b]	Multi-storey apartments	Typical residential area (2-storey homes); (low rise) commercial and industrial properties	Bungalows, mobile homes, busy roads, parks, single storey schools, campsites, etc.

[a]In this context, flood warning includes emergency planning, awareness and preparedness of the affected population, and preparing and issuing flood warnings.
[b]High and low 'nature of area' scores are intended to reflect the judgement of the assessor as to whether there are particular features of the area in question which will make people in the area significantly more or less at risk than those in a 'medium risk area'.

The sum of the three factors, with scores ranging from 3 to 9, indicates the vulnerability of the area as opposed to that of the people (Table V). This 'area vulnerability' score is multiplied by the hazard rating derived above to generate the value for X (the % of people exposed to risk) as shown in Table VI. Should the score exceed 100, this is simply taken as 100. Whilst this is not a true percentage, it is used as such and provides a practical approach to quantifying the assessed flood risk.

The final stage is to compute the numbers of deaths/injuries. This is achieved in our hypothetical example by multiplying the number of people exposed to the risk (N(ZE)), from Table IV, by a factor, Y, which is based on

Table V. Hypothetical example: area vulnerability scores

Distance from river/coast (m)	Flood warning	Speed of onset	Nature of area	Sum = area vulnerability
0–50	2	3	2	7
50–100	2	2	1	5
100–250	2	2	3	7
250–500	2	1	2	5
500–1000	2	1	2	5

Table VI. Hypothetical example: generating variable X (% of people at risk)

Distance from river/coast (m)	$N(Z)$	Hazard rating (HR)	Area vulnerability (AV)	X = HR × AV	N(ZE)
0–50	25	12.5	7	88%	22
50–100	50	7.6	5	38%	19
100–250	300	2.8	7	20%	59
250–500	1000	1.35	5	7%	68
500–1000	2500	0.25	5	1%	31

$N(Z)$ is the population in each hazard zone.
N(ZE) is the number of people exposed to the risk in each hazard zone.

the vulnerability of the people exposed. The factor we have used for Y is a function of two parameters that our experience suggests are particularly significant in relation to serious injury and loss of life in floods: the presence of the very old (P1); and those who are at risk due to disabilities or sickness (P2). In the first instance the values shown in Table VII can be used, but again these need further research in the future.

The sum for each area then provides an estimate of the Y values for each area which are then multiplied by the numbers of people exposed to the risk (as derived in Table VI) to give the numbers of injuries. In the hypothetical example in the relevant Tables, arbitrary percentages of the very old and infirm within each of the zones have been used to generate values for Y (Table VIII).

The resultant number of injuries is then is estimated by multiplying the number of people at risk (from Table VI) by Y, as shown in Table IX. In zones with a relatively high hazard rating, there would also be an increased probability of fatalities. We have assumed in this initial development of our method that a factor of twice the hazard rating is appropriate, expressed as a

Table VII. Hypothetical example: components of 'People Vulnerability' and their indicative scores

Parameter	10 – Low risk people	25 – Medium risk people	50 – High risk people
The very old (>75)	% well below national average	% around national average	% well above national average (including areas with sheltered housing)
Infirm/disabled/ long-term sick	% well below national average	% around national average	% well above national average (including hospitals)

Table VIII. Hypothetical example: generating values for Y (people vulnerability)

Distance from river /coast (m)	Presence of very old	Factor P1 (10/25/50)	Presence of infirm, etc	Factor P2 (10/25/50)	Y = P1 + P2 (as %)
0–50	Around national average	25	Around national average	25	50
50–100		25	Around national average	25	50
100–250	Above national average	50	Around national average	25	75
250–500	Below national average	10	Below national average	10	20
500–1000		10	Around national average	25	35

percentage, based on the results that this gives for our case studies (see below). Applying this factor in our hypothetical example yields a predicted 89 injuries of which 7 are fatalities (Table IX).

In summary, the above procedures illustrate how the key factors identified from past research are used to estimate the overall numbers of injuries and deaths. Clearly, the methodology could be 'tuned' with better weights for the different factors. In line with our aim of developing a map-based system, most of the required parameters are already available for UK floodplains and in many other countries (or there are surrogates for them). The possible

Table IX. Hypothetical example: generating estimates of the numbers of injuries and deaths

Distance from river/coast (m)	N(ZE), from Table VI	Y = P1 + P2 (as %)	No. of injuries including loss of life	Fatality rate = 2 × HR	No. of deaths
0–50	22	50	11	25%	3
50–100	19	50	10	15%	1
100–250	59	75	44	6%	2
250–500	68	20	14	3%	0.5
500–1000	31	35	11	1%	0
All			89		7

exception is data on flood water velocity, which is not collected systematically except at gauging stations.

4. An Application to Three Case Studies

The methodology has been tested by being applied to three historical flood incidents in the UK. Further such tests will be needed to refine the methodology.

4.1. GOWDALL, YORKSHIRE, 2000

Gowdall is a village which was extensively flooded from the River Aire in autumn 2000 to a depth of about 1 m. The estimated return period of the flood was 100 years and more than one hundred properties were flooded.

For simplicity, the whole of the flooded area was taken as a single hazard zone. Taking a depth of 1.0 m, an assumed velocity of 0.5 m/sec and a debris score of 0 (i.e., debris 'unlikely') gives a hazard rating (HR) of: $\{1 \times (0.5 + 1.5)\} + 0 = 2$. During the event in 2000 there was a flood warning (score 2), the speed of onset was very gradual (score 1) and the area is residential (score 2) to give an area vulnerability (AV) score of $2 + 1 + 2 = 5$. The percentage of those at risk, X, is simply $\mathrm{HR} \times \mathrm{AV} = 2 \times 5 = 10\%$. Taking the flooded population as 250, the population exposed to the risk is then $10\% \times 250 = 25$. A site visit suggested that the numbers of very old and infirm people are not significantly different from the national average. On this basis, the value for $Y = 25 + 25 = 50\%$.

The predicted number of injuries is therefore $25 \times 50\% = 13$. The associated fatality factor is 4% (twice the hazard rating of 2) giving 0.5 fatalities. These results appear reasonable and are consistent with the findings from parallel research on the health impacts of flooding (Risk and Policy Analysts, 2003). Here approximately one third (i.e., 36) of the flooded properties were subject to interviews. Although no fatalities were reported by those

interviewed, showing some overestimation of this hazard here, three direct injuries (i.e., physical injuries due to action of floodwaters) and eight indirect injuries (i.e., physical injuries due to over-exertion, etc.) were reported, giving an overall total of 11 to compare with the prediction of 13.

4.2. NORWICH 1912

Norwich suffered extreme flooding in 1912 with some 2,500 people flooded. The flood's estimated return period was 800 years and we have differentiated two hazard zones. The first, with 500 people, is close to the main river channel (within 50 m) and the second, with 2,000 people, is further away (Roberts and Son, 1912; Collins, 1920).

The derivation of the hazard rating is shown in Table X. There was no flood warning (score 3), the speed of onset was very gradual (score 1) and the area is residential (score 2) to give an area vulnerability (AV) score of $3 + 1 + 2 = 6$. The percentage of those at risk, X, is HR $\times$ AV and the population exposed to the risk is then $X \times N(Z)$ (Table XI). Because of the size of the population affected the percentages of very old and infirm people are not likely to be significantly different from the national average. On this basis, the value for Y is again 50%.

The predicted number of injuries is then 50% of the values presented in Table XI. The associated fatality factors are 7.5% and 3.4% (based on twice the hazard rating) for the two hazard zones (Table XII). Once again our methodology somewhat overestimates the fatality rate, in comparison with the reported four fatalities, but at least the result is the right order of magnitude.

Table X. Case study results: hazard rating for the Norwich flood (1912)

Distance from river	$N(Z)$	Typical depth, d (m)	Typical velocity, v (m/s)	Debris factor (DF)	Hazard rating = $d(v + 1.5) + \text{DF}$
<50 m	500	1.5	1	0	3.75
>50 m	2,000	1	0.2	0	1.7

Table XI. Case study results: generating X (% of people at risk) for Norwich, 1912

Distance from river	$N(Z)$	Hazard rating (HR)	Area vulnerability (AV)	X = HR $\times$ AV	N(ZE)
<50 m	500	3.75	6	23%	113
>50 m	2,000	1.7	6	10%	204

Table XII. Case study results: generating numbers of injuries and deaths for Norwich (1912 flood)

Distance from river	N(ZE), Table XI	Y = P1 + P2 (as %)	No. of injuries	Fatality rate = 2 × HR	No. of deaths
<50 m	113	50	56	7.5%	4
>50 m	204	50	102	3.4%	4
All			158		8

4.3. LYNMOUTH, 1952

Lynmouth suffered a devastating flood in August 1952 due to very rapid flow down the East and West Lyn rivers. The estimated return period was 750 years. Three hazard zones are taken here, based on the literature on the flood, related to the numbers of houses destroyed (38), severely damaged (55) and or just damaged (72).

The derivation of the hazard rating is shown in Table XIII. There was no flood warning (score 3), the speed of onset was rapid (score 3) and the area was predominantly residential (score 2) to give an area vulnerability (AV) score of $3 + 3 + 2 = 8$. The percentage of those at risk, X, is simply HR × AV and the population exposed to the risk is then $X \times N(Z)$ (Table XIV). Again, the percentages of very old and infirm people are not

Table XIII. Case study results: hazard rating for Lynmouth, 1952

Distance from river	$N(Z)$	Typical depth, d (m)	Typical velocity, v (m/s)	Debris factor (DF)	Hazard rating = $d(v + 1.5)$ + DF
Very close	100	3	4	2	18.5
Close	100	2	3	2	11
Nearby	200	1	2	1	4.5

Table XIV. Case study results: generating variable X (% of people at risk) for Lynmouth, 1952

Distance from river	$N(Z)$	Hazard rating (HR)	Area vulnerability (AV)	X = HR × AV	N(ZE)
Very close	100	18.5	8	100%[a]	100
Close	100	11	8	88%	88
Nearby	200	4.5	8	36%	72

[a]Since HR × AV = 148 which is greater than 100, X has been taken as 100%.

considered to be significantly different from the national average, so the value for Y is 50%.

The predicted number of injuries is therefore 50% of the values presented in Table XIV. The associated fatality factors are 37, 22 and 9% (again, based on twice the hazard rating) for the three hazard zones (Table XV). We have no precise numbers of people within each hazard zone in 1952, or good estimates of flood depths and velocities, but our assumptions do not appear unreasonable. The resultant prediction of 130 injuries, of which 31 would be fatal, is consistent with the actual death toll in 1952 of 34, this time showing some underestimation by our methodology of the actual loss of life.

4.4. EVALUATING THE TOLERABILITY OF OVERALL RISKS

In the recent UK government risk-based advice to land use planning authorities about development in flood plains – Planning Policy Guidance 25 (Department of Transport, Local Government and the Regions (DTLR), 2001) – flood likelihoods have been assigned degrees of tolerability, as follows:

1. "Little or no risk" – a probability of flooding <0.1% per year (i.e., less than 1 in 1000 per year floodplain);
2. "Low to medium risk" – a probability of flooding 0.1 – 1% per year (i.e., between 1 in 1000 and 1 in 100 per year) for fluvial flooding and 0.1 – 0.5% per year (i.e., between 1 in 1000 and 1 in 200 per year) for coastal flooding;
3. "High risk" – a probability of flooding >1% per year (i.e., greater than 1 in 100 per year floodplain) for fluvial flooding and >0.5% per year (i.e., greater than 1 in 200 per year) for coastal flooding.

A review of major floods since 1900 (JBA, 2000) shows that the risk of drowning is of the order of 1 in 1000 per major UK flood event. The implied borderline of intolerable risk for drowning as a result of fluvial flooding set in the PPG25 Guidance system is of the order of 1% per year ('medium' flood likelihood) × 0.001 (the probability of drowning), i.e., 1 in 100,000 per year.

Table XV. Case study results: generating numbers of injuries and deaths for Lynmouth, 1952

Distance from river	N(ZE) Table XIV	Y = P1 + P2 (as %)	No. of injuries	Fatality rate = 2 × HR	No. of deaths
Very close	100	50	50	37%	19
Close	88	50	44	22%	10
Nearby	72	50	36	9%	3
All			130		31

Table XVI. Presenting flood risks for the three case studies

Event	Likelihood (f) of a flood	Pop. within area (P)	No. of injuries	No. of deaths predicted	Deaths per year ($fN = D$)	Av. ind. risk (per year) (D/P)
Norwich, 1912	1 in 800 per year	2500	158	8	1.0×10^{-2}	1:250,000
Lynmouth, 1952	1 in 750 per year	400	130	31	4.1×10^{-2}	1:10,000
Gowdall, 2000	1 in 100 per year	250	13	0.5	5.0×10^{-2}	1:50,000

Although somewhat oversimplified, the average individual risks from the three case studies are presented in Table XVI. These show that the individual risks at Lynmouth in 1952 and Gowdall in 2000 were above the suggested target level of 1 in 100,000. The risk associated with the 1912 flood in Norwich was below the target level.

5. The Operational Framework and Sources of Data

The general approach to estimating flood risks to people derived from this methodology is outlined below (Figure 2). To avoid the need to collect new data on a large scale, existing or planned national data sets should be used, within a GIS system. In the foreseeable future, application of the methodology in many countries may require data to be collected locally for developing and calibrating the methods before they can be applied more widely.

Data sources will also vary in different countries, and different assumptions will be needed about the appropriateness of surrogate variables to match the needs of the different calculations.

5.1. STEP 1: DEFINE THE HAZARD ZONE

Options include, first, each hazard zone corresponding to a particular flood return period. This has the advantage that it could be derived from standard flood risk maps which have several return periods. Some of these exist already for the UK and others are planned. However this approach would not necessarily reflect accurately the actual hazard. For example, in a wide flat floodplain, the flood risk areas for all return periods will be very similar but the depth and velocity could vary considerably.

A second method could base the boundaries of hazard zones on distances from the river/coast. Standard values could be used for locations with similar characteristics (e.g., river size, valley slope, floodplain width, etc.).

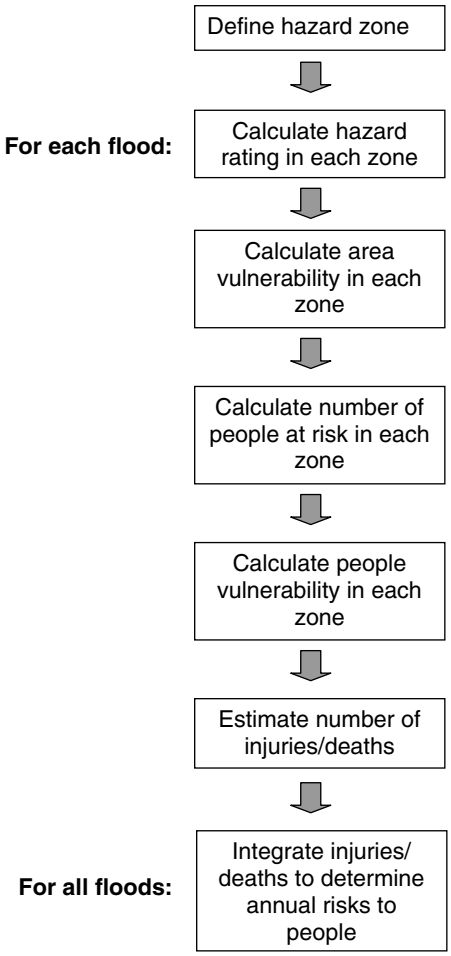

Figure 2. The approach advocated for estimating flood risks of serious of injury and loss of life to people in floods.

Alternatively, thirdly, each hazard zone could correspond to a range of values of flood hazard rating. This is technically a better approach, but requires the calculation of the flood hazard before defining each zone.

As the methodology now stands, we propose that the third approach above is adopted. The zones will be classified according to the degree of risk. For example, the zones may be classified as 'very high', 'high', 'medium' and 'low' risk. 'Very high' risk might correspond to a hazard rating value of greater than 10, and 'high' risk might correspond to a value in the range 7–10. The hazard zones can be based on the estimated 100-year flood (fluvial) and 200-year flood (coastal), and flood maps for these return periods are available for the whole of the UK.

Table XVII. UK flood mapping methods: the availability of flood velocity data

Flood mapping type and method	Availability of velocity data for floodplains
Fluvial Section 105 Survey: IH 130 method	Not available
Fluvial/Coastal Section 105 Survey: Historic flood outlines	Not available
Fluvial/Coastal Section 105 Survey: Flood basin model or projection of maximum levels	Not available
Fluvial/Coastal Section 105 Survey: 1-D hydrodynamic modelling	Velocity profile could be generated along a cross-section
Fluvial/Coastal Section 105 Survey: 2-D hydrodynamic modelling	Velocity vectors can be generated
National Fluvial Extreme Flood Outline using JFLOW	Velocity can be generated but accuracy is unknown
National Coastal Extreme Flood Outline (method not known)	Velocity can be generated from 2-D models that are used for about 70% of the coast but accuracy is unknown. The remainder is based on a projection of maximum levels approach (see above)
National fluvial flood mapping using Normal Depth method	Velocity profile can be generated along a cross-section but less accurate than a 1-D model

The main data deficiency is likely to be flow velocity. Only some of the mapping methods currently used in most countries, including the UK's mapping programme (Table XVII), provide relevant data. Where velocity data are unavailable, a velocity-equivalent could be estimated. This requires further investigation but possible methods include an equation of the form velocity $= f$ (depth, slope, roughness) in fluvial floodplains, or empirical equations for velocity where coastal defences fail or are overtopped, based on observations and detailed modelling results. That equation might be of the form velocity $= f$ (defence height, hydraulic head, distance from defence).

Debris potential is also likely to be difficult to determine. It can be a function of the land use in the upstream catchment/floodplain, but methods are not yet available to enable realistic predictions from this of debris concentrations, suggesting that more research is also needed here.

Hazard zones should take account of the proximity of flood defences. In general, areas close to defences should have a 'high' or 'very high' hazard rating. This could be linked to the condition of defences which, for the UK,

has been researched under a project on 'Risk Assessment for Strategic Planning' (RASP) (DEFRA/Environment Agency, 2003b).

5.2. STEP 2: CALCULATE THE HAZARD RATING IN EACH HAZARD ZONE

The hazard rating is calculated from information on flood depth, velocity and debris load, and for floods of several return periods in order to estimate the annual flood risk. Ideally the delineated hazard zones should then not change, but the hazard rating in each zone will change for different floods.

Applying the hazard rating in each hazard zone is not straightforward. Options include, first, using a single average value for each hazard zone. This will not identify variations within the zone, particularly in cases where a location with a high 'area vulnerability' or 'people vulnerability' score has a hazard rating value that differs significantly from the zone's average value. Alternatively, one could sub-divide the hazard zones and calculate a value of hazard rating for each sub-zone. This may be advisable where the area vulnerability score and/or the population vulnerability score vary significantly within the zone.

Over time and with more research the formula for calculating the hazard rating should be reviewed to ensure that it provides consistent values of flood hazard. In the absence of useful flood depth, velocity and debris load data, a first approximation could be made using the simple expression:

$$HR = (D_{\max}/D) - 1$$

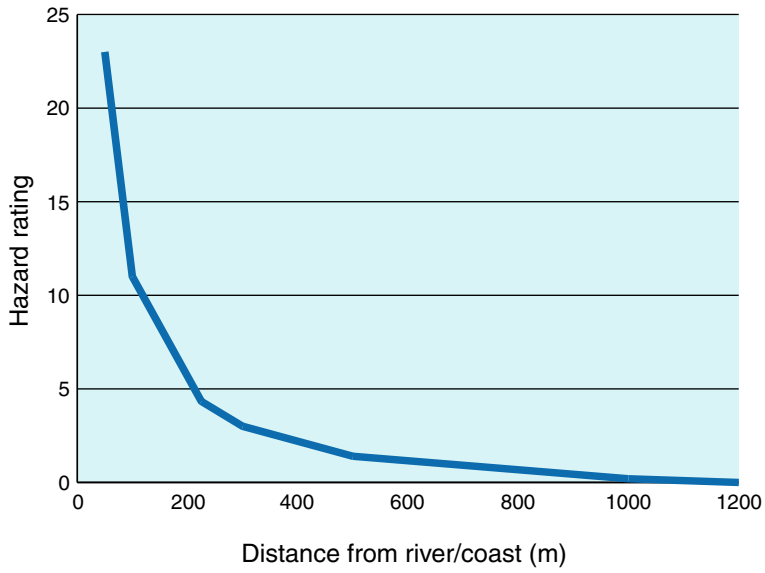

Figure 3. A default approach to assessing the hazard rating (for explanation see text).

where HR is the hazard rating at distance D, D_{max} is the extent of flooding from source (m), and D is the distance from flood source (m).

At $D = D_{max}$, HR = 0 since the flood depth will be zero. Figure 3 gives an illustrative plot of HR against D for $D_{max} = 1200$ m.

5.3. STEP 3: ESTIMATE THE 'AREA VULNERABILITY' IN EACH ZONE

'Area vulnerability' depends on several factors including the speed of onset of flooding, the availability of flood warnings, warning time, flood awareness and emergency planning, and the nature of the area including property types, size of floodplains, etc. Data on all these factors is needed, and combining them to produce an area vulnerability score for each flood hazard zone.

Data on the speed of onset of flooding is often patchy. Most catchment or meteorological agencies aim to provide flood warnings, so flood warning data is likely to be available in three categories of location: areas with a flood warning system; areas without a warning system because the available warning time is too short; and areas without a warning system for other reasons. Identifying locations where the warning time is less than 2 hours will be important, as these are where dangerous flash floods may occur.

Speed of onset is also affected by the presence of flood defences, as failure or overtopping of defences can cause very rapid flooding. Ideally a GIS layer showing relevant defences (i.e., raised embankments, walls and dams) should be developed but the greater difficulty here is predicting failure probability. This is generally low but the potential consequences are high. In the UK, RASP data could be used (DEFRA/Environment Agency, 2003b), since that research includes assessing the probability of defence failure.

Data on floodplain nature and extent should be readily available (e.g., on the UK Environment Agency flood maps). Property types in the floodplain may come from large and relatively detailed tax-related or other databases, or from databases capturing all properties to which mail is sent. In the UK for example the AddressPoint and Focus databases embrace the latter approach and they usefully include seasonal features such as campsites (DEFRA/Environment Agency, 2002b). Such databases may have limitations, however, such as not separating single storey dwellings. Either other databases should be sought, or local knowledge on property type will be needed, especially for high-risk areas.

5.4. STEP 4: CALCULATE THE NUMBER OF PEOPLE AT RISK IN EACH ZONE

Population data is generally available from national censuses. For the UK, data relates to Enumeration Districts (c. 200 properties), and calculations could be based on the existing methodology in the Modelling and Decision Support Framework (the MDSF) developed for catchment flood

management planning (DEFRA/Environment Agency, 2002b). This approach uses census data for each Enumeration District, and 'spreads' the population across the District in proportion to the number of residential properties there. An alternative approach would assume a constant population density throughout each District but this could lead to large errors because floodplains are often less developed than adjacent areas within the same census unit.

5.5. STEP 5: CALCULATE THE 'PEOPLE VULNERABILITY' IN EACH ZONE

The 'people vulnerability' measure requires information on the age and health of the population at risk, including the number of people with disabilities or sickness. Again, national population censuses should be useful.

For the UK some of this data is available from the national census and, in the MDSF system, a Social Flood Vulnerability Index (SFVI) has been calculated and mapped (DEFRA/Environment Agency, 2002, Tapsell *et al*., 2002a). This Index is concerned with the overall 'intangible' impacts of flooding, not just the risk of death/injury, and is based on three social variables (the elderly aged 75+; single parents; and the long-term sick) and four financial deprivation indicators (unemployment; overcrowding in households; non car-ownership; and non home-ownership). The rationale for the variables used is given in Tapsell *et al*. (2002) and was constrained by the need to use data that is available both for the whole of England and Wales and for small geographical areas to match the size of UK floodplains.

5.6. STEP 6: ESTIMATE THE NUMBER OF INJURIES/DEATHS

We outlined above the method for estimating the numbers of injuries/deaths. Some further work may be required to refine the method although the lack of reliable data currently on injuries in flood events – as opposed to fatalities – will make calibration difficult. Our three case examples appear to provide some reasonable results but these may not be typical of other situations. The overall error of prediction of fatalities across all three cases is less than 4%, but this error is smaller than one might expect. In reality we are not unduly dissatisfied with the Norwich result, given the low numbers involved, where the error is 50%.

5.7. STEP 7: DETERMINE ANNUAL RISKS

The method of determining annual risks needs data for a number of floods of different return periods. The results are then plotted against frequency of occurrence, and integrated to estimate the average annual risks (as with annual average damages (Penning-Rowsell *et al*., 2003)). In many countries including the UK, with sparse data nationally for a range of floods at any one

site, it may be possible to develop only an estimate of annual average risk based on a small number of flood events.

6. Assessment

The causes of death and serious injury due to flooding are many and varied, yet we have attempted to develop a simple model so as to try to predict their occurrence. From a review of the research literature we have proposed an approach to risk assessment that embraces the three groups of variables which appear to be most important in this respect, to take account of the likelihood of a flood, whether people will be exposed to it, and whether those exposed to that flood will be killed or seriously injured. The methodology presents flood risk in both societal terms (i.e. the estimated number of deaths per year caused by flooding in a unit of land, for example a flood cell) and in individual terms (i.e., the annual probability that an individual in a unit of land will die as a result of flooding).

Our method for estimating the number of deaths/injuries is based on determining a 'hazard rating' for different zones of the floodplain, a score for the 'area vulnerability' (in terms of flooding lead time, etc.), the population at risk and the population's vulnerability. The approach has been tested against three case study floods (Norwich 1912, Lynmouth 1952 and Gowdall 2000) and a satisfactory level of prediction appears to have been obtained.

However we recognise that the errors in predicting both serious injury and fatalities may in reality not match those found in our case examples, and more research is needed to put sensible confidence limits around the point estimates that the model generates. Better data is needed to refine the flood hazard rating formula, in different flood situations and in different countries. We need better ways of assessing the impacts of flood warning on risks to people, and on peoples' behaviour during floods.

To make the method readily applicable, such that policy makers could use it with some confidence, will require refinement of the overall methodology, the development of a GIS-based method, pilot testing of the method, more information on errors of prediction, and a system to guide careful interpretation of the results. Nevertheless we believe that we have made useful progress in developing a community scale model of loss of life and serious injury in floods, and that further research can build on this in the future.

References

Abt, S. R., Whittler, R. J., Taylor, A. and Love, D. J.: 1989, Human stability in a high flood hazard zone. *Water Res. Bull.* **25,** 881–890.

British Standard Institution: 1996, *BS 8800:1996 Occupational Health and Safety Management Systems*. British Standard Institution, London.

Collins, A. E.: 1920, *Report, Etc., of the City Engineer to the General Purpose Committee with respect to River Widening*. Norwich City Engineer's Office, Norwich.

Department of the Environment, Food and Rural Affairs and Environment Agency: 2002, *Risk, Performance and Uncertainty in Flood and Coastal Defence – A Review*, R&D Technical Report FD2302/TR1. HR Wallingford, Wallingford, Oxford.

Department of the Environment, Food and Rural Affairs and Environment Agency: 2002b, *Catchment Flood Management Plans, Development of a Modelling and Decision Support Framework (MDSF): MDSF Procedures and Technical Annexes*, Reports EX4495 and EX4497. HR Wallingford, Wallingford, Oxford.

DEFRA (Department of the Environment, Food and Rural Affairs): 2003a, *FCDPAG 4 – Approaches to Risk*. Department of the Environment, Food and Rural Affairs, London.

DEFRA (Department of the Environment, Food and Rural Affairs) and Environment Agency: 2003b, *Risk Assessment of Flood and Coastal Defence for Strategic Planning (RASP): Concept Note and Discussion Document*. HR Wallingford, Wallingford, Oxford.

DETR (Department of the Environment, Transport and the Regions): 2000, *Guidelines for Environmental Risk Assessment and Management, Revised Departmental Guidance,* Report by DETR, the Environment Agency and IEH. The Stationery Office, London.

DTLR (Department of Transport, Local Government and the Regions): 2001, *Planning Policy Guidance Note 25: Development and Flood Risk*. DTLR, London.

European Commission: 2000, *First Report on the Harmonisation of Risk Assessment Procedures*, DG Health & Consumer Protection. European Commission, Brussels.

Jonkman, S. N., Van Gelder, P. H. A. J. M., and Vrijling, J. K.: 2002, Loss of life models for sea and river floods, In: B. Wu, Z.-Y. Wang, G. Wang, G. G. H. Huang, and J. Huang (eds.), *Flood Defence 2002*, Science Press, New York, pp. 196–206.

Penning-Rowsell, E. C., Johnson, C., Tunstall, S., Tapsell, S., Morris, J., Chatterton, J. B., Coker, A., and Green C. H.: 2003, *The Benefits of Flood Alleviation and Coast Defence: Data and Techniques for 2003*. Middlesex University Flood Hazard Research Centre London.

Penning-Rowsell, E. C. and Wilson, T. L.: 2003, *The health effects of flooding: A European overview. Report for the cCASHh project*. Middlesex University Flood Hazard Research Centre, London.

Ramsbottom, D., Penning-Rowsell, E. C. and Floyd, P.: 2003, *Flood risks to people: Phase 1*. R&D Technical Report FD 2317. Department of the Environment, Food and Rural Affairs and Environment Agency, London.

Risk and Policy Analysts: 2003, *The Appraisal of Human-Related Intangible Impacts of Flooding*, DEFRA/Environment Agency R&D Report FD2005. Department of the Environment, Food and Rural Affairs and Environment Agency, London.

Roberts and Son: 1912, *Illustrated Record of the Great Flood, August 1912*. Roberts & Son, Norwich.

Royal Society: 1992, *Risk: Analysis, Perception and Management*. Royal Society, London.

Tapsell, S. M., Penning-Rowsell, E. C., Tunstall, S. M., and Wilson, T. L.: 2002, Vulnerability to flooding: Health and social dimensions. *Phil. Trans. R. Soc. Lond.*, **A360**, 1511–1525.

Natural Hazards (2005) 36: 65–80

Economic Hotspots: Visualizing Vulnerability to Flooding

ANNE VAN DER VEEN* and CHRISTIAAN LOGTMEIJER
Department of Business, Technology and Public Policy, University of Twente, P.O. Box 217, 7500 AE Enschede, The Netherlands

(Received: 30 October 2003; accepted: 30 June 2004)

Abstract. We simulate a large-scale flooding in the province of South-Holland in the economic centre of the Netherlands. In traditional research, damage due to flooding is computed with a unit loss method coupling land use information to depth-damage functions. Normally only direct costs are incorporated as an estimate of damage to infrastructure, property and business disruption. We extend this damage concept with the indirect economic effects on the rest of the regional and national economy on basis of a bi-regional input output table.We broaden this damage estimation to the concept of vulnerability. Vulnerability is defined as a function of dependence, redundancy and susceptibility. Susceptibility is the probability and extent of flooding. Dependency is the degree to which an activity relates to other economic activities in the rest of the country. Input–output multipliers form representations of this dependency. Redundancy is the ability of an economic activity to respond to a disaster by deferring, using substitutes or relocating. We measure redundancy as the degree of centrality of an economic activity in a network. The more central an activity is, the less it encounters possibilities to transfer production and the more vulnerable it is for flooding. Vulnerability of economic activities is then visualized in a GIS. Kernel density estimation is applied to generalize point information on inundated firms to sectoral information in space. We apply spatial interpolation techniques for the whole of the province of South-Holland. Combining information of sectoral data on dependency and redundancy, we are able to create maps of economic hotspots. Our simulation of a flood in the centre of Holland reveals the vulnerability of a densely populated delta.

Key words: risk, economic damage, vulnerability, GIS

1. Introduction

People and the environment are suffering increasingly from the effects of natural disasters due to high population growth and density, migration and unplanned urbanization, environmental degradation and possibly global climate change (UNEP, 2002). The number of people affected by disasters rose from an average of 147 million a year in the 1980s to 211 million a

* Author for correspondence. E-mail: a.vanderveen@ctw.utwente.nl

year in the 1990s. The consequences of climate change for low-lying countries like the Netherlands are potentially formidable (IPCC, 1998). From the seaside, the Netherlands faces an increase in the probability of being flooded, but also from the riverside, the delta has to deal with an increase in the discharge of water. On top of that, the Netherlands encounters subsidence. Physical processes due to ground water extraction and gas extraction challenge Dutch water policy from a new and different perspective.

Sea level rise in combination with subsidence will lead to a relative sea level rise, which is a danger to Dutch society. Policy measures concentrate on the coast and along the rivers Rhine and Meuse. For many years, the standard answer by Dutch Rijkswaterstaat was to raise the dikes along the rivers and the strengthening of weak positions in the dunes along the North Sea. However, this policy of raising dikes is now part of a nation wide discussion. The search is for alternative measures, which have the same effect. Accordingly, Rijkswaterstaat (2000) developed policy measures, which are aimed at giving water more space in the floodplain of the Dutch rivers. The reasoning behind this proposal is that allowing the river to expand in times of high water will decrease the pressure on the existing dikes and thus will decrease the risk to Dutch society.

Behind the concept of risk is the issue ''What is it we are protecting?'' A first and quick answer to this question is the value to society of the damage after an inundation. Probability times effect then is an indicator of risk to society.

In the following, we will shortly concentrate on the concept of risk. We will argue that the current measures of risk to society mainly focus on direct economic effects and do not cover indirect economic damage. Secondly, by concentrating on risk we refrain from the resilience of society after a disaster and the ability of society to adapt. Otherwise stated, the question is ''How vulnerable are we for disasters, can we cope with it and how do we measure such vulnerability?'' Finally, can we visualize vulnerability? The latter question leads us to the detection of economic hotspots. We will discuss the concepts of risk and vulnerability and illustrate the empirical content of vulnerability on basis of a simulation of a large-scale flood in the province of South-Holland in the Netherlands.

2. Risk and Vulnerability

Risk and vulnerability are words that have gone through a certain process changing its meaning and connotation. Out of a huge literature (see e.g. Blaikie *et al.*, 1994), Green (2003) defines risk as the probability of a negative perturbation to a system multiplied by the effect on that system.

He refers to the more engineering mode of dealing with the question how vulnerable society is for disasters. At the other extreme we find the literature on risk and uncertainty as proposed by Funtowicz and Ravetz (1993).

Common practice in the flooding (engineering) literature is to visualize risk and thus the underlying effect by counting unit losses (Parker *et al.*, 1987). With different flood-depths, depth-damage data is used to asses flood losses.

$$S = \sum_{i=1}^{n} \alpha_i m_i S_i$$

with

S = total damage;
α = damage factor;
m = number of entities in damage class i;
S_i = damage value for class i;
n = Number of damage classes i.

The current state of this type of models (Vrisou van Eck and Kok, 2001) is that data on land cover is collected and downloaded into a GIS environment. Damage assessment then counts the number of units of a certain type in the affected area and multiplies this with a damage factor. The latter is a relationship empirically derived from surveys, in which a relationship is established between depth and damage. The damage factor is the heart of the method and thus plays an important role in estimating damage. In standard research on flood management, the value of damage is based on a replacement value. However, as discussed in (Van der Veen *et al.*, 2003b) this might not reflect the economic value of the goods at risk (Cochrane, 1997; Cole, 1998; Rose and Benavides, 1998; MAFF, 2000; Freeman *et al.*, 2002; Rose and Lim, 2002). This annoying matter is caused by a few misunderstandings:

1. There is no agreement on the economic points of departure. Financial appraisals are mixed up with cost-benefit analyses (CBA). In the latter, the usual concept is economic cost, which relates to opportunity costs in welfare economics, whereas a financial appraisal is often base for investigating the sum of money to be recovered from insurance companies.
2. There is confusion on temporal and spatial scales: Financial appraisal limits itself to a single organization, whereas CBA requires wider borders, like a region, a nation, or the European Union.
3. There is confusion on the definition of direct costs: As stated by Cochrane (2003), "It is commonly asserted that total damage is the sum of direct damage (damage to building and contents) and lost *value added.*

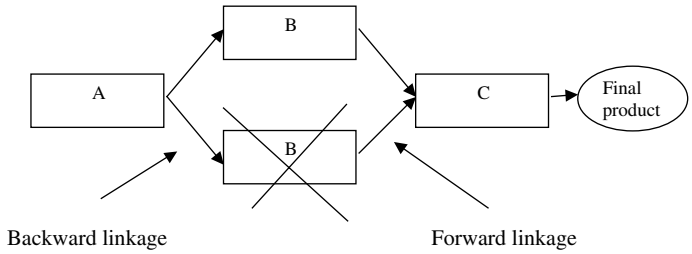

Figure 1. Forward and backward linkages in an economy, when factory B is damaged.

Double counting exists here because value added includes the services of capital, whereas direct damage should reflect the cost of replacing the undepreciated portion of such capital''.

4. Stock concepts are confused with flow concepts.
5. The borderline between direct and indirect costs is not well defined.

The distinction between direct and indirect costs is highlighted in Figure 1. (Cochrane, 1997). If factory B is flooded suppliers of goods and services are hit, as well as firms that purchase goods B. In the end, final demand of consumption, investment, export and government spending is touched. Part of a risk concept thus implies taking into account forward and backward linkages in a regional or national economy.

Note however that this extension does not allow for redundancy in an economy: if there is a second firm B that is able to take over the production, an economy is less vulnerable. See van der Veen *et al.* (2003a) for an extensive discussion on the problem of computing an aggregate indicator of the total economic costs of a large-scale disaster, incorporating the dynamics of an economy. In the next section we will define the concepts of vulnerability and redundancy more precisely.

2.1. VULNERABILITY

In this paper, we want to discuss the concept of vulnerability and pay attention to a method to visualize vulnerability in a disaggregated way in a GIS. By extending the concept of risk to a vulnerability concept we have to include the coping capacity of a region/nation to deal with floods. What is this coping capacity of society after a disaster?

As a point of departure we take the concept of vulnerability as introduced in a seminal paper by Parker *et al.* (1987). Vulnerability V is presented with the following formula:

$$V = f(S, D, T),$$

where S is Susceptibility, defined by the probability and extent to which the physical presence of water will affect inputs or outputs of an activity. D is Dependence, reflecting the degree to which an activity requires other activities to function normally. T is Transferability, the ability of an activity to respond to a disruptive threat by deferring or using substitutes or relocating.

Susceptibility refers to the geo-location of a site that is under investigation. Some sites are more prone to flooding and may encounter more often flooding. Susceptibility therefore relates to the geo-concept of damage. Dependency and transferability relate to the characteristics of the economic system. Dependency and transferability (nowadays we would say redundancy) are concepts best understood by representing the economic system as a network of interrelated activities. Within such a network, there are certain functions and sectors that are important for the functioning of the network as a whole. The first concept refers to how dependent we are upon output produced at a site and the latter refers to the local redundancy in the network. Both concepts are highly interrelated.

Note that by introducing concepts like dependency and redundancy we relate to the concept of economic costs in Cost-Benefit Analysis as discussed in EPA (2000). The concept of economic costs is a dynamic accounting for adaptations in an economic structure.

Note also that the concepts of vulnerability and redundancy in recent literature move to the term resiliency (Perrings, 2001). However, we feel more confident with the term vulnerability; as Green (2003) states: ''vulnerability can be defined as: ''*the time varying status of some desirable or undesirable characteristic(s) of the system in question*''. So, in turn, the resilience of a system is: ''*the dynamic response of vulnerability over time to the perturbations to which the system is subjected''*. A *resilient* system is then one which bends under stress but does not break, and which returns to a desirable state after the perturbation has passed''. End of quotation. Consequently, it is vulnerability, which has an empirical content.

In the following section, we will illustrate the concept of vulnerability based on a case in the Netherlands.

3. Simulating a Large-scale Flood: The Case of the Netherlands

The case we present is a large-scale flood due to a dike failure near Krimpen aan de IJssel, a small village in the Netherlands near Rotterdam. In 1953, the dramatic year of big floods in north western Europe, a dike in this village broke. However, by sailing in a small ship in the breach, a disaster was

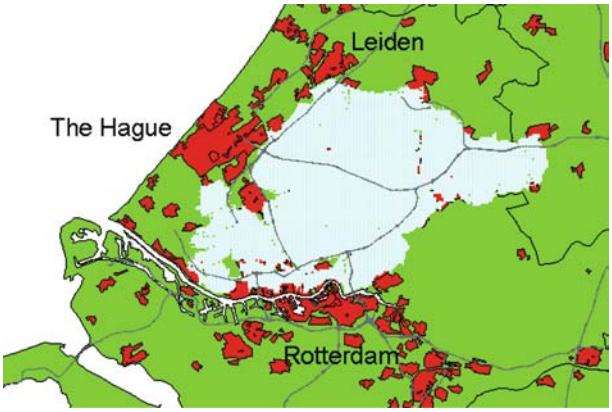

Figure 2. Simulating a large-scale flood in the Randstad of the Netherlands.

prevented. We now simulate this flood and try assessing the economic consequences. Delft Hydraulics supplied hydrological data and Rijkswaterstaat made GIS data available on firms, economic sectors and employment per grid (Vrisou van Eck and Kok, 2001). The blue area in Figure 2 represents the effect of the inundation after 10 days. In the middle of the area, water depth is −6 m. Moreover, we have at our disposal a bi-regional Input–Output Table (Eding *et al.*, 1995) representing the economic structure of the Province of South-Holland and the rest of the Netherlands. We distinguish 28 sectors in our economic model.

3.1. SUSCEPTIBILITY

Susceptibility is the physical characteristic of the location that makes an activity vulnerable. For our case study, we apply a simulation model, so we skip this element.

3.2. DEPENDENCY

Starting from the definition of dependency ''reflecting the degree to which an activity requires other economic activities as an input to function normally'', we refer to the idea of an economy as a network of linkages of interrelated industries. In doing so we can apply standard concepts in economics to estimate how much we depend on certain sectors for our regional and national welfare. From input–output analysis, (Leontief, 1952, 1986) we apply

the concept of multipliers[1] (Miller and Blair, 1985; Rose and Lim, 2002) to account for forward and backward linkages in the whole economy when a disaster hits a certain sector (Figure 1).

3.3. REDUNDANCY

Redundancy was defined by the ability of an activity (or system) to respond to a disruption by overcoming dependence by deferring, using substitutes or even relocating. Unused capacity, inventories and possibilities to import determine the coping capacity of the economy after a disaster (FEMA, 1999). See Figure 3.

For the USA the choice between alternatives in order to cope with the consequences of a disaster is elaborated in FEMA (1999). See Figure 4.

However, for the Netherlands data requirements for such a scheme are very demanding. In our case study, we have not the empirical detail at our disposal to copy the US FEMA approach. For the Dutch situation, we have to change over to a shortcut that reflects the detailed redundancy concept. We search for an alternative approach by looking at redundancy from a *network* perspective. Here the A matrix in economic input–output analysis can be viewed as a picture of the network of an economy. Our hypothesis is the following:

> *The more central the role of a sector is in a certain regional economy, the more difficult it will be to transfer production or to substitute production by a sector in the rest of the Netherlands.*

[1]Input–output analysis can be described as an economic method that focuses on the trade pattern between the constituent parts of the economy. These parts can be defined in very general terms, such as producers, consumers, the labour force, governmental agencies and foreign countries. Classifications may vary depending on the level of aggregation. For example, on the production side one may distinguish various types of industries or sectors such as agriculture, industry, several types of services, etc. The economic structure itself is modelled in terms of an input–output or inter-industry table, which represents the sales from one sector to another. The sales can be between industries, but also between firms and households or between workers and firms. The pattern of trade is interpreted in terms of regularities in the table, which can be analysed using various mathematical techniques. In conventional notation, X is referred to as an output vector and F – vector of final demand. The relationship between the two is established by

$$X = (I - A)^{-1}F$$

where A is the symmetric matrix of (constant) input coefficients, and $(I–A)^{-1}$ is the economy multiplier matrix (see Miller and Blair, 1985). Knowledge of the table enables us to calculate the effects of shifts in demand via multiplier analysis.

The tables are compiled at specialized institutes. In the Netherlands Statistics Netherlands (CBS) publishes these tables. In addition, other places such as universities sometimes compile specialized versions.

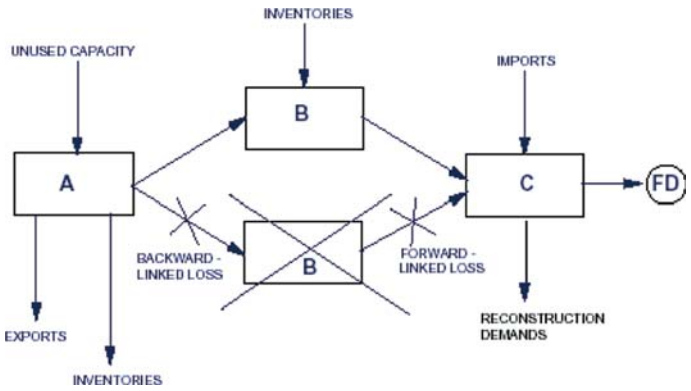

Figure 3. Transferability: choice between alternatives (FEMA, 1999).

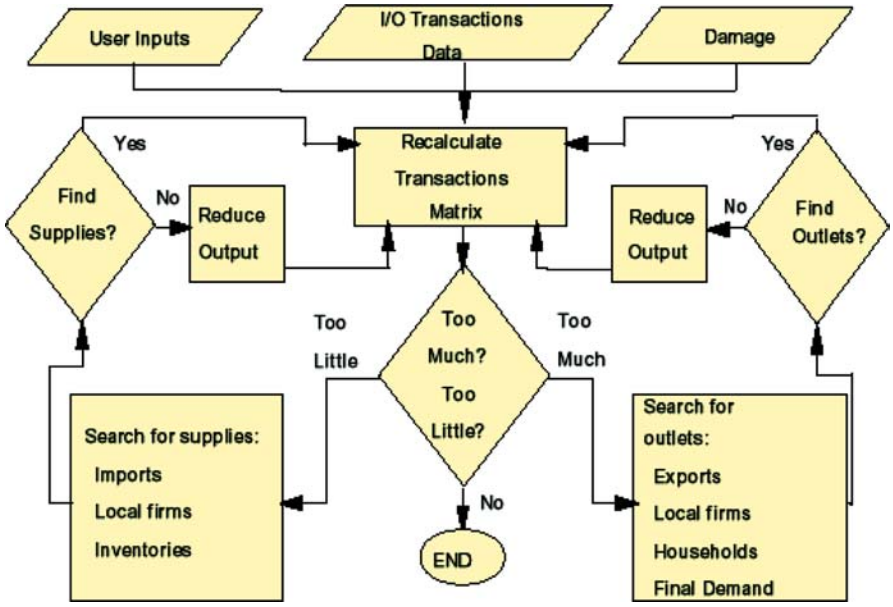

Figure 4. Determining redundancy in an economy (FEMA, 1999).

Comparing a measure of *centrality* of economic sectors in the province of South-Holland with a centrality measure for the same sectors in the Rest of the Netherlands will indicate redundancy in the flooded provincial economy. Indeed, this concept of centrality is an aggregate of the concept used by FEMA.

Centrality is a well-known concept in regional economics, measuring structural properties that can explain the performance of a network (Frank, 2002). It shows what sectors or entities play an important role and what sectors are strategic. Conventional measures of centrality relate to the identification of key sectors in an economy (Hazari, 1970). In more recent research Kilkenny and Nalbarte (1998) apply social network analysis (Leinhardt, 1977) to recognize central key sectors in a community.

Tallberg (2000) describes three measurements of centrality:

- The proportion of indirect contacts via a certain actor. This measurement is an important explanatory variable in studies of actor attributes.
- The number of direct contacts with other actors, being an indicator of the popularity of an activity.
- The distances and paths in a network, focusing on structural properties of a network.

We prefer to apply the second indicator measuring the popularity of activities of sectors in an economy. The Input–output A matrix (see footnote 1) can be viewed as a description of all relationships in an economy. By measuring the number and content of all contacts between economic sectors, we obtain a centrality indicator for individual sectors.

For our purpose, we like to extend the use of network analysis and the measure for centrality by incorporating the redundancy in the network. Our interest is in the importance of an economic sector relative to its bi-regional counterpart in the rest of the country. If the bi-regional counterpart is more central, we assume that this sector can replace production after a disaster. As a measure, we compute the quotient of the degree centrality of an economic sector in the province of South-Holland and the same economic sector in the rest of the Netherlands.

4. Visualizing Vulnerability

So far, we presented vulnerability as an aggregate concept. Now the question is, is it possible to disaggregate vulnerability and to relate it to a GIS environment? What are economic hotspots? The question thus is how to disaggregate redundancy and dependency to grids?

4.1. HOT SPOTS

In the literature, hotspots are defined as:

''Typically named hot spots, these are concentrations of incidents within a limited geographical context that appear over time'' (Levine, 2002).

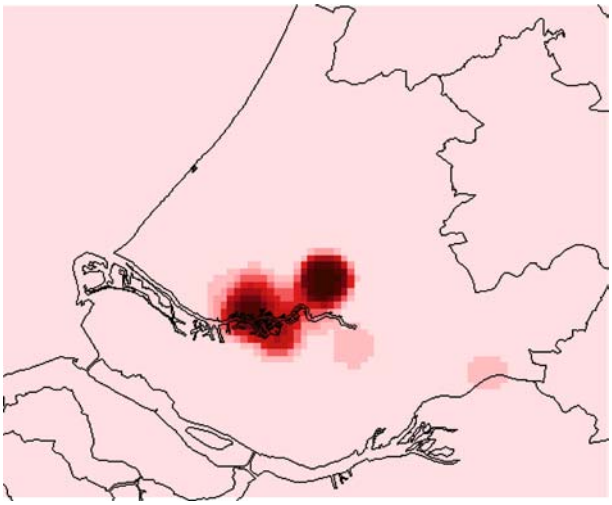

Figure 5. Clustering of value added of the petroleum industry in the province of South-Holland.

A hotspot thus measures the intensity of an incident in space. Examples can be found in applied research on crime and the formation of town centres (Thurstain and Goodwin, 2000; Thurstain *et al*., 2001; Levine, 2002). For our project, we want to detect the intensity of economic production in space measured by the economic concept of value added. Grids in space with high value added are labelled as hotspots.

4.1.1. *From Points to Grids*

As a first step in our empirical work, we have to generalize point information on firms to sectoral information in space. The data per grid are derived from employment data for individual firms per zip code, transformed into value added on basis of provincial data on value added and on employment. For details see van der Veen *et al*. (2003a). We distinguish 28 economic sectors ranging from agriculture and several types of industry to sectors of services.

We apply spatial interpolation techniques for the whole of the province of South-Holland. The result is a contour map of the phenomenon of value added. The available techniques offer several possibilities to cluster spatial information. Analogous to the work of (Thurstain and Goodwin, 2000) on town centres, we apply Kernel Density estimation (Levine, 2002) producing a circular area (kernel) of a certain bandwidth around an indicator.[2]

[2] One of the critical steps in using kernel-density estimation is to define the bandwidth in the formula. As an illustration we choose a bandwidth of 5000 m; for the rest of our empirical research we apply 2000 m. To test this ecological fallacy we have to perform an extensive sensitivity analysis in future research.

As an example we show in Figure 5 the clustering of the petroleum industry in the province of South-Holland. Here we measure the concentration of value added in the Petroleum Industry for all grids in the province.

4.1.2. *Combining Information*

In a second step we made similar figures as for the petroleum industry for the other 27 sectors in our provincial economy and applied an overlay procedure to combine and aggregate the data of the 28 sectors to a higher level. All sectors are added with no additional weights.

Results for the added value of the whole economy are presented in Figure 6. As can be seen, Rotterdam is a hotspot, but we also discover other important points in space.

4.1.3. *Adding Dependency and Redundancy Indicators*

Finally, density surfaces are combined with concepts of redundancy and dependency within ArcView GIS 3.3 software, by using a *weighted* overlay procedure. It is a technique for applying a common scale of values to diverse and dissimilar inputs in order to create an integrated analysis. This procedure enables us to add indicators of importance to layers.[3] The weights we use relate to multipliers in the Input-Output network and to the indicators of centrality.

We follow a step procedure to present economic hotspots. First, we insert information on multipliers as weights in the aggregating procedure in Figure 6. If a sector has indirect links to the rest of the Dutch economy the importance of the spot is increased. Figure 7 shows the result. New spots are added[4], to show that there are strong links within the Dutch economy increasing the vulnerability to floods.

Secondly, we insert information on redundancy in Figure 6. In Section 3.3 we discussed an indicator of centrality. We computed the quotient of the two indicators for the Province of South-Holland and for the Rest of the Netherlands. A high weight implies less redundancy in the rest in the economy.

Figure 8 presents the results: Indeed, comparing Figures 6 and 8 a slight decline in the number of hot spots is noticed; we observe that there is scope in the rest of the Dutch economy to take over some production.

In Figure 9 we combine Figure 6 with information on dependency and redundancy. The weight we use for each of the economic sectors is the

[3]As an alternative we suggest to use an arrhythmic overlay procedure. The main difference between these two procedures is in the way 'weights'' are dealt with in the procedure. In the case of a weighted overlay, all weights are related to each other and to the total value of the weights.

[4]Note that some spots disappear due to relative scaling.

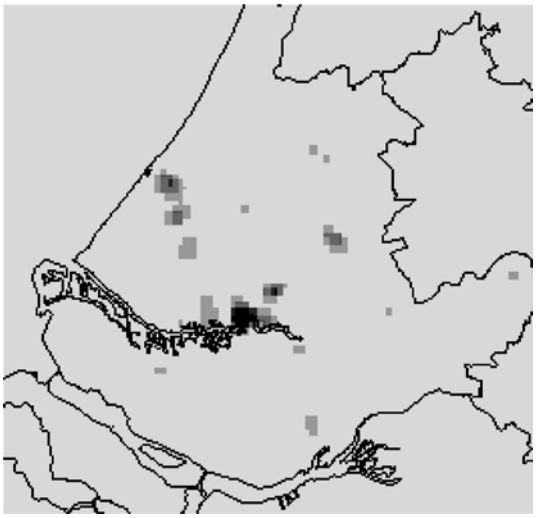

Figure 6. Economic hotspots in South-Holland; combining information on value added of 28 economic sectors.

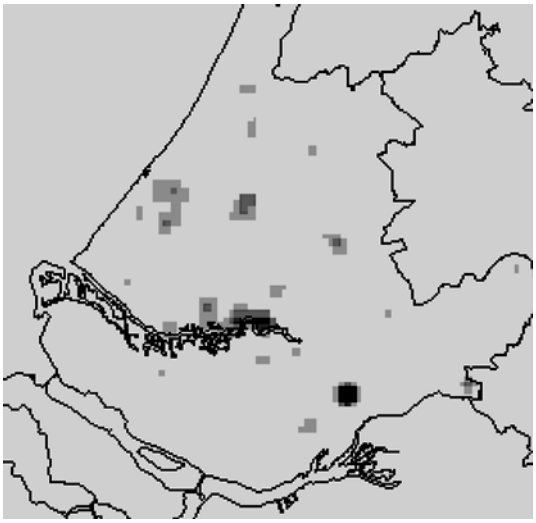

Figure 7. Economic hotspots in South-Holland; combining information on value added of 28 economic sectors with information on multipliers.

average of the multiplier and the centrality index. In the result we see the mutual influence of direct and indirect effects in an economy and the coping capacity of the Dutch economy to deal with a disaster like a flood.

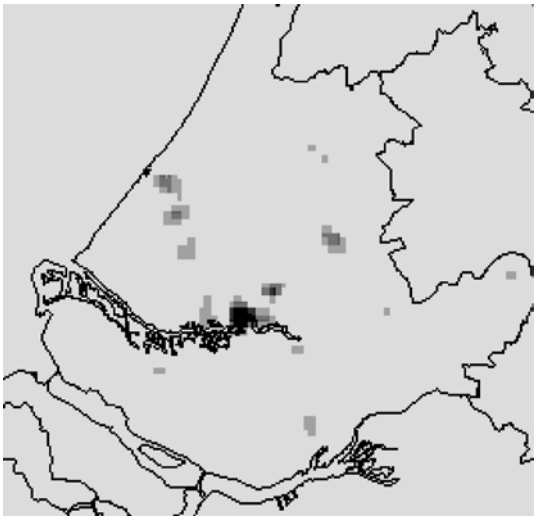

Figure 8. Economic hotspots in South-Holland; combining information on value added of 28 economic sectors with information on redundancy in the rest of the Dutch economy.

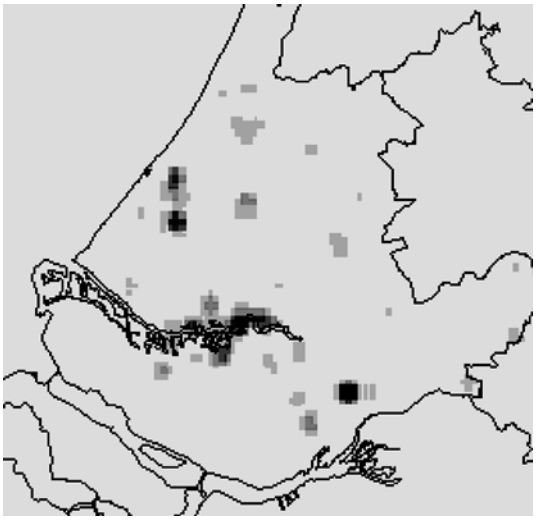

Figure 9. Economic hotspots in South-Holland; combining information on value added of 28 economic sectors with information on multipliers and information on redundancy in the rest of the Dutch economy.

Finally, in Figure 10 we reproduce Figure 9 in combination with the borderlines of the flood that was simulated. Moreover, we insert the main highways in the area.

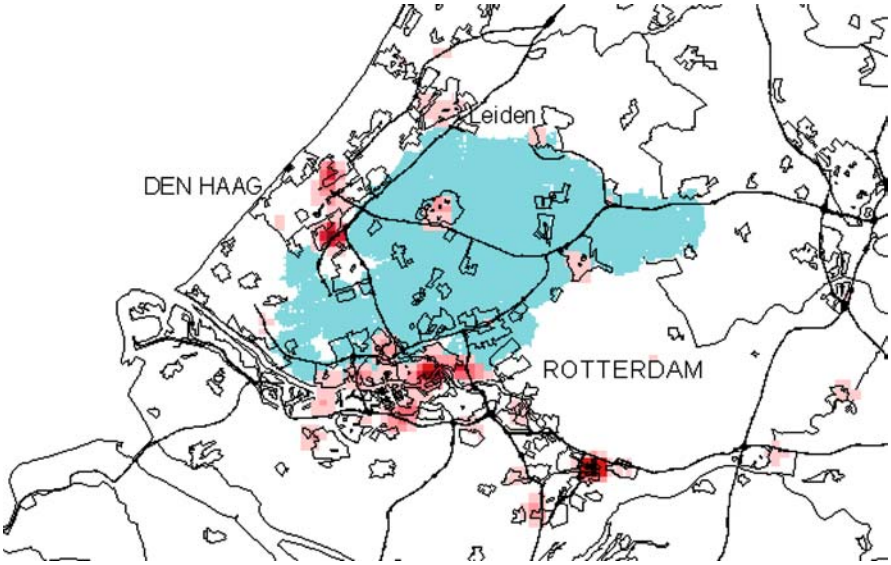

Figure 10. Economic hotspots in the province of South-Holland due to a simulated flood near Krimpen aan de IJssel.

The Figure reveals that some economic hot spots are situated outside the flooded area, but may also be heavily hit because the infrastructure of highways passes the flooded area. Especially the latter phenomenon asks for additional research on the role of economic lifelines (highways, cable infrastructure and electricity and gas lines) in the assessment of risk and vulnerability.

Research on the impact of disturbed lifelines requires a reformulation of our economic model. The accounting framework we chose in this paper is not capable to absorb this phenomenon. Our framework should be extended with a model that reflects the delicate relation between transportation costs and production.

5. Conclusions

Disasters like flooding have an enormous impact on local and national economies. Reasoning along the classical lines of risk misses the impact on the rest of the economy, but also does not take into account redundancy in an economy. A challenge is to visualize vulnerability: Where are the economic hotspots? By referring to the economy as a network we were able to develop a new and innovative tool visualising vulnerability. Additional research is necessary to test this instrument and the underlying indicators. Moreover, we envisage important new research around the role of economic lifelines in the concept of vulnerability.

References

Blaikie, P., Cannon, T., Davis, I. and Wisner, B.: 1994, *At Risk: Natural Hazards, People's Vulnerability, and Disasters*, Routledge, London.

Cochrane, H. C.: 1997, *Forecasting the Economic Impact of a Midwest Earthquake*. National Center for Earthquake Engineering Research Buffalo.

Cochrane, H. C.: 2003, Economic Loss: Myth and Measurement, A. Van der Veen, A. L. Vetere Arellano, and J. -P. Nordvik, Joint NEDIES and University of Twente Workshop: *In search of a common methodology on damage estimation*, EUR Report 20997 EN, Office for Official Publications of the European Communities, European Commission, Bruxelles.

Cole, S.: 1998. Decision support for calamity preparedness: socioeconomic and interregional impacts, M. Shinozuka, A. Rose and R. T. Eguchi, (eds.), *Engineering and Socioeconomic Impacts of Earthquakes*, MCEER, Buffalo.

Eding, G., Stelder, T. M., Vos, E. R., and Oosterhaven, J.: 1995, *Bi-regionale Interactie*, Groningen, REG, Stichting Ruimtelijk Economie Groningen.

EPA: 2000, Guidelines for preparing economic analyses, EPA 240-r-00-003, US Environmental Protection Agency.

FEMA: 1999, Hazus: Technical Manual, Volume 3, FEMA, Washington, USA.

Frank, O.: 2002. Using centrality modeling in survey networks, *Social Networks* **24**, 385–394.

Freeman, P. K., Martin, L. A., Mechler, R., Warner, K. and Hausmann, P.: 2002, *Catastrophes and Development; Integrating natural catastrophes into development planning*; Working papers series no. 4, The World Bank, Washington.

Funtowicz, S. O. and Ravetz, J. R.: 1993, Science for the post-normal age, *Futures* **25**(7), 739–755.

Green, C.: 2003, Evaluating vulnerability and resilience in flood management, A. Van der Veen, A. L. Vetere Arellano and J.-P. Nordvik (eds.), Joint NEDIES and University of Twente Workshop: *In search of a common methodology on damage estimation*, EUR Report 20997 EN, Office for Official Publications of the European Communities, European Commission, Bruxelles.

Hazari, B. R.: 1970, Empirical identification of key sectors in the Indian economy. *Rev. Econ. Statis.* **52**(3), 301–305.

IPCC: 1998. *The Regional Impacts of Climate Change: An Assessment of Vulnerability*. Cambridge University Press, Cambridge.

Kilkenny, M. and Nalbarte, L.: 1998, *Keystone Sector Identification*, TVA, Tennesee Valley Authority.

Leinhardt, S. (ed.), 1997 *Social Networks, a Developing Paradigm*. New York, Academic Press.

Leontief, W.: 1952. Some Basic Problems of Structural Analysis, *Rev. Econ. Statis.* **34**(1), 1–9.

Leontief, W.: 1986, Input–Output Economics. In Leontief, W. *Input Output Economics*, 2nd edn. Oxford University Press, New York and Oxford; 3 18. Previously published: 1951.

Levine, N.: 2002, *CrimeStat II: A Spatial Statistics Program for the Analysis of Crime Incident Locations, Crimestat Manual*, Ned Levine & Associates, TX, Natinonal INstitue of Justice, Washington DC.

Lomborg, B.: 1998. *The Skeptical Environmentalist*, Cambridge University Press, Cambridge.

MAFF: 2000, Flood and Coastal Defense Project Appraisal Guidance: Economic Appraisal, Ministry of Agriculture, Fisheries and Food, London, UK.

Miller, R. E. B., Blair, P. D.: 1985. *Input–Output Analysis: Foundations and Extensions*. University of Pennsylvania, USA, pp. 100–147.

Parker, D. J., Green, C. H. and Thompson, P. M.: 1987, *Urban Flood Protection Benefits, a Project Appraisal Guide*. Gower, Aldershot.

Perrings, C.: 2001. Resilience and Sustainability, H. Folmer *et al.* (eds.), *Frontiers of Environmental Economics*. Cheltenham, UK, Elgar; distributed by American International Distribution Corporation, Williston, VT.: Northampton, MA, pp. 319–41.

Rijkswaterstaat: 2000, *Ruimte voor rivieren*, Ministerie van Verkeer en Waterstaat, Directoraat-Generaal, Rijkswaterstaat, Den Haag.

Rose, A. and Benavides, J.: 1998. Regional economic impacts. *Engineering and Socioeconomic Impacts of Earthquakes*. M. Shinozuka, A. Rose and R. T. Eguchi. MCEER, Buffalo.

Rose, A. and Lim, D.: 2002. Business interruption losses from natural hazards: Conceptual and methodological issues in the case of the Northridge earthquake, *Environ. Hazards* **4**, 1–14.

Tallberg, C.: 2000, *Comparing Degree-based and Closeness-based Centrality Measures*, Department of Statistics, Stockholm University, Stockholm.

Thurstain, M., Batty, M., Hacklay, M., Lloyd, D., Bodt, R., Hyman, A., Batty, S., Tomalin, C., Cadell, C., Falk, N., Sheppard, S., and Curtis, S.: 2001, *Producing Boundaries and Statistics for Town Centres*, CASA, Center for Advanced Spatial Analysis, London.

Thurstain, M. and Goodwin, D. U.: 2000, Defining and Delineating the Central Areas of Towns for Statistical Monitorin Using Continuous Surface Representations, Paper 18, Centre for Advanced Spatial Analysis, London.

UNEP: 2002. *Global Environmental Outlook 3*, Earthscan, London.

Van der Veen, A., Steenge, A. E., Bockarjova, M. and Logtmeijer, C. J. J.: 2003a, Structural economic effects of large scale inundation: a simulation of the Krimpen dike breakage, A. Van der Veen, A. L. Vetere Arellano and J.-P. Nordvik (eds.) Joint NEDIES and University of Twente Workshop: *In search of a common methodology on damage estimation*, EUR Report 20997 EN, Office for Official Publications of the European Communities, European Commission, Bruxelles.

Van der Veen, A., Vetere Arellano, A. L., and Nordvik, J.-P.: 2003a, Joint NEDIES and University of Twente Workshop *In search of a common methodology on damage estimation*, EUR Report 20997 EN, Office for Official Publications of the European Communities, European Commission, Bruxelles.

Vrisou van Eck, N. and Kok, M.: 2001, Standaard methode schade en slachtoffers als gevolg van overstromingen, HKV & Dienst Weg- en Waterbouwkunde, Lelystad & Delft.

Natural Hazards (2005) 36: 81–102

Stochastic Modelling of the Impact of Flood Protection Measures Along the River Waal in the Netherlands

SASKIA VAN VUREN[1,2,★], HUIB J. DE VRIEND[1], SONJA OUWERKERK[1] and MATTHIJS KOK[1,2]
[1]*Delft University of Technology, P.O. Box 5048, 2600 GA Delft, The Netherlands;* [2]*HKV Consultants, P.O. Box 2120, 8203 AC Lelystad, The Netherlands (E-mail: m.kok@hkv.nl)*

(Received: 30 October 2003; accepted 30 June 2004)

Abstract. River flooding is a problem of international interest. In the past few years many countries suffered from severe floods. A large part of the Netherlands is below sea level and river levels. The Dutch flood defences along the river Rhine are designed for water levels with a probability of exceedance of 1/1250 per year. These water levels are computed with a hydrodynamic model using a deterministic bed level and a deterministic design discharge. Traditionally, the safety against flooding in the Netherlands is obtained by building and reinforcing dikes. Recently, a new policy was proposed to cope with increasing design discharges in the Rhine and Meuse rivers. This policy is known as the Room for the River (RfR) policy, in which a reduction of flood levels is achieved by measures creating space for the river, such as dike replacement, side channels and floodplain lowering. As compared with dike reinforcement, these measures may have a stronger impact on flow and sediment transport fields, probably leading to stronger morphological effects. As a result of the latter the flood conveyance capacity may decrease over time. An *a priori* judgement of safety against flooding on the basis of an increased conveyance capacity of the river can be quite misleading. Therefore, the determination of design water levels using a fixed-bed hydrodynamic model may not be justified and the use of a mobile-bed approach may be more appropriate. This problem is addressed in this paper, using a case study of the river Waal (one of the Rhine branches in the Netherlands). The morphological response of the river Waal to a flood protection measure (floodplain lowering in combination with summer levee removal) is analysed. The effect of this measure is subject to various sources of uncertainty. Monte Carlo simulations are applied to calculate the impact of uncertainties in the river discharge on the bed levels. The impact of the "uncertain" morphological response on design flood level predictions is analysed for three phenomena, viz. the impact of the spatial morphological variation over years, the impact of the seasonal morphological variation and the impact of the morphological variability around bifurcation points. The impact of seasonal morphological variations turns out to be negligible, but the other two phenomena appear to have each an appreciable impact (order of magnitude 0.05–0.1 m) on the computed design water levels. We have to note however, that other sources of uncertainty (e.g. uncertainty in hydraulic roughness predictor), which may be of influence, are not taken

★ Author for correspondence. Phone: +31-15-27-84735; Fax: +31-15-27-85124; E-mail: b.g.vanvuren@ct.tudelft.nl

into consideration. In fact, the present investigation is limited to the sensitivity of the design water levels to uncertainties in the predicted bed level.

Key words: river morphodynamics, flood protection and forecasting, stochastic modelling, uncertainty analysis, Monte Carlo simulation, numerical integration

1. Introduction

In the past few years many rivers flooded all over the world, such as the Jamuna river in Bangladesh, the Yangtze in China, the Oder and the Vistula in Poland, the Moldau in the Czech Republic and the Elbe in Germany. A large part of the Netherlands lies below sea level and below river flood levels (Figure 1). Without flood defences much of the country would be flooded regularly. In the Netherlands, the 1995 flood event in the Rhine caused 250,000 people to be evacuated. Although no major flooding occurred at the time, the economical and social damage was considerable. It may be expected that in the future, due to the changing climate, higher discharge levels will occur, leading to more frequent flooding of the rivers, unless adequate measures are taken to prevent this.

World-wide, this leads to an increasing demand for reliable flood level predictions supporting the river managers to take decisions with respect to the design of flood protection measures. To that end, often use is made of hydrodynamic models with a fixed bed, provided that its geometrical

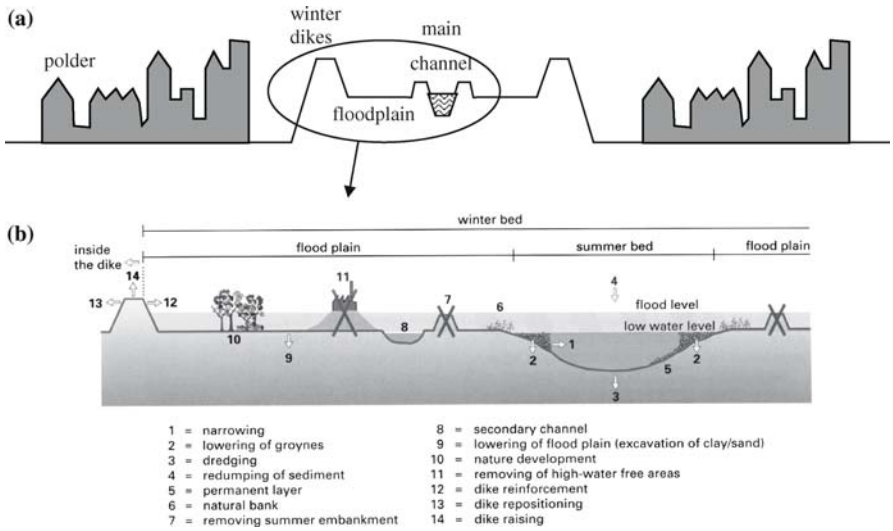

Figure 1. (a) layout of the Rhine river basin in the Netherlands. (b) Flood protection measures proposed in the Room for the River study in the Netherlands (Silva *et al.*, 2001).

schematisation is an adequate representation of the "actual" state of the river. However, the adequacy of the geometrical schematisation is critical. An *a priori* judgement of safety against flooding on the basis of fixed-bed forecasting in morphodynamic river systems can be quite misleading (De Vriend, 2002). The sensitivity of flood levels to morphological changes is assessed in this paper. The problem is addressed using a case study of one of the Rhine branches in the Netherlands: the river Waal.

Flood protection is embedded in Dutch laws and is summarised in the Flood Protection Act (1995). According to this law, the Netherlands are divided into 53 so-called dike rings, each with its own level of protection, according to its location. The dike rings along the Rhine have a protection level of 1/1250 per year. This means that the flood defences are designed for water levels with a probability of exceedance of 1/1250 per year. These water levels are known as design water levels (DWLs). The DWLs are computed with a fixed-bed hydrodynamic model based on the "actual" (latest-measured) cross-sections of the river. The model is driven by the design discharge hydrograph. The peak of this hydrograph has a probability of exceedance of 1/1250 per year, derived from a statistical analysis of all flood events on record. The shape of the discharge hydrograph is derived from averaging the wave shapes of historical flood events that are linearly scaled up to this peak event. This means that only one stochastic variable is involved in the establishment of the design water levels: the peak discharge.

Traditionally, the safety against flooding is obtained by building and strengthening dikes. Recently, the Room for the River (RfR) policy has been proposed by the government (Silva *et al.*, 2001). This policy boils down to "no dike strengthening, unless...". It focuses on measures to increase the flood conveyance capacity, such as lowering of groynes and floodplains, implementation of secondary channels and detention basins, removing obstacles and setting back river dikes (Figure 1). As compared with dike reinforcement, these flood protection measures reduce the DWLs and may have an extra impact on the flow and sediment transport fields in the river. This may result in extra morphological effects. As a consequence of the latter, the river's flood conveyance capacity may decrease over time. Hence, the determination of DWLs using a fixed-bed hydrodynamic model (instead of a morphodynamic model) may suggest an unrealistic safety level for RfR policies.

In the present paper, we consider a RfR flood protection measure: floodplain lowering in combination with summer levee removal along the Waal. We investigate whether this reduces the DWLs and if it induces a stronger morphological response than in the reference situation with dike reinforcement.

Although we consider a two-dimensional problem, we use a one-dimensional morphodynamic model of the Rhine to analyse the hydraulic and

morphological changes in the river system. In that way, we neglect the two-dimensional processes such as the lateral sediment transport exchange between the main channel and the floodplains and the asymmetry of river cross-sections. With this simplification, model uncertainties are introduced. In addition, various input uncertainties and other assumptions in the one-dimensional Rhine model introduce uncertainties in the hydraulic and morphological predictions.

In this study, we analyse first the DWL reduction of the floodplain measure in a deterministic way, meaning that the impact of uncertainties on this reduction is neglected. Subsequently, with respect to the morphological changes we consider the impact of only one uncertainty source, namely the river discharge, on bed levels. To account for this uncertainty, we make Monte Carlo simulations (MCS) with the Rhine model, meaning that the model is run a large number of times, each time with a different, but statistically equivalent discharge time series. MCS results in a large number of simulated morphological states with equal probability. It provides insight into the stochastic variation of the bed level predictions.

Additionally, we will analyse the impact of the ''uncertain'' morphological response on design flood level predictions for three phenomena, viz. (1) the impact of the spatial morphological variation over years, (2) the impact of the seasonal morphological variation and (3) the impact of the morphological variability around bifurcation points. We will investigate to what extent there is a feedback of these three phenomena on the design water levels and whether it is justified to use a fixed-bed hydrodynamic model for design water level computations. Furthermore, we will analyse how the three morphological phenomena affect the exceedance probability of water levels, which may subsequently lead to second order changes in DWLs and changes in the exceedance frequency of the current DWLs.

2. Stochastic Modelling of River Morphology

2.1. CASE STUDIES

The Rhine rises in Switzerland as a snowmelt-fed mountain river and eventually ends as a rain- and snowmelt-fed lowland river in the North Sea (Figure 2). The river Waal is one of the branches of the Rhine in the Netherlands. In the 20th century the main channel of the Waal was fixed by groynes and the floodplain protected from frequent flooding by small embankments – the summer levees. The winter dike, which acts as the main flood defence, protects the hinterland.

In this paper, we consider floodplain lowering in combination with summer levee removal along the river Waal. Over a distance of 27 km (section between

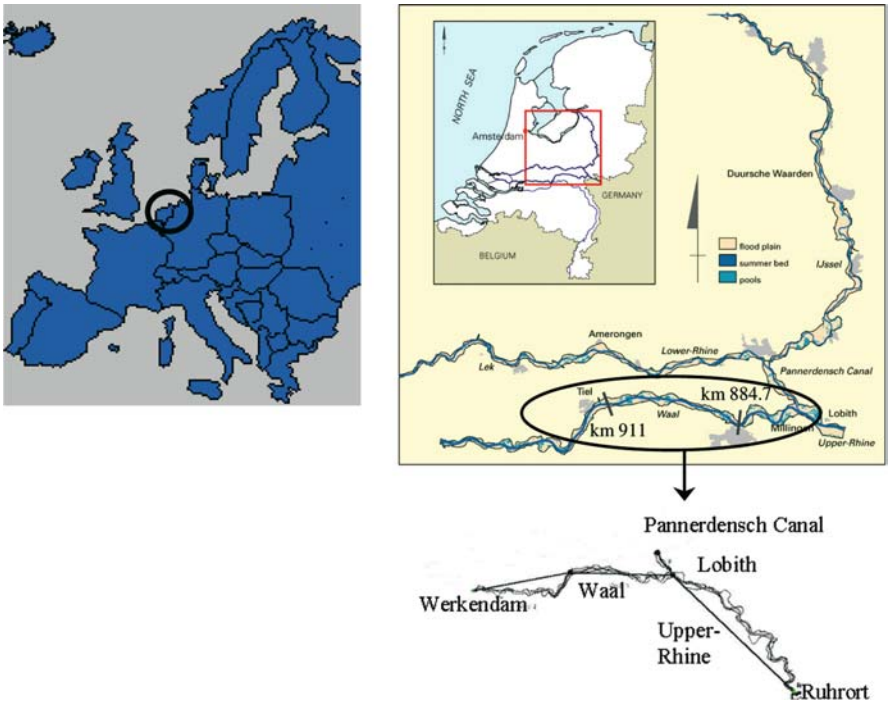

Figure 2. The Rhine branches in the Netherlands and the schematisation of three main branches in the Rhine model as a network of nodes and branches.

Nijmegen – 884.7 km – and Beneden-Leeuwen 911 km, see Figure 2) the floodplain level is lowered by 1.5 m. This leads to a DWL reduction of several decimetres. Generally speaking, this will cause additional changes in sediment transport gradients, leading to a permanent sedimentation in the main channel at the location of the intervention and temporary or permanent erosion downstream. Removal of summer levees leads to more frequent flooding of the floodplains, hence to a greater morphological response. The further evolution of the system (in space and time) is compared to the one in the reference situation, i.e. with dike reinforcement, in order to assess to what extent the ''new'' flood protection measures in the Waal result in more bed level variability. In this study, the morphological evolution of the upstream part of the Waal between Pannerdense Kop (867 km) and Tiel (915 km) is analysed.

2.2. ONE-DIMENSIONAL RHINE MODEL

In the Netherlands six main branches of the Rhine can be distinguished: Upper-Rhine, Waal, Pannerdensch Canal, IJssel, Lower-Rhine and Lek. Two bifurcation points connect the different branches (Figure 2). In this study, we simulate the hydrodynamic and morphological responses in the

Waal branch. To that end, we use an adapted version of the morphodynamic Rhine model (Jesse and Kroekenstoel, 2001), based on the SOBEK software package of Institute for Inland Water Management and Wastewater Management (RIZA) and WL|Delft Hydraulics. This model solves the 1-D cross-sectionally integrated shallow-water equations, while retaining a distinction between the main channel, the groyne section, the flow-conveying floodplains and the storage area. It uses the sediment transport rate and the sediment balance equations to determine the morphological changes. Lateral sediment transport from the main channel into the floodplains or *vice versa* is neglected. All sediment transport and all morphological changes therefore occur in the main channel. Since the Rhine model is a one-dimensional model, the computed hydraulic and morphological changes in the main channel are cross-sectionally averaged.

The Rhine model consists of a network of nodes and branches. It includes the branches Upper-Rhine, Pannerdensch Canal and Waal and the bifurcation point Pannerdensche Kop. At this bifurcation approximately 66% of the Rhine discharge is directed to the Waal. The remaining 34% flows into the Pannerdensch Canal. The model has an upstream boundary at Ruhrort (upstream of Lobith) and two downstream boundaries at Werkendam and at 1 km downstream of the Pannerdense Kop. The river is by no means a prismatic channel with a plane sloping bed. Many variations in the river are noticed, such as variation in geometry, in floodplain width, in floodplain vegetation type and variation in the presence or absence of summer dikes, flood-free areas and storage and conveying parts in the floodplains. These variations are schematised in the model.

As Froude numbers in the Rhine branches are usually in the order of 0.1–0.35, a quasi-steady approach (Jansen *et al.*, 1979) can be followed. This means the river is considered as a morphodynamic system, including the dynamic feedback between water motion, sediment transport, sediment balance and bed level changes. The sediment transport capacity depends on the flow velocity and the sediment characteristics, like density, grain size distribution, shape and uniformity. In general, the water motion tends to pick up sediment and deposit it elsewhere. If the water motion is interrupted, spatial gradients in the sediment flux cause morphological changes. These morphological responses influence the water motion and the sediment transport, which in their turn, affect the sediment balance and the bed topography. This dynamic loop is run through for each numerical time step of 10 days: when computing the water motion, the bed is held fixed, and when computing the bed level changes, the water motion is kept invariant to changes in the bed level.

The entire computation period is 20 years. The spatial grid size is 500 m. Hydrodynamic and morphological responses at intermediate time steps of 10 days and spatial steps of 500 m can be predicted.

The following boundary conditions are required: a hydraulic and a morphological condition at the upstream boundary and a hydraulic condition at the two downstream boundaries. These conditions comprehend the following: (1) a discharge hydrograph and a fixed-bed level (presence of a natural clay-layer) at the upstream boundary, (2) a rating curve (discharge-water level relationship) at the downstream boundary Werkendam, (3) a discharge hydrograph at the downstream boundary in the Pannerdensch Canal (in order to maintain the discharge distribution at the bifurcation constant under all discharge conditions). Three initial conditions are required. The bed level, the water level and the discharge distribution are given at the beginning of the model run.

2.3. MONTE CARLO SIMULATIONS

The Rhine model is affected by various uncertainties, including those in the model schematisations and in the specification of the model input (for example boundary conditions, initial conditions) and the model parameters. Van der Klis (2003) and Van Vuren *et al.* (2002) have shown that the future discharge hydrograph is one of the most important sources of uncertainty. In order to quantify the corresponding uncertainty in the morphological response, Monte Carlo simulations are performed with the Rhine model. For the time being, uncertainties introduced by the model schematisation and the specification of model inputs, other than the river discharge, are left out of consideration.

The principle of Monte Carlo simulation (MCS) (Hammersly and Handscomb, 1964) is to run a deterministic model repeatedly, each run with a different set of model inputs. In this study the Rhine model is run 300 times, each time with another discharge time series of 20 years duration that has been randomly generated according to a prescribed probability distribution. On the basis of the set of outputs of all model simulations, the morphological response statistics are analysed in terms of expected value, variance, percentile values of 5 and 95% and confidence intervals.

2.4. SYNTHESIS OF DISCHARGE TIME SERIES

Van Vuren and Van Breen (2003) and Duits (1997) derive a method to randomly synthesise discharge time series. The generation of the discharge time series is based on 100 years of daily discharge measurements at Lobith, where the Rhine enters the Netherlands. The method accounts for the seasonal dependency of the discharge and the correlation of the discharges in successive periods.

To fit the discharge time series with the numerical time step applied in the simulation, we used 10-day averaged discharges based on the daily measurements. To that end, each year is split into 36 periods of approximately 10 days each. For each of these periods, the weighted average discharge Q_w

of the daily discharges Q_d is estimated, such that the total sediment transport capacity in each period T, S_{tot} remains unchanged:

$$T \cdot S(Q_w) = S_{tot}(T)\left(= T \cdot E(S) = T \cdot \int_0^\infty S(Q_d)p(S)dS\right) \quad (1)$$

with $p(S)$ is the probability density of sediment transport $S(Q_d)$.

This results in 36 sets of 100 data points. The Spearman rank correlation method (Dahmen and Hall, 1989) is used to test the presence of a trend in each of the 36 data sets and in the yearly peak discharge. No statistically significant trends are observed, which indicates the independence of subsequent data points within each data set.

A statistical description of these data sets have been derived in three consecutive steps:

- To randomly synthesise discharge time series use is made of a multivariate distribution function that is derived on the basis of marginal probability distribution functions for each ''10-day''-period (data set) and the auto-correlation function that accounts for the correlation between discharges in successive periods.
- For each period i, the parameters of a marginal probability distribution function – a shifted lognormal distribution – are statistically derived for the discharge Q_{w_i}: the distribution parameters μ and σ and the location parameter a (Figure 3a). The location parameter is equal to the lowest observed river discharge in that period. Period 1 is the beginning of January and period 36 is the end of December.
- The auto-correlation function that accounts for the correlation between discharges in successive periods is estimated (Figure 3b). The figure illustrates that discharges in periods close to each other are strongly correlated (auto-correlation coefficient close to 1). This correlation reduces if the intermediate period between successive discharges increases.

The correlation between three successive periods is considered next. This means that the discharge in a certain period i depends on the discharge in two preceding periods, $i-1$ and $i-2$. The correlation with the other periods is neglected.

- A multivariate lognormal distribution function is constructed on the basis of the marginal distribution functions for each period and the auto-correlation function.

In this study 300 discharge time series of 20 years duration each (20 years of 36 periods) have been synthesised by random sampling from this multivariate distribution function. These time series are used in the MCS with the Rhine model.

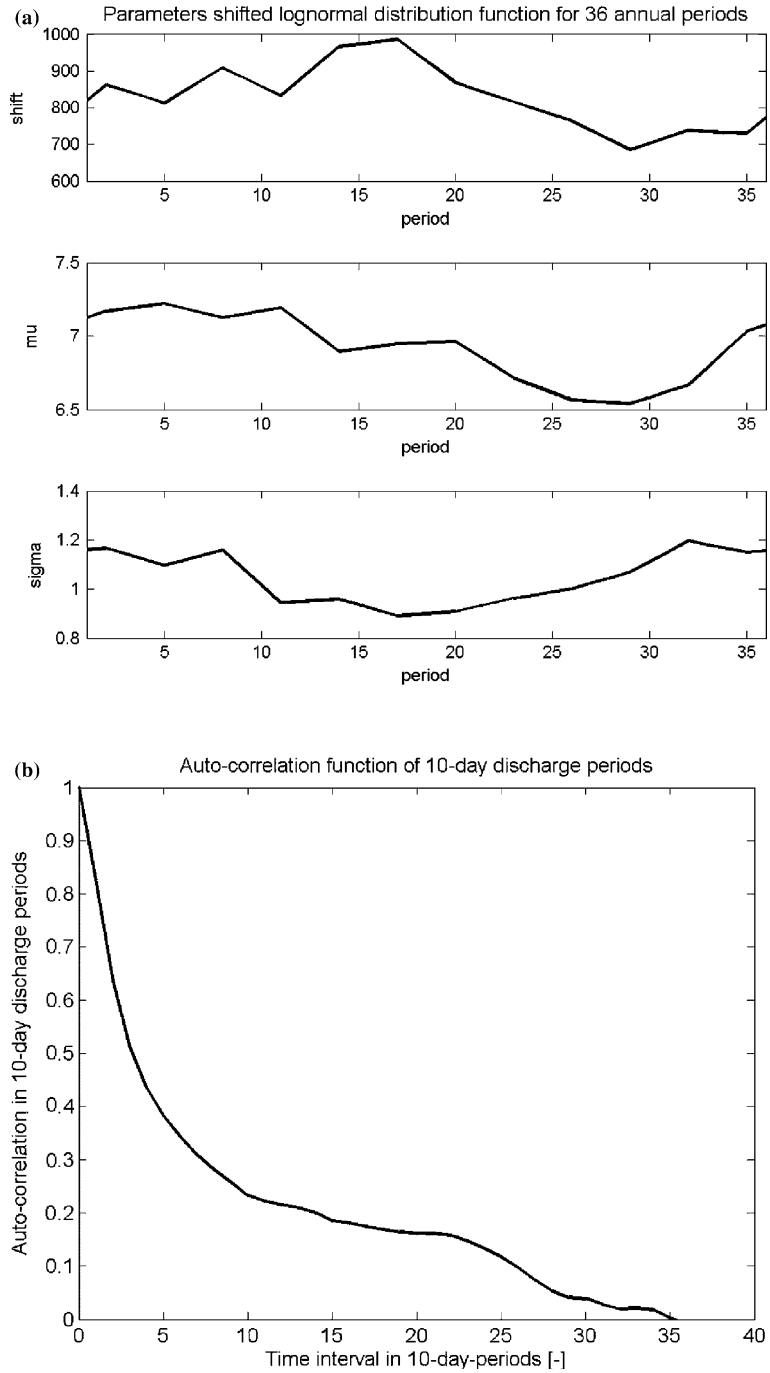

Figure 3. (a) Parameters of the shifted lognormal distribution for the 36 annual periods. (b) Auto-correlation that describes the correlation between discharges in successive "10-day"-periods.

2.5. SPATIAL VARIATION OF STOCHASTIC MORPHOLOGICAL RESPONSE IN THE WAAL

First, the stochastic nature of the morphological evolution in the main channel of the Waal in the reference situation with dike reinforcement is analysed on the basis of 300 model runs of a computation period of 20 years. Subsequently, the situation with floodplain lowering in combination with summer levee removal is analysed. Each run is driven by one of the synthesised discharge time series. This results into a morphological response per model run, reflecting just one possible future state. The lines in Figure 4 represent the morphological response of two simulations of a period of 20 years and the moving averaged discharge series over a time window of 3 months. The morphological state at any particular moment in time depends very much on the short-term history of the discharge time series. Hence it makes a difference whether the 20-year time series is ended in the high-water season or in the dry season.

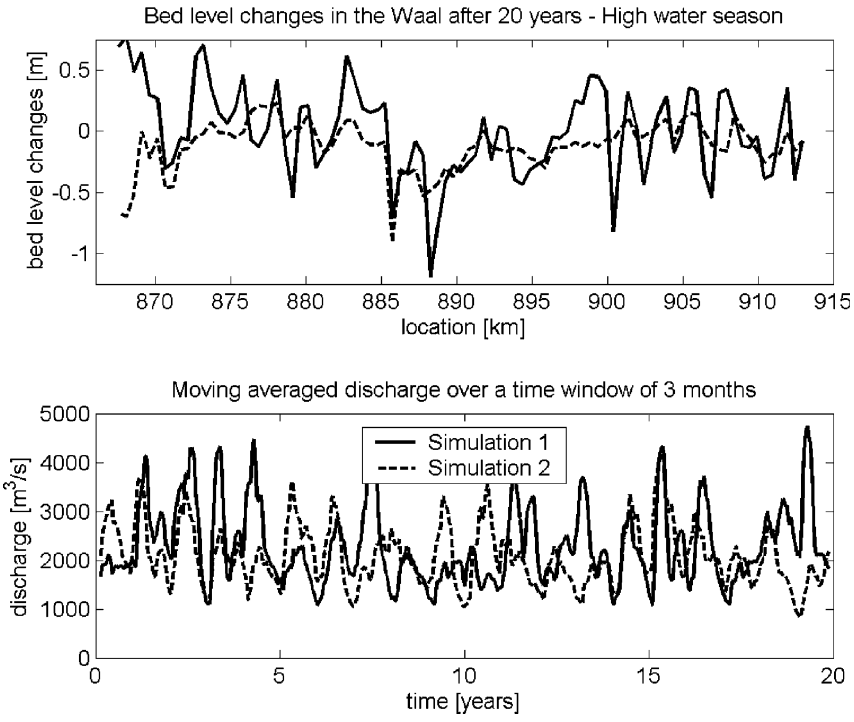

Figure 4. The cross-section averaged morphological response in the main channel of the Waal after 20 years in the high-water season for two model simulations in the reference situation with dike reinforcement and the moving-averaged discharge series over a time window of 3 months.

In the last century large-scale tilting of the river Waal is observed. Large-scale erosion is noticed in the upstream part of the Waal. Near Tiel there is a hinge point, downstream of which long-term sedimentation takes place. The Rhine model computations show a continuation of this large-scale tilting. Figure 5 shows the prediction of general scour for the upstream part of the Waal. On top of that, the figure illustrates that the uncertain discharge together with the changes in the river geometry, such as width variation and man-made structures (such as riverbed protection), leads to an uncertain morphological response. Each change in the river geometry acts as a generator of new bottom waves, which travel downstream and may lead to large uncertainties.

At locations with large changes, a local increase in bed level variability is observed – reflected by an increase in standard deviation in Figure 5. This increase in standard deviation is more pronounced in the high-water season than in the dry season.

Lowering the floodplains combined with removal of the summer levees results in a DWL reduction of 0.3 up to 0.6 m. Furthermore, this measure

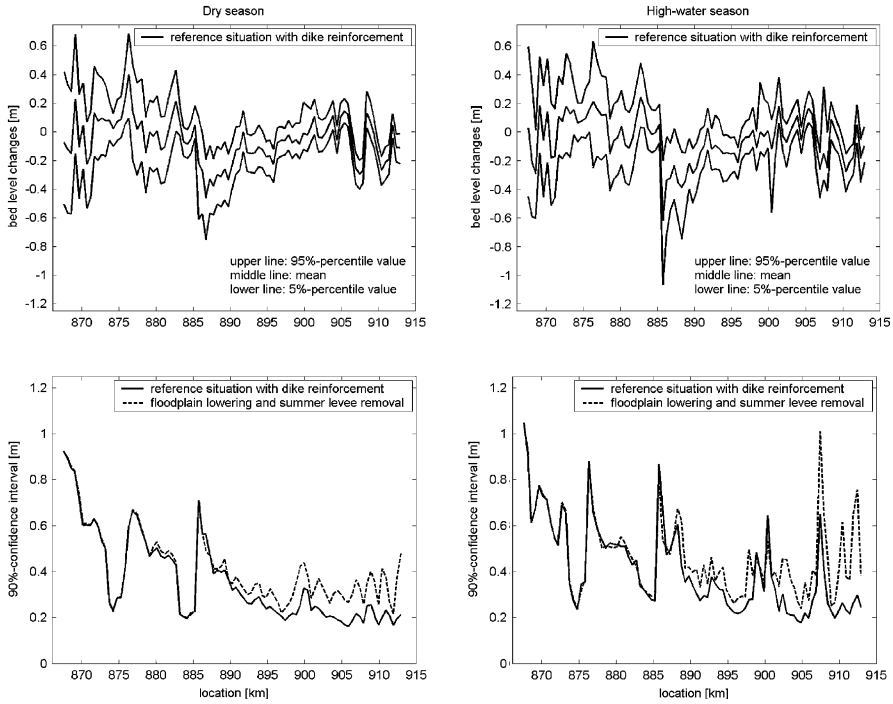

Figure 5. Spatial variation of the statistical properties of the cross-sectionally averaged bed level changes in the Waal after 20 years in the high-water season and the dry season computed with the one-dimensional Rhine model.

leads to a much stronger and more uncertain morphological response than the reference situation with dike reinforcement. The measure results in more frequent and more extensive flooding of the floodplains, whence their impacts are more pronounced (Figure 5). Not only does the mean bed level increase at the location of the floodplain lowering also the size of the confidence interval increases. The latter is especially noticed in the river sections with the large discontinuities, such as location 907.4 km (see Figure 6).

Examples of locations where changes in river geometry cause large standard deviation in bed level changes are:

- The bottom protection structures at Erlecom (873–876 km) and at Nijmegen (882–885 km). These structures are designed for navigation purposes that prevent the riverbed from scouring. In the model the structures are schematised as fixed bed layers imposing a lower bound on the bed level. At both locations the morphological response after 20 years shows a bar in the riverbed and a dip in the confidence interval. The fixed layers prevent further erosion, while they lead to extra scour and bed level variability downstream.
- The locations with large variation in the floodplain width: Hiensche Waarden and Affendensche Waarden (898–901 km), Ochtense Buitenpolder (902–906 km) and Willemspolder and Drutense Waard (906–913 km). At these locations an increase in the size of the confidence interval is noticed. For example, there is a large open water area between 906 and 908 km in the floodplain "Willemspolder"). An increase in flood-conveying width results in sedimentation; a decrease leads to erosion in the main channel. At the transition points this results in an increase in bed level variability, hence a larger confidence interval.

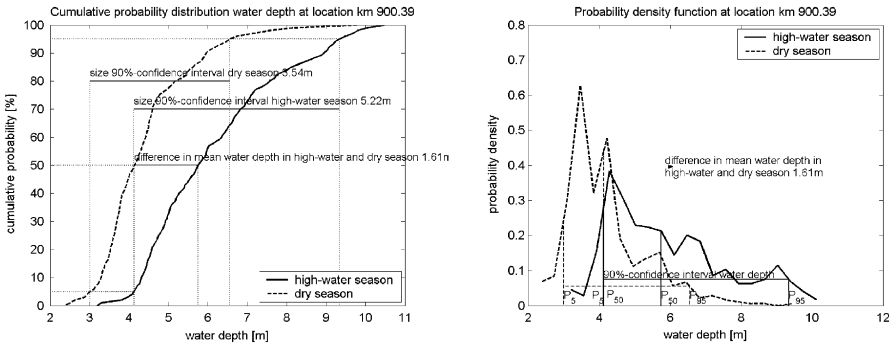

Figure 6. Cumulative probability distribution and probability density function of the computed cross-sectionally averaged bed level change at river location 907.4 km after 20 years in the high-water season for the reference situation with dike reinforcement and floodplain lowering in combination with summer levee removal.

- The bifurcation Pannerdense Kop (867 km). The actual discharge distribution and the sediment distribution at this point depend very much on the local morphological situation, which is strongly variable (as indicated by the large confidence interval).

2.6. TEMPORAL VARIATION OF STOCHASTIC MORPHOLOGICAL RESPONSE IN THE WAAL

The above results show the spatial morphological response statistics after a period of 20 years that ends in the high-water season and in the dry season. The temporal variation of the response statistics is analysed for two locations (see Figure 8): a location in a river section with a large change in river geometry (907.4 km; see Figure 7) and a location in a more or less prismatic river section (895.3 km).

In the section with the large change in river geometry, the seasonal variation in the morphological response statistics is considerable. It reflects the seasonal variation in river discharge. The seasonal fluctuation of the standard deviation is significant, with the largest values found in the high-water season and the smallest ones in the dry season (see Figure 8). At 907.4 km (the transition from a narrow to a wide cross section), a net sedimentation occurs in the main channel. The 95%-percentile strongly oscillates, and the 5%-percentile much less so. This can be explained by the fact that at discharges above bankfull, bottom waves (sedimentation) are initiated in the main channel. These bottom waves migrate downstream and (partly) damp during discharges below bankfull, when the flow stays within the main channel. Therefore, the seasonal variation in the 5%-percentile is limited.

At location 895 km, a uniform river section, the seasonal signature is much less pronounced. The uncertainty in the bed level change at this location is affected by the bottom waves initiated at other locations in the

Figure 7. River section "Willemspolder" (906–908 km) with a large variation in floodplain width (courtesy of Rijkswaterstaat – DON).

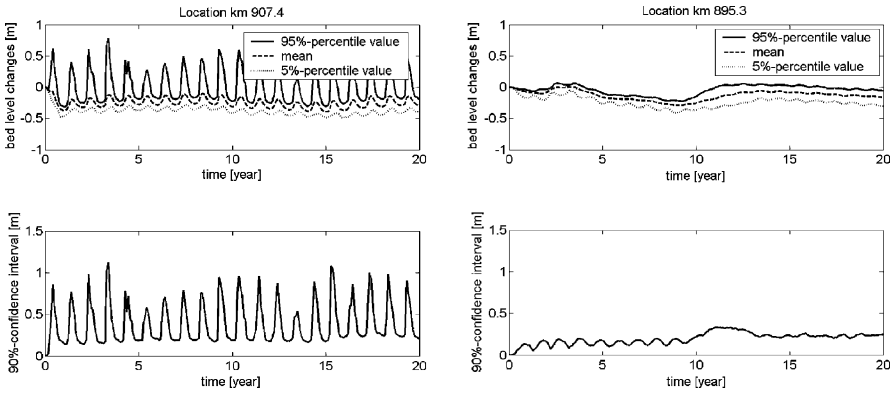

Figure 8. Temporal variation of the statistical properties of the cross-sectionally averaged bed level changes computed with the one-dimensional Rhine model at a location in where the geometry of the river section changes (907.4 km) and at a location in a more or less prismatic river section (895.3 km) in the reference situation with dike reinforcement.

river, which propagate downstream and at a certain moment pass by 895.3 km.

The largest uncertainty in bed level variability in the study area occurs in the high-water season in the Willemspolder (907.4 km): the size of the confidence interval is approximately 1.5 m. The smallest uncertainty is predicted for the Waal bend at Nijmegen (884 km) in the low water season. The size of the confidence interval is less than 0.15 m.

3. Potential Effect of Morphological Changes on Flood Conveyance

In the foregoing we have shown that the bed level in the Waal exhibits a strong spatial and temporal variation. The uncertain discharge together with large changes in the river geometry leads to an uncertain morphological response. The stochastic approach does not only show that many possible morphological states can occur. It also shows that in some reaches the spatial and temporal bed level variations are more pronounced than in others.

Large-scale floodplain lowering in combination with removal of summer levees strongly enhances the morphological response as compared to the reference situation with dike reinforcement. On average, the uncertainty in the morphological response increases with 22%.

Consequently, the river's flood conveyance capacity will vary over time. Hence, the determination of DWLs using a fixed-bed hydrodynamic model, instead of a morphodynamic model, may underestimate the DWLs. In the next section, we will investigate to what extent the bed level variability affects

the design water level (DWL) and to what extent it is justified to compute this DWL with a fixed-bed hydrodynamic model. To that end, we will use two different methods (see Sections 4.1 and 4.2) to analyse the effect of three morphological phenomena on the computed design water levels, namely:

- spatial variation of the bed morphology over a period of years,
- morphological evolutions at a seasonal scale,
- morphological variability around the bifurcation point Pannerdense Kop.

The latter phenomenon is of interest, because the present management policy is to maintain the discharge distribution at the bifurcation point under all discharge conditions. Yet, the discharge distribution varies slightly with time, as a result of time-dependent morphological changes around the bifurcation point. The question is to what extent this may lead to substantial differences in the DWL.

4. Impact of River Morphology on Predicted Flood Levels

4.1. APPLICATION OF MONTE CARLO SIMULATION TO THE CURRENT DESIGN WATER LEVEL PREDICTION METHOD

Design water levels are derived from a fixed-bed hydraulic model, driven by the design discharge hydrograph. The "fixed-bed" is the latest-measured state of the river. Since bed level surveys are made through the year, this probably does not represent a "snapshot" of the actual state of the river at any point in time. The design discharge is based upon a statistical analysis of the yearly peak discharges from 100 years of daily discharge measurements at Lobith. A combination of 3 probability distributions – a Gumbel distribution, a Pearson III distribution and a lognormal distribution – is used to extrapolate the data to the design probability of exceedance (Parmet *et al.*, 2002). These probability distribution types fit the best to the discharge measurements. The design discharge is revised every 5 years. As a consequence of the 1993 and 1995 flood events, the probability curve has changed and the discharge has gone up from 15,000 m^3/s to 16,000 m^3/s. The relation between the yearly exceedance frequency f and the river discharge Q is given by:

$$Q = 1517.8 \cdot \ln(1/f) + 5964.6 \quad 1/2 \leq f \leq 1/25 \tag{2a}$$

$$Q = 1316.4 \cdot \ln(1/f) + 6612.6 \quad 1/25 \leq f \leq 1/10000 \tag{2b}$$

The wave shape of the design discharge hydrograph is found by linear scaling up the discharge hydrograph of historical flood events. Each discharge hydrograph is therefore multiplied with the ratio of the design discharge to the peak discharge of this hydrograph. The average hydrograph of the upscaled hydrographs is used as wave shape of the design discharge hydrograph.

In order to determine to what extent morphological changes affect the design water levels, MCS is applied to the current prediction method. To that end, 300 morphological model runs were made with statistically equivalent discharge time series. The bed topography resulting from each run at a certain point in time is fixed and a standard design flood computation is made on top of that bed topography. During this flood computation the morphological evolution during the flood is not taken into consideration. The computations yield 300 design water levels at each location and at each timepoint in the flood computation. This gives insight into how morphological changes may affect the design water level.

4.2. EXTENDED METHOD FOR DESIGN WATER LEVEL COMPUTATION

The current method of DWL computation is extended with a second random variable, river morphology, in order to determine the effects of uncertainties in the river's morphological state on the exceedance probability of water levels. The extended method results in general in higher DWL compared with results using the current method. The reason is that the tail of the probability distribution of the water levels becomes bigger, and therefore the water level with exceedance probability of 1/1250 will be higher. However, in this case we also see erosion in some parts of the river, and erosion results in lower design water levels. Hence, it may be expected that in some parts of the rivers there will be lower design water levels, where in other parts there will be higher water levels. On average, there will be lower bed levels in all parts of the river.

The extended method involves the following steps (Van Vuren *et al.*, 2003):

1. Again, 300 morphological states at a certain point in time T are computed with a morphodynamic model run in MSC-mode. The resulting morphological states are statistical equivalent, each with a probability of occurrence $P(\mathrm{M}_j)$ of 1/300.
2. This time, the flood model is run on each of the 300 bed topographies, using a range of 15 constant discharges varying from 13,000 till 20,000 m^3/s, with a discretisation step of 500 m^3/s. Again, the morphological evolution during these high discharges is not considered. The probability P of the discharge level Q_i is derived from formula (2):

$$P(Q \leq Q) = f(Q) = \exp - \left(\frac{Q - 6612.6}{1316.4} \right) \tag{3a}$$

$$P(Q_{\mathrm{i}}) = P(\mathrm{Q} \leq Q_{\mathrm{i}} + 250) - P(\mathrm{Q} \leq Q_{\mathrm{i}} - 250) \tag{3b}$$

This results in 15 water level distributions per simulated morphological bed.

3. The probabilities of the morphological state $P(\mathrm{M}_j)$ and the discharge level $P(Q_i)$ are multiplied to determine the probability of the computed water levels $P(\mathrm{W}L_{ij})$.
4. On the basis of the set of outputs (4500 water levels and their corresponding probability), a cumulative probability distribution of the water level at each location is determined by numerical integration. The probability of exceedance indicated by this curve includes the potential effect of morphological changes. The water level with a probability of exceedance of 1/1250 per year ($\mathrm{DWL}_{\mathrm{new}}$) can now be compared with the value computed with the traditional method (DWL_0). Moreover, the curve can be used to determine an "updated', exceedance probability of the DWL_0, now including morphological effects.

4.3. IMPACT OF SPATIAL MORPHOLOGICAL VARIATION OVER A PERIOD OF YEARS

At a time-scale of decades to a century, the large-scale tilting of the Waal is expected to continue. Hence, long-term erosion is to be expected in the part of the Waal between 867 km and 915 km, considered herein (Figure 5). This leads to an ongoing reduction of the DWLs (Figure 9). Near Tiel (913 km) there is a hinge point, downstream of which long-term sedimentation takes place. Clearly, this comes with an ongoing increase of the water level in the reach below Tiel.

The uncertainty in this long-term morphological response is reflected in the DWLs, as becomes apparent from Figure 9. This figure shows the spatial distribution of the statistical properties of the ΔDWL ($= \mathrm{DWL_T} - \mathrm{DWL_{T0}}$), after a period of respectively 5 and 20 years in the high-water season for the

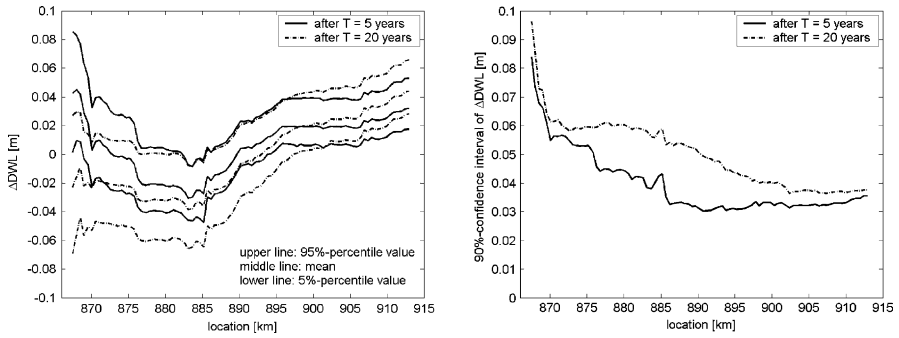

Figure 9. Spatial variation of the statistical properties of ΔDWL ($= \mathrm{DWL_T} - \mathrm{DWL_{T0}}$) along the Waal after a period T of respectively 5 and 20 years for the reference case with dike reinforcement.

reference case with dike reinforcement. The 90%-confidence interval gives an indication of the variation in ΔDWL resulting from differences in morphological state. The confidence interval increases as a function of time. Since the water levels in the downstream direction towards Tiel are determined to an increasing extent by the downstream water level, the confidence interval decreases in downstream direction. The DWLs vary with a probability of 90% within a range of 5–10 cm, which is not much as compared to the expected uncertainty originating from other sources (e.g. in bed roughness predictor).

The application of the extended method for design water level computations results in a set of 4500 water level computations and their corresponding probability. These are used to derive the cumulative probability distribution of the water levels per river location. Figure 10 shows this curve at 884.7 km, after a period of 20 years of morphological evolution. In the same figure, the curve derived with the hydrodynamic model with a fixed-bed level at time T_0 is shown.

The figure shows a decrease in DWL of 0.06 m in 20 years, when the uncertain morphological changes are taken into account. According to the new curve, the exceedance probability of DWL_0 comes down from 1/1250 to 1/1460 per year. Given the other sources of uncertainty playing a role at this extreme end of the probability distribution, these differences are minor.

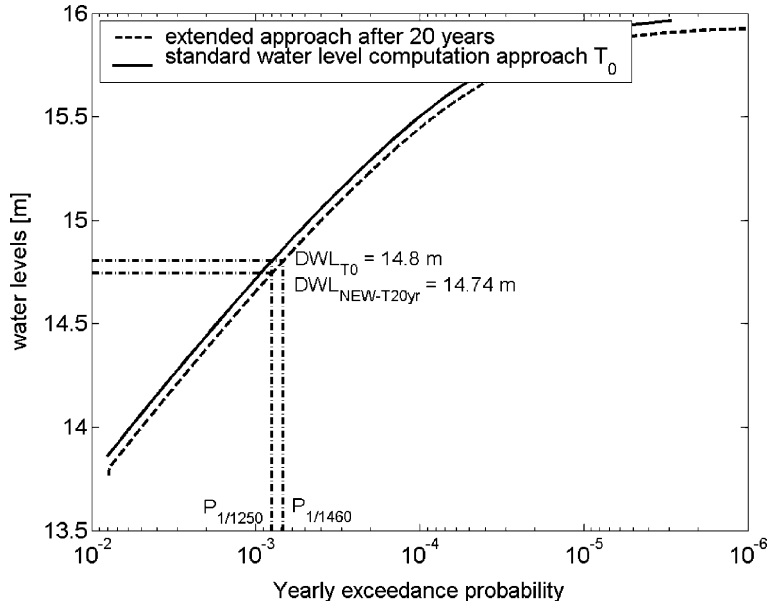

Figure 10. Exceedance probability of water levels at location 884.7 km at T_0 and after 20 years.

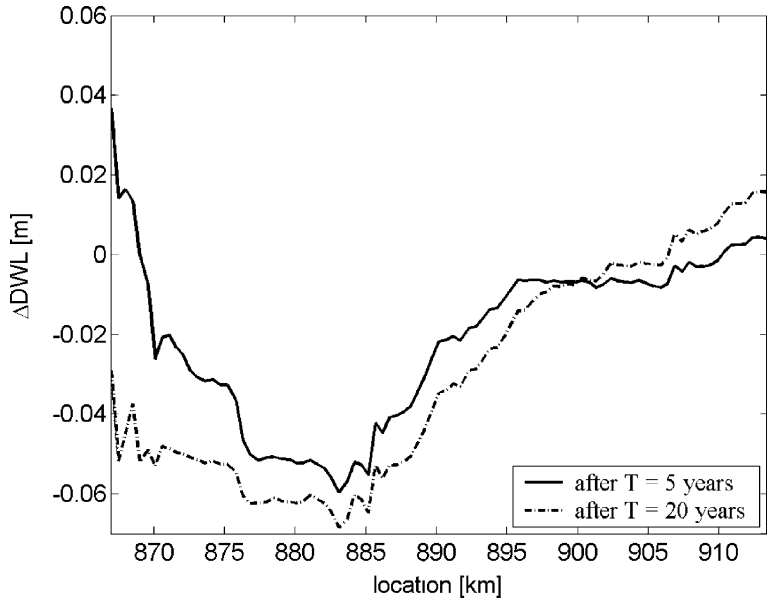

Figure 11. Spatial distribution of ΔDWL ($= DWL_T - DWL_{T0}$) along the Waal after a period T of respectively 5 and 20 years for the reference case with dike reinforcement.

Doing this for all locations along the Waal leads to the spatial distributions of ΔDWL shown in Figure 11. The conformity with the large-scale rotation around the hinge point near 900 km is striking. Apparently, this rotation is the prime cause of the long-term changes in DWL.

4.4. IMPACT OF SEASONAL MORPHOLOGICAL VARIATION

We noticed a large seasonal variation of the statistical properties of the morphological response in Figures 5 and 8. The largest uncertainties in the morphological response are found in the high-water season. Computations have shown that seasonal variations in the river morphology hardly affect the DWLs.

4.5. MORPHOLOGICAL VARIABILITY AROUND BIFURCATION POINT

Local morphological changes around the bifurcation point Pannerdensche Kop may lead to variations in the discharge distribution. Discharge measurements show variations between tens and hundreds of cubic metres per second. In the computations so far, we have kept the discharge distribution at the bifurcation point fixed. We will now adopt a statistical description of the discharge distribution, based upon daily discharge measurements at the Pannerdensche Kop in the period 1961–2000. For each

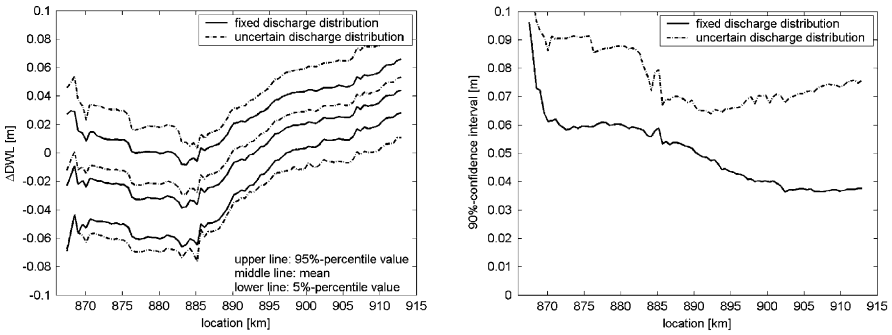

Figure 12. Spatial variation of the statistical properties of ΔDWL ($= DWL_T - DWL_{T0}$) along the Waal after a period T of 20 years for the reference situation with the fixed and the uncertain discharge distribution, respectively.

fixed-bed hydrodynamic model run of a computation period of 20 years a new discharge distribution is drawn from this statistical description.

The effect of this uncertain discharge distribution on the DWL predictions is shown in Figure 12. This figure shows the spatial distributions of the statistical properties of ΔDWL after 20 years, for the fixed and the uncertain discharge distributions, respectively. On average, ΔDWL for the uncertain discharge distribution is slightly larger than that for the fixed distribution. The variation in ΔDWL, however, is significantly enhanced by the uncertainty in the discharge distribution, up to more than 10 cm.

4.6. EFFECTS OF RIVER IMPROVEMENT MEASURES

Floodplain lowering in combination with summer levee removal seems to enhance the morphological variability as compared with the reference situation with dike reinforcement. The flood protection measure leads to an increase of the flood conveyance capacity, hence to a reduction of the DWLs.

Clearly, if the measures are effective, the exceedance probability of the water level will come down. This results in a significant decrease of the design water levels as compared with the reference situation. A second order lowering of DWLs is due to the long-term general scour that comes with the tilting of the river Waal. The combined effect is much stronger than that of the increased morphological activity induced by these measures.

5. Conclusions and Recommendations

With the introduction of the new flood protection policy Room for the River, the reduction of flood levels will be achieved by measures increasing the discharge capacity of the river by increasing its cross-sectional area. Our analysis of the morphological impact of floodplain lowering in combination with summer levee removal shows a significant effect on the morphological activity in the Dutch river Waal. Monte Carlo simulation reveals that not only the morphological response is much stronger, also the uncertainty involved with morphological predictions increases (on average with 22%).

Given this uncertainty in the predictions of the morphological evolution, the question arises to what extent the computation of design water levels with a fixed-bed hydrodynamic model based on the present state of the river is appropriate. Three phenomena of morphological uncertainty are considered. The effects of seasonal morphological variations turn out to be negligible. The other two phenomena (long-term spatial variation over years and the morphological variability near the bifurcation point) appear to have a larger effect on the computed design water levels (order of magnitude 0.05–0.1 m). Absolutely speaking, this is still rather small, given the other uncertainties in the model and those in the determination of the design discharge. These will add up to the uncertainty, so the values found here are at best an indication of the lower bound. It is recommended to investigate the impact of other sources of uncertainty that contribute to uncertainties in DWLs. Amongst others, the uncertainty involved with the hydraulic roughness predictor is expected to have a significant effect, since it affects both the hydraulic and the morphodynamic computations.

The uncertainty ranges found here are not so small as compared with the centimetre-accuracy claimed for the design water levels for the assessment of the flood defences. In the Netherlands, there are plans to spend millions of Euros to river improvement measures that reduce the design water level by a few centimetres. The present analysis puts this into perspective.

Acknowledgements

The work presented herein was mainly done in the framework of the project "Stochastic modelling of low-land river morphology no. DCB 5302" founded by the Foundation for Technical Sciences (STW), and, as far as the third author is concerned, as an MSc-thesis project at Delft University of Technology. The authors wish to acknowledge the Institute for Inland Water Management and Wastewater Management (RIZA) for the permission to use the Rhine model. They also would like to thank H. Havinga of the Ministry of Transport, Public Works and Water Management and H.J. Barneveld of $HKV_{CONSULTANTS}$ for their valuable inputs into this project.

References

Dahmen, E. R. and Hall, M. J.: 1989. *Screening of Hydrological Data. Tests for Stationary and Relative Consistency*. ILRI (International Institute for Land Reclamation and Improvement Publication) Vol. 49. Wageningen, The Netherlands. ISBN 9070754 231.

De Vriend, H.: 2002. Model-based morphological prediction: From art to science. In: Vol. 2, D. Bousmar and Y. Zech. A. A. (eds), *Proceedings of River Flow 2002*, Balkema Publishers, Rotterdam, pp. 3–12. ISBN 905809 509 6.

Duits, 1997. *Dredging Optimisation in River Bends*. Delft University of Technology and HKV Consultants, report P086, Delft [in Dutch: Baggeroptimalisatie in rivierbochten].

Flood Protection Act, 1995. [in Dutch: Wet op de Waterkering, 21 december 1995].

Hammersly, J. M. and Handscomb, D. C.: 1964. *Monte Carlo Methods*. Methuen & Co., London.

Jansen, P. Ph., Bendegom, J., van den Berg, J., De Vries M., and Zanen, A.: 1979. *Principles of River Engineering, The Non-tidal Alluvial River*. Delftse Uitgevers Maatschappij, 509 p. ISBN 90 6562 146 6.

Jesse, P. and Kroekenstoel, D. F.: 2001. 1-D *Morphodynamic Rhine Branches Model*. RIZA report 2001.040. [in Dutch: 1-D Morfologisch Sobek Rijntakken model]. ISBN 9036953952.

Parmet, B. W. A. H., Van de Langemheen, W., Chbab, E. H., Kwadijk, J. C. J., Diermanse, F. L. M., and Klopstra, D.: 2002. *Design Discharge of the Rhine at Lobith*. report 2002.012. [in Dutch: Analyse van de maatgevende afvoer van de Rijn te Lobith]. ISBN 9036954347.

Silva, W., Klijn, F., and Dijkman, J.: 2001. *Room for the Rhine Branches, Summary of Research Results*. RIZA and WL|Delft Hydraulics. ISBN 9036953871.

Van der Klis, H.: 2003. *Uncertainty Analysis Applied to Numerical Models of River Bed Morphology*. PhD thesis. Delft University of Technology, Delft, The Netherlands. ISBN 90-407-2440-7.

Van Vuren, S. and Van Breen, L. E.: 2003. Morphological impact of floodplain lowering along a low-land river: a probabilistic approach. In: Korfiatis, G. and Christodoulou, G. (eds), *Proceedings of the XXX IAHR Congress, August 2003, Thessaloniki, Greece – Theme D Hydroinformatics and Advanced Data Technology in Engineering Practice*, pp. 191–200. ISBN 960-243-598-1.

Van Vuren, S., Kok, M., and Ouwerkerk, S. J.: 2003. Impact of river morphology on extreme flood level prediction: A probabilistic approach. In: *Proceedings of the European Safety and Reliability Conference 2003*, June 2003, Vol. 2. Maastricht, The Netherlands, pp. 1653–1662. ISBN 190 5809 595 9.

Van Vuren, S., Van der Klis, H., and De Vriend, H.: 2002. Large-scale floodplain lowering along the River Waal: A stochastic prediction of morphological impacts. In: Vol. 2, D. Bousmar and Y. Zech. A. A. (eds), *Proceedings of River Flow 2002*, Balkema Publishers, Rotterdam, pp. 903–912. ISBN 905809 509 6.

Natural Hazards (2005) 36: 103–123

National Floodplain Mapping: Datasets and Methods – 160,000 km in 12 months

KATE BRADBROOK[1,★], SIMON WALLER[1] and DAVE MORRIS[2]
[1]*JBA Consulting, South Barn, Broughton Hall, SKIPTON, North Yorks BD23 3AE, UK;*
[2]*Centre for Ecology and Hydrology, Maclean Building, Crowmarsh Gifford, Wallingford, Oxon OX10 8BB, UK*

(Received: 17 November 2003; accepted: 30 June 2004)

Abstract. This paper describes two projects requiring production of national floodplain maps for England and Wales – some 80,000 km of river. The novel solutions developed have brought together a national Digital Elevation Model (DEM), automatically-generated peak flow estimates at intervals along the watercourses and two alternative methods of calculating the outlines: normal depth calculation; and a purpose-built 2-dimensional raster-based floodplain model, JFLOW. The DEM was derived using Interferometric Synthetic Aperture Radar (IFSAR) techniques and has a vertical precision of ±0.5 m–1.0 m (RMSE) and a 5 m horizontal resolution. The flow estimates were derived by automating Flood Estimation Handbook (FEH) techniques. The normal depth calculations are applied at a number of discrete cross-sections with linear interpolation between to form a 3-dimensional water surface. This is overlain on the DEM to produce the flood outline. Careful manual checking is required at a number of stages. The JFLOW model is based on a discretised form of the 2-dimensional diffusive wave equation and directly simulates the flood outline in a series of overlapping short (1 km) reaches. Flood outlines from the overlapping reaches are merged to produce the overall flood envelope. The model has been written to work as a screen-saver, allowing distributed processing across all computers in an office and manual intervention is minimal. In simple valley situations both methods give similar results, but show differences in more complex areas. Each has advantages and disadvantages, but both have been shown to be a practicable solution to allow production of 160,000 km of flood outline in 12 months.

Key words: automated floodplain mapping, 2-dimensional raster model, normal depth calculation, flood estimation handbook, synthetic aperture radar

1. Introduction

The UK has suffered widespread flooding in recent years, notably in Easter 1998 and autumn 2000. This has raised the profile of flooding in the country, particularly in the insurance sector and has resulted in a re-evaluation of provision of flood insurance. This is currently included as part of normal household cover. In future insurers may have the option to increase or refuse premiums for high risk properties. Additionally, new Government planning

★ Author for correspondence. E-mail: kate.bradbrook@jbaconsulting.co.uk

guidance in England and Wales increases the significance of flooding as a material consideration in planning applications. The planning guidance, PPG25 (DTLR, 2001), requires the Environment Agency of England and Wales to produce flood zones in order to facilitate the application of these new policies. The flood zones will show the nominal 0.1% flood outline (1 in 1000-year flood), outside of which flooding will not form a constraint on development, and the 1% flood outline (1 in 100-year flood), inside which development may only take place under special circumstances. In general, these outlines will be used as screening tools to trigger further, more detailed studies, for individual development plans. This paper discusses two projects to produce national flood outlines: one for the insurance company Norwich Union and one for the Environment Agency. The aim of the paper is to report on the challenges that had to be overcome in deriving practicable methods for these projects and to compare the similarities and differences between them.

The current understanding of national flood risk is represented by the Indicative Floodplain Map (IFM), which is held by the Environment Agency and published on the Internet (www.environment-agency.gov.uk). This dataset is a compilation of: (i) historic flood outlines; (ii) the results of detailed local studies; and (iii) a comparatively low resolution nationwide flood outline produced in 1996 by the then Institute of Hydrology (now Centre for Ecology and Hydrology). This nationwide outline is known as IH130 after the report describing its generation (Morris and Flavin, 1996). The 100-year flood depth was calculated using catchment characteristics (area, rainfall and soil) for every point on the river network where the catchment area exceeded 10 km^2. This was translated into a flood outline using a ground model with a 50 m grid spacing. This was the first time that a nationwide outline had been attempted, but the relatively coarse spatial resolution has resulted in areas shown at flood risk that are in fact well above the river channel. Similar problems result from use of some of the historical outlines which were also based on records held on relatively low resolution mapping (e.g., 1:50,000). In addition, the return period of the historical outlines is not always known.

The aim of the studies reported in this paper was to improve the understanding of national flood risk through the application of consistent flow and ground data and methods across the country. The resulting outlines needed to offer a substantial improvement on the early generalised models (e.g., IH130) whilst giving reasonably close matches in known flood risk areas to outlines from historic floods or more detailed studies. Detailed modelling on a national scale is not possible. Such studies typically cost several thousand euros per km of river channel and a study covering a 50 km reach would usually take over 12 months to complete. The studies that are the topic of this paper needed to provide national coverage at more than one return period in

approximately 2 years (including development) with costs of only a few euros per river km.

The data requirements for producing a flood outline are: (i) a ground model; (ii) flood flows; and (iii) a method to relate flow to water depth. The challenge was to find an appropriate level of detail that uses datasets which could be obtained on a national scale and processing techniques that were practicable within the required timescales.

2. Ground Model

The ground model must provide a spatial description of elevation in valley bottoms so that a particular water level can be related to a flood extent. Because typical errors of estimation of ground elevations in floodplains in existing national DEMs were greater than errors of estimation of flood depths, the choice of DEM was likely to have the largest impact – larger than that of the choice of flow estimation or flood modelling methods – on the final flood outlines. In terms of national scale mapping there were three options: (i) use the best existing data at each location resulting in a ''patchwork'' of data quality; (ii) use an existing national dataset; or (iii) purchase a new national dataset.

Either option (ii) or (iii) was favoured in order to provide consistency across the country. In the UK, the best existing national data set was Ordnance Survey (OS) 'Profile' data. This has been built up over a long period from a variety of data sources and has been stored as contour lines with a 5 m elevation interval. The vertical precision of the original data sources is quoted as ± 1.5 m, but the interpolation required to produce a ground model grid introduces additional errors. The fact that the DEM has been derived from contour lines also leads to a noticeable lack of detail in valley bottoms and both the valley lateral and long profiles tend to be flatter than in reality. For flood outlines, the topographic data in the valley bottoms is particularly important. Pilot studies with the OS Profile data suggested that as soon as the flow was out-of-bank, the full extent of floodplain was inundated and there was little variation in flood extent for different flow depths.

A new ground model was therefore procured. For national coverage, a remote sensing technique was a prerequisite, and most such techniques (e.g. SAR, LiDAR, satellite systems) have a trade-off between coverage, which is related to flying height for airborne systems, and accuracy. The DEM used is known as NEXTMap Britain and was derived by Intermap Technologies Corporation (Intermap) using Interferometric Synthetic Aperture Radar (IFSAR), an airborne remote sensing system. This gives nationally consistent coverage at a particular time (the data collection took place over a three month period). The data are supplied on a 5 m grid with a stated vertical RMSE of 0.5 m or 1.0 m (the better precision is obtained in south-east

England due to lower flying heights). An orthorectified image (ORRI) is also produced.

A feature of remotely-sensed elevation data is that the Digital Surface Model (DSM) produced by the imagery generally includes vegetation and buildings. This can cause problems for flood modelling: for example a bridge could appear to be a barrier to flow, and a woodland area would seem to be elevated above the floodplain. (A DSM can sometimes be used to good effect at high resolution, particularly in urban areas, but the 5 m resolution of the NEXTMap DSM would not adequately distinguish flow paths between buildings and trees.) To get around this, flood modellers often use a bare-earth model in which vegetation and man-made objects are removed by using a variety of filtering techniques. Intermap have developed software, TerrainFit®, to derive a bare-earth model automatically (e.g., Coleman, 2001). Whilst this is convenient for the modeller and facilitates smooth running of the models, in some circumstances it can create far greater flood extents (for example if an embankment is removed that actually acts as a flood defence). A compromise used by NEXTMap Britain is to supply a version of the ground model that includes major embankments and flood defences. These are defined as structures that are clearly 'visible' in the terrain model (a subjective criteria) or shown on OS 1:50,000 scale mapping. Editors ensure a continuous embankment surface, interpolating levels where a point may have missed the top of the embankment. The line is only broken where there are clear flow path openings (e.g., watercourse and road bridges) but this will not pick up smaller culverts or underpasses. Similarly, smaller flood defences, which are not included in the original DSM, will not be shown.

Other special measures were required along the watercourse. The conveyance in and around the channel represents a significant proportion of the capacity of the entire floodplain. IFSAR does not receive a return from surface water and where data are missing (generally for watercourses >25 m wide), the editing process imposes a flat surface within the channel banks. The level of this surface is generally below the lowest river bank but is artificial and includes steps in the downstream direction. Any approach to modelling therefore needs to take account of the conveyance of the channel and the artificial channel shown in the DEM. This poses a challenge to the modelling which is discussed below. Similarly, in many locations the watercourse may be obscured by woodland or culverts. The first of these situations causes real problems for modelling since the filtering process removes trees but the resulting ground profile may not reflect the true valley profile. As yet there are no real solutions, even with manual editing, which will adequately reproduce the true ground profile in areas where the remote sensing has been unable to see enough of the ground. In such areas, the flood outline may not be as accurate as in other locations.

3. Flow Estimates

Nationwide estimates of T-year flood peaks were produced by CEH using an automated version of the UK's standard method, the FEH statistical procedures (Robson and Reed, 1999). The procedures had been automated primarily as a means of assessing their performance (Morris, 2003) with the secondary objective of creating network-wide flood estimates for use in flood risk mapping. This part of the paper summarises the procedures, and explains how they were automated to produce estimates of flood peaks for return periods of between 2 and 1000 years at four million locations on the UK river network.

3.1. THE FEH STATISTICAL PROCEDURES

The FEH statistical procedures enable the T-year flood peak to be estimated at almost any location (*subject site*), gauged or ungauged, on the UK river network. They comprise two main, and independent, procedures: the estimation of (i) an *index flood*, the median annual flood (QMED); and (ii) a *growth factor*, the ratio of the T-year flood to the index flood.

At an ungauged site QMED is initially estimated from a regression equation that takes into account catchment area, annual average rainfall, soils properties, and the effects of reservoirs and lakes. For non-rural catchments ($>2.5\%$ urbanised) this is increased by an urban adjustment factor (UAF) based on urban extent and catchment permeability. This catchment descriptor based estimate is known as $QMED_{CD}$.

Because $QMED_{CD}$ is known to be considerably less reliable than QMED estimated from gauged floods ($QMED_{obs}$), it is adjusted where possible using data from similar gauged catchments. The most reliable adjustments come from what are termed *donors*, gauging stations that are upstream or downstream of the subject site or on adjacent similar tributaries. More distant catchments, termed *analogues*, may also be used. $QMED_{CD}$ at the subject site is adjusted by multiplying it by $QMED_{obs}/QMED_{CD}$ (the *adjustment factor*) from the donor/analogue site. Occasionally the adjustment is based on two or three donors or analogues. At gauged subject sites, QMED is usually estimated directly from the gauge record.

Growth factors at ungauged sites are estimated from hydrologically-similar gauged catchments, which must be rural and have at least eight years of data. Similarity is quantified in terms of nearness in a three-dimensional space whose axes are based on catchment size, wetness and soils. For the T-year growth factor the 'closest' gauged catchments to give a combined record length of at least 5T years are used. This set is termed the *default pooling-group*. The user may revise it to take into account other factors such as lakes. Weighted averages of moments of the distribution of annual floods at the pooling-group sites are used to define the parameters of a selected statistical distribution (usually the generalised logistic). This is used to estimate growth factors at the subject site.

For subject sites with non-rural catchments the estimated growth factors are reduced by a factor that ranges from UAF at $T = 1000$ down to 1.0 (no reduction) at $T = 2$. Together with the urban adjustment to QMED the net effect on the T-year flood ranges from none at $T = 1000$ (when urbanisation is considered unlikely to affect flood peaks) up to a factor of UAF at $T = 2$.

For gauged subject sites, T-year growth factors may be estimated from the gauge data alone, provided that the record length is at least $2T$, (termed *single-site analysis*). A combination of single-site and pooled analysis is recommended for sites with a record length in the range T to $2T$. If needed, flood volume can be estimated using a standard hydrograph profile with a time-to-peak estimated from catchment descriptors.

The FEH statistical procedures superseded those of the Flood Studies Report (FSR) (NERC, 1975), bringing the following benefits: a more robust index flood (FSR used the mean, which is more influenced by extremes); national methods for index flood and growth factor estimation, eliminating inconsistencies caused by regional boundaries; ability to use new flood data as they become available; stations for estimating flood growth selected on hydrological, not geographical criteria; and analyses based on digital spatial datasets, promoting ease and consistency of use. The principal limitation of the statistical procedures for this application is that they are not recommended for use on catchments that are strongly affected by lakes or reservoirs or are heavily urbanised (a small minority of locations), where a rainfall-runoff modelling approach is preferred. An allowance has been made for the former (see below), but the effects of using the method in heavily urbanised catchments have not been quantified. It is expected that estimates from an automated FEH rainfall-runoff model will be available for use in future projects.

3.2. AUTOMATING THE FEH STATISTICAL PROCEDURES

Three procedures have been automated: the computation of $QMED_{CD}$; the determination of the donor/analogue adjustment; and the estimation of growth factors. Initial results were produced using automation in strict accordance with FEH procedures, but these were subsequently revised following identification of problems in the original results. Flood estimates using both the original and revised procedures have been produced for most of Great Britain. Values have been computed at every point where the catchment area is greater than 0.5 km^2 on the drainage network derived from the CEH integrated hydrological digital terrain model (IHDTM) (Morris and Flavin, 1990), which has a grid interval of 50 m.

Often the revisions were introduced to promote *spatial coherence* – to minimise the incidence of adjacent estimates that are clearly inconsistent. Whilst spatial coherence does not indicate correctness, spatial incoherence

does indicate incorrectness, and so, other factors being equal, a set of estimates that is spatially coherent is preferable to one that is not. For example, the revisions aim to ensure that the influence of any one gauging station varies gradually with distance along a river reach.

Network-wide computation of $QMED_{CD}$ was straightforward, as values of the required FEH catchment descriptors were available at every grid point. To maintain spatial coherence the urban adjustment was no longer truncated where catchment urbanisation fell below 2.5%. Instead, it was allowed to taper off smoothly. This eliminated a step in QMED of up to 53% on permeable catchments.

Two problems were encountered when network-wide adjustment factors were derived from donors and analogues selected in accordance with FEH guidance. Firstly, at locations on a river reach where a donor or analogue ceased to apply (because the difference between its catchment and that of the subject site exceeded the FEH suggested limits) there could be a step in the adjustment factor that resulted in a large rise or fall in QMED. Secondly, at over 60% of locations, there were no qualifying donors or analogues. Major revisions were needed to overcome these problems. These included relaxation of the similarity criteria for donor/analogue selection, used in combination with a gradual moderation of adjustment factors so that they did not suddenly cut in or out; the use of up to seven donor/analogues with gradually varying weights based on similarity to the subject site and relative position on the river network; and capping the influence of analogues and donors that were not upstream or downstream of the subject site. These changes led to a marked improvement in spatial coherence, and at least one donor or analogue at over 85% of subject sites, and were further vindicated when they were shown to reduce estimation error (see Section 3.3). (The automated adjustment procedure ensured that, at gauged sites, $QMED = QMED_{obs}$).

When network-wide growth factors were estimated using default FEH pooling-groups for a range of return periods from 5 to 1000 years two problems were apparent. There were unjustifiable steps in growth factors within river reaches, and numerous locations where the T-year growth factor was lower than that for a lesser return period. The former were eliminated by improving the station weighting method and including at least ten stations in a pooling-group (FEH pooling-groups for short return periods often consisted of just one or two stations). The latter were mainly due to using a different pooling-group for each return period, although some occurrences were traced to the effect of the urban adjustment. They were eliminated by using a single pooling-group for all return periods (the 200-year pooling-group was adopted as it was considered that anything much larger would lead to excessive averaging of growth-curves) and revising the growth-factor urban adjustment (whilst retaining the end-point properties at $T = 2$ and 1000 described above). The generalised logistic distribution was used at all

times. (In the automated method, pooling-groups were used at both gauged and ungauged sites.)

3.3. ACCURANCY AND APPLICABILITY OF THE AUTOMATED ESTIMATES

When assessed at 730 gauged locations, mainly in England and Wales, the estimated factorial standard error (fse) in $QMED_{CD}$ was 1.62. This fell to 1.56 after adjustment following FEH guidelines and 1.46 using the revised procedures. The latter figure implies that at approximately 68% of locations the QMED estimate will be within 0.68 times and 1.46 times the 'true' value. Growth factor estimation performance, assessed at 437 gauged rural UK catchments, ranged from an estimated fse of 1.2 for $T = 10$ increasing to 1.3 at $T = 50$. Due to the length of records at gauging stations, no assessment was possible for higher return periods. The revisions for spatial coherence had led to small improvements in accuracy.

As well as improving accuracy of estimation and spatial coherence within river reaches, the revisions also improved the consistency of flood estimates at confluences with, for example, the proportion of confluences displaying serious inconsistencies in estimated QMED (outflow QMED less than 90% of the highest inflow QMED, or greater than 110% of the sum of the inflow QMEDs) falling from 22% to 4%.

Whilst these automatically-produced estimates from the revised procedures are acceptable for input to regional flood risk models, it is important to note that they will not be as reliable as those produced for individual locations by an experienced hydrologist. Further, they should be used with particular caution at subject sites with heavily urbanised or reservoired catchments, where this method is not recommended.

It should be noted that the flow calculated at each flow point is for a unique event at that location of a particular probability of occurrence. This will be a slightly different event from the one which gives the same probability at neighbouring points. The combined dataset does not represent a single event that passes down a catchment, but a collection of individual events.

Similarly, the flow points produced from FEH were not explicitly related to each other. In order to calculate normal depth, knowledge of the location of each point within the network was required (because slope is taken from upstream and downstream directions). A semi-automated approach was derived to label the points within the flow network. The catchment area and distance to surrounding points was used to apply logic to a dendritic numbering system in which the river, reach and node point were combined to identify each point uniquely and its place in the river network for that catchment. This was manually amended in complex areas (e.g., where two rivers were close together).

The flow data is based on a 50 m grid whereas the DEM is a 5 m grid. It proved necessary to move automatically each of the 600,000 points to the

bottom of the valley as defined by the higher resolution DEM. Without doing this, both approaches would have produced distorted flood extents. For the JFLOW method, a hydrograph rather than just peak flows was required and a standard FEH design hydrograph shape was used. The shape of the hydrograph can be very important in low-lying areas where volume is a defining factor in flood extents. It also proved necessary to make adjustments to the hydrograph downstream of lakes to account for their routing effects on hydrograph shape.

4. Flood Outline Methods

The main difference in requirements of the two projects is that the Norwich Union project required outlines for six different return periods from the 10-year event to the 1000-year event, whereas the Environment Agency project only required the 100-year and 1000-year outlines. In addition, the Norwich Union project originally required flood depths only and not the full outlines, although the latter are now being produced. For these reasons, the two different methods have been used, but based on the same datasets, which allows comparison of the techniques.

The Norwich Union project uses Normal Depth, which – once cross-sections are set-up at the inflow points – allows flood depths to be quickly calculated for a range of peak flows. Subsequent generation of flood outlines requires interpolation of the water surface between the cross-sections and comparison of this with the ground model at intervening grid cells.

The Environment Agency project uses a 2-D Diffusion Wave Model (JFLOW) to route a flow hydrograph over a 1 km reach downstream of each inflow point and directly generate the flood outline for that point. Individual outlines from each point are then merged to produce the overall envelope of flooding.

4.1. CHANNEL CAPACITY

As discussed earlier, the shape of the channel below the banks is not included in the DEM and it was not possible to obtain a national dataset of such information. It was therefore necessary in both methods to make an assumption about the missing conveyance. Largely for pragmatic reasons in the absence of data, it was assumed that the bankfull channel capacity is equivalent to QMED (the flow with a 2-year return period). This is based on well-known geomorphological arguments regarding the magnitude and frequency of channel forming events (Wolman and Miller, 1960; Dury, 1976) and is similar to assumptions made in previous work (Morris and Flavin, 1996).

As flows increase above bankfull, the velocity of flow above the channel is likely to be greater than the adjacent flow on the floodplain, and this introduces complex shear and momentum transfer processes (Sellin, 1964; Knight, 1981). An assessment of possible ways of dealing with this in the JFLOW model is given in Bradbrook *et al*. (2004), which concluded that it was appropriate to adopt the simple solution of accounting for the missing channel area in the DEM by subtracting QMED from the flow estimate at each point before analysis. This solution is used for both methods. The limitations of this assumption will be most marked in areas where channel engineering has artificially increased the natural channel capacity. This is most likely in urban areas, and if sufficient data on channel capacity were available, appropriate adjustments could be made.

5. Normal Depth Method

The normal depth method is based on Manning's equation:

$$Q = \frac{AS^{1/2}R^{2/3}}{n} \tag{1}$$

where Q is flow (m^3/s), n is Manning's coefficient, A is flow area (m^2), S is slope, and R is hydraulic radius (m) which is given by A/WP where WP is the wetted perimeter (m). For a general application of Manning's equation, the slope would be the energy gradient. In a normal depth calculation the slope is set equal to the bed slope. This assumes that there is no backwater effect from downstream.

The calculation is applied at a cross-section, which is split into segments of an equivalent width to the DEM cell size (Figure 1). For a given water level, the flow area and hydraulic radius of each segment can be calculated. The wetted perimeter is given by the distance along the ground only: the boundary between flow segments is not included. A value of Manning's n was estimated for each segment based on landuse at that location derived from image analysis of the IFSAR data (DEM and orthorectified image). Analysis of texture of the orthorectified image, combined with calculation of the difference between the DEM and DSM (greater in areas with buildings or vegetation) was used to classify areas into one of 8 landuse types. These were assigned typical Manning's n values as shown in Table I. Manning's equation is applied to each segment and the resulting flow contributions from each segment are summed to give the overall flow for that water level. This process is repeated for a number of different water levels to produce a rating curve for the cross-section. The water level for a particular flow rate can then be derived by interpolation.

The inherent assumptions in this method include: (i) flow in all segments is moving perpendicular to the cross-section; (ii) the water level is

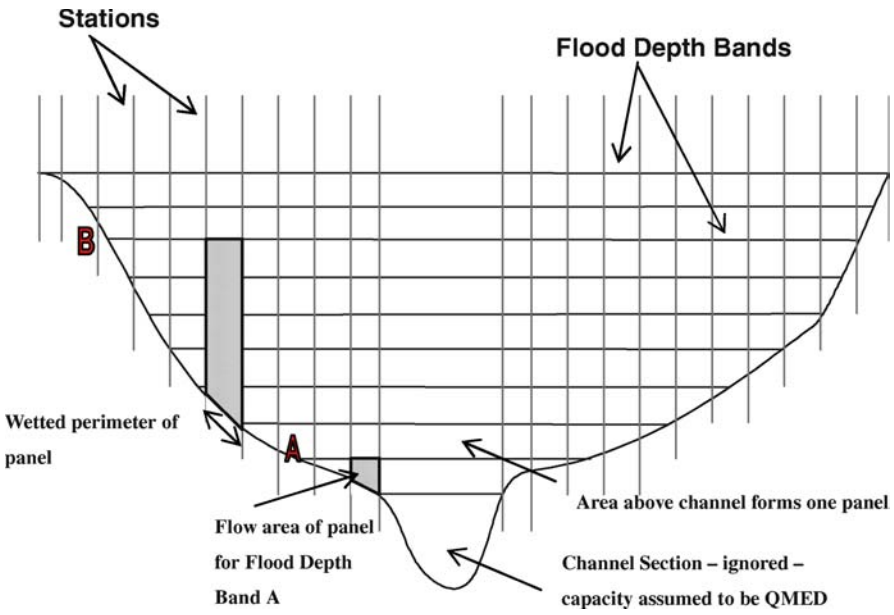

Figure 1. Normal depth calculation.

Table I

Landuse category	Manning's *n* value
Water	0.04
Grass	0.06
Moor	0.07
Crop	0.08
Urban	0.10
Forest	0.10
Dense forest	0.15

horizontal across the section and flow paths exist to fill parts of the section with a ground level lower than the water level but which may be separated from the inflow point by a ridge of higher ground; and (iii) there is sufficient volume of water to fill the cross-section to the normal depth level.

These assumptions lead to the observation that the definition of the cross-section has an overwhelming influence on the normal depth calculated. For example, if the cross-section is not extended far enough, such that the water surface intersects with higher ground at the edges, then water

depths could be vastly overestimated. A slight change in orientation of the cross-section could lead to large changes in flow area for a given water level.

Derivation of the slope presents a challenge since the DEM only gives bank levels and not bed levels. The bank levels can have substantial local variation and it was therefore necessary to derive an average slope over approximately 4 km. This was achieved automatically by using the network numbering and extracting bank levels at the point 10 sections away in both the upstream and downstream directions. This can still result in negative gradients in some low-lying areas so a minimum gradient of 1:10,000 was imposed.

The cross-sections defined consisted of three components: left floodplain; right floodplain; and channel. An automated tool was developed which sought to produce a 'first pass' cross section by recognising the average direction of flow within the floodplain, which could be different to that in the river. This was successful in small, well defined valleys but only provided a starting point elsewhere and 60% of the cross-sections needed manually refining. As discussed above, the definition of the cross-section is vital in defining the flood depth using the normal depth method.

The calculation of normal depth does not result in a smooth long profile of the water surface that constantly increases in elevation with upstream distance. The water surface rises and falls due to local changes in conveyance. In order to get sensible results it is necessary to impose a simple rule that stops water level from falling upstream. This is a simple representation of the backwater effect that would occur in reality, but does not take account of whether there is adequate volume to fill the cross-section or of attenuation. At some sections, the water surface calculated is so high that it is necessary to ignore these results as they would result in unrealistic levels upstream. Identification of these is subjective, but undertaken within a quality-assurance (*QA*) software environment. Once identified, these values are removed and the water level from downstream is carried upstream. This gives a horizontal water surface gradient over short distances (200 m), which, whilst it may not be locally realistic (except in strong backwater situations), results in more reasonable long profiles for the reach as a whole.

The QA software (Figure 2) enables users to view valley long sections and cross-sections within a mapping environment along with their automatically produced rating curves. A number of automatic checks were incorporated in order to assist the user in assessing whether a valid normal depth has been created. Once the long sections have been passed in the QA environment, the resulting water surface is imposed on each of the sections. Using standard GIS software a 3-dimensional water surface is created using linear interpolation between sections. The ground level from the DEM is then subtracted

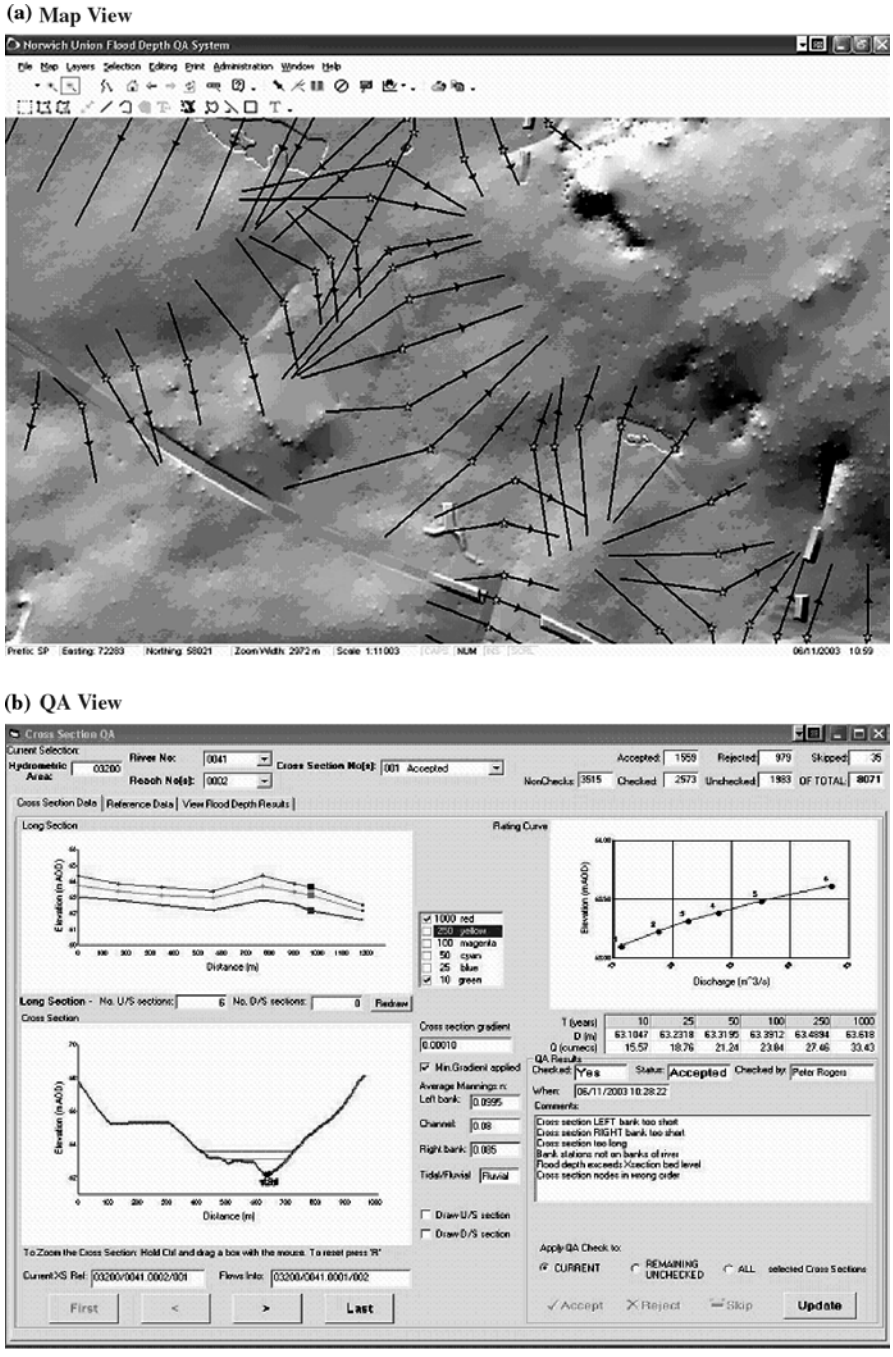

Figure 2. QA environment for normal depth calculations.

from this surface to give a grid of flood depth from which polygons defining the flood extent are derived.

Further manual checking of the outlines is then carried out to ensure that they are representative of flooding. For a large catchment (15,000 km of river), it may take a week to check the cross-sections. Due to its importance, checking of the cross-sections is fairly labour intensive, but once this has been completed, the normal depth for flows of a number of different return periods can be calculated very quickly, requiring only a few hours per catchment. Further checking of the normal depth calculations using the QA software may then take a further 2 weeks. Generation of the 3-D water surface and flood outlines can require overnight processing for each return period. A further 2 days would then typically be spent checking the first flood outlines to ensure that the result is realistic.

6. 2-D Diffusion Wave Modelling

In cases where flow is relatively shallow, topographically-driven 2-dimensional diffusion wave models have been shown to provide similar quality answers to fully-hydrodynamic 2-dimensional models (e.g., Horrit and Bates, 2001), but require fewer computational resources. In deeper flows, inertial terms, missing from the diffusion wave equation, become more important. Thus such models are ideal for simulating floodplain flows, but not within-channel flows. 2-D difffision wave models are becoming increasingly recognised as useful tools for use along with digital elevation models to predict flood extents (Wicks *et al*., 2003).

The JFLOW model uses a discretised form of the 2-dimensional diffusive wave equation, which can be represented by a 2-dimensional application of Manning's Equation (1) between grid cells (Figure 3), coupled with the continuity equation applied to each grid cell. The slope is the local water surface slope between grid cells. The model is described in more detail in Bradbrook *et al*. (2004), along with validation tests. That paper showed that the model could simulate flow at 45° to the grid cells, but nevertheless the model domain for each inflow point was extracted from the overall DEM so that the flow grid was approximately orthogonal to the main valley direction (Figure 4).

A hydrograph is applied at the upstream end of the model domain. As the flow increases, the water spreads out according to the topography and water surface gradients (Figure 4). As the flow decreases, the water will drain back towards the low points in the topography and the depths will reduce. A depth in each grid cell and the overall flood outline is calculated every timestep, but usually just the maximum depth and extent are recorded.

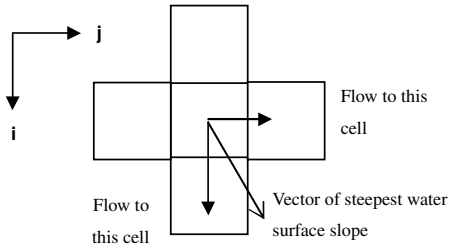

Figure 3. Flow between floodplain nodes in JFLOW.

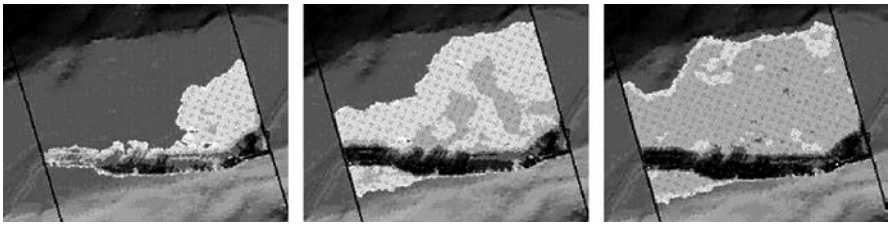

Figure 4. Floodwave progression in JFLOW (screen shots showing depth contours).

As a result of it being topographically driven, the model naturally accounts for all features in the DEM and calculates flow paths directly. This means that embankments will cause backing up, and flow will only cross over to lower ground behind a topographic ridge if there is a suitable low point in the ridge. Thus, DEM editing is more important than for the normal depth approach.

Special consideration was needed to develop such a model for application on a national scale. As discussed above, the flow value for each inflow point refers to a unique event occurring at that location. The flood outline associated with that event was therefore simulated at that point, and for a distance of 1 km downstream. A critical depth downstream boundary is imposed at the end of the 1 km reach. Since inflow points were generally at a 200 m spacing, the 1 km downstream distance will give an overlap with several other points (Figure 5). The outlines are merged to produce an overall flood envelope showing the largest flood extent at any one location. This approach helps automation of the process as: (i) a small portion of the DEM is extracted for each simulation, and processing of each individual point does not require large computational resources; and (ii) each inflow point can be processed independently, in any order and several can be processed at the same time.

The process of producing the flood depth grid is fully automated and runs as a distributed application, utilising all available computers on an office

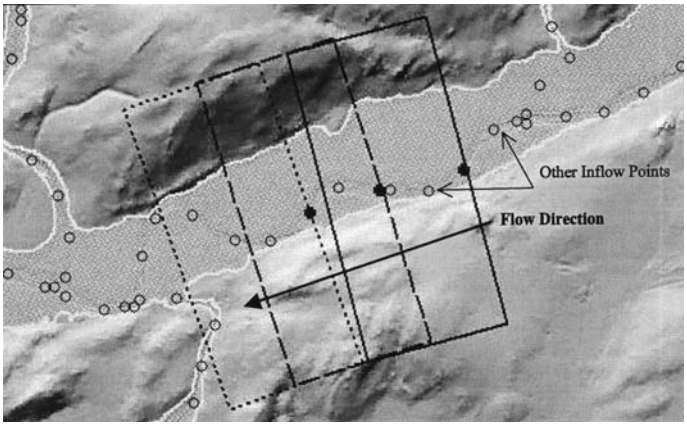

Figure 5. Calculation areas in JFLOW For 3 inflow points.

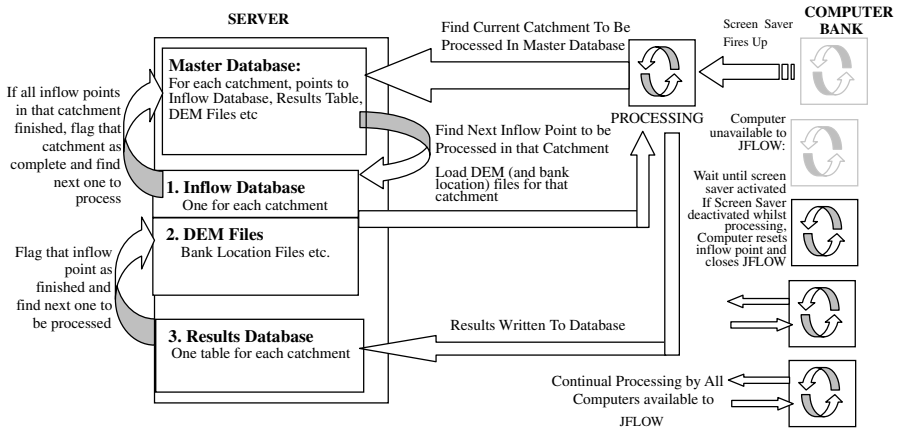

Figure 6. Distributed processing for fluvial extreme flood outline using JFLOW.

network. Figure 6 illustrates this operation. A central database holds details of all the inflow points to be processed with their hydrographs and grid file. The JFLOW application is written as a screen saver. When it is run, it interrogates the central database to find details of the next point to be processed. On finishing that point, the results are written to the central database and details of another point retrieved. A dedicated computer is used to produce the flood outline from the results for individual points once a full catchment is complete. A large catchment (15,000 km of river) may take 48 h of processing for 1 return period, running on 50 computers (20 full-time and 30 part-time only when screen saver activated).

7. Discussion

Table II summarises the main theoretical similarities and differences between the two methods as discussed in the previous sections. To assess the effect of these on the resulting flood outlines, Figure 7 shows the 1000-year flood outlines generated for part of the upper Severn on the English–Welsh border, to the west of Shrewsbury. Inset (a) around Welshpool is for a largely rural river in a well-defined valley. As would be expected, both methods give largely similar results. Inset B is for a broad area of floodplain at the confluence of the Severn and Vernwy rivers and Inset C shows the river Severn through the town of Shrewsbury. These are two of the most complex areas simulated and in these situations the two methods do show differences in results. For the normal depth calculations in particular, definition of cross-section orientation and width was particularly important in these areas and careful manual checking was used to improve the flood outline. In the simpler valleys upstream and downstream of these complex locations, the outlines from the two methods are similar.

For lower return periods, both methods have been validated against historic outlines within these study areas and elsewhere. In general the comparisons are good (e.g., see Waller *et al.*, 2003, Bradbrook *et al.*, 2004) and show that the outlines are realistic. Within Shrewsbury, both methods generally overestimated relative to historic outlines for the 100-year flow – this may reflect the fact that through this urban area, engineering works to the channel are likely to mean that its capacity is greater than QMED, or that the historic flood was smaller than the 100-year event.

Sensitivity tests on the Manning's value were undertaken for the 1000-year flood. Whilst the water depth showed sensitivity to Manning's n value (where a 30% increase in Manning's n gave an average depth increase of 0.2 m), this did not generally result in significant differences in flood outline. This is partly due to the 5 m horizontal resolution of the DEM but also because, in many locations, this extreme flood fills the valley bottom and is contained by steeper ground where increases in depth do not result in large changes in extent.

There are some circumstances where normal depth cannot be calculated. An example of this is where a tributary enters the floodplain of a larger river (e.g. A on Figure 7a). It is difficult to define a cross-section for the tributary floodplain. The normal depth would spread out over several kilometers if the cross-section perpendicular to the tributary flow direction were extended until it met high ground. There are similar problems in low-lying areas where flooding could be estimated to spread out a long distance whereas in a real event this may be limited by the volume of water.

The use of linear interpolation for the water surface can cause problems. Although the sections are closely spaced (200 m), the ground profile between sections may not be linear. This can result in gaps in the flood extent where

Table II

	Normal depth	2-D Diffusion wave
Manning's equation	1-D form applied to cross-section. Slope is bed slope	2-D form applied between each grid cell. Slope is local water surface gradient between cells
Water surface	Horizontal across section; interpolated between sections	Can vary between grid cells
Flow paths	Assumed flow paths to all points in section below water level	Calculated directly by model
Inflow	Peak flow only – assumed sufficient volume to fill section to normal depth level	Full hydrograph needed. Volume in hydrograph can limit flood extent in low-lying areas
Backwater	Independent levels calculated at each section assuming no backwater effects – subsequent adjustments are required in practice (Section 5)	Flood outline for event is simulated independently of other inflow points. Backwater effects can occur from constrictions in the topography but not from other inflow points
DEM features	Very sensitive to cross-section orientation and valley profile at cross-section location. Less sensitive to DEM features blocking flow paths.	DEM features blocking flow paths will cause backing up until water level is high enough to spill over feature

the ground profile is convex, or exaggerated depth and extent if the ground is concave. This is particularly noticeably in steep rivers where gaps can be quite commonplace (e.g., B on Figure 7a).

The checking of the JFLOW outline focuses on looking for modelling anomalies which largely fall into two categories. Firstly, where the flood extent has exceeded the flow simulation area, resulting in the flood extent exhibiting a straight line. These points must be re-run for a larger simulation area. Secondly, as in the normal depth calculations, where water surface peaks are caused by a local reduction in conveyance, a parallel effect in JFLOW can result in steps of several metres in depth in the floodplain between flow simulation areas. As with the normal depth calculations, the solution is to skip the results from certain inflow points. However some steps in the flood outline at overlap areas can remain. A full solution would require taking account of downstream water levels on the upstream flow simulation area. However this then violates the unique event assumptions. Another solution would be to use very long simulation areas, but then flow attenuation within the reach can become significant. The real answer to this problem in both methods may lie in the estimate of channel conveyance: at floodplain constrictions, it would be expected that the channel capacity and velocities are higher than where such constrictions do not exist.

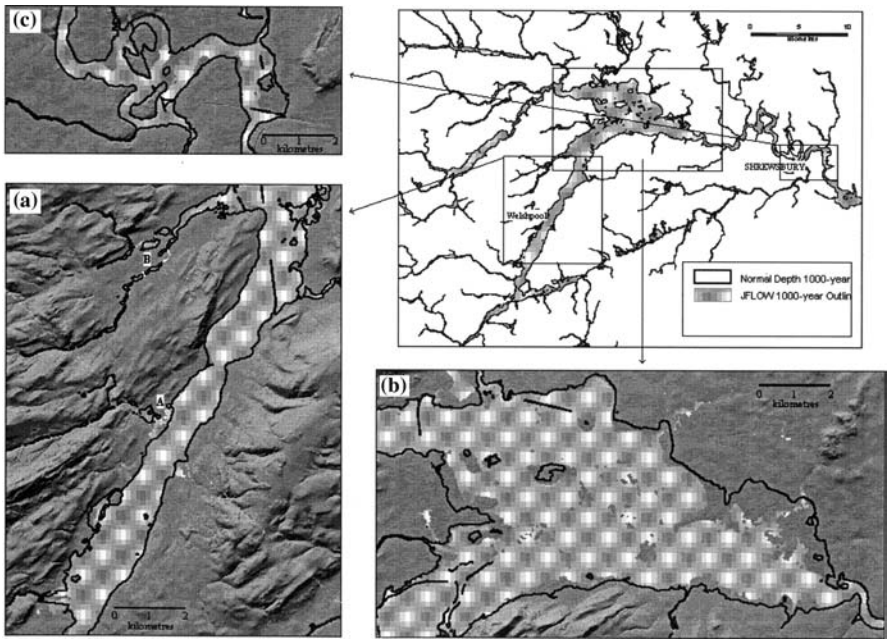

Figure 7. Results for the river Severn.

JFLOW results can also have problems in low-lying areas, where the 1 km simulation reach length may not be long enough for the water levels at the upstream end of the reach to be independent of the downstream boundary condition, and the flood outline can be strongly determined by the hydrograph volume. The assumed hydrograph shape is therefore critical to the final outline produced in such areas. This may explain why the JFLOW outline in Insets (b) and (c) in Figure 7 is generally smaller than the normal depth outlines. Alternatively, this may relate to choice of high water levels in the normal depth results that have been carried upstream as a backwater effect.

8. Conclusions

The datasets required to generate floodplain mapping are a high quality ground model and flow estimates. Errors in ground models have potentially a greater influence on the final flood outlines than uncertainties in the other components. The ground model used in this study was obtained using IFSAR and has elevations with a vertical RMSE of 0.5–1.0 m on a 5 m horizontal resolution. Use of such data for floodplain mapping requires preprocessing to remove vegetation and man-made features.

A national flow data set was obtained by automating the standard UK Flood Estimation Handbook techniques. These will not necessarily match detailed site-specific estimates made by experienced users but provide the coverage required for a national-scale mapping project. In future, improved flood peak estimates will become a available as a result of better and longer records of gauged floods, and further-development of the FEH procedures and their automation techniques.

Two methods have been developed to calculate flood outlines from the flow and ground data. In simple valley situations, they tend to give similar results. In complex situations such as major river confluences, particularly careful checking of cross-sections and water surface long profiles is required for the normal depth calculations, however this manual intervention stage can be used to ensure improved comparisons with any historical data. Both methods have their advantages and disadvantages but have been shown to be practicable in terms of processing over 160,000 km of river and produce realistic national floodplain maps within a timescale of approximately 12 months.

Acknowledgements

JBA consulting would like to acknowledge the help and support of Intermap Technologies Corporation, Norwich Union and the Environment Agency in these projects.

References

Bradbrook, K. E., Lane. S. N., Waller, S. G., and Bates, P.: 2004, Two dimensional diffusion wave modelling of flood inundation using a simplified channel representation, *J. River Basin Manage*. **2**, 211–223.

Coleman, D.: 2001, Radar Revolution: Revealing the Bald Earth, *Earth Observat. Mag*. November Issue, 30–33

Dury, G. H.: 1976, Discharge prediction, present and former, from channel dimensions, *J. Hydrol*. **30**, 219–245.

DTLR: 2001. *Planning Policy Guidance Note 25: Development and Flood Risk*. (Now available from the Office of the Deputy Prime Minister at www.planning-odpm.gov.uk.)

Horritt, M. S. and Bates, P. D.: 2001, Predicting floodplain inundation: raster-based modelling *versus* the finite element approach. *Hydrolog. Process*. **15**, 825–842.

Knight, D. W.: 1981, Boundary shear stress in smooth and rough channels, *J. Hydraul-Div*. ASCE, **107**, 839–851.

Morris, D. G.: 2003, *Automation and Appraisal of the FEH Statistical Procedures for Flood Frequency Estimation*. Report to DEFRA. CEH, Wallingford, UK.

Morris, D. G. and Flavin, R. W.: 1990, A digital terrain, model for hydrology. *Proceedings of the 4th International Symposium on Spatial Data Handling*. Vol. 1, July 23–27, Zurich, 250–262.

Morris, D. G. and Flavin, R. W.: 1996, *IH Report No. 130: Flood Risk Map for England and Wales,* Institute of Hydrology, Wallingford, UK.

NERC.: 1975. *Flood Studies Report* (5 volumes). Natural Environment Research Council. Reprinted 1993 with Supplementary Reports and additional bibliography. Institute of Hydrology, Wallingford.

Robson, A. I. and Reed, D. W.: 1999, *Flood Estimation Handbook, Volume 3: Statistical Procedures for Flood Frequency Estimation*. Institute of Hydrology, Wallingford, UK.

Sellin, R. H. J.: 1964, A laboratory investigation into the interaction between the flow in the channel of the river and that over its floodplain, *La Houille Blanche*, **7**, 783–801.

Waller, S. G.: Bradbrook, K. F.: Huband, M., Mitchell, G., and Gilkes, P.: 2003, *The Extreme Flood Outline*, *Proceedings of the 38th DEFRA Flood & Coastal Management Conference*, 07.2.1–07.2.11.

Wicks, J., Mocke, R., Bates, P., Ramsbottom, D., Evans, E., and Green, C.: 2003, *Selection of Appropriate Methods for Flood Modelling*, *Proceedings of the 38th, DEFRA Flood & Coastal Management Conference*, 09.2.1–09.2.8.

Wolman, M. G.: and Miller, J. P.: 1960, Magnitude and frequency of forces in geomorphic Processes, *J. Geolog*. **68**, 54–74.

Natural Hazards (2005) 36: 125–145

The Influence of Floodplain Compartmentalization on Flood Risk within the Rhine–Meuse Delta

D. ALKEMA[1,★] and H. MIDDELKOOP[2]
[1]*Department of Earth Systems Analysis, International Institute for Geo-Information Science and Earth Observation (ITC), P.O. Box 6, 7500 AA Enschede, The Netherlands;* [2]*Department of Physical Geography, Faculty of Geographical Sciences, Utrecht University, P.O. Box 80.115, 3508 TC Utrecht, The Netherlands*

(Received: 12 November 2003; accepted: 30 June 2004)

Abstract. The present compartmentalization layout within the river polders in the Dutch Rhine–Meuse delta is the result of abandonment and partial removal of secondary dikes and the construction of modern infrastructure embankments. These structures will guide the flow of water in case the polder would inundate. Through the application of a 2-D flood propagation model in the polder *Land van Maas en Waal* this study explores whether restoration or removal of old dike remnants would contribute to a reduction of the risk and damage during an inundation. A systematic set of 28 flood scenarios was simulated and for each scenario an additional damage and risk assessment was carried out. It is concluded that a simple removal or total restoration will not reduce flood damage, but that this must be achieved by a strategic compartment plan. With such a plan old dike remnants and present embankments can be used to keep water away from vulnerable and valuable areas for as long as possible and to guide the floodwater to areas that are considered less vulnerable.

Key words: flood risk, flood hazard, 2-D modelling, polders

1. Introduction

This study explores the role of historic and modern compartmentalisations on the potential damage resulting from inundation of river polders in the Rhine–Meuse delta. These polders are protected against river floods by primary dikes that are designed to prevent inundation for discharge peaks lower than the 1250-year recurrence time flood (or: annual probability of occurrence of 0.0008). For the Rhine this corresponds with a discharge of 16,000 m^3/s at the Dutch/German border and 3,800 m^3/s for the Meuse at the Dutch/Belgium border. However, since the magnitude of this design flood has to be determined by statistical extrapolation from a 100-year record of observations, there is a considerable uncertainty band around the estimated design discharge. Furthermore, it is anticipated that due to climate change,

★ Author for correspondence. E-mail: alkema@itc.nl

peak flows in the Rhine and Meuse might increase during the forthcoming century (Middelkoop *et al.*, 2001; Silva *et al.*, 2001). For this reason, water management in the Netherlands considers a "worst-case" scenario with an increase of the design discharge of the Rhine to 18,000 m^3/s and for the Meuse to 4600 m^3/s (Silva *et al.*, 2001). This rise in discharge implies that – when no measures are taken – the probability of overtopping or breaching of the dikes would increase as well and the safety of the polder and its inhabitants would fall below the required safety standard. Furthermore, there is a growing awareness that it is impossible to guarantee totally secure defence against floods: the inundation of river polders in the Netherlands therefore is no longer unimaginable. Recently, the option of using retention areas outside the present high-water bed of the rivers is considered as flood reduction measure (Silva *et al.*, 2001). Furthermore, the idea of appointing some river polders as temporary emergency retention basins has been put forward in order to alleviate flood risk in the densely populated and low-lying downstream parts of the Netherlands in case a flood higher than the design discharge would occur. To allow controlled flooding of certain polders, parts of the dike will be designed as spill-over that can withstand overtopping by large amounts of flood water without breaching. Before such decisions can be taken, the potential damage in different polders must be assessed, and measures to reduce damage in the eventual case of inundation must be thoroughly considered. This demands quantitative information on the hydraulic characteristics of the inundation process of a river polder, depending on the elevation, land use and the occurrence of embankments within the polder. These embankments subdivide a polder into different compartments, which greatly controls the rate and sequence of the inundation. The present-day compartmentalization of the polders consists of the remains of compartment dikes have been erected in historic times and embankment of modern infrastructure (highways, rail). Because of the effect of these embankments on the inundation, therefore, strategies to reduce the inundation damage of a polder should focus at the design of the compartmentalization layout to minimize the potential number of casualties and damage caused by the inundation.

The aim of this study was to determine the hydraulic characteristics (i.e., propagation rate, flow depth, inundation time) of the inundation of a river polder along the lower Rhine and Meuse rivers and the resulting damage, depending on the compartment layout of the polder. In addition to quantifying the effect of the present compartmentalization on the inundation propagation, we focused at assessing to what extent the inundation damage of river polders may be reduced by restoring the functioning of the old compartment dikes. For this purpose we simulated the inundation of a river polder using a two-dimensional flood propagation model for 28 inundation scenarios. The scenarios are based on a set of seven different dike-failures

including catastrophic breaches and controlled overtopping of different sections of the primary river dikes along the Waal and Meuse rivers, and four combinations of modern and (restored) historic topographic layouts of the polder. Each inundation scenario was evaluated by assessing the potential damage caused by the inundation. The study was carried out for the polder *Land van Maas en Waal*, located between the Waal (the largest distributary of the lower Rhine river) and the Meuse river (Figure 1).

2. Historic Background

By nature, the Rhine–Meuse delta is characterized by alluvial ridges with natural river levees intersecting low-lying back-swamps. During periods of increased river discharge these swamps were flooded and remained inundated for a long period due to poor drainage. The natural levees along the rivers consist mainly of sandy material and formed the natural higher ground in the area. When the first inhabitants entered the area, the levees were their natural choice for settlement and the starting point for the further development of the back-swamps. For protection against river flooding artificial mounds and dikes were constructed. The first dikes were built perpendicular to the natural levees, upstream from the settlement to divert the flood water around the settlement (Driessen, 1994). The enclosure of the river area by dikes was completed between the 13th and 14th century. To exploit the agricultural potential of the back-swamps, the drainage was improved by digging a network of canals. Also, compartment dikes were raised within the polders to control drainage, and in the event of a dike breach, to prevent areas from flooding. Between the 16th and 19th century, a polder system was created

Figure 1. Location of the study area.

surrounded by primary river dikes and with secondary dikes that formed closed compartments within the polder, each with its own drainage system of canals, sluices and pumps. The polder *Land van Maas en Waal* is a typical example of such a polder system (Figure 2). This defence system offered protection against smaller floods but it could not avoid that occasionally large floods overtopped or breached the primary river dikes (e.g., Driessen, 1994). During the onset of the flood, the system of compartments diverted the flow of the floodwater and delayed the propagation by forcing the water to fill up the polder compartment by compartment (Hesselink *et al*., 2003). This increased the time for evacuation and distributed the impact of the flood more evenly over the polder.

During the 20th century the condition of the main river channels and quality of the primary river dikes had greatly improved, and inundation of a river polder in the Netherlands has not occurred since 1926. As a consequence, the appreciation and valuation of maintaining a secondary defence system within the polders declined and many compartmentalization dikes were subject to neglect or were completely removed. Large-scale development of the polder, with rapid expansion of urban and industrial area and land reallocation contributed to their decline. Embanked infrastructure gradually developed as additional compartmentalizing elements within the polder. This started in the late 19th century with railway lines and progressively developed in the 20th century with the construction of highways and motorways. Although these embankments were not designed as flood barriers, they will play a significant role in directing the floodwaters in case of inundation. Viaducts and bridges will funnel water and create increased flow-velocities. With the

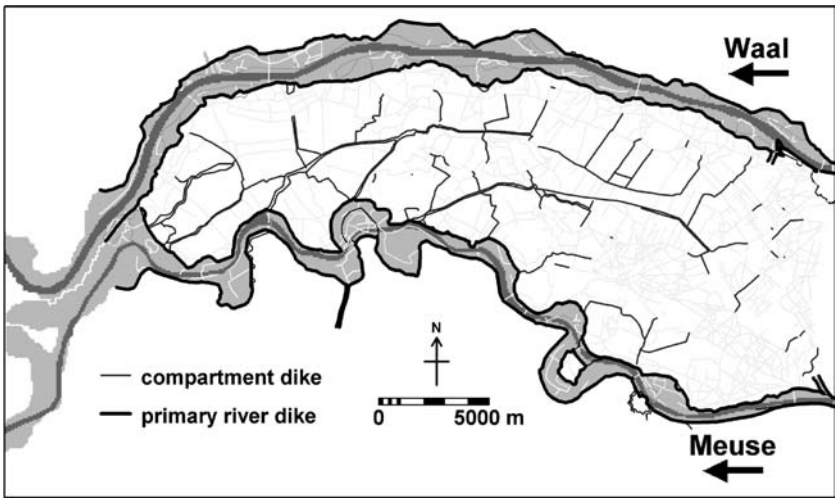

Figure 2. Historic map of the *Land van Maas en Waal* around 1850.

coinciding decline of the secondary dike system by end of the 20th century, the old compartment system was replaced by a non-systematic compartmentalization of the polder consisting of old dike remnants and new embankments.

3. Inundation Scenarios

The evaluation of the inundations was carried out for different combinations of failure of the primary river dikes and topographic layouts of the polder.

3.1. DIKE FAILURES

A dike failure can be either a catastrophic breach or a controlled overtopping of the dike at a predetermined spill-over location. In total seven failures were simulated at five locations, five spill-overs and two breaches. Three locations are along the Waal river and two along the Meuse (Figure 3). At Weurt and Overasselt, both a breach and an overtopping were simulated. The choice for the locations was based on three considerations: (1) they are distributed more or less evenly along the rivers, so that differences between the scenarios will become sufficiently apparent; (2) they are not located too far downstream because that would result in very small inundations; (3) they are positioned in between urban areas, because it would be unrealistic to construct a spill-over near a village. The location of Weurt for the breaching scenario was chosen because of the availability of historic data from the 1805 flood-reconstruction simulations carried out by Hesselink (2002).

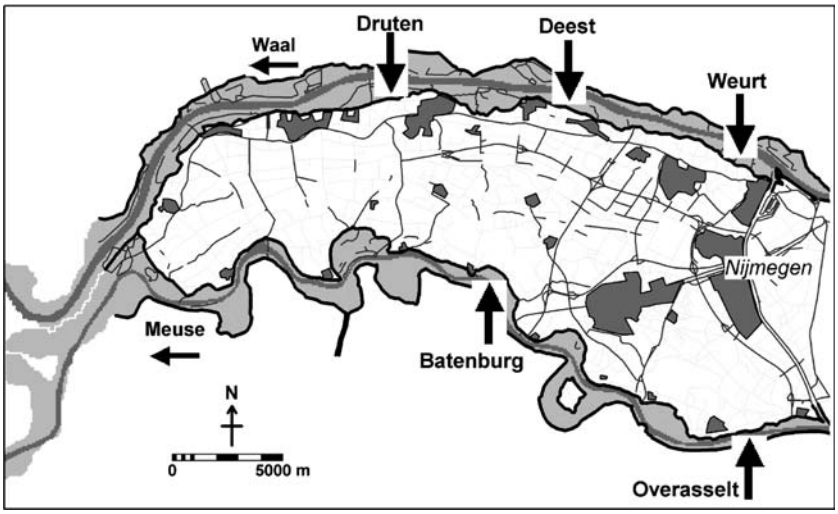

Figure 3. Location of the spill-overs and dike breaches.

3.2. SPILL-OVERS

The aim of a spill-over into a retention area is to cut off the peak of a flood wave in order to alleviate the flood risk in downstream areas. When compared to a dike breach, a spill-over allows controlled inundation over a predefined dike stretch, at an *a priori* known flood stage in the river. As no scour hole develops, the amount of water entering the polder depends on the river discharge and eventual technical means to reduce the level of the spill-over threshold. To optimize the effect of the spill-over on reducing the downstream river flood stages, the peak of the flood wave has to be cut off at exactly the right moment. In this study, we considered a spill-over that will be activated as soon as the present-day design discharge of the Waal and Meuse rivers are exceeded, which is 10,160 m^3/s and 3800 m^3/s, respectively. At that moment the threshold height of the dike is reduced by 20 cm over a width of 525 m for the Waal and 300 m for the Meuse.

3.3. BREACHES

The dimensions of the Weurt breach (i.e., gap width and scour hole depth, Figure 4) are based on the historic dike breach that occurred at this location in 1805. This flood disaster was reconstructed in detail by Hesselink (2002). The breach location along the Meuse river was selected near Overasselt since a dike breach occurred here in 1820 (Driessen, 1994), although this event was not documented and analyzed in the same detail as the 1805 flood. The dimensions of this breach and the scour hole were therefore not based on documentation, but on circumstantial evidence, like comparison with other Meuse dike breaches and shape of the reconstructed dike.

Apart from the ultimate dimensions of the dike breach, the rate at which the breach develops determines the amount of water flowing into the polder.

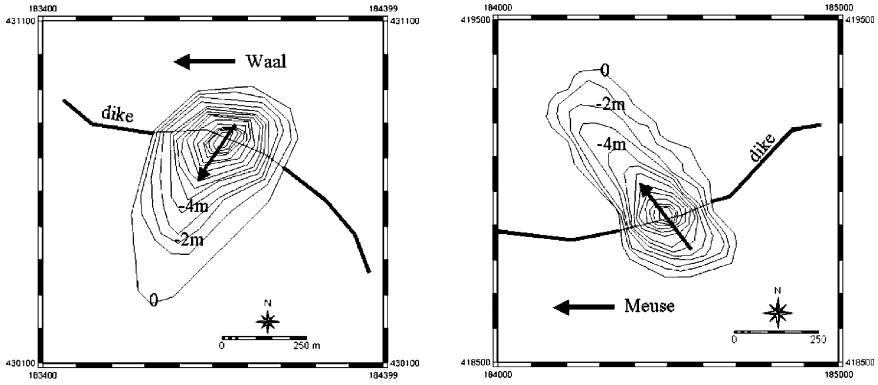

Figure 4. Dimensions of the dike breach near Weurt (left) and of the dike breach near Overasselt (right).

In this study, it was assumed that the final dimensions of the dike breach gap and scour hole were reached 3 h after the dike collapsed.

3.4. TOPOGRAPHY

Four different lay-outs of the polder interior were constructed, based on: (A) a current Digital Terrain Model provided by the Province of Gelderland (Van Mierlo *et al.*, 2001) and (B) on the DTM of the polder as it was in the first half of the 19th century, reconstructed by Hesselink (2002) with a complete compartmentalization (Figure 5). The historic DTM is based on 35,868 elevation points measured between 1950 and 1965 (before large land levelling and re-allocation schemes had taken place), complemented with data from a land survey carried out along five transects in the beginning of the 19th century and dike-height measurements carried out in 1801. The current DTM is derived from a laser-altimetric survey with a vertical accuracy of a few centimetres. Comparison between the topographic maps of 1850 and 2000 showed which former secondary dikes had disappeared and which remnants had survived. A field survey provided information of the height of these elements and of the embankments of modern infrastructure. For modelling purposes a grid size of 75 m was chosen and a check with elevation points derived from the topographic map showed that vertical accuracy was within 10 cm for 90% of the control points. The four different layouts are (Figure 6).

A: Present situation, including dike remnants and modern embankments (present);
B: Present situation with all remnants removed (cleaned-up);
C: Present situation with the 1850 compartmentalization complete restored (restored);
D: Present situation with strategic adaptations to protect vulnerable (urban) areas (strategic).

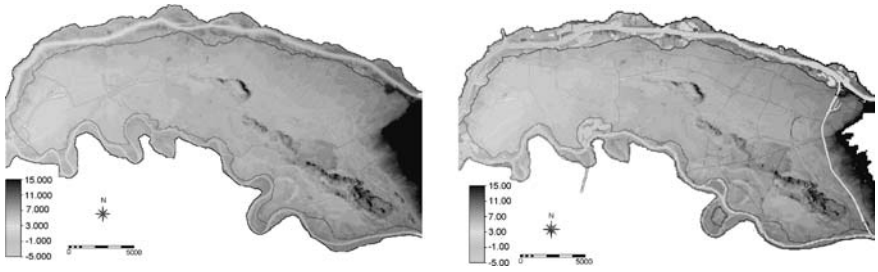

Figure 5. Digital Elevation Model (DEM) of the study area around 1850 (left) and around 2000 (right).

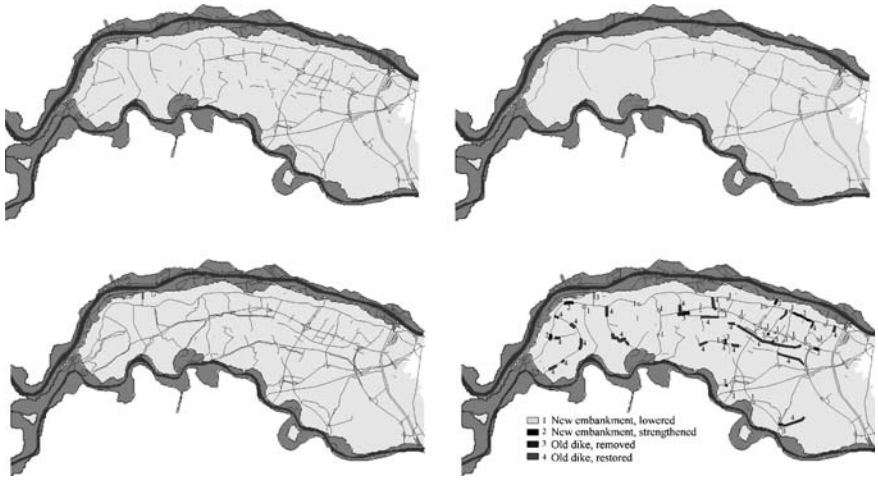

Figure 6. The 4 compartment layouts. Top left: present situation (A). Top right: all old elements removed (B). Lower left: all old elements restored (C). Lower right: strategic adaptations (D).

The aim of layout D is to reduce the impact of the flood in terms of damage or risk by selective changes in the present compartment layout. This involves both repair of previously removed dikes as well as removal of dike sections. The adopted strategy aims at directing the water flow away from, or around the urban areas and to guide it towards the less vulnerable agricultural areas in the centre of the polder (Figure 7).

4. The 2-D-flood Propagation Model Delft-FLS

To assess the effects of linear elements within the polder on the flood characteristics, we used the two-dimensional flood propagation model Delft-FLS, developed at WL|Delft Hydraulics (Stelling *et al.*, 1998). This model was designed to simulate overland flow over initially dry land and through complex topography. It includes internal boundary conditions that allow the correct modelling of dike-breach scenarios, which makes it very suitable tool to simulate dike-failure related floods in polder areas. The scheme used in Delft-FLS is based upon the following characteristics:

- The approximation of the continuity equation is such that (a) mass is conserved, not only globally but also locally and (b) the total water depth is guaranteed to be always positive which excludes the necessity of flooding-and-drying procedures;
- The momentum equation is approximated such that a proper momentum balance is fulfilled near large gradients.

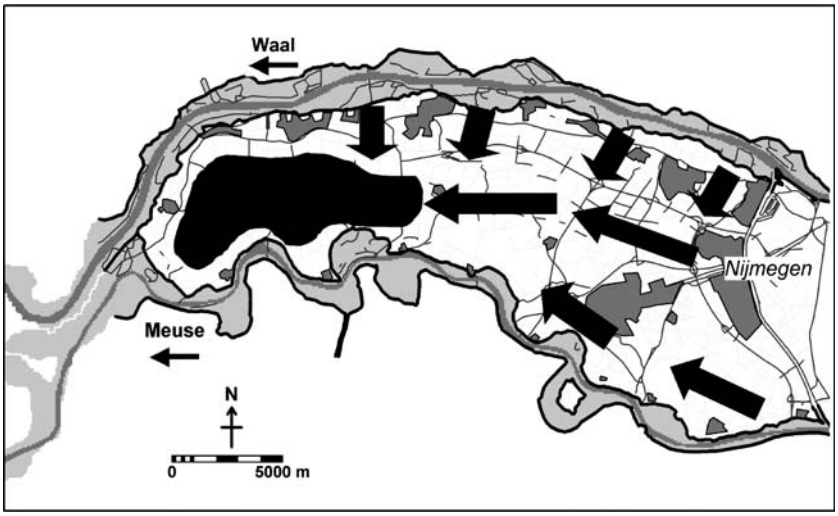

Figure 7. Strategic plan to use old and new barriers to keep the water away from vulnerable areas for as long as possible and to guide it towards less vulnerable parts of the polder.

The combination of positive water depths and mass-conservation assures a stable numerical solution. A proper momentum balance provides that this stable solution converges. The robust numerical scheme allows for the correct simulation of sub-critical and super-critical flow. Further information regarding the model properties can be found in Stelling *et al.* (1998) and Hesselink *et al.* (2003).

4.1. DATA REQUIREMENTS

Delft-FLS requires the following information:

- An accurate digital terrain model (DTM) that includes all topographical features with their correct heights and depths, like dikes, embankments, channels, sluices, tunnels, etc.;
- Land surface cover information in terms of hydraulic roughness coefficients both for 'dry' (polder) and the 'wet' (channels) surfaces;
- Discharge or water-level time-series at the inflow boundary and a stage-discharge relation at the outflow boundary;
- Dimensions of the dike breach and their development through time.

All spatial data has to be available in raster format.

4.2. MODEL OUTPUT

The model produces three types of output: (1) raster maps at predefined time-steps that show the spatial distribution of the water depth and flow-velocity;

(2) time-series at regular intervals of the water level and flow-velocity at predefined locations and discharges though predefined cross-sections; (3) animation file showing the dynamic behaviour of the flood as it propagates through the polder.

4.3. MODEL SENSITIVITY

Hesselink *et al.* (2003) carried out a sensitivity analysis of inundation patterns simulated with Delft-FLS for varying surface roughness and topographic detail in the same area as the present study. They concluded that hydraulic roughness affects the speed at which the polder fills, but does not influence the maximum inundation depth. Furthermore, the model results were highly sensitive to the terrain topography and the inclusion of secondary compartment dikes within the polder. Alkema and De Roo (in press) tested the model on the inundation of the Ziltendorfer polder during the 1997 Oder flood in Germany. This polder is comparable in size and land-use, although it is not as compartmentalized as the *Land van Maas en Waal*. The results of this study also confirmed the model sensitivity reliability, with the addition that for accurate water depth predictions a good discharge-stage curve is essential. These studies demonstrated that the Delft-FLS model is well capable of accurately simulating inundation depth and propagation rate of an inundation. Validation of other parameters, such as flow velocity, was not possible from these studies.

5. Boundary Conditions and Model Calibration

5.1. RIVER DISCHARGE

In accordance with the upper estimates of future design discharge (1250-year recurrence time) due to climate change considered by Dutch water management (Silva *et al.*, 2001) we carried out model simulations for a design flood equal to 18,000 m^3/s for the Rhine at the Dutch/German border and 4600 m^3/s for the Meuse at the Dutch/Belgian border. Assuming that the Waal River then discharges 63.5% of the Rhine discharge the corresponding peak discharge in the Waal River equals 11,400 m^3/s. The shape of this increased design flood wave was obtained from Dutch Institute for Water Management and Waste Water Treatment (RIZA, pers. comm., http://www.riza.nl/index-uk.html; Figure 8). Likewise, the peak-discharge of the Maas will reduce as it travels downstream. Near the study area it is estimated that the peak discharge will be reduced by approximately 1000 m^3/s, giving a peak discharge of around 3650 m^3/s, but the width of the flood wave is much more stretched than further upstream (RIZA, pers. comm.).

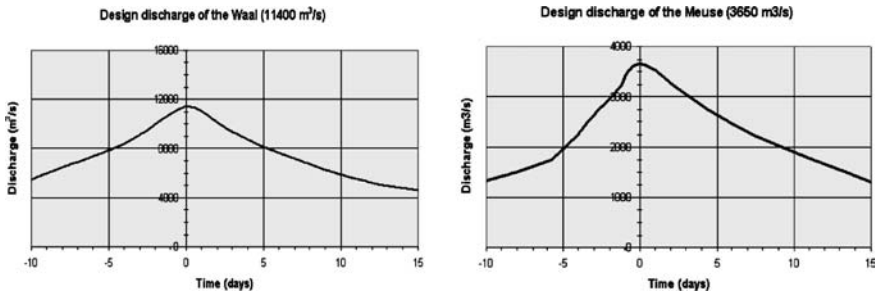

Figure 8. Discharge curve of the Waal used in this study (left) and that for the Meuse (right).

5.2. STAGE DISCHARGE RELATIONS WAAL AND MEUSE

Stage-discharge relations of the Waal and Meuse rivers at the downstream boundaries of the modelling area (villages of Opijnen and Empel) were provided by the water authorities of the province of Gelderland (Figure 9). During the model calibration the relation for the Waal River was slightly adapted to compensate for errors in the representation of the riverbed in the DTM. For the Meuse this was not necessary.

5.3. SURFACE ROUGHNESS COEFFICIENTS

The flow of water is hindered by the resistance of surface features. The surface roughness depends largely on the type of land cover and is often expressed as Manning's coefficient. Table I gives an overview of the land cover classes and the corresponding values of Manning's coefficients as they are found in literature (e.g., Chow, 1959; Albertson and Simons, 1964; Barnes, 1967) with the exception of the values for the riverbed and the floodplain. The latter were obtained by model calibration and partially correct for inaccuracies in the representation of the riverbed. This explains their low values. Figure 10 shows the resulting surface roughness map.

5.4. MODEL CALIBRATION

The discharges that are used as boundary condition in this study have never been recorded in the Waal and Meuse, so no measured water levels are available to calibrate the model. However, previous modelling studies have provided estimates of flood water levels in the rivers occurring at these extreme discharges (WL|Delft Hydraulics, pers. comm., http://www.wldelft.nl/gen/intro/english/index.html). The outcomes of these studies were used to verify the water stages in the rivers calculated in this study (Table II).

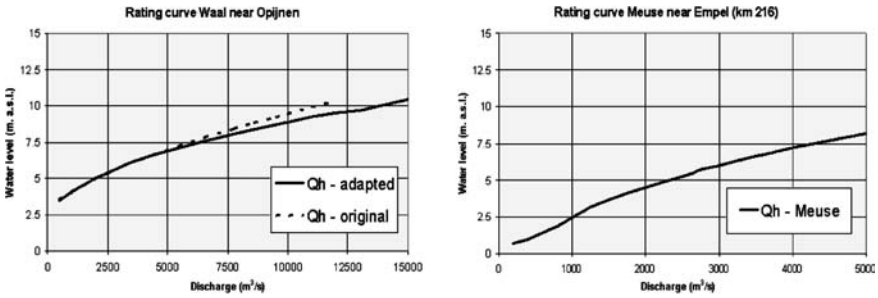

Figure 9. Stage-discharge curves for the Waal near Opijnen (left) and for the Meuse near Empel (right).

Table I. Roughness values for different land cover types used in the model simulations

Landcover type	Manning's coeff.
Riverbed	0.008
Floodplain	0.011
Urban area	0.100
Forest	0.150
Arable land	0.050
Dike	0.030
Heather	0.050
Main road	0.020
Railway	0.020
Secondary road	0.015
Water	0.012
Grassland	0.018

6. Flood Hazard Assessment

The model results, hourly maps of flow-velocity and water depth, were transformed into seven indicator maps that describe the various aspects of a flood. For each of the 28 scenarios a set of these indicator maps was calculated. Figure 11a–g shows such a set for a catastrophic dike breach near Weurt with the present topography.

All maps are the result of an aggregation of 150 h of simulation time (150 h maps). Maximum water depth and maximum flow velocity were derived directly from the water depth and flow-velocity maps that were generated by Delft-FLS. The indicator ''impulse'' was calculated as the product of the water depth and the flow velocity at each time step. It indicates the momentum of the water flow. The indicator ''maximum rising'' is based on the difference of water

Figure 10. Manning's surface roughness coefficients.

Table II. Comparison between water stage predictions of previous studies and the results of this study at various locations along the rivers

WAAL	Nijmegen (885 km)	Bridge A50 (894 km)	Druten (904 km)	Ben. Leeuwen (911 km)	Dreumel (920 km)
Previous studies	15.00 m	13.60 m	12.50 m	11.80 m	10.80 m
This study	14.99 m	13.64 m	12.48 m	12.07 m	10.93 m
MEUSE	Heumen (166 km)	Overasselt (171 km)	Batenburg (185 km)	Heerewaarden (205 km)	
Previous studies	12.70 m	12.00 m	10.10 m	7.30 m	
This study	12.20 m	11.90 m	10.10 m	7.54 m	

depth at a certain time step and the water depth at an hour earlier. It shows those locations where the water level will rise very quickly. The indicator map ''flood propagation'' shows how the floodwater moves through the polder and how barriers such as dikes and embankments diverted it. It gives an estimated time of arrival for the first floodwater in hours after the dike-breach. The indicator map ''duration'' is based on a natural draining of the polder near its lowest point (lower left corner, towards the Meuse river) through a 75-m wide gap in the Meuse primary river dike. The indicator map ''sedimentation/erosion'' gives a rough estimate on sedimentation and erosion rates. It is based on the Rouse criterion that gives the ratio between the upward lifting forces in the turbulent flow and the downward oriented gravitational forces. This criterion was calculated at the hourly time steps, for sediment particles with a diameter of 210 μm. Three additional assumptions were made: (1) The sediment-load of the

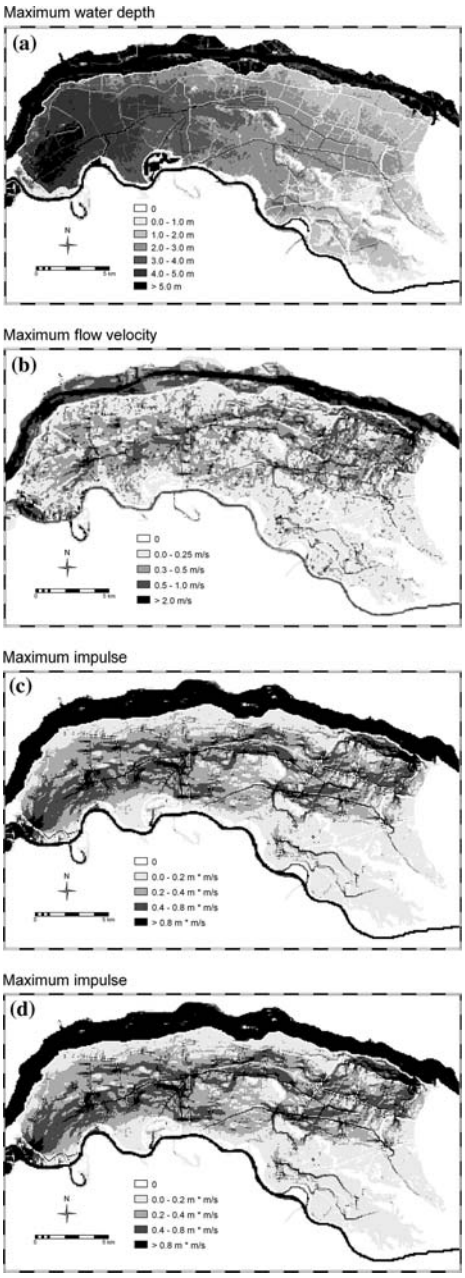

Figure 11. Flood hazard indicator maps. (a) Water depth; (b) Flow velocity; (c) Impulse; (d) Rising of the water level; (e) Flood propagation; (f) Duration; (g) Sedimentation/erosion.

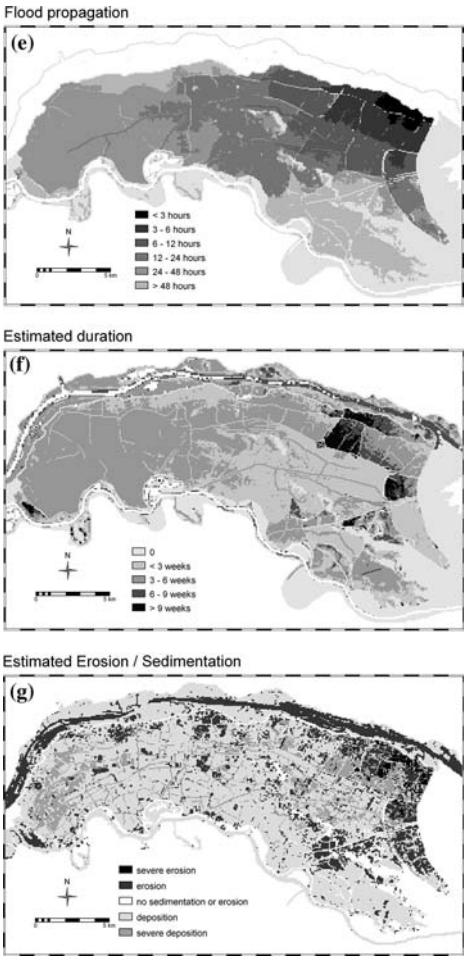

Figure 11. Continued.

water that has flown into the area decreases linearly with time; (2) The input of sediment at a certain location at a certain time depends on the amount of inflowing water and the change in storage; and (3) sedimentation and erosion occur only in the first 150 h of the flood. This approach does not give absolute values for sedimentation and erosion, but provides an indication of where large accumulations may be expected.

7. Flood Damage Estimation

A standard way used to estimate flood damage is the so-called stage-damage curve, that describes for each land cover type the damage factor on a scale

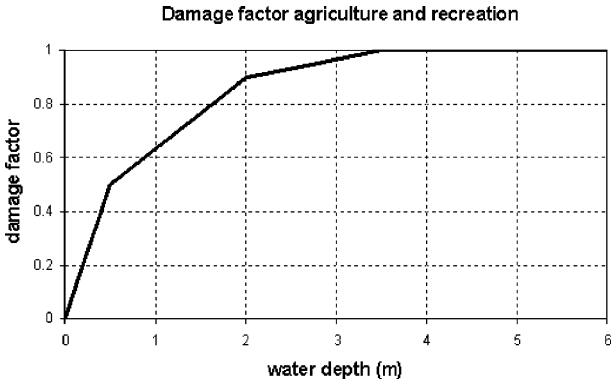

Figure 12. Stage-damage curve for agriculture and recreational areas. (Source: Kok *et al.*, 2002.)

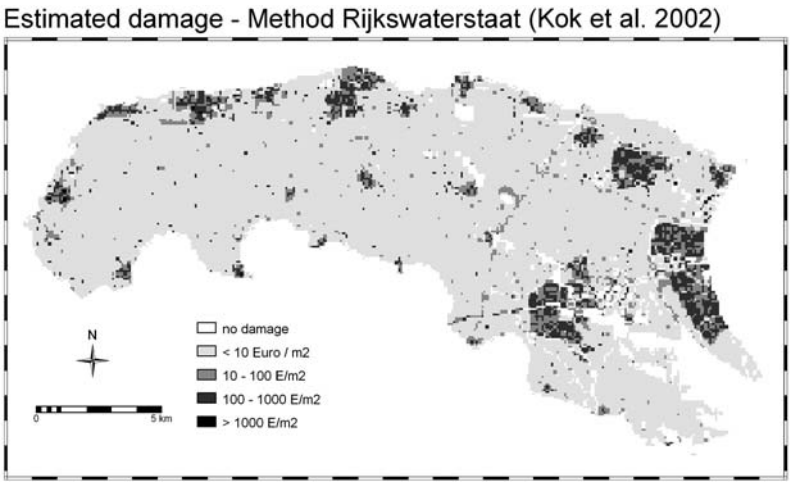

Figure 13. Flood damage map in euros/m^2, based on the method of Rijkswaterstaat.

from 0 (no damage) to 1 (complete destruction) as a function of inundation depth (Figure 12). The absolute damage is obtained by multiplying the damage factor with the value of the unit.

In the Netherlands, a standardized method has been developed by the Directorate-General for Public Works and Water Management (Rijkswaterstaat) to estimate the possible monetary damage for flood scenarios (Kok *et al.*, 2002). This method was applied to the 28 flood scenarios in our study. An example of the damage map is given in Figure 13. The summed-up totals for all scenarios are listed in Table III.

Table III. Overview of flood damage for the 28 scenarios (in million euros)

Type	Present situation (A)	Cleaned-up situation (B)	Restored situation (C)	Selective changes (D)
(1) Weurt (Waal)				
Breach	5,400	5,300	5,500	4,300
Spill-over	1,900	1,700	2,000	905
(2) Deest				
Spill-over	740	740	761	711
(3) Druten				
Spill-over	627	629	645	588
(4) Overasselt (Maas)				
Breach	2,600	2,600	2,700	2,500
Spill-over	1,400	1,400	1,400	1,300
(5) Batenburg				
Spill-over	859	906	907	946

8. Multi-Parameter Flood Hazard Estimation – An Example

Flood damage estimation methods based on depth-damage curves have several limitations. First, there is usually lack of data to establish reliable curves. Second, the methods often only consider maximum water depth to estimate the damage, neglecting other relevant flood parameters, such as flow velocity, sedimentation and duration of the inundation. Third, all consequences of the flood are expressed as monetary losses due to inundation, while aspects related to evacuation success, such as warning time and speed of the rising of the water level, are not considered. Therefore, a more elaborated impact assessment method was developed for this study that is based on the set of indicators that was calculated for each scenario (Figure 11: maximum water depth; maximum flow velocity; maximum impulse; maximum rate of water level rise; flood propagation time; flood duration). This approach is derived from decision support systems described by Beinat and Nijkamp (1998) and Van Herwijnen (1999).

Aggregation of the indictors was done in three steps: (1) Rescaling of the indicator value range to a normalized scale of 0 to 1; (2) Assigning weights to each indicator; (3) Defining one of the scenarios as standard and to calculate for all other scenarios the ratio value. The process of normalization and weight assignment is subjective, but it is transparent. It includes more than one aspect of a flood and it allows a wider interpretation of the consequences of inundation than just damage (money). This approach does not provide absolute risk, damage or casualties values, but presents hazard classes on an ordinal scale where low classes stand for low hazard and high classes for high hazard. Table IV shows the weights and normalised values for an example

Table IV. Example of normalizing and weighing a set of flood hazard parameters (weights are between brackets)

Water depth (0.2)		Inpulse (0.2)		Rising (0.1)		Duration (0.1)		Sedimentation (0.1)		Propagation (0.3)	
Class (m)	Value	Class (m^2/s)	Value	Class (m/h)	Value	Class (weeks)	Value	Class	Value	Class (h)	Value
0	0	0	0	0	0	0	0	Severe erosion	1	0	0
0.0–0.2	0.1	0.0–0.1	0.1	0.0–0.1	0.2	< 2	0.2	Medium erosion	0.85	< 3	1
0.2–0.5	0.25	0.1–0.2	0.2	0.1–0.3	0.4	2–4	0.4	Light erosion	0.7	3–6	0.8
0.5–1.0	0.5	0.2–0.3	0.4	0.3–0.5	0.6	4–6	0.6	Equilibrium	0.5	6–12	0.6
1.0–1.5	0.7	0.3–0.4	0.6	0.5–0.75	0.8	6–8	0.8	Light deposition	0.7	12–24	0.4
1.5–2.5	0.85	0.4–0.8	0.8	0.75–1.0	0.9	> 8	1	Medium deposition	0.85	24–48	0.2
2.5–3.5	0.95	> 0.8	1	> 1.0	1			Severe deposition	1	> 48	0.1
> 3.5	1										

Table V. Comparison of the aggregated relative hazard values for all scenarios. The scenario with a breach at Weurt and the present topography is used as standard

Type	Present situation (A)	Cleaned-up situation (B)	Restored situation (C)	Strategic changes (D)
(1) Weurt (Waal)				
Breach	1	0.98	1.01	0.89
Spill-over	0.46	0.45	0.50	0.35
(2) Deest				
Spill-over	0.32	0.32	0.34	0.31
(3) Druten				
Spill-over	0.23	0.24	0.24	0.20
(4) Overasselt (Meuse)				
Breach	0.63	0.64	0.65	0.59
Spill-over	0.40	0.40	0.41	0.37
(5) Batenburg (Meuse)				
Spill-over	0.33	0.35	0.35	0.33

where six parameters were used for the assessment. Table V presents the results of this multi-parameter hazard assessment. It shows the aggregated total hazard values for all scenarios as ratio of the standard scenario, based on the assumed weights indicated in Table IV.

9. Results and Conclusions

The results of 28 flood scenarios in terms of damage and relative hazard are shown in Tables III and V. From these tables can be seen that the further downstream the failure locations are situated, the lower the damage and hazard because a smaller part of the polder is flooded. Failure at the most upstream located point of the polder will result in the highest damage. Furthermore, the damage and hazard associated with a catastrophic dike breach are significantly higher than in case of a spill-over inundation. The breaching of the dike creates an enormous gradient between the water level in the river and the low-lying polder surface. This results in a much higher flux of floodwater into the polder than of a controlled overtopping at a spill-over location. So from a safety and damage reduction point of view it can be concluded that it makes sense to prefer controlled overtopping over catastrophic breaching. Embankments and internal dikes not only control the inflowing flood water, but also create storage locations that drain badly and could extend the inundation time up to 2 months.

Comparison between the different topographies showed that the complete restoration of the old secondary dike systems does not result in a

significant improvement, not for the damage nor for the hazard. The same holds for the scenarios where all the old dike-systems were removed. There are two explanations for this: (1) Most secondary dikes are too low to block the water flow completely and therefore do not affect significantly the maximum water depth in the polder. Especially for methods that only use the maximum water depth as hazard indicator, like the method of Rijkswaterstaat, the results will be similar. (2) Compartmentalizing has both positive and negative consequences. Inside the compartment the water level will rise faster and the maximum water depth may be higher than without the compartmentalization. Outside the compartment there will be a delay in the arrival time of the floodwater (or no flood at all) and the flow-velocities will be reduced. Whether the positive consequences outweigh the negative ones depends on the distribution of vulnerable (and valuable) areas – e.g., urban areas – in relation to the compartments. In the scenarios that consider the complete restoration or removal of old dikes the positive effects are balanced by the negative consequences. In the D-scenarios a strategic plan was developed with the aim of guiding the water away from the vulnerable urban areas where a lot of valuable property is concentrated. The water was guided to the more rural parts of the polder. This strategic approach does reduce the damage or hazard in the inundated area. It can therefore be concluded that complete restoration or removal will not improve the safety situation in the polder, unless a strategy is followed to protect the more vulnerable parts. Instead, this can be achieved by a well-designed compartment layout, comprising both modern and (repaired) historic embankments.

Acknowledgements

This research was funded by the Belvedere bureau of the Dutch ministry of Housing, Spatial Planning and the Environment. Nathalie Asselman (WL|Delft Hydraulics), Annika Hesselink (Utrecht University/RIZA), Dré van Marrewijk and Oswald Lagendijk (Belvedere) provided useful feedback to the design and evaluation of the scenarios. WL|Delft Hydraulics is gratefully acknowledged for the use of Delft-FLS.

References

Albertson, M. L. and Simons, D. B.: 1964, Fluid mechanics, flow in open channels. In: Chow (ed.), *Handbook of Applied Hydrology*, McGraw-Hill, New York, USA.

Alkema, D. and De Roo, A. (in press), Testing of a 2D flood propagation model by reconstructing the inundation of the Ziltendorfer Niederung (Germany) during the 1997 Oder flood. *J. Hydrol.*

Barnes, H. H.: 1967, Roughness characteristics of natural channels. Geologic Survey Water-supply paper 1849. United States Printing Office, Washington. http://water.usgs.gov/pubs/wsp/wsp_1849/html/pdf.html

Beinat, E. and Nijkamp, P.: 1998, *Multicriteria Evaluation for Land Use Management*. Kluwer Academic Publishers, Dordrecht, The Netherlands.

Chow, V. T.: 1959, *Open Channel Hydraulics*. McGraw-Hill, New York, USA.

Driessen, A. M. A. J.: 1994, *Watersnood tussen Maas en Waal. Overstromingsrampen in het rivierengebied tussen 1780 en 1810*. Walburg Pers, Zutphen, The Netherlands.

Hesselink, A. W.: 2002, History makes a river. Morphological changes and human interference in the river Rhine, The Netherlands. PhD thesis. Faculty of Geographical Sciences, University of Utrecht, NGS 292.

Hesselink, A. W., Stelling, G. S., Kwadijk, J. C. J. and Middelkoop, H.: 2003, Inundation of a Dutch river polder, sensitivity analysis of a physically based inundation model using historic data. *Water Resources Res.* **39**(9), art. no. 1234.

Kok, M., Huizinga, H. J., Meijerink, T. C., Vrouwenvelder, A. C. W. M., and Vrisou van Eck, N.: 2002, Standaardmethode 2002. Schade en Slachtoffers als gevolg van overstromingen. Eindrapport. Dienst Weg en Waterbouwkunde, Rijkswaterstaat Delft, The Netherlands.

Middelkoop, H., Daamen, K., Gellens, D., Grabs, W., Kwadijk, J. C. J., Lang, H., Parmet, B. Schädler, B.W.A.H., Schulla, J., and Wilke, K.: 2001, Impact of climate change on hydrological regimes and water resources management in the Rhine basin. *Climatic Change* **49,** 105–128.

Silva, W., Klijn, F., and Dijkman, J.: 2001, Room for the Rhine branches in the Netherlands: What research has taught us. Report of the Ministry of Transport, Public Works and Water Management, Directorate-General for Public Works and Water Management, The Hague, The Netherlands.

Stelling, G. S., Kernkamp, H. W. J., and Laguzzi, M. M.: 1998, Delft Flooding System: A powerful tool for inundation assessment based upon a positive flow simulation. In: Babovic and Larsen (eds.), *Hydroinformatics '98*. Balkema, Rotterdam, The Netherlands.

Van Herwijnen, M.: 1999, Spatial decision support for environmental management. PhD thesis. Faculty of Economic Sciences and Econometry, Free University, Amsterdam, The Netherlands.

Van Mierlo, M. C. L. M., Overmars, J. M. S., and Gudden, J. J.: 2001, Delft-FLS inundatie simulaties van de Ooij-Düffelt polder en de Land van Maas en Waal polder. http://www.compuplan.nl/pe-resultaten-delftfls.htm.

Natural Hazards (2005) 36: 147–164

National-scale Assessment of Current and Future Flood Risk in England and Wales

JIM W. HALL[1,*], PAUL B. SAYERS[2] and RICHARD J. DAWSON[3]

[1]*School of Civil Engineering and Geosciences, Cassie Building, University of Newcastle-upon-Tyne NE1 7RU, UK;* [2]*HR Wallingford, Howbery Park, Wallingford, Oxfordshire OX10 8BA, UK;* [3]*Department of Civil Engineering, University of Bristol, Queen's Building, University Walk, Bristol BS8 1TR, UK*

(Received: 11 November 2003; accepted: 30 June 2004)

Abstract. In recent years, through the availability of remotely sensed data and other national datasets, it has become possible to conduct national-scale flood risk assessment in England and Wales. The results of this type of risk analysis can be used to inform policy-making and prioritisation of resources for flood management. It can form the starting point for more detailed strategic and local-scale flood risk assessments. The national-scale risk assessment methodology outlined in this paper makes use of information on the location, standard of protection and condition of flood defences in England and Wales, together with datasets of floodplain extent, topography, occupancy and asset values. The flood risk assessment was applied to all of England and Wales in 2002 at which point the expected annual damage from flooding was estimated to be approximately £1 billion. This figure is comparable with records of recent flood damage. The methodology has subsequently been applied to examine the effects of climate and socio-economic change 50 and 80 years in the future. The analysis predicts increasing flood risk unless current flood management policies, practices and investment levels are changed – up to 20-fold increase in real terms economic risk by the 2080s in the scenario with highest economic growth. The increase is attributable primarily to a combination of climate change (in particular sea level rise and increasing precipitation in parts of the UK) and increasing economic vulnerability.

Key words: flood risk, flood defence reliability, climate change, socio-economic scenarios

1. Introduction

Over 5% of the UK population live in the 12,200 km^2 that is at risk from flooding by rivers and the sea (HR Wallingford, 2000). These people and their property are protected by 34,000 km of flood defences. Traditionally, this important and safety-critical infrastructure system has been managed locally. It is now become increasingly apparent that flood risk can be managed more effectively by adopting strategic approaches applied at catchment, regional and national scales. These strategic approaches provide the opportunity to coordinate management of flood defence infrastructure with other

* Author for correspondence. E-mail: jim.hall@ncl.ac.uk

measures, such as techniques to reduce runoff, control the urbanisation of floodplains and organisation of flood warning and evacuation. Strategic catchment-scale flood risk management coincides with the catchment-scale approach adopted in the EU Water Framework Directive.

Broad-scale flood risk analysis is a prerequisite for strategic flood risk management. A risk-based approach to decision-making requires that the risks and costs of all decision options, including the *status quo*, are evaluated in quantified terms. Such an approach also has the potential to put flood management decisions on the same footing as risk-based decision-making in relation to other natural and man-made hazards that policy-makers are bound to address. However, it is important to recognise the contrasting nature of different risks (Royal Society, 1992) and the varying sources of uncertainty in the quantified risk analyses that are conducted in different fields, so considerable caution should be exercised in comparing risk estimates. Nonetheless, regional and national-scale risk analysis does potentially provide decision-makers with powerful tools to develop targeted and potentially synergistic mitigation strategies.

National-scale risk assessment is by no means straightforward, because of the need to assemble national datasets and then carry out and verify very large numbers of calculations. Increasingly, however, national-scale datasets are becoming available. Aerial and satellite remote sensing technologies are providing new topographic and land use data. Commercial organisations are generating and marketing increasingly sophisticated datasets of the location and nature of people and properties. In 2002 the Environment Agency, the organization responsible for operation of flood defences in England and Wales, introduced a National Flood and Coastal Defence Database (NFCDD), which for the first time provides in a digital database an inventory of flood defence structures and their overall condition. Together, these new datasets now enable flood risk assessment that incorporates probabilistic analysis of flood defence structures and systems. Once the necessary datasets are held in a Geographical Information System (GIS) they can then be manipulated in order to explore the impact of future flood management policy and scenarios of climate change.

In the following section of this paper, an overview of the national-scale flood risk assessment methodology for flood risk analysis is provided. Section 3 summarises application of the methodology to all of England and Wales. In Section 4, the same methodology is used to predictions of flood risk under scenarios of climate and socio-economic change.

2. Overview of the Methodology

Flood risk is conventionally defined as the product of the probability of flooding and the consequential damage, summed over all possible flood events. It is often quoted in terms of an expected annual damage, which is

sometimes referred to as the ''annual average damage''. For a national assessment of flood risk, expected annual damage must be aggregated over all floodplains in the country. An overview of the methodology by which this can be achieved is given in Figure 1 and described in outline below. Further details can be found in Hall *et al.* (2003).

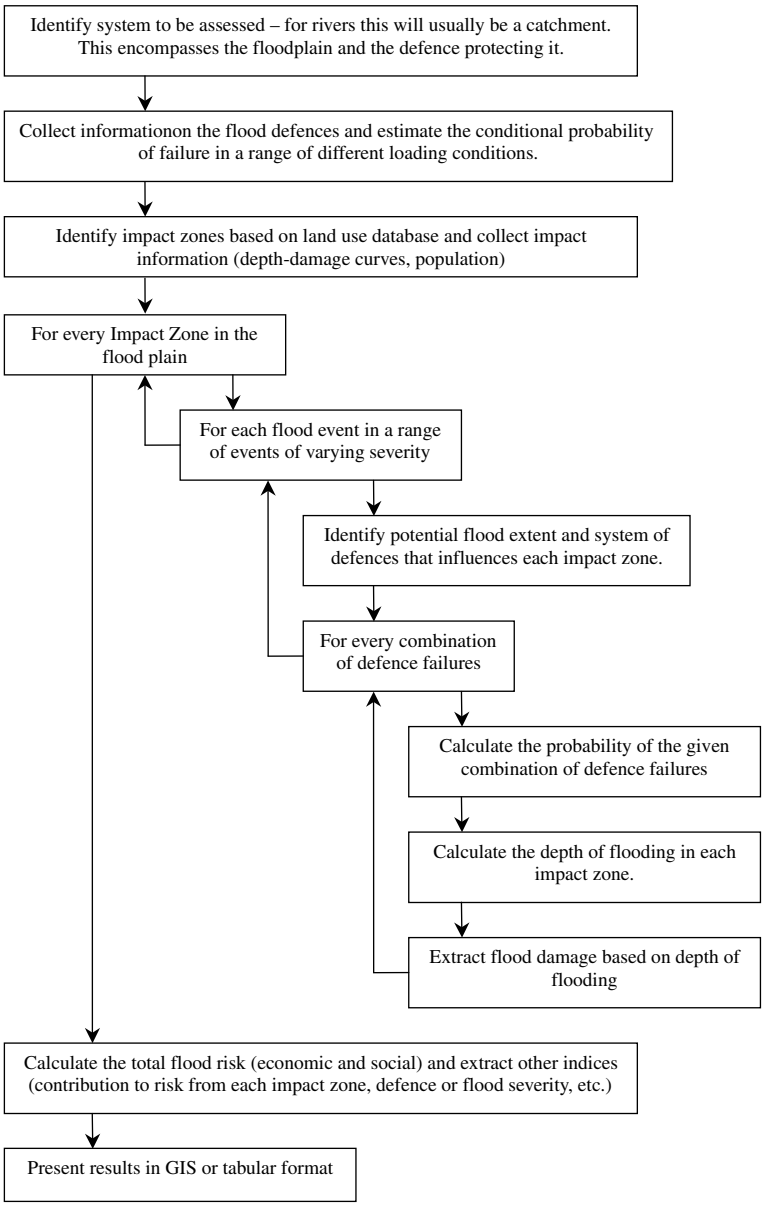

Figure 1. Overview of the national flood risk assessment methodology.

The most significant constraint on a national-scale flood risk assessment methodology is the availability of data. The methodology presented here has been developed to make use of the following national GIS datasets and no other site-specific information:

1. *Indicative Floodplain Maps (IFMs)* are the only nationally available information on the potential extent of flood inundation. The IFMs are outlines of the area that could potentially be flooded in the absence of defences in a 1:100-year return period flood for fluvial floodplains and a 1:200-year return period flood for coastal floodplains.
2. *1:50,000 maps with 5 m contours*. The methodology has been developed in the absence of a national topographic dataset of reasonable accuracy. Topographic information at 5 m contour accuracy has only been used to classify floodplain types as it is not sufficiently accurate to estimate flood depths.
3. *National map of the centreline of all watercourses*.
4. *National Flood and Coastal Defence Database* provides a national dataset of defence location, type and condition.
5. *National database of locations of residential, business and public buildings*.
6. *Land use maps and agricultural land classification*.

The 34,000 km of flood defences in England and Wales protect areas most at risk from severe flood damage. An essential aspect of flood risk analysis is therefore to assess the reliability of the flood defence infrastructure. These infrastructures must be dealt with as systems if the flood risk is to be accurately estimated. In the absence of more detailed information on flood extent, in the current methodology the Indicative Floodplain is adopted as the maximum extent of flooding and is further sub-divided into Impact Zones, not greater than 1 km $\times$ 1 km. Each flood Impact Zone is associated with a system of flood defences which, if one or more of them were to fail, would result in some inundation of that zone.

Reliability analysis of flood defences potentially requires a huge quantity of data, which are not available for all of the flood defences in England and Wales. An approximate reliability method has therefore been developed that makes use of the so-called Standard of Protection (SOP), which is an assessment of the return period at which the defence will significantly be overtopped. Flood defence failure is addressed by estimating the probability of failure of each defence section in a given load (relative to SOP) for a range of load conditions. Generic versions of these probability distributions of defence failure, given load, have been established for a range of defence types for two failure mechanisms: overtopping and breaching.

Having estimated the probability of failure of individual sections of defence, the probabilities of failure of combinations of defences in a system are calculated. To do so, it is assumed that the probability of hydraulic loading of

individual defences in a given flood defence system is fully dependent. The probabilities of failure of each of the defences in the system, conditional upon a given load, are assumed to be independent. For each failure combination an approximate flood outline, which covers some proportion of the IFM, is generated using approximate volumetric methods. These methods estimate discharge through or over the defence and inundation characteristics of the floodplain, based on an assessment of floodplain type.

In the absence of water level and topographic data, estimation of flood depth has been based on statistical data. These data were assembled from 70 real and simulated floods for a range of floodplain types and floods of differing return periods. These data were used to estimate flood depth at points between a failed defence and the floodplain boundary, in events of a given severity. Flood depth estimates from a range of floods were used to construct an estimate of the probability distribution of the depth of flooding for each Impact Zone (Figure 1).

The numbers of domestic and commercial properties and area of agricultural land in each Impact Zone were extracted from nationally available databases. These data were combined with relationships between flood depth and economic damage that have been developed from empirical analysis of past flooding events (Penning-Rowsell *et al.*, 2003a). For a given Impact Zone the expected annual damage R is given by

$$R = \int_0^{y_{\max}} p(y)D(y)\,dy$$

where $y_{\max}$ is the greatest flood depth from all flooding cases, $p(y)$ is the probability density function for flood depth and $D(y)$ is the damage in the Impact Zone in a flood of depth y m. The total expected annual damage for a catchment or nationally is obtained by summing the expected annual damages for each Impact Zone within the required area.

The population at risk was estimated from the number of inhabitants within an Impact Zone using 2001 census data. The Social Flood Vulnerability Indices (SFVI) (Tapsell *et al.*, 2002) were used to identify communities vulnerable to the impacts of flooding. Social vulnerability is ranked from "very low" to "very high" and is based on a weighting of the number of lone parents, the population over 75 years old, the long term sick, non-homeowners, unemployed, non-car owners and overcrowding, obtained from census returns. The risk of social impact is obtained as a product of probability of flooding to a given depth and the SFVI, providing a comparative measure for use in policy analysis.

3. Methods for Scenarios-based Future Flood Risk Assessment

There is increasing concern about the potential impacts of climate change on flood risk. Of equal, if not greater, potential significance, are the impacts that

socio-economic changes will have on vulnerability to flooding. Flood management decisions, such as the introduction of new land use planning policies or the construction of major new flood defence infrastructure can take decades to implement. For example studies are now under way to plan the upgrading of the Thames Barrier, even though it will continue to provide the required standard of flood protection until 2030. There is therefore a need to develop long term scenarios of flood risk in order to assist the development of robust long-term flood risk management policies.

A scenarios-based approach explicitly acknowledges that the distant future is uncertain and that several plausible trajectories of societal change can be sketched out. Scenarios are not intended to predict the future. Rather they are tools for thinking about the future, recognising that the future is shaped by human choice and action, and is unlikely to be like the past. Scenarios development involves rational analysis and subjective judgement (DTI, 2003).

Flood defence is an interesting application of the scenarios-based approach because it involves integrated use of two different types of scenario:

- Climate change projections are based on *emissions scenarios*, used to establish the global emission of greenhouse gases to the atmosphere.
- *Socio-economic scenarios* provide the context in which flood management policy and practice will be enacted and relate to the extent to which society may be impacted upon by flooding.

The UK Climate Impacts Programme scenarios for the UK published in 2002 (usually referred to as UKCIP02) (Hulme *et al.*, 2002) have been used. These scenarios are based on four emissions scenarios: Low emissions, Medium-low emissions, Medium-high emissions and High emissions corresponding to the Intergovernmental Panel on Climate Change's Special Report on Emissions Scenarios (usually referred to as SRES) scenarios B1, B2, A2 and A1F1, respectively (IPCC, 2000). The UKCIP02 scenarios predict that annual average precipitation across the UK may decrease slightly, by between 0 and 15% by the 2080s depending on scenario. The seasonal distribution of precipitation will change, with winters becoming wetter and summers becoming drier, the biggest relative changes being in the South and East. Under the High Emissions scenario winter precipitation in the South and East may increase by up to 30% by the 2080s. By the 2080s the daily precipitation intensities that are experienced once every 2 years on average may become up to 20% heavier. By the 2080s and depending on scenario relative sea level may be between 2 cm below and 58 cm above the current level in western Scotland and between 26 and 86 cm above the current level in south east England. For some coastal locations a water level that at present has a 2% annual probability of occurrence may have an annual occurrence probability of 33% by the 2080s for Medium-High emissions. The climate change scenarios included within UKCIP02 do not

include allowance for model error and do not therefore represent the maximum potential range of climate change effects.

The Foresight Futures socio-economic scenarios (SPRU *et al.*, 1999; UKCIP, 2001; DTI, 2003) are intended to suggest possible long term futures, exploring alternative directions in which social, economic and technological changes may evolve over coming decades. The scenarios are represented on a two-dimensional grid (Figure 2). On the vertical dimension is the system of governance, ranging from autonomy where power remains at the national level, to interdependence where power increasingly moves to other institutions. On the horizontal dimension are social values, ranging from individualistic values to community oriented values. The four Foresight Futures that occupy this grid are summarised in Tables I and II.

There is no direct correspondence between the UKCIP02 scenarios and the Foresight Futures 2020, not least because the Foresight Futures are specifically aimed at the UK whereas the emissions scenarios used in UKCIP02 are *global* greenhouse emissions scenarios. However, an approximate correspondence can be expected, as shown in Table III.

The national-scale flood risk analysis model outlined above was used to analyse long term change by making appropriate changes to the model parameters to reflect the time and scenario under consideration. The four scenarios listed in Table III were analysed for the 2080s and chosen to coincide with the years for which climate scenarios were available (Hulme *et al.*, 2002). The input data required by the risk analysis model do not correspond exactly to the information provided in either in climate change or socio-economic

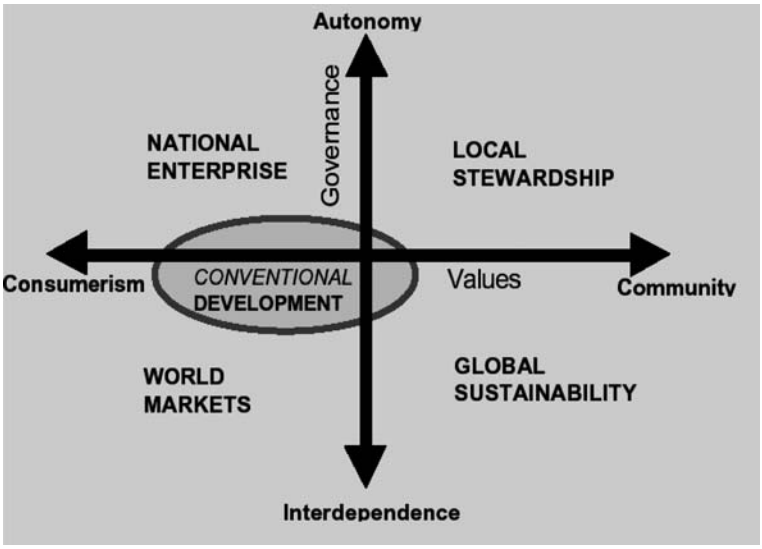

Figure 2. Socio-economic scenarios.

Table I. Summary of Foresight Futures (DTI, 2003)

	World markets	National enterprise	Global sustainability	Local stewardship
Social values	Internationalist, libertarian	Nationalist, individualist	Internationalist, communitarian	Localist, co-operative
Governance structures	Weak, dispersed, consultative	Weak, national, closed	Strong, co-ordinated, consultative	Strong, local, participative
Role of policy	Minimal, enabling markets	State-centred, market regulation to protect key sectors	Corporatist, political, social and environmental goals	Interventionist, social and environmental
Economic development	High growth, high innovation, capital productivity	Medium-low growth, Low innovation, maintenance economy	Medium-high growth, high innovation, resource productivity	Low growth, low innovation, modular andsustainable
Structural change	Rapid, towards services	More stable economic structure	Fast, towards services	Moderate, towards regional systems
Fast-growing sectors	Health & leisure, media & information, financial services, biotechnology, nanotechnology	Private health and education, domestic and personal services, tourism, retailing, defence	Education and training, large systems engineering, new and renewable energy, information services	Small-scale manufacturing, food and organic farming, local services
Declining sectors	Manufacturing, agriculture	Public services, civil engineering	Fossil fuel energy, traditional manufacturing	Retailing, tourism, financial services
Unemployment	Medium-low	Medium-high	Low	Medium-low (large voluntary sector)
Income	High	Medium-low	Medium-high	Low
Equity	Strong decline	Decline	Improvement	Strong improvement

Table II. Snap shot statistics for 2050 (UKCIP, 2001)

	Mid 1990s	World markets	National enterprise	Global sustainability	Local stewardship
UK population (million)	58.5	59	57	57	55
Gross domestic product growth per year	+2%	+3%	+1.75%	+2.25%	+1.25%
Gross domestic product per capita	£10,500	£61,000	£31,000	£41,000	£24,000
Land use (%)					
Agricultural	75%	60%	70%	70%	75%
Urban	15%	22%	19%	15%	14%
Forest and other	10%	18%	11%	15%	11%

Table III. Correspondence between UKCIP02 scenarios and Foresight Futures

SRES[a]	UKCIP02[b]	Foresight Futures 2020[c]	Commentary
B1	Low emissions	Global sustainability	Medium-high growth, but low primary energy consumption. High emphasis on international action for environmental goals (e.g. greenhouse gas emissions control). Innovation of new and renewable energy sources.
B2	Medium-low emissions	Local stewardship	Low growth. Low consumption. However, less effective international action. Low innovation.
A2	Medium-high emissions	National enterprise	Medium-low growth, but with no action to limit emissions. Increasing and unregulated emissions from newly industrialised countries.
A1F1	High emissions	World markets	Highest national and global growth. No action to limit emissions. Price of fossil fuels may drive development of alternatives in the long term.

[a] Special Report on Emissions Scenarios (IPCC, 2000).
[b] UK Climate Impacts Programme 2002 scenarios (Hulme *et al.*, 2002).
[c] DTI (2003).

scenarios. It was therefore necessary to construct approximate relationships between the variables for which scenarios information was available and the variables required for flood risk analysis. A summary of the relationships adopted in the analysis of risks from river and coastal flooding is provided in Table IV. A quantified estimate was made of the effect in each scenario that a given change, for example urbanisation, would have on the relevant variables in the risk model (Table IV). The cumulative effect of each of the changes in the given scenario was then calculated. Where feasible, regional variation was applied to these adjustments in order to take account of, for example, regional differences in climate or demographic projections. There is no unique mapping between a scenario, which is an inherently vague entity, and a realization of the risk model. In other words, there is not a unique representation of the scenario in the risk model. The quantified analysis presented here is one of many equally plausible representations of the same four scenarios. Whilst no claim is made to the uniqueness of these results, they do illustrate some striking contrasts between different scenarios of change and provide the basis for exploring responses to flood risk that are robust across plausible futures.

Future flood risk is greatly influenced by flood management policy and practice, perhaps more so than it is by changes outside the control of the flood manager, such as climate change or economic growth. However, in the analysis described here current flood defence alignment and form, as well as the levels of investment in maintenance and renewal were kept the same across all scenarios. Clearly flood defence policy will change in the future and will tend to reflect the nature and public expectations of future society i.e. flood defence is scenario-dependent. However, the aim of the current study was to inform present-day policy makers and in order to do that, the present day flood defence policy was subjected to particular scrutiny, by analysing its effectiveness in a range of scenarios. Changing scenarios were super-imposed on this fixed flood defence policy (including the current pattern of expenditure and technical approach), in order to assess the capacity of the current policy to cope with long term changes.

3.1. RESULTS FOR THE PRESENT SITUATION

The national-scale risk assessment methodology described above was applied to all of England and Wales in 2002. The results are reported on a 10 km $\times$ 10 km grid (though, as described above, the analysis was conducted on the basis of Impact Zones not greater than 1 km $\times$ 1 km). Figure 3 shows the proportion of each 10 km $\times$ 10 km grid cell that is occupied by floodplain. It indicates the very high proportions of floodplain around the Wash and the Humber estuary on the east coast of England and in several other coastal areas.

Comparison of the extent of the Indicative Floodplain with residential, commercial and land use databases revealed that in England and Wales there

Table IV. Representation of future scenarios in risk model

Variable used risk model	Explanation	Changes that may be represented with this variable
Standard of Protection (SoP) of flood defences	The return period at which the flood defence (or where none exists the river bank) is expected to overtop.	Climate change[a] Changes in land use management (which may change run-off and hence river flows and water levels) Morphological change (that may also influence the conveyance of the river and hence water levels)
Condition grade of flood defences	An indicator of the robustness of the defences and their likely performance when subjected to storm load.	Morphological changes Maintenance regimes
Location of people and properties in the floodplain	Spatially referenced database of domestic and commercial properties. Census data on occupancy, age etc.	Demographic changes Urbanisation Commercial development
Flood depth-damage relationships	Estimated flood damage (in £ per house or commercial property) for a range of flood depths	Changes in building contents Changes in construction practices
Social flood vulnerability indices[b]	An aggregate measure of population vulnerability to flooding, based on census data	Changes in demographics (e.g. age) Changes in equity
Agricultural land use classification in the floodplain	Agricultural land grade from 1 (prime arable) to 5 (no agricultural use)	Changed agricultural practices Agricultural land being taken out of use
Reduction factors	Measures that will reduce total flood damage, e.g. flood warning and evacuation can be reflected by factoring the estimated annual average damage	Flood warning (including communications technologies) and public response to warning Evacuation Community self-help

[a] For example a scenario in which if climate change is expected to increase water levels by 20% is represented by reducing the SoP of flood defences by an appropriate increment.
[b] Tapsell *et al.* (2002).

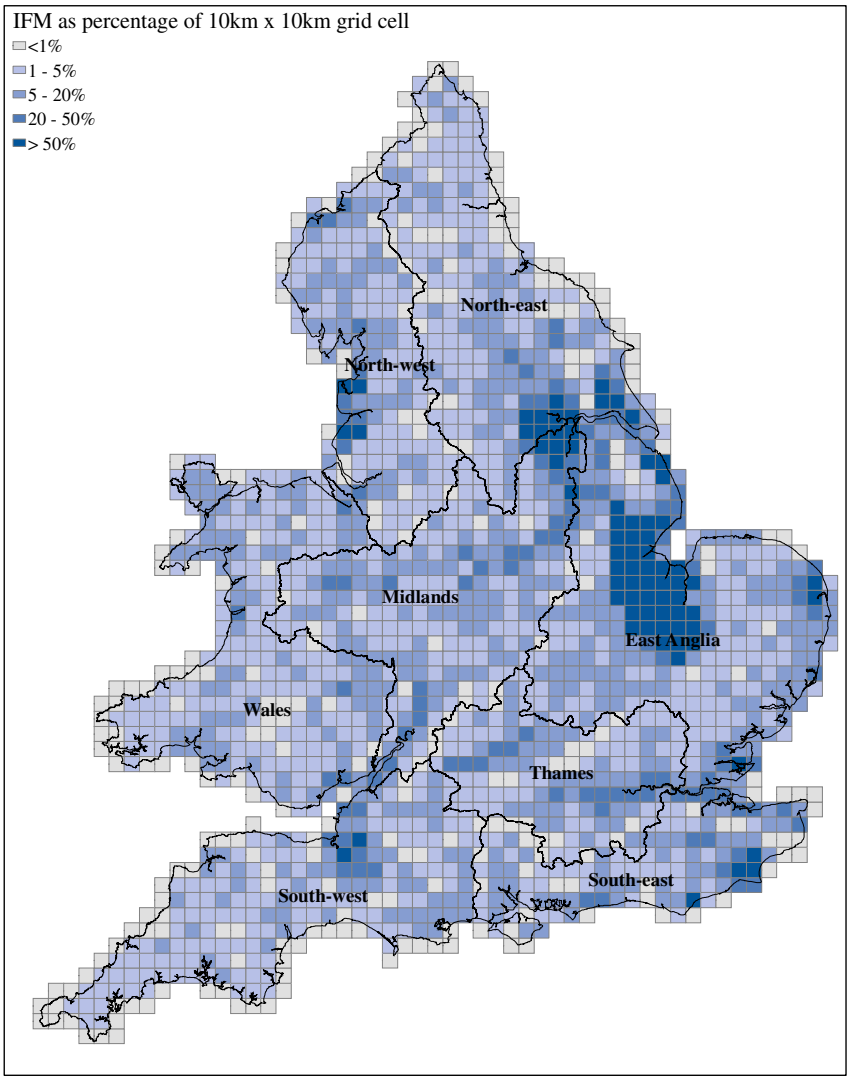

Figure 3. Proportion of land in Indicative Floodplain.

are 1.61 million residential properties and 131,000 commerical properties in the Indicative Floodplain, together with 1.43 million hectares of agricultural land. Comparison on census data with the Indicative Floodplain yields an estimated 4.47 million people resident within the Indicative Floodplain. The total value of residential property at risk is £208 billion.

The national-scale risk analysis yielded an estimated Expected Annual Damage due to flooding of £1.0 billion, with an uncertainty range between £0.6 billion and £2.1 billion. The spatial distribution of economic risk from

flooding is illustrated in Figure 4. Highest economic risk is located in floodplain areas of high economic value, notably Greater London despite very high standards of flood protection. A number of areas of high coastal flood risk are located along the south, east and north-west coasts of England. The expected annual damage to agriculture is estimated to be £5.9 million, accounting for only about 0.5% of economic damage due to flooding. This loss is very small in economic terms, but can represent considerable impact on the rural economy.

The risk analysis has been compared with recent flood events to assess the dependability and uncertainties in the methodology (HR Wallingford, 2003). The annual average flood damage estimate of roughly £1 billion is of the same order to but somewhat larger than annual losses due to flooding experienced in recent years. For example, floods in Autumn 2002 resulted in economic losses of the order of £750 million (Penning-Rowsell *et al.*, 2003b). Some of the inconsistency is explained by reporting of recent flood events and by assumptions in the model (particularly the exclusion of emergency repair works). Although a single event provides only limited basis for validation of annual average risk estimates, the reasonably good correspondence between model and observations indicates that the model does provide a sound basis for policy appraisal and comparative evaluation of future scenarios.

3.2. RESULTS FOR FUTURE SCENARIOS

The results of the flood risk scenarios analysis are summarised in Table V. No discounting or inflation is applied to economic risks. Risk is estimated at time points in the future using today's prices.

Large increases in the number of people occupying the floodplain in the UK are envisaged in the relatively loosely regulated World Markets and National Enterprise scenarios. Most of this increase is predicted to occur by the 2050s, representing predictions of very rapid growth in the first half of this century which is envisaged to approach a limit associated with a fairly stable population and spatial constraints. Floodplain occupancy is kept stable in the Global Sustainability and Local Stewardship scenarios. However, increasing flood frequency, primarily due to climate change means that even with stable numbers of people in the floodplain, the number of people at risk from flooding more frequently than 1:75 years will increase in all scenarios, assuming that current flood defence systems are continued into the future. Greater climate change by the 2080s, together with the increased floodplain occupancy noted above mean that the World Markets and National Enterprise scenarios will see more than doubling of the number of people at risk from flooding more frequently than 1:75 years.

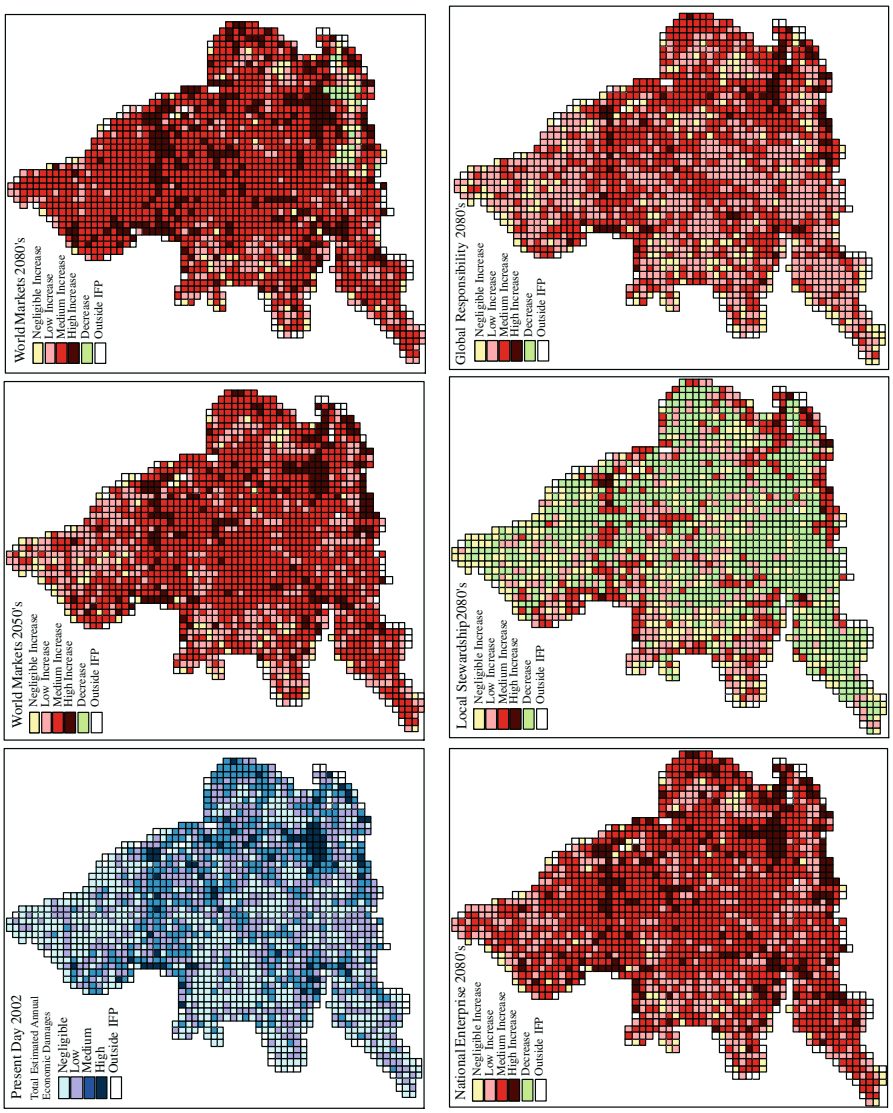

Figure 4. Expected annual economic damage for 2002 and future scenarios.

Table V. Summary of flood risk scenarios

	2002	World Markets 2050s	World Markets 2080s	National Enterprise 2080s	Local Stewardship 2080s	Global Sustainability 2080s
Number of people within the indicative floodplain (millions)	4.5	6.2	6.9	6.3	4.5	4.6
Number of people exposed to flooding (depth > 0 m) with a frequency > 1:75 years (millions)	1.6	3.3	3.5	3.6	2.3	2.4
Expected annual economic damage (residential and commercial properties) (£ billions)	1.0	14.5	20.5	15.0	1.5	4.9
Annual economic damage relative to Gross domestic product per capita	0.10%	0.15%	0.14%	0.31%	0.05%	0.06%
Expected annual economic damage (agricultural production) (£ millions)	5.9	41.6	34.4	41.3	63.5	43.9

In all scenarios other than the low growth, environmentally/socially conscious Local Stewardship scenario, annual economic flood damage is expected to increase considerably over the next century assuming the current flood defence policies are continued in future. A roughly 20-fold increase by the 2080s is predicted in the World Markets scenario, which is attributable to a combination of much increased economic vulnerability (higher floodplain occupancy, increased value of household/industrial contents, increasing infrastructure vulnerability) together with increasing flood frequency.

Change in the ratio of flood risk to per capita GDP provides an indication of how severe or harmful (in economic terms) flooding will be when compared with economic growth over the next century. In the World Markets and National Enterprise scenarios flooding is expected to remove a

greater proportion of national wealth than it currently does (and thus merit a greater investment to reduce risk). In the Local Stewardship and Global Sustainability scenarios flooding is predicted to remove a lesser proportion of national wealth since these scenarios will tend to be less vulnerable to flood damage and are expected to be subject to somewhat less climate change.

The pattern for flood damage to agriculture is rather different to the pattern from economic damage as a whole. In the globalised World Markets scenario the contribution of agricultural damage to overall economic damage is projected to decrease, with a greater proportion of agricultural products being imported (though the effect of climate change on agriculture globally has not been considered) and low-grade agricultural land being taken out of production. Agricultural damage in the more self-sufficient National Enterprise and Local Stewardship scenarios is expected to be more significant.

Figure 4 shows the distribution of the increase in expected annual economic damage for the World Markets 2050s scenario and all four scenarios for the 2080s, relative to the estimated risk in 2002. Increasing risk is predicted to be concentrated in broadly the same areas as where it is currently highest. Coastal flooding makes an increasing contribution to total flood risk, increasing from 26% in 2002 to 46% in the 2080s. The increasing probability of overtopping the Thames Barrier that protects central London makes a significant contribution to this increase in risk.

Analysis of environmental and socio-economic phenomena over a timescale of 30–100 years in the future involves formidable uncertainties. Model uncertainties in climate projections up to the 2050s exceed the differences between emissions scenarios. There is considerable disagreement about the spatial patterns of climate change down-scaled to the UK. Changes in some climate variables, for example extreme sea levels and short, high intensity rainfall events are particularly difficult to predict. Socio-economic change, which on a global scale leads to changing greenhouse gas emissions trajectories and on the UK scale also determines economic and social vulnerability to flooding, is even more difficult to predict and, it is argued, succumbs only to a scenarios-based approach which seeks to illustrate some of the potential range of variation between different futures. The flood risk scenarios presented here are therefore subject to very considerable uncertainties. They do, nonetheless, provide insights into the sources and impacts of future flood risk and the implications of continuing current flood defence policies into the future.

4. Conclusions

A national-scale flood risk assessment methodology, which includes the effect of flood defence systems, has been applied to all of England and Wales, making use of nationally available datasets. The analysis estimates expected

annual damage due to flooding of roughly £1 billion, a figure that is slightly higher than, but comparable to economic damage due to flooding in England and Wales in recent years. The largest contribution to this risk is in the Greater London area, despite the very high standard of protection from flooding.

Socio-economic and climate scenarios have been used in combination in order to generate self-consistent projections of potential future variation in flood risk, assuming stable flood defence policy. In all scenarios the frequency of flooding is projected to increase, more so on the coast than on rivers. The increase is greatest in high-emission scenarios. The risk of flooding is strongly modified by societal vulnerability and the scenarios analysis demonstrates how widely that vulnerability may vary according to the trajectory of socio-economic change. The risk that actually prevails in the future will be further modified by flood management activity, which will itself be a reflection of society's values and expectations.

Acknowledgements

The research described in this paper formed part of a project entitled ''RASP: Risk assessment for flood and coastal defence systems for strategic planning'', funded by the Environment Agency within the joint DEFRA/EA Flood and Coastal Defence R&D programme. The National Flood Risk Assessment 2002 was funded by the Environment Agency. The scenarios analysis was funded by the UK Office of Science and Technology as part of the Foresight Flood and Coastal Defence programme. The paper expresses the views of the authors and not the UK Government.

References

DTI: 2003, *Foresight Futures 2020: Revised Scenarios and Guidance*, Department of Trade and Industry.

Hall, J. W., Dawson, R. J., Sayers, P. B., Rosu, C., Chatterton, J. B., and Deakin, R.: 2003, A methodology for national-scale flood risk assessment. *Water Maritime Eng*. **156**(3), 235–247.

HR Wallingford: 2000, National appraisal of assets at risk from flooding and coastal erosion, Technical Report volumes 1 and 2, HR Wallingford Report TR107.

HR Wallingford: 2003, National flood risk assessment 2002, HR Wallingford Report EX4722.

Hulme, M., Jenkins, G. J., Lu, X., Turnpenny, J. R., Mitchell, T. D., Jones, R. G., Lowe, J., Murphy, J. M., Hassell, D., Boorman, P., McDonald, R., and Hill, S.: 2002, Climate change scenarios for the United Kingdom: The UKCIP02 scientific report, Tyndall Centre for Climate Change Research, School of Environmental Sciences, University of East Anglia, Norwich, UK.

IPCC: 2000, Special report on emissions scenarios (SRES): A special report of working group III of the Intergovernmental Panel on Climate Change, Cambridge University Press, Cambridge.

Penning-Rowsell, E. C., Johnson, C., Tunstall, S. M., Tapsell, S. M., Morris, J., Chatterton, J. B., Coker, A., and Green, C.: 2003a, *The Benefits of Flood and Coastal Defence: Techniques and Data for 2003*, Flood Hazard Research Centre, Middlesex University.

Penning-Rowsell, E. C., Chatterton, J., Wilson, T., and Potter, E.: 2003b, *Autumn 2000 Floods in England and Wales: Assessment of National Economic and Financial Losses*, Flood Hazard Research Centre, Middlesex University.

Royal Society: 1992, Risk analysis, perception and management, Report of the Royal Society Study Group, The Royal Society, London.

SPRU, CSERGE, CRU, PSI: 1999, Socio-economic futures for climate impacts assessment, Final Report, Science and Technology Research, University of Sussex.

Tapsell, S. M., Penning-Rowsell, E. C., Tunstall, S. M., and Wilson, T. L.: 2002, Vulnerability to flooding: health and social dimensions, *Phil. Trans. R. Soc. Lond.* **A360**(1796), 1511–1525.

UKCIP: 2001, *Socio-economic Scenarios for Climate Change Impact Assessment: A Guide to Their Use in the UK Climate Impacts Programme*, UKCIP, Oxford.

Natural Hazards (2005) 36: 165–189

Summer Floods in Central Europe – Climate Change Track?

ZBIGNIEW W. KUNDZEWICZ[1,3,★], UWE ULBRICH[4], TIM BRÜCHER[2], DARIUSZ GRACZYK[1], ANDREAS KRÜGER[2], GREGOR C. LECKEBUSCH[4], LUCAS MENZEL[3], IWONA PIŃSKWAR[1], MACIEJ RADZIEJEWSKI[1] and MAŁGORZATA SZWED[1]

[1]*Research Centre for Agricultural and Forest Environment, Polish Academy of Sciences, Bukowska 19, 60-809 Poznań, Poland;* [2]*Institute for Geophysics and Meteorology, University of Cologne, 50923 Köln, Germany;* [3]*Potsdam Institute for Climate Impact Research, 14412 Potsdam, Germany;* [4]*Institute of Meteorology, Free University of Berlin, 12165 Berlin, Germany*

(Received: 14 October 2003; accepted: 30 June 2004)

Abstract. In Central Europe, river flooding has been recently recognized as a major hazard, in particular after the 1997 Odra /Oder flood, the 2001 Vistula flood, and the most destructive 2002 deluge on the Labe/Elbe. Major recent floods in central Europe are put in perspective and their common elements are identified. Having observed that flood risk and vulnerability are likely to have grown in many areas, one is curious to understand the reasons for growth. These can be sought in socio-economic domain (humans encroaching into floodplain areas), terrestrial systems (land-cover changes – urbanization, deforestation, reduction of wetlands, river regulation), and climate system. The atmospheric capacity to absorb moisture, its potential water content, and thus potential for intense precipitation, are likely to increase in a warmer climate. The changes in intense precipitation and high flows are examined, based on observations and projections. Study of projected changes in intense precipitation, using climate models, for several areas of central Europe, and in particular, for drainage basins of the upper Labe/Elbe, Odra/Oder, and Vistula is reported. Significant changes have been identified between future projections and the reference period, of relevance to flood hazard in areas, which have experienced severe recent floodings.

Key words: flood hazard, flood risk, intense precipitation, river flow, climate change, climate change impact, central Europe

1. Introduction

According to the global data of the Red Cross for the time period 1971–1995, floods killed, in an average year, over 12,700 humans, affected 60 million people and rendered 3.2 million homeless. Berz (2001) examined temporal variability of great flood disasters (understood as events where international

★ Author for correspondence. E-mail: zkundze@man.poznan.pl or zbyszek@pik-potsdam.de

or inter-regional assistance is necessary). His data show that recently the number of great flood disasters worldwide has considerably grown. In the nine years 1990–1998 it was higher than in the three-and-half earlier decades 1950–1985, together (Kundzewicz, 2003). Since 1990, there have been over 30 floods worldwide, in each of which material losses exceeded one billion US$ and/or the number of fatalities was greater than one thousand. The highest material flood losses, of the order of 30 billion USD, were recorded in China in the summer of 1998, while the storm surge in Bangladesh during two days of April 1991 caused highest number of fatalities (140,000).

It is estimated that the material flood damage recorded in the European continent in 2002 has been higher than in any single year before. According to Munich Re (2003), the floods in August of 2002 alone caused damage at the level exceeding 15 billion Euro (therein 9.2 in Germany, and 3 each in Austria and in the Czech Republic). During severe storms and floods on 8–9 September 2002, 23 people were killed in southern France (Rhone valley), while the total damage went up to 1.2 billion USD. Several destructive flood events also occurred overseas in 2002. In July and August of 2002, floods and landslides in northeastern and eastern India, Nepal and Bangladesh killed 1200. A flood in central and western China in June caused 3.1 billion USD losses and killed 500, while another one, in central and southern China in August, caused 1.7 billion USD damage and killed 250.

In recent years, several catastrophic floods have occurred in large central European rivers: Elbe/Labe, Oder/Odra and Vistula. The present paper will put these destructive flood events in perspective.

2. Flood Risk on the Rise? In Search of Causal Mechanism

Having observed that flood risk and vulnerability is likely to have grown in many areas, one is curious to understand the reasons for growth. A review of possible mechanisms of changes (in terrestrial systems, in socio-economic systems, and in climate) is presented in Table I.

Flood risk may have grown due to a range of land-use changes, which induce land-cover changes, hence changes of hydrological systems. Deforestation, urbanization, and reduction of wetlands empoverish the available water storage capacity in a catchment. Urbanization has adversely influenced flood hazard in many watersheds by increase in the portion of impervious area (roofs, yards, roads, pavements, parking lots, etc) and increase of the runoff coefficient. In result, higher peaks of runoff responses to intensive precipitation have been observed and the time-to-peak has decreased. Timing of river conveyance may also have been considerably altered by river regulation measures (channel straightening and shortening, construction of embankments).

Flood risk has substantially grown due to considerable changes in socio-economic systems, corresponding to development of flood-prone areas.

Table I. Possible reasons for changes in flood risk and vulnerability in central Europe

- Changes in terrestrial systems (hydrological systems and ecosystems; land-cover change, river regulation – channel straightening, embankments, changes of conditions of transformation of precipitation into runoff leading to a higher peak and shorter time-to-peak).
- Changes in socio-economic systems (increasing exposure and damage potential – floodplain development, growing wealth in flood-prone areas, land-use change: urbanization, deforestation, elimination of natural inundation areas (wetlands, floodplains causing land-cover changes in terrestrial systems), changing risk perception).
- Changes in climate (holding capacity of the atmosphere, intense precipitation, seasonality, circulation patterns).

Shortage of land, attractiveness of floodplains, and unjustified belief in absolute safety of structural flood protection schemes (dikes, dams), cause the tendency of massive human encroaching into flood-prone areas, and investing in infrastructure there. Many wrong locational decisions have been taken, which cause the flood loss potential to increase. In the same time, much of the natural flood storage volume is lost, ecosystems are devastated and riparian wetlands destroyed.

In addition to the changes specified above, also changes in climate are likely to play an important role in changing flood risk and vulnerability.

According to IPCC (2001a), a statistically significant increase in global land precipitation over the 20th century has been noted. This refers to both mean values and extremes, but the extremes in precipitation are likely to change more than the mean. It results directly from physics (Clausius–Clapeyron law) that the atmosphere's capacity to absorb moisture (and its absolute potential water content, pool of precipitable water, and thus potential for intensive precipitation) increases with temperature. This is a sufficient condition, *caeteris paribus*, for an increase in flood hazard. Indeed, higher and more intense precipitation has been already observed in many areas of the mid- and high latitudes, e.g. in the USA and in the UK (IPCC, 2001a), and this trend is expected to strengthen in the future, warmer world.

It is very likely (IPCC, 2001a) "that in regions where total precipitation has increased … there have been even more pronounced increases in heavy and extreme precipitation events. The converse is also true." Moreover, increases in "heavy and extreme precipitation" have also been documented in some regions where the total precipitation has decreased or remained constant. That is, the number of days with precipitation may have decreased more strongly than the total precipitation volume. As stated in (IPCC, 2001a), changes in the frequency of heavy precipitation events can arise from several causes, e.g., changes in atmospheric moisture or circulation. Over the latter half of the 20th century, it is likely that there has been a 2 to 4%

increase in the frequency of heavy precipitation events reported by the available observing stations in the mid- and high latitudes of the Northern Hemisphere. The area affected by most intense daily rainfall is growing and significant increases have been observed in both the proportion of mean annual total precipitation in the upper five percentiles and in the annual maximum consecutive 5-day precipitation total. The latter statistic has increased for the global data in the period 1961–1990 by 4% (IPCC, 2001a). The number of stations reflecting a locally significant increase in the proportion of total annual precipitation occurring in the upper five percentiles of daily precipitation totals outweighs the number of stations with significantly decreasing trends by more than 3 to 1 (IPCC, 2001a).

Where data are available, changes in river flow usually relate well to changes in total precipitation (IPCC, 2001a). There are a number of studies reporting that high flows have become more frequent (cf. Kundzewicz, 2003). Many increases of annual maxima and peak-over-threshold (POT) variables have been found in a part of the river flow data in different areas, e.g. in the UK (particularly in Scotland and in southeastern England), and in the USA. However, this does not directly translate into general finding on changes in flood flows everywhere. No globally uniform increasing trend in maximum river flow has been detected. In some stations, a statistically significant decrease has been reported, while in many stations – no statistically significant change has been found.

The links between flood-risk growth and climate variability and change have found extensive coverage in the Third Assessment Report (TAR) of the Intergovernmental Panel on Climate Change (IPCC, 2001a, b; Kundzewicz and Schellnhuber, 2004). In (IPCC, 2001b), floods have been ubiquitously identified on short lists of key regional concerns.

The general conclusion drawn from the science of the climate change is as follows: the hydrological cycle is likely to accelerate in the warmer climate. Yet, there is a great deal of uncertainty in findings about future climate change impacts on water resources, and this refers particularly to extreme events. Part of the problems is due to a spatial and temporal scale mismatch between coarse-resolution climate models and hydrological (catchment) spatial scale and between monthly/daily data and daily/hourly dynamics of flood routing. Only in some, but not all, areas, the projected direction of change of hydrological processes is consistent across different scenarios (emissions of greenhouse gases, which drive climate models) and across different models.

Studies of links between hydrological extremes and climatic variability (e.g., oscillations in the Ocean–Atmosphere system, such as the El Niño–Southern Oscillation (ENSO) or North-Atlantic Oscillation (NAO) lead to interesting findings. The frequency and intensity of ENSO have been unusually high since the mid 1970s, as compared with the previous 100 years

of instrumental records (IPCC, 2001a). This is likely to have direct consequences related to changes in flood hazard, since in some regions of South America, intensive precipitation and floods occur frequently in the El Niño phase (IPCC, 2001b).

Regional changes in timing of floods have already been observed in many areas, with increasing late autumn and winter floods (caused by rain and/or earlier snowmelt) but lower spring snowmelt flows and less ice-jam-related floods, e.g. in central Europe. This has been a robust result. Yet, intensive and long-lasting precipitation episodes happening in summer, especially those induced by the Vb cyclone (see Section 5), have led to disastrous recent flooding in Europe. Certainly, one should be very careful with attempts to attribute the responsibility for occurrence of a particular flood to global changes (e.g. of climate). A particular flood may have well manifested the natural variability of the river flow process – virtually any maximum flow rate, which was observed recently, had been exceeded some time in the (possibly remote) past. Yet, increased probability of intense summer precipitation and floods fits well into the general image of the changing (warming) globe with intensified, accelerated hydrological cycle.

Changes in future flood frequency are likely to be complex (Arnell and Liu, 2001). They depend on the flood-generation mechanism. Increasing flood magnitudes are likely to occur where floods result of heavy rainfall. Decreasing magnitudes are expected where floods are generated by spring snowmelt. All in all, climate change is likely to cause an increase of the risk of riverine flooding across much of Europe.

The climatic impact on water resources depends, in general, not only on changes in the characteristics of streamflow, but also on such system properties, as: pressure (stress) on the system, its management (also organizational and institutional aspects), and adaptive capacity. Climate change may challenge existing water resources management practices by contributing additional uncertainty, but in a particular place, non-climatic changes may have posed a greater impact.

3. Recent Floods in Central Europe in a Nutshell

In the basins of three large international rivers in central Europe: the Labe/Elbe (drainage basin in Czech Republic and Germany), the Odra/Oder (drainage basin in Czech Republic, Poland and Germany), and the Vistula (most of drainage basin in Poland, with basins of tributaries located also in Slovakia, Ukraine, and Belarus), cf. Figure 1, the water resources are rather scarce. However, even if the mean annual flow values are low, the hydrological variability is considerable, hence floods have not been uncommon. After the recent floods on three large rivers and their tributaries, floods have

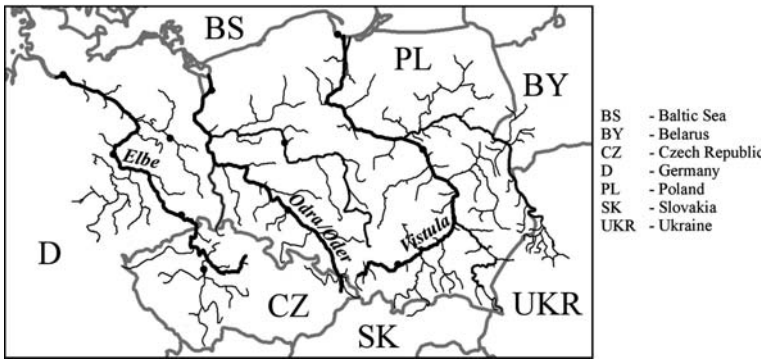

Figure 1. Location of the drainage basins of the rivers. Labe/Elbe, Odra/Oder, and Vistula.

been broadly recognized as a major hazard. The most destructive floods in central and eastern Europe, which occurred in 1997 in the basins of the Odra/Oder and the Vistula and 2002 in the basin of the Labe/Elbe, caused 114 and 36 fatalities, respectively, while the material damage reached 6.5 and 15.2 billion euro, respectively. The 2002 data include the flood on the Danube and its tributaries.

The three most recent floods; 1997 (Odra/Oder, Vistula, and their tributaries), 2001 (Vistula and its tributaries), and 2002 (Labe/Elbe and its tributaries) have several commonalities. All three flood events occurred in summer and were caused by similar atmospheric drivers – Vb atmospheric circulation type (cf. Figure 2). The floods were generated by intensive precipitation during a longer wet spell, which covered vast areas. Very fast, violent flash floods occurred in small and medium catchments of mountainous tributaries of large rivers and in the upper reaches of the main rivers. Huge masses of water propagated downstream the main rivers, causing dyke failures, and inundating urban areas, therein large towns. Since levees were broken and vast, mostly agricultural, areas were inundated, this was a relief to downstream areas. The flood wave flattened as part of it was trapped in a temporary storage. The return period of flood flow decreased downstreams; from very rare events in headwaters to more common events in lower (lowland) courses.

3.1. ODRA FLOOD OF 1997 – A POLISH PERSPECTIVE

In the second half of June 1997, abundant precipitation filled the natural storage and saturated the soil in a large part of the upper Odra/Oder catchment. From the 4th to the 10th of July, a quasi-stationary low-pressure trough developed, covering the catchment area of the upper Odra and its

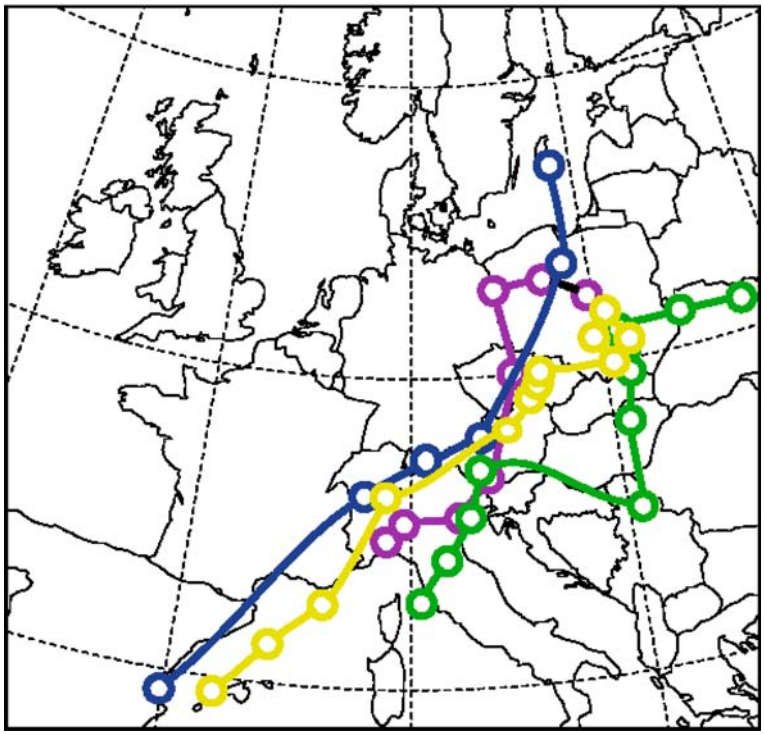

Figure 2. Cyclone track for 1997, 2001, and 2002 floods, with positions given in 12-hourly intervals. All lows shown have a north-eastward track. Green: low named "Xolska", 4 July 1997 00 UTC to 9 July 1997, 00 UTC; Yellow: low named Zoe, 16 July 1997 00 UTC to 21 July, 12 UTC; Blue: low named "Axel", 15 July 2001 00 UTC to 17 July 2001, 00 UTC. Pink: low named "Ilse", 10 August 2002, 00 UTC to 13 August 2002, 12 UTC. Results obtained within the MICE Project in the Institute for Geophysics and Meteorokogy, University of Cologne.

tributaries, with a front dividing humid air masses of largely different temperatures.

The heavy and long-lasting rains in the beginning of July, covering large areas, caused destructive flooding in Czech Republic and Poland. Yet, a few days later, another train of intensive rains occurred with up to 300 mm precipitation recorded from 17 to 22 July. A third wet spell, in the third decade of July 1997, occurred basically in the drainage basin of the river Vistula. Figure 3 presents the spatial distribution of precipitation over central and eastern Europe in July 1997 in relation to long-term July averages based on the 1961–1990 data.

One could distinguish three stages of the 1997 Odra flood in Poland. In the first stage, after the intensive rainfall in the catchments of the upper Odra and its headwater tributaries, river flows increased very fast. The flood was very

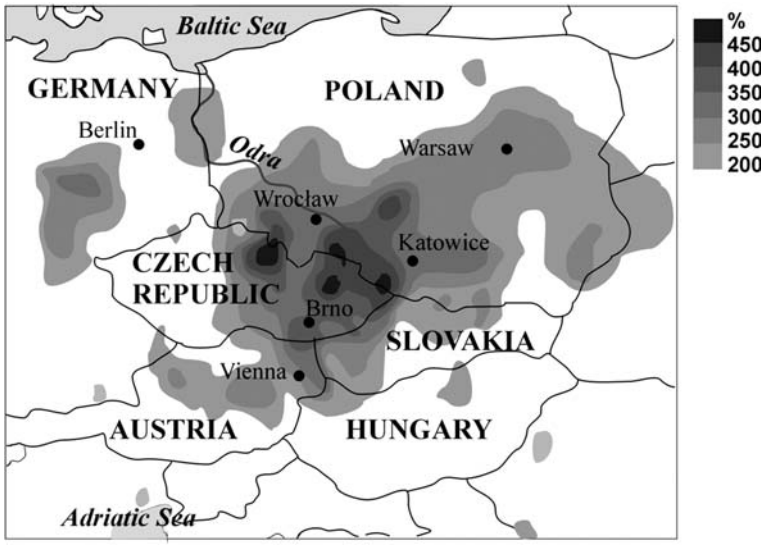

Figure 3. Precipitation in July 1997, compared to a mean monthly value (by courtesy of Dr Bruno Rudolf, Global Precipitation Climatology Centre (GPCC), German Weather Service, Offenbach).

destructive and dynamic – it virtually ruined the town of Kłodzko (31,000 inhabitants) located at the river Nysa Kłodzka, tributary to the Odra. It also destroyed several staff gauges, including the one in Racibórz-Miedonia, where all-time record was observed on 9 July before the records discontinued, as illustrated in Figure 4. In Racibórz-Miedonia, the former record stage of 838 cm and the record discharge of 1630 $m^3 s^{-1}$ of 1985 were marked out by the much higher values of 1045 cm and 3260 $m^3 s^{-1}$, respectively, in July 1997. The flow rate of the exceedance probability of 1% (100-year-flood) estimated in this cross-section, based on seven decades of records, reads 1680 $m^3 s^{-1}$.

In the second stage, a huge flood wave, which was already in the river channel of the Odra, propagated downstream and inundated towns located upon the river. Due to the huge size of the wave it was not possible to avoid urban flooding, yet, thanks to the time lag, some preparation could be made. The flood devastated large riparian towns located on the Odra, such as Racibórz (65,000 inhabitants), Opole (131,000) and Wrocław (700,000). In Opole, water level outstripped the absolute historic maximum by 173 cm (777 cm in 1997, as compared to 604 cm in 1813 and 584 cm in 1985) and the peak flow reached 3500 $m^3 s^{-1}$. The flood protection system of Wrocław was designed for a flow rate of 2400 $m^3 s^{-1}$, and was generally perceived as

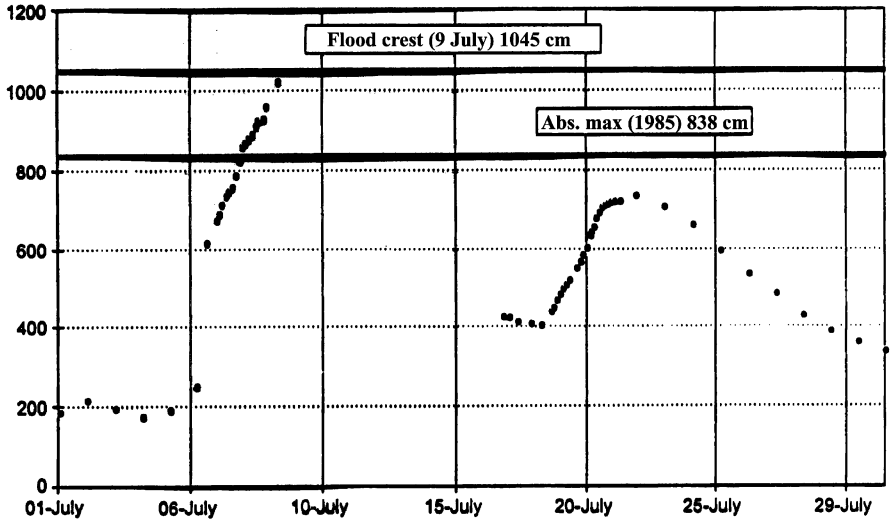

Figure 4. Stage hydrograph for the river Odra, gauge Racibórz-Miedonia in July 1997. (Source: Kundzewicz *et al*., 1999, based on IMGW data.)

adequate. However, the peak flow rate in July 1997 was higher nearly by half than the design value, and large parts of the city were inundated. Due to dike failures and massive inundations, the flood wave in the Odra lost part of its impetus. The peak flow of the flood wave decreased while travelling downstream, so that the return period of the maximum discharge, being of the order of at least several hundreds up to thousands years in the headwaters (Grünewald, 1998), was far more common downstreams.

Finally, in the third stage of the flood, high water reached the boundary stretch (state border between Poland and Germany) and the lower Odra. There was more time for preparation – heightening and strengthening of embankments. The fight to save the dikes was largely successful on the Polish side. On the German side, several dike breaches occurred and significant material losses were recorded.

In Poland, the nation-wide toll for both the Odra and the Vistula floods of summer 1997 was an all-time high as far as the economic damages are concerned. The number of flooded towns and villages was 2592, the number of evacuees was 162,000, and around 665,000 ha of land were flooded, of which agricultural fields constitute over 450,000 ha. More detailed information can be found in Kundzewicz *et al*. (1999).

The 1997 Odra flood was a surprise to many, since there have been no disastrous floods on the Odra for several decades before the recent deluge. However, many destructive events were recorded earlier in historic times; both winter floods, related to snowmelt and ice-jams, and summer

rain-caused floods (typically in June and July). For example, in July 1310, a large flood hit Kłodzko, inundating suburbs and killing between 1500 and 2000 people. Floods usually occurred either on the upper and middle Odra (e.g. 1813, 1854, 1903, 1977 and 1985) or on the Lower Odra (e.g. 1855, 1940). Floods covering the whole length of the river have been more rare and usually very dramatic. The flood in the summer of 1997 was an extreme one in this category.

The flood of 1997 lasted long. The wave travelled slowly downstream and, at several gauging stations, the alarm levels were exceeded uninterruptedly during several weeks. The exceedance of the historic absolute maximum water levels lasted from 4 to 7 days at the upper Odra to about 16 days in Połłęcko.

The existing flood protection system in the drainage basin, consisting of dikes, reservoirs (including dry flood protection reservoirs) and relief channels at the Odra and its tributaries, and a system of polders, could not accommodate such a gigantic flood wave as the one occurring in 1997. The structural flood defences, for several larger towns upon the Odra and its tributaries and for vast areas of agricultural land, proved to be dramatically inadequate for such a rare flood. No wonder, indeed, flood defences, are designed to withstand smaller, more common floods (of the order of tens to 100-year return interval), and fail when exposed to a much higher pressure of an extraordinarily high flood. Indeed, if a flood record is doubled and the flood recurrence interval gets into the range of several hundreds or thousands of years, i. e. very much higher than the design value (Grünewald, 1998), there is no way to avoid high material losses. One notable exception is the Dutch regulation, whereby major river dikes have been designed to withstand a very rare flood.

The event made the broad public aware of how dangerous and destructive a flood can be. It also unveiled the weaker points of the existing flood defence system and helped identify the most pressing needs for improvements. Indeed, every link in the chain of the operational flood management was found to be in need of considerable strengthening.

The flood of 1997 was the most extreme event on record, both in hydrological terms (peak stage, flow, inundated area) and in economic terms (material losses). It was an effect of exceptionally intensive and persistent precipitation covering a large area. This very rare hydrological event was superimposed on a complex, and dynamically changing, socio-economic system of Poland – a country with economy in transition from centralized to market-based system.

3.2. ELBE FLOOD OF 2002 IN PERSPECTIVE

The meteorological mechanism responsible for occurrence of heavy precipitation included composite events: two low-pressure systems (Hanne and Ilse),

commencing near Ireland four days after each other, and then moving southeast over the Mediterranean, and further towards Northeast, meeting colder air masses. The Vb cyclone brought moisture from the Mediterranean area to central Europe (cf. Ulbrich *et al.*, 2003a, b). Intense, long-lasting precipitation was recorded, which covered large areas. Monthly precipitation in August 2002 is presented in Figure 5.

According to Czech data (Kubát *et al.,* 2003), for over a week since 6 August, every day, intensive precipitation was measured in one or several Czech raingauges. For instance, in Staré Hute (altitude 792 m, county Ceské Budejovice), there were three days, with daily precipitation in excess of 100 mm each (101.4 mm on 6 August, 152.9 on 7 August during the first train of intense precipitation and 107.4 on 12 August, during the second train of intense precipitation). In Knajpa (county Jablonec n. Nisou), precipitation observed on 12 August and 13 August was 75.6 mm and 278 mm, respectively. Extremely high precipitation of 312 mm was measured at the station Cínovec (county Teplice) on 12 August, but rainfall observed there in adjacent days was also high (68 mm on 11 August and 26 mm on 13 August).

Two waves of intense precipitation: 6–7 and 11–12 August (first one largely filling the storage capacity in the catchments) turned out to be fatal for

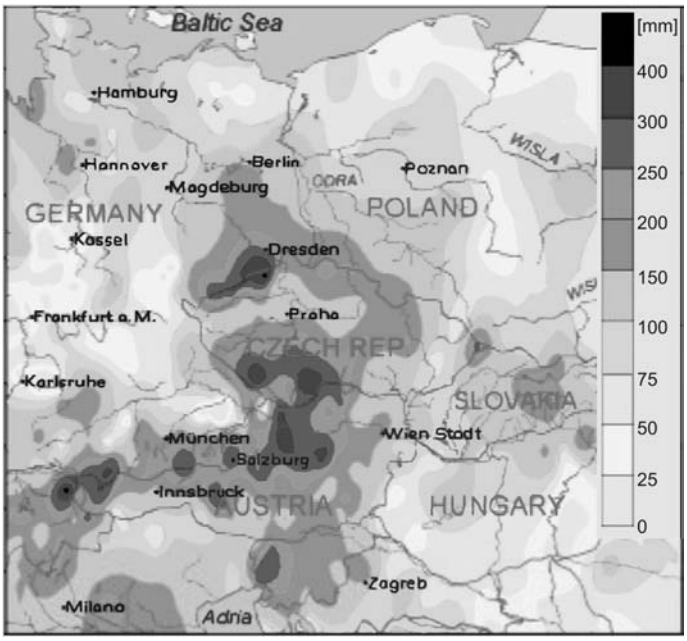

Figure 5. Precipitation in August 2002 (from: Rudolf and Rapp, 2003).

the Czech capital, Prague, jeopardized by the main river, Vltava (Moldau) and its tributaries (Sazava and Berounka). Upstream reservoirs in the Vltava basin (mostly multi-purpose, with hydropower as the main task, and corresponding operation rules) were filled during the first flood wave and could not accommodate high inflows during the second flood wave. The 2002 flood peak level in Prague exceeded all the events recorded in the last 175 years (Kubát *et al.*, 2003). This is the only instance when the flow rate of 5000 m^3/s^{-1} was exceeded. Between 1941 and 2001 Vltava flow never reached 2500 m^3/s^{-1}. Three exceedences of the $Q_{100} = 3700$ m^3/s^{-1} were observed within five decades of the 19th century (1845, 1862, 1890).

In four precipitation observing stations, the 24-hour precipitation in August 2002 has qualified into the ten highest observations ever recorded in the Czech Republic (Cinovec 312 mm in the Ore Mountains, Knajpa, 278 mm, Smedavská hora, 271.1 mm, and Jizerská 247.8 mm – all three stations in Jizerské mountains). Also in the category of two-day precipitation, the 2002 record at Cinovec (380 mm) was the highest in the history of observation record. However, in the category of three-day event, the Cinovec mark (406 mm) did not reach the top. It ranked ninth on record, while the top six three-day rainfalls, on the list of national records, stem from July 1997 (Kubát *et al.*, 2003).

The 24-hr precipitation of 312 mm was also recorded in Germany, beating the all-time national record. In Zinnwald-Georgenfeld (Saxony), 312 mm of precipitation was recorded from 12 August 2002, 6 a.m. UTC to 13 August 2002, 6 a.m. UTC (usual time interval for measuring one-day precipitation). However, since hourly values are available, it has been found that maximum 24-hour precipitation recorded from 12 August 2002, 5 a.m. UTC to 13 August 2002, 5 a.m. UTC was even higher and reached 352.7 mm (Rudolf and Rapp, 2003). The maximum 24-hr and 72-hr precipitations recorded in Zinnwald-Georgenfeld in August 2002 are expected to occur less frequently than once in a hundred years. High precipitation in Zinnwald and vicinities caused a catastrophic flood of the river Müglitz (Figure 6), which destroyed the village Weesenstein (south of Dresden).

The return periods of some flood flows in August 2002 in Czech Republic and Germany were of the order of several hundred years.

The water level of the Elbe in the profile Dresden on 17 August 2002, i.e. 940 cm, has considerably (by 63 cm) exceeded the former highest mark, while records are available since 1275. The second highest water level, 877 cm, dating back to 31 March 1845, was related to snowmelt and ice-jam flood. In the past, stages in excess of 800 cm were observed in Dresden five times during less than a century – from 1785 to 1879 (four out of five times – in February or March), but this level has never been reached more recently in the over 120-year time period after 1880, until the 2002 flood. However, such a long period of lower annual maxima has not been uncommon in the

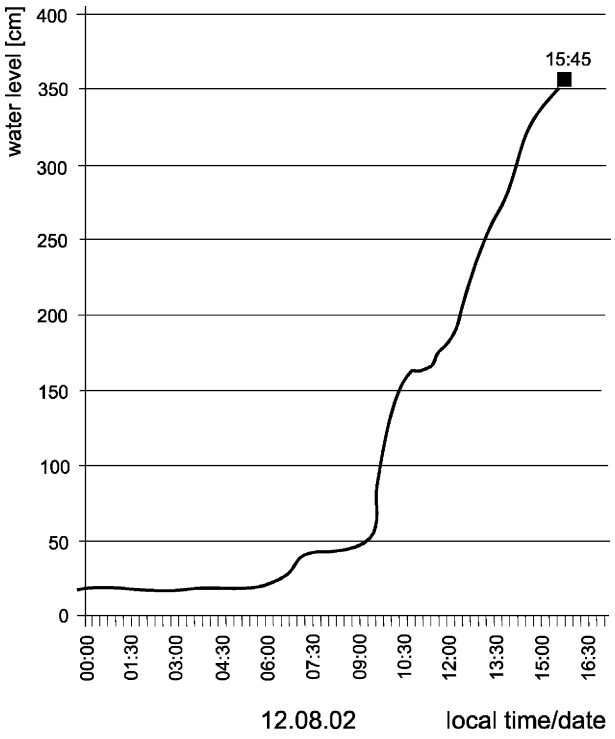

Figure 6. Stage hydrograph for the river Müglitz, gauge Dohna on 12 August 2002. Data were provided by Dr Höhne, Saxonian State Office for Environment and Geology (Sächsisches Landesamt für Umwelt und Geologie).

historical data. For instance, between 1502 and 1783, i.e. 281 years, the level of 800 cm was exceeded only once.

Figure 7 illustrates the spatial-temporal changes of flow of the river Elbe, for different cross-sections. It results from Figure 7 that the tributaries of particular importance during this event were: the Mulde (increase of flow in the Elbe due to strikingly high inflow) and the Havel (decrease of flow in the Elbe due to massive polder inundation).

Greatest devastation was caused by flooding on tributaries to the Elbe. Some rivers rose by up to 4 m, as the river Mulde (adjacent to the river Müglitz) in Grimma. The Dresden Central Station was inundated to the depth of 1.5 m by the river Weißeritz, which during the 2002 flood turned back to the old bed. Evacuation of people and wealth was necessary, including most valuable cultural treasures (e.g. musea in Dresden and Semper Opera house).

The breakdown of 2002 flood damage in Germany (the Elbe, the Danube, and their tributaries) amounting to 9.2 billion euro, after Munich Re (2003), reads: private households 2.1 billion euro, infrastructure belonging to state

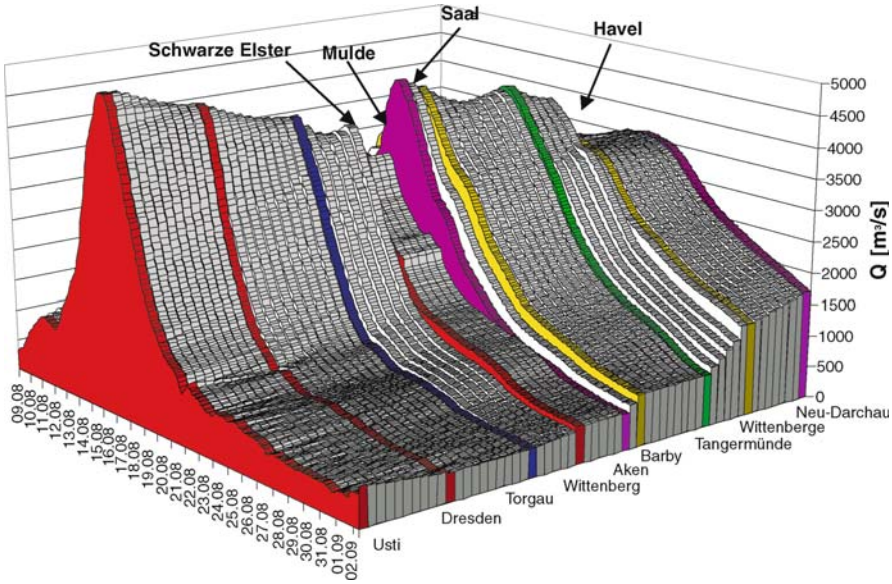

Figure 7. Spatial-temporal diagram of flow of the river Elbe. Courtesy of Dr Engel, Bundesanstalt für Gewässerkunde, Koblenz, Germany.

and local authorities 1.8, trade and industry 1.7, federal infrastructure 1.6, agriculture 0.29, other losses 1.7.

The 2002 deluge resembled historic events from remote past. For example, on 21 July 1342, a St. Magdalene's flood, caused by intensive rain, devastated large areas of Europe, causing thousands fatalities and immense destruction. Yet, apart from the record set in Dresden, the all-times historic flood records on the river Mulde in Döbeln (1897) and Grimma (1573) were exceeded in August 2002 by 126 cm, and 136 cm, respectively (Becker and Grünewald, 2003). The two types of disastrous floods occurring in the past were: summer floods in June–July–August, caused by intense precipitation, and winter floods caused by snowmelt, ice-advances and ice-blocking.

From the viewpoint of spatial extent of precipitation, its intensity and duration (a wave of two wet spells), hence – precipitation totals, the August 2002 event was exceptional.

During the 2002 flood, the structural defences – important element of the flood preparedness system – occurred to be insufficient. Dikes were found to be in need of heightening and strengthening. However, since the building of dikes has taken most of natural inundation areas, a strong opinion was voiced for a need "to give rivers their floodplains back". Sealing of land surface reduced retention and accelerated runoff. Careless development of areas exposed to flooding has amplified the impact. Most riparians have not been aware that indeed no technical protection gives a perfect safety, and that there

exist no measure preventing inundations during really extreme floods, which are rare, but not impossible. So, in case of a rare flood, even an optimal flood protection system, composed of both structural and non-structural measures, can only minimize the damage, rather than guarantee a complete protection.

3.3. HAS THERE BEEN A TREND?

Mudelsee *et al.* (2003) found no upward long-term trends in the occurrence of extreme floods in central Europe. In their considerations, they included such factors as reservoirs and deforestation, and found that they have had minor effect on flood frequency. The instrumental database used in their study was extended by concatenation of the historical database, of a largely different (lower) accuracy. In the instrumental dataset, decrease in winter flood occurrence over the last century was observed, with fewer events of strong freezing. For 1920–2002, and for 1852–2002, decreasing numbers of winter floods were observed for the Oder and the Elbe, respectively. Indeed, winter floods, which were so frequent in the past, have become quite rare now. For instance, the last ice flood on the Elbe and the Oder took place in 1947. Mudelsee *et al.* (2003) found trends for major summer flood events (classes 2–3) at significance level of 90% neither on the Elbe nor on the Oder, except for an upward trend for all flood events (including minor ones) and with correction for reservoirs. In their analysis of extreme precipitation events during the 20th century, Mudelsee *et al.* (2003) found increasing trend (90% level) for gridded monthly precipitation values at 50° N and 15° E (containing nearly the entire catchment of the Elbe at Dresden and part of the catchment area of the Oder at Eisenhüttenstadt) and no significant trend at 50° N and 18.75° E (containing eastern and southern parts of the Oder catchment plus large areas beyond the basin). Historical precipitation data consisted of homogeneized monthly estimates for grid boxes of the size of 2.5° latitude × and 3.75° longitude. Even if Elbe and Oder are large rivers, yet monthly interval is not adequate temporal resolution for studying intense precipitation and floods.

However, it is important to note that climate is just one of several important factors controlling the process of river flow. Figure 8 illustrates changes in annual maximum river flow of the river Warta (large right-hand tributary to the Odra) at the Poznań gauge. There has been a clearly decreasing long-term tendency in annual maximum flow, which is difficult to explain by climatic impacts. The tendency can be explained by direct human interference (changes in storage, land use, and melioration).

4. Intense Precipitation – What Changes are Expected in Central Europe?

Based on results of climate models, it is projected that changes of mean precipitation will significantly differ from changes of the potential future

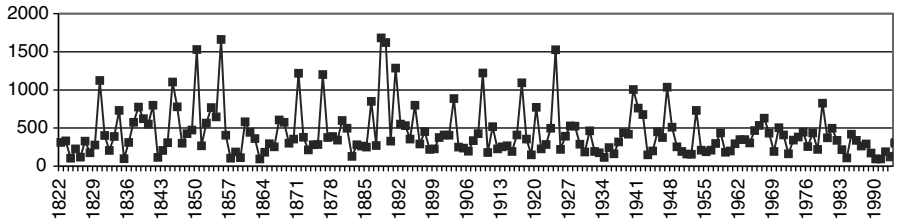

Figure 8. Maximum annual flow of the river Warta, gauge Poznań. (Source: Graczyk *et al*., 2002.)

occurrence of extreme precipitation events in central Europe, which are likely to become more intense and more frequent. For example, Christensen and Christensen (2003) used the regional climate model HIRHAM4 (Christensen *et al*., 1998), arriving at the conclusion that the amount of summer precipitation exceeding the 95th percentile is very likely to increase in many areas of Europe, even if the mean summer precipitation may decrease over a substantial part of the European continent. However, climate models are not overall consistent with respect to the direction of change on mean summer precipitation over central Europe (IPCC, 2001a). But, up to recent results, it seems likely that for broad parts of the investigation area the mean summer precipitation will decrease, corroborating the general projection of enhanced summer drying over continental interiors, while the amount of precipitation related to extreme events will increase.

The regional climate model considered here is the Hadley Centre (Bracknell, UK) model HadRM3. It is driven by the global atmospheric model HadAM3, following the dynamical downscaling technique. Details about the model physics and used parametrizations of the Hadley Centre model family can be found e.g. in Pope *et al*. (2000), Gordon *et al*. (2000) or Collins *et al*. (2001). In order to study a climate change signal, two 30-year time periods are compared. For present-day climate conditions the period 1961–1990 is assumed as representative, whereas a possible future scenario is represented by the period 2070–2099. The climate model experiments were based on the IPCC SRES (Special Report on Emission Scenarios) marker scenario A2 (cf. Nakicenovic *et al*., 2000).

One index used for the quantification of intense precipitation events is defined via the number of days with 24-h precipitation, exceeding an arbitrarily selected threshold of 10 mm. For Europe, the climate change signal for 2070–2099 (Figure 9) reveals a reduction in the number of intense rainfall events in the southern Europe and an increase over northern Europe.

Understanding of intense precipitation can be enhanced, when the daily precipitation produced by the model is separated into different intensity classes. The lower percentiles of daily precipitation over the upper part of the

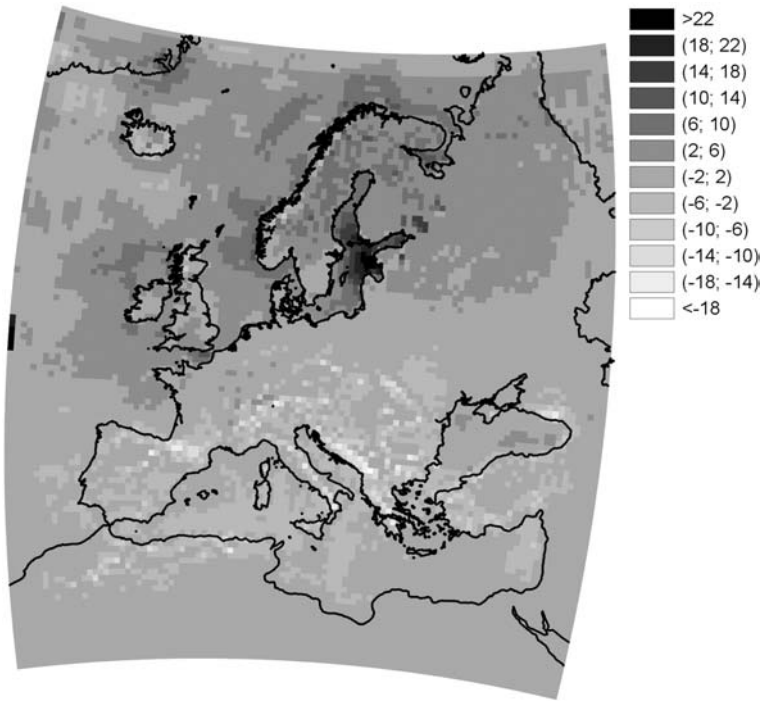

Figure 9. Number of days with 24 h precipitation, exceeding a threshold of 10 mm. Comparison of climate change signal simulated by HadRM3-P for the control period in the 20th century (1961–1990) and the future horizon of interest (2070–2099). The climate model experiment was run for SRES scenario A2a. Results obtained in the Research Centre of Agricultural and Forest Environment, Polish Academy of Sciences within the MICE Project.

Odra/Oder river basin are projected to decrease slightly, while the higher ones are likely to increase considerably (Figure 10). Looking at the drainage basins of all three large rivers of central Europe – Elbe (Labe), Odra (Oder), and Vistula, where dramatic flooding have occurred recently, one can note an increase in heavy precipitation (Figure 11) in projections for future maximum daily precipitation, likely to have important, and adverse, consequences for flood risk.

A corroborating result is produced when different global climate models are considered. The global models ECHAM4/OPYC3 (cf. Roeckner *et al*., 1992, 1996) and HadCM3, both representing state-of-the-art coupled climate models, have been selected for analysis. The validation of global simulation (ECHAM4/OPYC3 and HadCM3) precipitation data has proved that the general characteristics of summer and winter half-year precipitation compare well to the station data for areas in central Europe, reproducing trends existing in the observations in the last 40 years (decrease in summer and

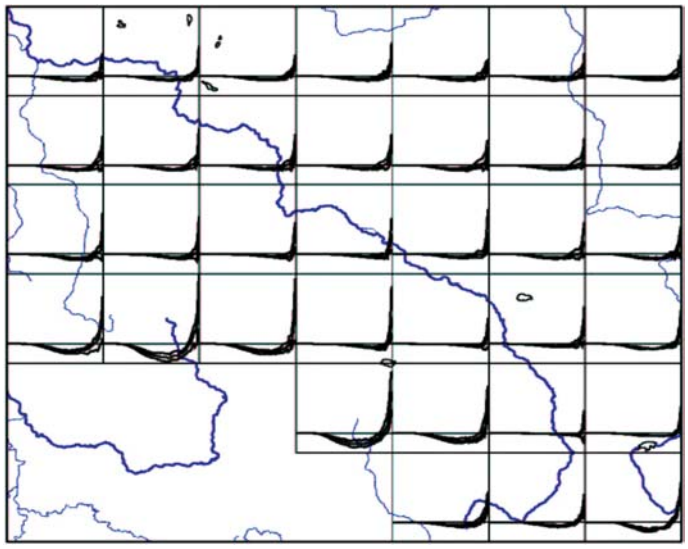

Figure 10. Climate change signal for different intensity classes of daily precipitation for the Odra basin (HadRM3 grid cells). Comparison of 1961–1990 and 2070–2099. For every grid cell considered, there is a diagram of changes of precipitation in different intensity classes. The *x* and *y* axes represent, respectively, precipitation intensity and change in precipitation of a particular intensity. Diagrams presented in individual grids show a decrease in low-intensity precipitation and an increase in high-intensity precipitation. Results were obtained in the Research Centre of Agricultural and Forest Environment, Polish Academy of Sciences within the MICE Project.

increase in winter), cf. Krüger (2002). For the Dresden area, changes of the daily precipitation amount per intensity class are shown in Figure 12 for summer (June, July, August) and for time intervals 2060–2089 *versus* 1930–1959. For ECHAM4/OPYC3 (a spectral model with a horizontal resolution of T42) the grid box area centred around 51.6257° N and 14.06257° E was selected, for HadCM3 four grid cells were chosen, for the regional model (HadRM3), nine grid cells have been selected. This was done in order to achieve a higher level of representativeness, as especially in the regional model the analysis of one grid cell is insufficient. The classification was done separately for each grid cell, and afterwards accumulated to one signal. From analysis of the climate model outputs it becomes clear that in HadCM3 and ECHAM4/OPYC3 simulations, the amount of precipitation related to events with daily precipitation less than 16 mm per day are reduced, whereas the amount related to intense precipitation events (>16 mm) will increase under climate change conditions. For HadRM3 simulations, the increase of intense precipitation event under climate change is projected only for the most extreme events (>32 mm).

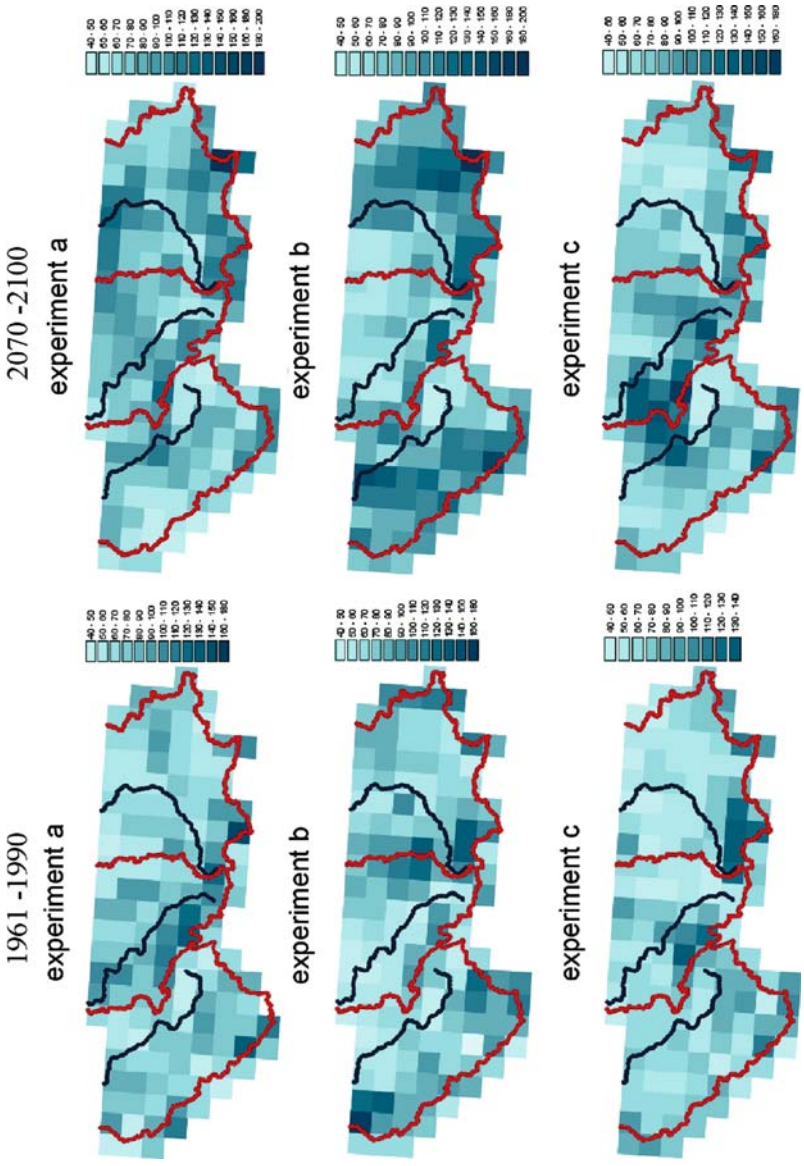

Figure 11. Maximum daily precipitation – comparison of projections for 2070–2099 *versus* the control period 1961–1990, based on HadRM3, for three model runs (a, b, c) for the upper parts of the catchments of the rivers Elbe (Labe), Odra (Oder) and Vistula. Results obtained in the Research Centre of Agricultural and Forest Environment, Polish Academy of Sciences within the MICE Project.

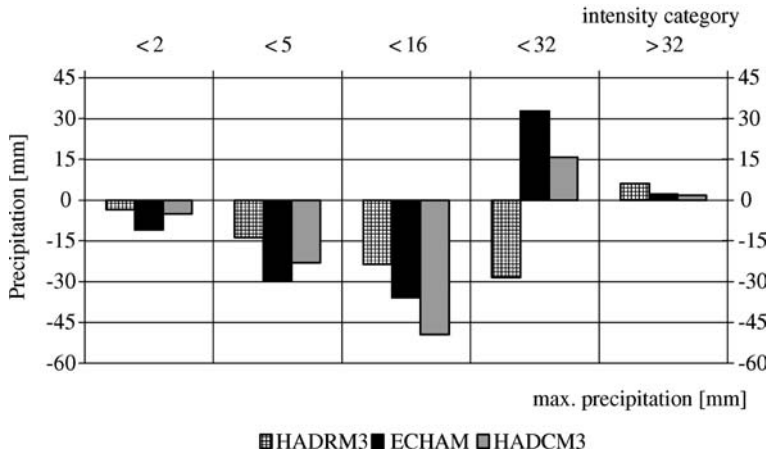

Figure 12. Changes in the daily summer (June, July, August) precipitation in different intensity classes for ECHAM4/OPYC3, HadCM3, and HadRM3, for grid box areas surrounding the city of Dresden for time intervals: 2060–2089 and 1930–1959. Result obtained in the Institute for Geophysics and Meteorology, University of Cologne.

Thus, summarizing the results presented so far, under future climate conditions (SRES A2 scenario) a tendency to a higher amount of extreme daily precipitation for summer rainfall can be diagnosed for the investigation area. This increase in intense precipitation, which is likely to increase the flood risk, is of significant concern for water management in these regions.

However, not all studies agree as to the direction of future changes in intense precipitation and flood frequency in selected catchments in central Europe. The mountainous area at the Czech-German border of the Elbe catchment, where floods along the Elbe and its tributaries frequently originate, has been investigated in terms of future flood development. In a first step, the rainfall-runoff model HBV-D (Bergström and Forsman, 1973; Menzel and Bürger, 2002) has been applied with observed climate data to reproduce historical discharge conditions, and found to perform well in the sense of mean values, showing reduction of mean discharge conditions over the scenario period. Subsequently, climate scenarios have been delivered from the stochastic method STAR (Werner and Gerstengarbe, 1997) which combines large-scale temperature change projections and locally measured, long-term time series of temperature and related climate parameters. Regional climate scenarios agree in their projections of a general mean precipitation decrease in the investigated regions and show a tendency of increasing precipitation intensities both in summer and winter, although not in a consistent way (statistically significant increases for some stations only). However, results of river flow simulations indicate reduced flood risk in the scenario period for the catchment in question. This is in contrast to clear

increase in flood risk found, using the same methodology, for another examined catchment in western part of Germany. There are indeed large uncertainties resulting from the discrepancies between climatic models, problems with hydrological models (which are still not capable to reproduce small-scale, intense floods, especially when they occur during summer), and problems with the fit of the Gumbel distribution, used in flood frequency studies. Hence, further investigations are needed to confirm (or disprove) these results.

5. Possible Synoptic Causes and their Relation to Climate Change

The existence of a so called ''Vb-track'' situation in summer has accompanied recent occurrences of extreme precipitation events over Central Europe (cf. Ulbrich *et al.*, 2003a, b). The name ''Vb-track'' originates from a work of van Bebber (1891), who classified tracks of European lows. A Vb-track situation is characterized by a cyclone system travelling from the Gulf of Genoa northeastwards to central Europe. Occurrence of such situations in summer and comparison of the role of these cyclone tracks for extreme rainfall under present-day and future climate conditions are investigated. In order to detect changes of weather regimes connected with the occurrence of Vb-tracks, a specific analysis of Vb-tracks under climate change conditions, as well as an objective classification method of weather situations (Grosswetterlagen, GWL) were applied.

For the vegetation season (April to September), an algorithm from Murray and Simmonds (1991) was used for the identification and tracking of cyclone cores over the North Atlantic and European sector. This investigation was done using simulation data of the Global Climate Model ECHAM4/OPYC3, for the climatology of 1861–1930 as well as for enhanced greenhouse gas concentrations. A validation of the results with respect to NCEP-re-analysis data reveals a systematical underestimation of the number of tracks due to the model time and spatial resolution, whereas the distribution pattern (e.g. of the track density) is well reproduced (Pinto, 2002). From these identified systems only those following the pathway of typical Vb-tracks were considered. For historical climatology, the track density reaches a maximum above the Gulf of Genoa with up to 5 systems per summer, reducing to 2 or 1 system over the investigation area. The climate change signal of Vb-tracks reveals an overall reduction of the track density of the order of 20 to 30%. Thus, under changed climate, a tendency to a reduced number of Vb-track situations in summer is identified. However, the amount of rainfall related to extreme precipitation events increases. Thus, additionally an analysis of *Groswetterlagen* connected with heavy rainfall events (cf. Hess and Brezowsky, 1977; Gerstengarbe and Werner, 1993; Gerstengarbe *et al.*, 1999) was applied. Details of the applied

objective classification method can be found in Krüger (2002) and Krüger and Ulbrich (submitted). Thirty different GWLs are distinguished, whereof mainly the GWL Trough Central Europe (TCE) is connected with the occurrence of Vb-track situations. In ECHAM4/OPYC3, for all days during the vegetation season, a reduction of the frequency of the TCE GWL is simulated, consistent with the reduced Vb track density. If only the days with precipitation above the 90th percentile (intensive rainfall) are considered, both models simulate an increase of the TCE GWL in summer (June to August). Thus, for days with intense rainfall events, Vb-track related circulation pattern become more important under enhanced greenhouse gas concentrations than for the present-day climate. While there are less Vb situations under enhanced GHG forcing, these situations are likely to lead to extreme rainfall more frequently than under present conditions. This increased risk is of considerable importance for flood preparedness systems.

6. Concluding Remarks

Even if the mean precipitation over catchments of large rivers in Central Europe is low, the rainfall variability is high and intense precipitation may occur, in particular in the headwaters area. After the 1997 Odra /Oder flood, the 2001 Vistula flood, and the most destructive 2002 deluge on the Labe/Elbe, river flooding has been recently recognized as a major hazard in the region.

Having observed that flood risk and vulnerability are likely to have grown in many areas, one is curious to understand the reasons for growth. These can be sought in socio-economic domain (humans encroaching into floodplain areas, land-use change), terrestrial systems (land-cover change resulting from land-use change, river regulation), and climate system. The atmosphere's capacity to absorb moisture, its potential water content, and thus potential for intense precipitation, increase in a warmer climate. General acceleration of hydrological cycle in the warming world, observed already to some extent and projected in the future to a larger extent, leads to the conclusion that intense summer precipitation events could be on the rise.

Projections show more intense precipitation events in the warming climate also for central and eastern Europe. Significant changes have been identified for the catchments of the large rivers in central Europe, between future projections and the reference period. They are of direct relevance to increase of flood hazard in areas, which have experienced severe recent floodings.

It is an open question, whether or not the Vb circulation track, responsible for major flooding has become more frequent. This type of circulation occurred several times in the year 2002. Also the search for eventual changes in cyclone tracks, subject to ongoing research, has not led to conclusive results yet.

Acknowledgements

A major part of the research reported has been carried out in the framework of the MICE (Modelling the Impact of Climate Extremes) Project financed by the European Commission under the Fifth Framework Programme for Scientific Research. The climate-model data, produced by the Hadley Centre, have been provided to MICE by the LINK Project, funded by the UK Department of the Environment, Food and Rural Affairs. Dr Radziejewski was also supported by the Foundation for Polish Science. Useful and constructive remarks of an anonymous reviewer of this paper, which helped improve the presentation, are gratefully acknowledged.

References

Arnell, N. and Liu, Chunzhen (Coordinating Lead Authors): 2001, Hydrology and water resources. Chapter 4 in: J. J. Mc Carthy, O. F. Canziani, N. A. Leary, D. J. Dokken and K. S. White (eds.), IPCC (Intergovernmental Panel on Climate Change) *Climate Change 2001: Impacts, Adaptation and Vulnerability*. Contribution of the Working Group II to the Third Assessment Report of the Intergovernmental Panel on Climate Change, Cambridge University Press, Cambridge, UK.

Becker, A. and Grünewald, U.: 2003, Flood risk in Central Europe, *Science* **300**, 1099.

Bergström, S. and Forsman, A.: 1973, Development of a conceptual deterministic rainfall-runoff model. *Nord. Hydrol.* **4**, 147–170.

Berz, G.: 2001, Climatic change: effects on and possible responses by the insurance industry. In: J. L. Lozán, H. Graßl and P. Hupfer (eds.), *Climate of the 21st Century: Changes and Risks*. Office: Wissenschaftliche Auswertungen, Hamburg, Germany, 392–399.

Bürger, G.: 2002, Selected precipitation scenarios across Europe. *J. Hydrol.* **262**, 99–110.

Christensen, J. H. and Christensen O. B.: 2003, Severe summertime flooding in Europe, *Nature* **421**, 805.

Christensen, O. B., Christensen, J. H., Machenhauer, B., and Botzet, M.: 1998, Very high-resolution regional climate simulations over Scandinavia – present climate. *J. Clim.* **11**, 3204–3229.

Collins, M., Tett, S. F. B., and Cooper, C.: 2001, The internal climate variability of HadCM3, a version of the Hadley Centre coupled model without flux adjustments. *Clim. Dynam.* **17**, 61–81.

Gerstengarbe, F.-W. and Werner, P. C.: 1993, Katalog der Grosswetterlagen Europas nach Paul Hess und Helmuth Brezowski 1881–1992, *Berichte des Deutschen Wetterdienstes Nr. 113*, 4 Aufl., Selbstverlag des Deutschen Wetterdienst, Offenbach a. M., 249 pp.

Gerstengarbe, F.-W., Werner P. C. and Rüge, U.: 1999, *Katalog der Grosswetterlagen Europas nach P. Hess und H. Brezowski 1881–1992*, 5. Aufl. – Potsdam Institut für Klimafolgenforschung, Potsdam, Germany, 138 pp.

Gordon, C., Cooper, C., Senior, C. A., Banks, H. T., Gregory, J. M., Johns, T. C., Mitchell, J. F. B. and Wood R. A.: 2000, The simulation of SST, sea ice extents and ocean heat transports in a version of the Hadley Centre coupled model without flux adjustment. *Clim. Dynam.* **16**, 147–168.

Graczyk, D., Kundzewicz, Z. W. and Szwed, M.: 2002, Zmienność przepływów rzeki Warty w Poznaniu, 1822–1994 (Variability of flow of the river Warta, 1822–1994). In: *Detekcja zmian klimatu i procesów hydrologicznych* (Detection of changes in climate and hydro-

logical processes) Z. W. Kundzewicz, and Radziejewski, M. (eds.), Sorus Publishers, Poznań, Poland, 55–65.

Grünewald, U. (ed.): 1998, *Ursachen, Verlauf und Folgen des Sommer-Hochwassers 1997 an der Oder, sowie Aussagen zu bestehenden Risikopotentialen* (Causes, course and consequences of the summer flood of 1997 on the Oder and assessment of existing risk potential; in German). Deutsche IDNDR Reihe 10a, Bonn, Germany.

Hess, P. and Brezowsky, H.: 1977, Katalog der Grosswetterlagen Europas. *Berichte des Deutschen Wetterdienstes* No. 113, Vol. 15, 2. Aufl. Selbstverlag des Deutschen Wetterdienstes, Offenbach a. M., 70 pp.

IPCC (Intergovernmental Panel on Climate Change): 2001a, *Climate Change 2001: The Scientific Basis* J. T. Houghton, Y. Ding, D. J. Griggs, M. Nouger, P. J. van der Linden, X. Dai, K. Maskell, and C. A. Johnson (eds.), Contribution of the Working Group I to the Third Assessment Report of the Intergovernmental Panel on Climate Change, Cambridge University Press, Cambridge, UK.

IPCC (Intergovernmental Panel on Climate Change): 2001b, *Climate Change 2001: Impacts, Adaptation and Vulnerability* J. J. McCarthy, O. F. Canziani, N. A. Leary, D. J. Dokken, and K. S. White (eds.), Contribution of the Working Group II to the Third Assessment Report of the Intergovernmental Panel on Climate Change, Cambridge University Press, Cambridge, U.K.

IPCC (Intergovernmental Panel on Climate Change): 2001c, *Climate Change 2001: Synthesis Report*. Watson, R. T. and the Core Writing Team (eds.), Contribution of Working Groups I, II and III to the Third Assessment Report of the Intergovernmental Panel on Climate Change, Cambridge University Press, Cambridge, UK.

Krüger, A.: 2002, Statistische Regionalisierung des Niederschlags für Nordrhein-Westfalen auf Grundlage von Beobachtungsdaten und Klimaszenarien. Mitteilungen aus dem Inst. für Geopysik und Meteorologie, Universität zu Köln, Köln, Germany, 125 pp, ISSN 0069-5882.

Kubát, J. *et al.*: 2003, Summary Report on Hydrometeorological Situation during the August 2002 Floods. Czech Hydrometeorological Institute, Prague, Czech Republic.

Kundzewicz, Z. W.: 2003; Extreme precipitation and floods in the changing world. In: *Water Resources Systems – Hydrological Risk, Management and Development* G. Blöschl, S. Franks, M. Kumagai, K. Musiake and D. Rosbjerg (eds.), IAHS Publ. No. 281, IAHS Press, Wallingford, pp. 32–39.

Kundzewicz, Z. W. and Schellnhuber, H.-J.: 2004, Floods in the IPCC TAR perspective, *Nat. Hazards* **31**(1), 111–128.

Kundzewicz, Z. W., Szamałek, K. and Kowalczak, P.: 1999, The Great Flood of 1997 in Poland. *Hydrol. Sci. J.*, **44**, 855–870.

Menzel, L. and Bürger, G.: 2002, Climate change scenarios and runoff response in the Mulde catchment (Southern Elbe, Germany). *J. Hydrol.* **267**, 53–64.

Mudelsee, M., Börngen, M., Tetzlaff, G. and Grünewald, U.: 2003, No upward trends in the occurrence of extreme floods in central Europe, *Nature* **421**, 166–169.

Munich Re: 2003, Annual Review: Natural Catastrophes 2002. Topic 10.

Murray, R. J. and Simmonds, I.: 1991, A numerical scheme for tracking cyclone centres from digital data. Part I: development and operation of the scheme. *Aust. Met. Magazine* **39**, 155–166.

Nakicenovic N. *et al.*: 2000, *IPCC Special Report on Emission Scenarios*. Cambridge University Press, Cambridge, UK.

Pinto, J. J. G.: 2002, *Influence of Large-scale Atmospheric Circulation and Baroclinic Waves on the Variability of Mediterranean Rainfall*. Mitteilungen aus dem Inst. für Geopysik und Meteorologie, Universität zu Köln, Köln, Germany, 134 pp.

Pope, V. D., Gallani, M. L., Rowntree, P. R., and Stratton, R. A.: 2000, The impact of new physical parametrizations in the Hadley Centre climate model – HadAM3. *Clim. Dynam.* **16**, 123–146.

Roeckner, E., Arpe, K., Bengtsson, L., Dümenil, L., Esch, M., Kirk, E., Lunkeit, F., Ponater, M., Rockel, B., Sausen, R., Schlese, U., Schubert, S. and Windelband, M.: 1992, Simulation of present-day climate with the ECHAM model: Impact of model physics and resolution. Report No. 93, Max-Planck-Institut für Meteorologie, Hamburg.

Roeckner, E., Arpe, K., Bengtsson, L., Christoph, M., Claussen, M., Dümenil, L., Esch, M., Giorgetta, M., Schlese, U., and Schulzweida, U.: 1996, The atmospheric general circulation model ECHAM4: Model description and simulation of present-day climate. Report No. 218, Max-Planck-Institut für Meteorologie, Hamburg.

Rudolf, B. and Simmer, C.: 2002, Niederschlag, Starkregen und Hochwasser. In: G. Tetzlaff (ed.), Wissenschaftliche Mitteilungen aus dem Institut für Meteorologie der Universität Leipzig. Sonderheft zum Jahr der Geowissenschaften – Atmosphäre November 2002, 28–43.

Rudolf, B. and Rapp, J.: 2003, The century flood of the River Elbe in August 2002: Synoptic weather development and climatological aspects, Quarterly Report of the Operational NWP-Models of the Deutscher Wetterdienst, Special Topic July 2002, Offenbach, Germany, 7–22.

Ulbrich, U., Brücher, T., Fink, A. H., Leckebusch, G. C., Krüger, A, and Pinto, J. G.: 2003a, The Central European Floods in August 2002, Part I: Rainfall periods and flood development. *Weather* **58**, 371–376.

Ulbrich, U., Brücher, T., Fink, A. H., Leckebusch, G. C., Krüger, A., and Pinto, J. G.: 2003b, The Central European Floods in August 2002 , Part II: Synoptic causes and considerations with respect to climatic change. *Weather* **58**, 434–441.

van Bebber, W. J.: 1891, Die Zugstraßen der barometrischen Minima nach den Bahnenkarten der Deutschen Seewarte für den Zeitraum von 1875–1890. *Meteorol. Z.* **8**, 361–366.

Werner, P. C. and Gerstengarbe, F.-W.: 1997, Proposal for the development of climate scenarios. *Clim. Res.* **8**, 171–182.

Natural Hazards (2005) 36: 191–206

Dealing with Uncertainty in Flood Risk Assessment of Dike Rings in the Netherlands

HERMAN VAN DER MOST[1,★] and MARK WEHRUNG[2]
[1]*WL Delft Hydraulics, P.O. Box 177, 2600 MH Delft, The Netherlands;* [2]*Ministry of Transport, Public Works and Water Management, P.O. Box 5044, 2600 GA Delft, The Netherlands*

(Received: 21 November; accepted: 30 June 2004)

Abstract. Current flood protection policies in the Netherlands are based on design water levels. This concept does not allow for a proper evaluation of costs and benefits of flood protection. Hence, research is being carried out on the introduction of a flood risk approach, which looks into both the probability of flooding and the consequences of flooding. This research is being carried out within the framework of a major project called the Floris project (FLOod RISk in the Netherlands). To assess the probability of flooding the Floris project distinguishes different failure modes for dikes and structures within the dike ring. Based on a probabilistic analysis of both loads and resistance the probability of failure is determined for each failure mode. Subsequently the probabilities of failure for different failure modes and dike sections are integrated into an estimate of the probability of flooding of the dike ring as a whole. In addition the Floris project looks into the different consequences of flooding, specifically the economic damages and the number of casualties to be expected in case of flooding of a particular dike ring. The paper describes the approach in the Floris project to assess the flood risk of dike rings in the Netherlands. One of the characteristics of the Floris project is the explicit attention to different types of uncertainties in assessing the probability of flooding. The paper discusses the different starting-points adopted and presents an outline on how the Floris project will deal with uncertainties in the analysis of weak spots in a dike ring as well as in the cost benefit analysis of flood alleviation measures.

Key words: flood risk, dike rings, uncertainty, failure modes, flooding probability, the Netherlands

1. (Current) Flood Protection Policy in the Netherlands

Historically, the containment of floods has been a main concern in Dutch water management. As most part of the ''low countries'' are actually below sea level, water management is largely about *keeping our feet dry*. From the first settlers some 5000 years ago, flood risk has been a part of life in the Netherlands. At first people lived on higher ground. Over time this higher ground was connected by dikes. Dike rings were created to protect the land

★ Author for correspondence. E-mail: herman.vdmost@wldelft.nl

from flooding. In dealing with flood risk the focus shifted from controlling the damage to minimizing the probability of flooding.

In 1953, a storm tide hit the Netherlands. Catastrophic flooding occurred in the South Western Delta area. Almost 2000 people died during these floods and the economic damage was enormous. The conceivable reaction was: ''This must never happen again''. The *Delta committee*, established soon after the event, published its important *Delta Plan* in 1960. It comprised a large set of engineering works to raise protection from the sea: the Delta Works.

The Delta committee also introduced a completely new approach to determine the required level of protection against flooding. After the last ''real'' flood event in 1926, engineers had determined the required height of the embankments on the basis of the following principle: *the highest observed water level plus* 1 m. On the basis of a *cost-benefit analysis,* the Delta committee determined a new optimum level of protection, formulated as *return period* for the design water level. Taking into account the variances in risk and possible damage, different return periods for the Delta and rivers were established (see Figure 1).

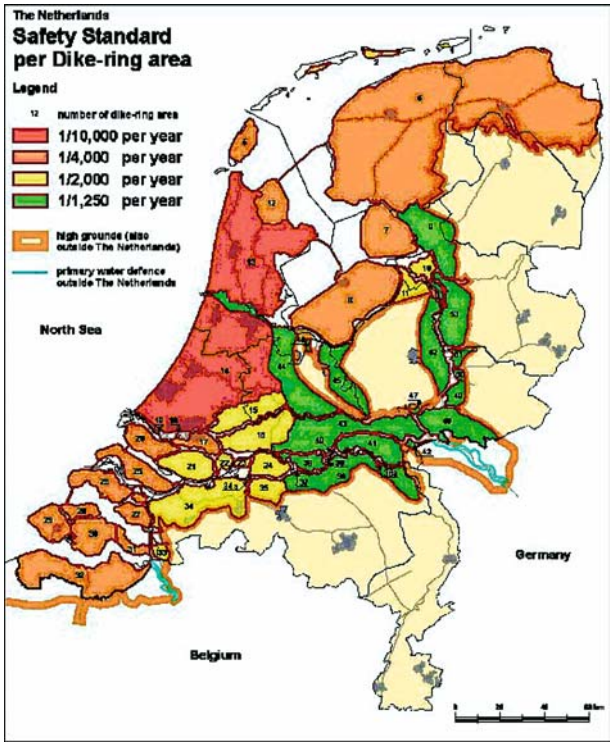

Figure 1. Dike rings in the Netherlands with their associated protection level.

For the central western part of the Netherlands where the main cities Amsterdam, Rotterdam and The Hague are located, a return period of 10,000 years was adopted; for the dikes along the river Rhine, a return period of 3000 years was proposed. The protection level along the branches of the river Rhine was adjusted to a return period of 1250 in the 1970s as a response to growing protest against the rigorous dike reinforcement programs which led to destruction of landscapes and cultural-historic sites.

As the Netherlands receive a large inflow of water from Germany and Belgium through the rivers Rhine and Meuse a part of the country is also susceptible to flooding from rivers. In 1993 and 1995, serious flooding occurred in the basin of the river Meuse. On both occasions, there were no casualties but the economic damage mounted up to 200 million Euro. Early 1995, there was an even more serious risk that the dikes of the river Rhine would collapse. This would lead to the inundation of a large area along the river with depths up to 6 m and a sincere risk of casualties. The authorities evacuated 250,000 inhabitants in the areas at risk. In the end, the dikes did not collapse but the evacuation costs were substantial and it seriously disrupted daily and economic life.

The 1995 flood placed the dike-reinforcement program high on the political agenda. A *Delta law* for the large rivers was rushed through parliament. The dike reinforcement program gained momentum and by the year 2000 nearly all parts of the reinforcement program of hundreds of kilometers of river dikes had been realized. The 1995 flood event also triggered a rather proactive policy response: the policy directive ''Room for the river'' was passed in parliament. This policy directive restricted the use of land for construction and commercial activities in areas prone to floods. The floods of 1993/1995 in combination with the international debate on the effects of global warming raised the awareness about the risks of floods and droughts.

Considering the fact that flood management is vital, the Dutch Law on Water Defences orders that hydraulic boundary conditions, i.e., design water levels and wave heights, should be updated every 5 years and that water defences should be evaluated for these new conditions. The flood events of 1990, not only put flood management higher on the political agenda it also led to a significant adaptation of the river flow statistics. The new boundary conditions for 2001 implied a further reinforcement of the dikes by 0.5–1 m, at a time when the reinforcement program based on the former statistics was nearly completed. Understandably, water managers proved very reluctant to further raise the river dikes. At the turn of the millennium, serious doubts were raised whether the Netherlands could go on enforcing the dikes. Now, alternatives were studied and debated in order to reach a more sustainable response to the impacts of climate change and improve the spatial quality of the flood plain areas. The alternatives relied on strengthening the resilience of rivers and nature by giving room to the rivers to counteract the expected rise

in the design water level. Typical measures include widening the flood plain through dike realignment and excavating side channels in the flood plains (Dijkman and Heynert, 2003). In a relatively short period of time, the policy paradigm of policy makers, engineers and water managers changed significantly: dike reinforcement changed from most preferred to least preferred option, only to be used when other flood protection measures such as giving space to the rivers were unfeasible.

The current flood protection policy is still based on design water levels. The current approach only looks into the probability of flooding. Dike reinforcements are designed to cope with the design conditions. The designs look for minimum costs, while preserving the values of landscape, nature and cultural-historic sites. A major drawback of the current approach is that is not possible to compare the costs and benefits of flood protection measures. Also it is difficult to evaluate measures that aim to minimize damage, such as spatial planning and emergency measures. To overcome such limitations the Technical Advisory Committee on Flood Defence initiated the development of a flood risk approach.

2. New Developments: Introduction of Flood Risk Approach

The methodology developed for assessing flood risk differs from the current approach on a number of aspects (Technical Advisory Committee, 2000).

1. The analysis is no longer limited to individual dike sections; the dike ring as a whole is being analysed. So the analysis provides insight into the strength of an entire dike ring, which typically consists of dikes, hydraulic structures and dunes.
2. The analysis takes account of all failure modes of a dike ring, whereas the current approach focuses mainly on the failure mode of overtopping.
3. All uncertainties are explicitly included in the calculation in a systematic and verifiable way.

The calculation of the flooding probability of a dike ring is based on the principle that a ''chain is as strong as its weakest link''. The calculation reveals all the weak links in a dike ring. It also shows that not every weak link contributes in an equal manner to the total flooding probability. This understanding provides opportunities for a step-wise improvement of a dike ring. Improvement measures may include raising the crest of a dike, improving the operation of a hydraulic structure or reinforcing the dunes. Addressing the weakest link first is often the most beneficial measure to reduce the calculated flood probability. So, application of the method may assist in prioritizing the different weak spots that may be present in a dike ring.

When calculating flooding probabilities, various forms of uncertainty are taken into account in a systematic and verifiable way. This is an important difference to the current approach based on exceedance frequencies, which only considers the natural uncertainty in water level. In the current approach, after determining the design water level, a safety margin is added to include non-explicit uncertainties. The calculation of the flooding probability includes uncertainties in water levels and wind, in strength of dikes and structures and in calculation models for the different failure modes. It should be noted that the calculated flooding probability is always an estimate of the actual flooding probability. As the uncertainty in models and data decreases, the approach will improve in accuracy.

The development of the methods started in the 1990s. During its development the methodology was applied to illustrative case-studies. The development was concluded with a successful application to four different types of dike ring (Technical Advisory Committee, 2000).

3. Floris Project

The application of the newly developed methodology to the four dike rings also revealed the presence of a number of weak spots within these dike rings. Especially structures like sluices and dams appeared to be relatively weak links within the water defence system. The findings of the study triggered the Ministry of Transport, Public Works and Water Management to launch a major project (the VNK or Floris project) to assess the probability of flooding for all dike ring areas in the Netherlands. The objective of the Floris project is to gain insight in the probabilities of flooding in the Netherlands, the consequences of possible floods and the uncertainties that effect the assessment of both probabilities and consequences (Parmet, 2003). The execution of the project will help to identify weak spots within a dike ring. Also cost estimates will be made for the improvement of weak spots. Along with the insight in the consequences of a flood, these outputs provide information for a soundly based appraisal of the desirability to reinforce the weak spots within the various dike rings.

The project is carried out by the national government in cooperation with the water boards and the provinces. The water boards provide the available information of the flood defence structures, whereas the provinces share their knowledge of the inner dike ring area. The national government compiles all required data and carries out the necessary calculations with the assistance of various engineering consultants. Transfer of knowledge and technology to the private sector is also an objective of the Floris project. That is why the major Dutch consultancy firms are involved in the execution of the project.

4. Dealing with Uncertainty: The Starting-Points

Many uncertainties play a role in the assessment of the flood risk of a dike ring. Table I presents an overview. A distinction is made between inherent uncertainties and knowledge uncertainties. Of these types of uncertainties, only knowledge uncertainties may be reduced through research within a reasonable span of time. To deal with natural variability, the concept of probability is commonly adopted. Knowledge uncertainty, however, is dealt with in very different ways, ranging from neglecting the uncertainty to approaches in which all uncertainties are taken into account in a comprehensive manner.

The traditional approach to deal with knowledge uncertainties is to make conservative assumptions (''better safe than sorry'', ''worst case''). This approach has one major disadvantage: it is quite difficult to assess what degree of safety is actually provided. To overcome this problem probabilistic approaches or risk analyses have been developed. All uncertainties (in input) are described using probability distributions. The outcome of the analysis is a probability distribution as well. Based on such distribution, conclusions can be drawn for example on the probability of failure.

Table I. Overview of uncertainties in determination of flood risk (examples)

Type	Source			
	Categories of uncertainty	Hydraulic loads	Strength of water defences	Consequences of flooding
Inherent uncertainties	Natural variation	Temporal variation of discharges, waves and water levels	Spatial variation of soil properties	Economic consequences of flooding
	Future developments/ policies	Climate change, Space for river policy		Economic and demographic development
Knowledge uncertainties	Lack of data (statistical uncertainty)	Probabilistic model of discharges, waves and water levels	Characteristics of dikes and subsoil, Idem structures	Casualties in relation to evacuation
	Lack of knowledge of processes (model uncertainty)	Mathematical models for water levels and waves	Mathematical models for failure mechanisms 'Aging' of dikes, structures	Mathematical models of flood dynamics, Behaviour of people during floods

The Floris project has defined a number of starting-points on how to deal with the uncertainties in the assessment of flood risk due to the whims of nature and human failure. The major starting-point of the Floris project is that all uncertainties are included in the analysis to avoid unnecessary conservative assumptions. To promote mutual comparability of calculated flood risk between dike rings, all uncertainties identified are dealt within a systematic and consistent manner. To this end a probabilistic approach is adopted. This approach shows how uncertainties affect the outcome of the analysis, e.g., it becomes clear which uncertainties have the largest influence on the calculated flood risk. Based on such understanding a deliberate choice can be made to either reinforce the water defences or to reduce the uncertainties through research.

Although there is a lot of knowledge available on different aspects and processes that affect the flood risk, there are still areas where knowledge is lacking. These include the possible existence of residual strength, the possible impact of emergency measures and the systems behaviour of dike rings along rivers. Time and budget constraints of the Floris project did not allow to develop a proper probabilistic model for these areas. In these cases a deliberate choice was made to adopt conservative assumptions to avoid unjustified optimism. As a consequence ''pleasant surprises'' will be more likely to occur than disappointments when knowledge increases over time after appropriate research.

Due to knowledge uncertainties the calculated flood risk has a limited reliability. This reliability may be expressed through reliability intervals. Decision-makers, however, generally have difficulty in dealing with reliability intervals. When is information sufficiently accurate to make decisions? It is the art of engineering to draw sufficient conclusions from insufficient data. Within the Floris project another approach is adopted in dealing with uncertainty. All available information is integrated in a statistically justified way. The calculated flood risk comprises the best estimate of the flood risk *given the available knowledge*. Uncertainties are directly incorporated in the decision-making process by raising the question to what extent the reliability of the calculated flood risk can be increased through (additional) research.

This definition implies that the calculated flood risk may not only change because of physical reinforcements but also because of research which may reduce uncertainties. Whether research results in a lower probability of failure depends on the actual outcome of the research. The extent to which uncertainties can be reduced for that matter is limited. Uncertainties in knowledge of local circumstances may be reduced through field research. Model research may reduce uncertainties in ''failure'' models. It should be realised, however, that more sophisticated models generally are more data intensive. As a consequence the uncertainty may shift from model uncertainty to statistical uncertainty. Unless additional field research is carried, the

net gain may be limited. Statistical uncertainties in hydraulic conditions can not be reduced through research within a reasonable period of time. The period of observation is generally too short compared to the return period of the events considered.

5. Assessment of Probability of Flooding of Dike Rings

A dike ring normally consists of large segments of dikes or dunes interrupted by a few hydraulic structures such as locks, pumping stations, tunnels, discharge sluices, etc. Engineering experience shows that there are many different modes that may lead to failure of flood defence structures. Insufficient height may lead to large overtopping rates, which will erode the inner slope. Structures can also be undermined through eroded ''pipes'' in the subsoil. Then of course water pressures can build up and lead to loss of stability. Slope protection of dikes (grass, stones or asphalt) may get washed away under severe wave attack, which leads to erosion of core material and possibly a breach. The gateway function of hydraulic structures adds another failure mode: the non-closure of the gate. Human failure may play a very important role with this failure mode. Figure 2 depicts the different failure modes of dikes within a dike ring.

To be able to determine the failure probability of a particular failure mode both the hydraulic load to the dike as well as the strength of the dike section are described in probabilistic terms. The failure probability is then the probability that the load is larger than the strength of the dike or structure.

The probability of failure of a particular dike section is subsequently assessed by combining the probabilities for each possible failure mode, taking

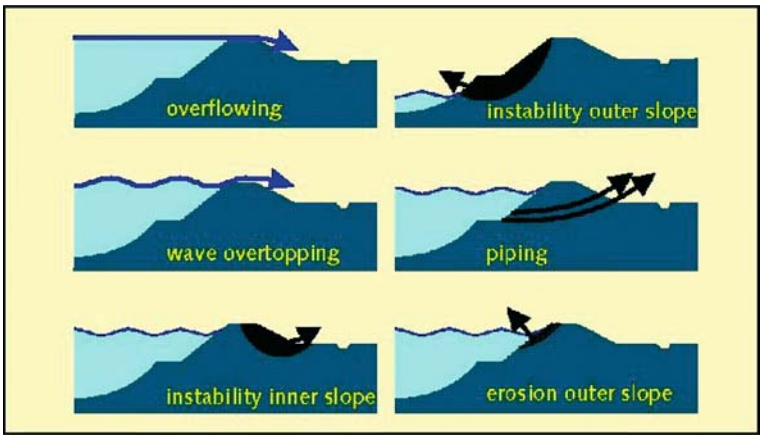

Figure 2. Overview of failure modes for dikes.

into account the dependences between the failure modes. Each failure mode is modelled in such a way that its occurrence will lead to an initial breach. So the result of the calculation is actually the probability of an initial breach in a dike section. With the same combination procedure the failure of different dike sections is combined into the failure of dike rings (Lassing *et al.*, 2003). The dependence between the dike sections is taken into account in this process. Actually this dependence is already introduced at the lowest level: the input variables of the calculation models for the different failure modes. For each variable a correlation function (in space or time) is specified.

The model generates two main results for every single "element" within the dike ring: the probability of failure (often described by the reliability index β) and a set of coefficients of influence for all input variables (often described as α_i). The combination procedure combines the output of two elements and the coefficients of correlation into a combined reliability index and a new set of α_i. This procedure is repeated until all elements within the system are dealt with.

The importance of taking into account the dependency between dike sections can be shown with the following example. Consider a dike ring situated along the Rhine consisting of 25 dike sections. For each dike section the probability of failure due to overtopping is 1/1250 per year. The probability of failure due to piping for each dike section is taken ten-times smaller, 1/12,500 per year. A first indication of the system's probability of failure can be found by calculating an upper boundary (sum of the probabilities of failure of all elements) and a lower boundary (probability of failure of the weakest link). This leads to the following estimates for the dike ring as a whole:

$$\begin{aligned} 1/1250 &< P_{\text{f, overtopping, dike ring}} < 1/50 \\ 1/12500 &< P_{\text{f, piping, dike ring}} < 1/500 \\ \hline 1/1250 &< P_{\text{f, dike ring}} < 11/500 \end{aligned}$$

A calculation which takes into account all dependencies results in:

$$\begin{aligned} P_{\text{f, overtopping, dike ring}} &= 1/1000 \\ P_{\text{f, piping, dike ring}} &= 1/850 \\ \hline P_{\text{f, dike ring}} &= 1/800 \end{aligned}$$

The failure probability of the dike ring for overtopping appears to be close to the lower boundary, the weakest link approach. This can be explained by the dominating influence of the discharge of the river Rhine. A high discharge leads to high water levels for all dike section. As a result there is a strong dependence of failure of these dike sections. The failure probability of the dike ring for piping tends more to the upper boundary. For piping the influence of the discharge of the Rhine is less dominant; the influence of specific soil characteristics is more important. These soil characteristics are

relatively independent, which leads to relatively independent failure of the dike sections. Although piping has the largest probability of failure for the ring as a whole, there is still some influence of overtopping on the overall probability of failure of the dike ring.

6. Assessment of Consequences of Flooding

The assessment of the consequences of flooding comprises the determination of the hydraulic consequences, the economic damage and the number of casualties. To determine the hydraulic consequences of flooding both global and detailed models are being used. Global models make use of simplifying assumptions to obtain a quick estimate of the maximum inundation depths and associated damage that may occur. Detailed inundation models, based on the generic Delft 1D2D model, are used to analyse the dynamics of an inundation due to a breach in the dike (Hesselink *et al.*, 2003; Stelling *et al.*, 1998). The magnitude of the hydraulic consequences of a dike breach will depend on the location of the breach and the speed with which the breach will grow. Also limitations in the incoming discharge may play a role. To account for these factors different inundation scenarios are analysed. The application of the inundation model requires a detailed schematisation of the dike ring area. This includes a digital terrain model (including relevant line elements that may obstruct the flow) and the land use because of the hydraulic resistance. The detailed inundation model provides a regionally distributed picture of the development over time of inundation depths, stream velocities as well as the rate of water level rise (see Figure 3 for an example).

The hydraulic consequences are input to the assessment of economic damages and the number of casualties due to flooding. The economic damages are calculated using a standard method (Vrisou van Eck *et al.*, 2000). Information on economic value and vulnerability to flooding of land use is combined with information on the expected inundation depths of dike rings. Figure 4 illustrates the procedure.

The assessment of economic damages includes both direct and indirect economic damages. The direct material damage is defined as damage to objects, capital goods and movables due to the direct contact with the water. This includes repair damage to real estate, repair damage to means of production, damages to household effects and damages due to loss of raw materials and products (including agricultural yields). Also economic losses due to stagnation in production is taken into account.

The indirect economic damages pertains to damages to supplying and buying companies outside the flooded area as well as to additional travel costs due to interruption of traffic though the flooded area.

The Floris project also looks into the number of casualties to be expected. This number of casualties will depend on the characteristics of the flood. Very

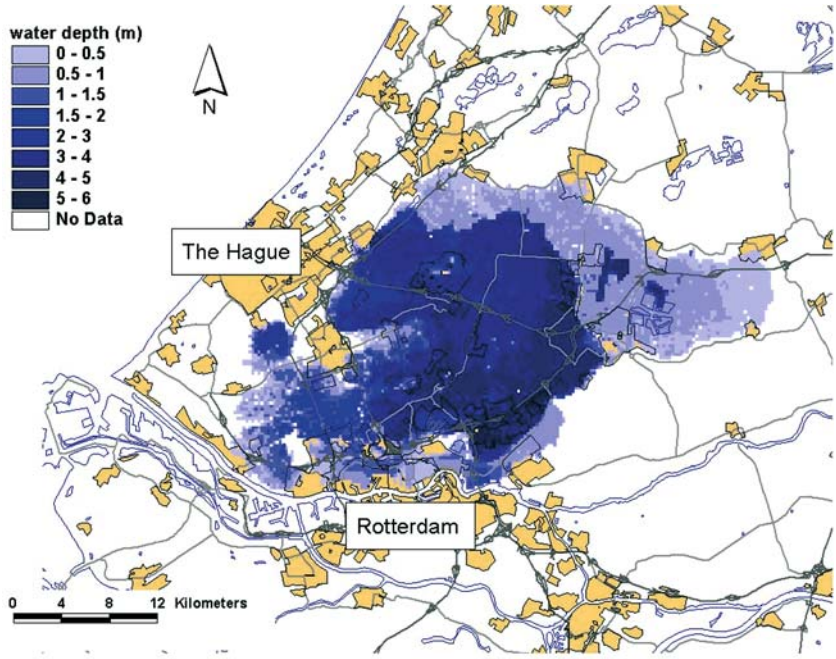

Figure 3. Example of calculated pattern of inundation depths for a dike ring.

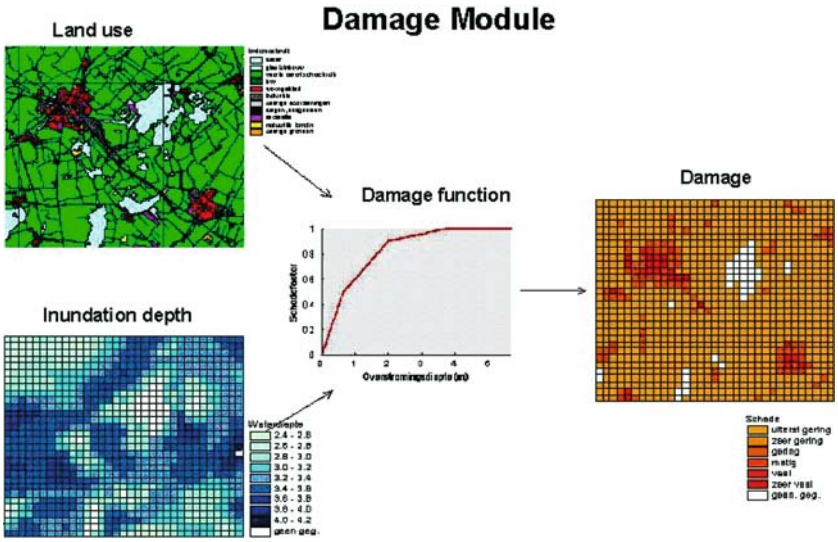

Figure 4. Combining hydraulic consequences and land use into economic damages.

important is of course the inundation depth, but also stream velocities and the rate of water level rise play a role. Experience shows that it is in particular the combination of high rates of water level rise with larger inundation depths that result in relatively large numbers of casualties.

Another important factor is whether or not preventive evacuation has been carried out. To assess the contribution of preventive evacuation in reducing the number of casualties of a possible flood, a Preventive Evacuation Model is being developed. This model estimates which fraction of the inhabitants of the dike ring will be evacuated in the course of time. Time is the key factor in a successful evacuation. The model looks into both the time needed and the time available for evacuation. The time *needed* depends on the extent of preparation and the presence of infrastructure. The time *available* depends on the predictability of the flood, which in its turn depends on the type of threat (from the sea or from a river).

Not all people that are present in a dike ring during flooding will become a victim of drowning. A large part of the people will be able to flee to safe places or will be rescued. Evidence from past floods suggests that many casualties are to be expected close to the breach in the dike. Due to high stream velocities people lose their balance; also buildings in which people have found shelter may collapse. It is assumed that buildings will collapse when the stream velocity amounts to more than 2 m/s and the product of inundation dept and stream velocity is larger than 7 m^2/s (Rescdam, 2002).

For the areas further away from the breach the percentage of casualties depends on the inundation depth and the rate of water level rise. The Floris project distinguishes between two different situations. In areas with a high rate of water level rise (rate of more than 1 m/h) people will have difficulty in reaching safe places. As a consequence the number of casualties due to drowning is relatively large. In other areas with a lower rate of water level rise it is assumed that people generally will succeed in finding shelter temporarily. In such cases casualties will have other causes. People may die due to hypothermia or fatigue or they may get stuck in houses that collapse later on during the flood. Figure 5 shows a casualty function for the situation with a high rate of water level rise (Asselman and Jonkman, 2003).

With these casualty functions information on hydraulic consequences together with information on the presence of people and buildings can be combined to obtain estimates of the expected number of casualties in a particular dike ring.

7. Analysis of Weak Elements Within the Dike Ring

The Floris project has adopted a systematic and consistent approach in dealing with uncertainties in the determination of flood risk. Dealing with

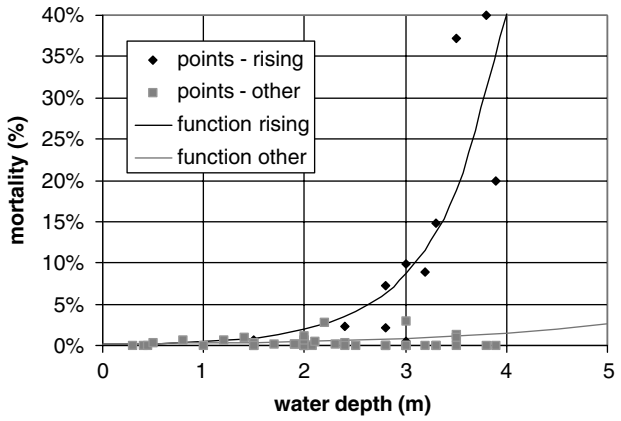

Figure 5. "Casualty function": mortality as a function of inundation depth.

uncertainties, however, goes beyond the mere quantification of flood risk. It is also important to incorporate uncertainty in *decisions* on the protection against flooding. Knowledge uncertainty is e.g., an important factor in the identification of weak spots within a dike ring. Is a particular dike section indeed a weak element or is the large contribution to the flooding probability of the dike ring mainly due to knowledge uncertainty?

Within a dike ring there will be stronger and weaker dike sections and hydraulic structures. Based on its contribution to the probability of flooding of the dike ring a dike section or hydraulic structure can be identified as a weak spot. The calculated contribution reflects the best estimate given the available information. Additional research may provide different inputs to the failure models. The outcome of additional research is of course not known beforehand. One can only make assumptions on the outcome. A structured *sensitivity analysis* can be carried out to investigate the possible consequences of additional research.

For strong sections within the dike ring an unfavourable outcome of additional research is assumed. If under such conditions the contribution to the flooding probability of the dike ring is still negligible, then the section can be most probably be considered as strong. Similarly for weak spots it is investigated whether a favourable outcome of additional research or field work would change the perception of the section being weak. Figure 6 summarizes the approach. For the category "(yet) undetermined" actual additional research has to clarify whether these sections/structures are really weak spots or not.

The sensitivity analysis focuses on the stochastic variables which have most impact on the probability of failure. The sensitivity analysis is only applied to knowledge uncertainties; these are the uncertainties that may be

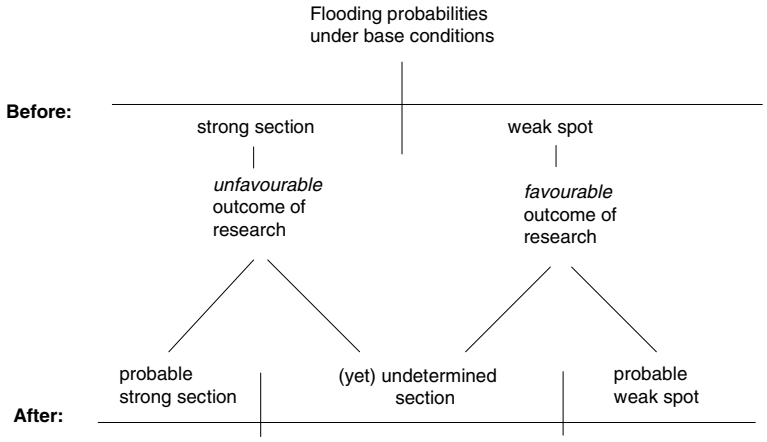

Figure 6. Classification of dike sections into weak, strong and undetermined.

reduced with additional research or field work. The classification in weak spots and strong sections can subsequently be used to develop a cost effective program for additional (field) research. It also provides a comprehensive picture of the quality of the dike ring. Such understanding can be used in defining alternative reinforcement programs for dikes and hydraulic structures within the particular dike ring.

8. Cost–benefit Analysis of Flood Alleviation Measures

Uncertainties play also a role in the cost benefit analysis of flood alleviation measures. In a general cost benefit analysis the benefits of an activity are compared with the costs of the activity. If the benefits are higher than the costs, the activity is attractive (it generates an increase in economic welfare). In flood management this means that the costs of flood alleviation measures are compared with the decrease in expected flood damage (risk reduction). Costs include investments costs (fixed and variable) and costs for maintenance and management.

The attractiveness of a measure will depend on the ratio between investments and damage reduction. If the ratio is (sufficiently) higher than 1.0, it will be economically attractive to carry out the measure. In the Floris project it is recognized that both costs and benefits are not exactly known; they contain a certain amount of uncertainty. Costs for instance are not based on a specific design, but assessed with the use of unit costs. Therefore the accuracy is limited. Due to the lack of knowledge some safe assumptions are made in the calculation of the risk reduction which probably results in an overestimation of the benefits of the measure. Hence it is conceivable that for

a certain measure the costs will be higher than the benefits, although the ''average'' benefit–cost-ratio exceeds 1.0.

The issue of how to deal with uncertainties in the cost–benefit-analyses has not yet been solved. The idea of a classification of measures based on their ''average'' benefit–costs-ratio (for instance very attractive, attractive, possibly attractive and non-attractive) has been suggested. The establishment of boundaries between these classes will require a probabilistic approach to both costs and benefits of the measure. This will be further investigated within the project.

9. Conclusions and Outlook

The paper has presented an outline of the flood risk approach, which is currently being developed and applied to the various dike rings in the Netherlands. The focus in the Floris project is on a detailed assessment of the contribution of dikes, dunes and hydraulic structures to the flooding *probability* of a dike ring. For most dike rings the consequences of flooding are assessed in a rather global way. This is done for pragmatic reasons. For some dike rings, however, the consequences will be analysed in more detailed way as described in this paper.

The current application shows that not all required information is readily available. Adequate information on subsoil and inner material of dikes as well as on the foundation of hydraulic structures is lacking in quite a few cases. In the absence of sufficient data, (conservative) assumptions have to be made. Additional field research will help to reduce such uncertainties. The methodology developed, provides a systematic framework for assessing which research may offer the largest gain in reducing the flooding probability.

The Floris project introduces a new concept of safety against flooding. Hence, communication of approach and findings of the project is given ample attention. The project will not only provide information on flooding probability, but also information on flood risk in terms of economic damage and expected number of casualties. These types of outcomes open a new arena for use in policy making. Flood risk in terms of casualties may be compared with other risks in society such as industrial risks and risks in transport and aviation; see Jonkman *et al.* (2003) for an overview of quantitative risk measures for loss of life and economic damage. Such comparison should of course be carried out with great care, as different sets of assumptions may have been used in risk assessments for the various domains.

Information on flood risk in terms of economic damage may provide input to a societal debate on the required level of protection to flooding (Vrijling, 2001). The current flood protection levels of the various dike rings were determined in the 1960s. Thanks to economic and demographic

developments the values that are protected have increased enormously. In addition there is the impact of climate change, which will result in larger loads on the water defence structure. Overall there appears to be enough reason for a reconsideration of the current protection levels of the various dike rings. The Floris project will provide valuable information to support such a process.

References

Asselman N. E. M. and Jonkman, S. N.: 2003, Consequences of floods: the development of a method to estimate the loss of life, Delft Cluster report DC1-233–7.

Dijkman, J. P. M. and Heynert, K. V.: 2003, Changing approach in flood management along the Rhine River in the Netherlands, In: *''Dealing with Flood Risk''*, *Proceedings of an interdisciplinary seminar on the regional implications of modern flood management*. Delft Hydraulics Select Series 1/2003, Delft University Press, Delft.

Hesselink, A. W., Stelling, G. S., Kwadijk, J. C. J., and Middelkoop, H.: 2003, Inundation of a Dutch river polder, sensitivity analysis of a physically based inundation model using historic data, *Water Res. Res.* **39**(9).

Jonkman, S. N., van Gelder, P. H. A. J. M., and Vrijling, J. K.: 2003, An overview of quantitative risk measures for loss of life and economic damage, *J. Hazard. Mater*. **A99**, 1–30.

Lassing, B. L., Vrouwenvelder, A. C. W. M., and Waarts, P. H.: 2003, Reliability analysis of flood defence systems in the Netherlands, In: Bedford and Van Gelder (eds.), *Proceedings of ESREL 2003: Safety and Reliability*.

Parmet, B. W. A. H., 2003, Flood risk assessment in the Netherlands, In: *''Dealing with Flood risk'', Proceedings of an interdisciplinary seminar on the regional implications of modern flood management*. Delft Hydraulics Select Series 1/2003, Delft University Press, Delft.

Rescdam.: 2002, *The Use of Physical Models in Dam-break Flood Analysis*, Helsinki University of Technology, 2002

Stelling, G. S., Kernkamp, H. W. J., and Laguzzi, M. M.: 1998, Delft flooding flow simulation: A powerful tool for inundation assessment based upon a positive flow simulation, In: V. Babovic and L. C. Larsen (eds.), Hydroinformatics '98, Balkema, Rotterdam, pp. 449–456.

Technical Advisory Committee for Flood Defence in the Netherlands.: 2000, *From Probability of Exceedance to Probability of Flooding*.

Vrijling, J. K.: 2001, *Probabilistic Design of Water Defense Systems in the Netherlands*, Reliability Engineering and System Safety **74**, 337–344.

Vrisou van Eck, N., Kok, M., and Vrouwenvelder, A. C. W. M.: 2000, *Standard Method for Predicting Damage and Casualties as a Result of Floods*, Lelystad, HKV Consultants and TNO Bouw.

Natural Hazards (2005) 36: 207–220

The Development and Application of a Flood Risk Model for the Czech Republic

HARVEY J. E. RODDA
Peter Brett Associates, Caversham Bridge House, Waterman Place, Reading RG1 8DN, UK; Current address: Hydro-GIS Ltd, 12 Sandy Lane, Cholsey, Oxfordshire, OX10 9PY, UK (E-mail: harvey.rodda@hydro-gis.co.uk)

(Received: 1 December 2003; accepted: 30 June 2004)

Abstract. A flood risk model was developed for the Czech Republic to calculate the probability of insured losses from flood events. The model was GIS based, making use of a 100 m horizontal resolution DTM and a network of the major rivers in the country. A review of historical flooding was undertaken to define the worst and most widespread flood events. Synthetic flood events were generated based on a study of the spatial variation in magnitude of river flows from selected historical flood events going back to 1935. A total of 30 synthetic events were generated each providing peak flows at 25 gauging stations throughout the country. The flows were converted into flood levels using rating equations based on information provided by the Czech Hydrological and Meteorological Institute. The extent of and depth of flooding was mapped on a cell by cell basis by applying an automated procedure developed using the grid option within the Arc/Info GIS. The flood depths were combined with maps of the postal codes to define an average flood depth per post code. The model was calibrated using maps of the observed flood extents from 1997 and 2002.

Key words: flood modelling, flooding, Czech Republic, GIS, insurance

1. Introduction

In June 2002 a project was initiated by Benfield Ltd. (re-insurance brokers) and Peter Brett Associates (consulting engineers) to model flood risk in the Czech Republic. Flooding had been identified as the natural hazard which caused the greatest risk to the Czech Republic as illustrated by the damaging floods of July 1997 which caused $US 2–4 billion of damage and 54 deaths (Kundzewicz, 2000); and the recent catastrophic flooding of August 2002. Since the 1997 event flood insurance had become much more widespread within the Czech republic. Within the insurance sector, models are required in order that reinsurance needs can be determined (and technically priced) to ensure the financial solvency of primary insurers.

Flood risk modelling for insurance purposes is a fairly recent application of hydrological modelling. Most studies have mapped the flood outlines from a design flood, commonly 1 in 100 years, for a whole river network in a given country (e.g. Morris and Flavin, 1995). These types of maps are very good for planning purposes or emergency operations and

have also been produced for the Czech Republic by the Czech Hydrological and Meteorological Institute (CHMI). However, one major disadvantage is that they do not consider the relationships between the degree of flooding for individual river basins. This is of particular importance for the insurance industry where the primary insurer needs to know whether losses can be paid without requiring cover from a re-insurer and the re-insurer needs to control portfolio risk aggregation. Against this background, it was evident that a model was required which could simulate flooding on an event basis.

2. Study Area and Data Requirements

Developing a model for a whole country is a difficult task since the balance between an adequate level of model accuracy and the large extent of the study area has to be reached. The detail and extent of the model was constrained by time and cost limitations on the project and also since the study considered the insured loss due to flooding it was not necessary to model flooding in sparsely populated areas.

A more significant constraint for the hydrological aspects of the study was the availability and cost of the data. Time series data in the form of mean daily flows, design flood flows and flow/level rating curves were required for an adequate number of gauging stations to provide a reasonable representation of the river network. A river network was defined (Figure 1) by selecting gauging stations for catchments with a record going back to at least 1935 and over 1000 km^2. The year 1935 was taken as the cut-off since a large number of stations were built in this year. The number of stations was limited to 25 due to the high costs of data from the CHMI. The final network comprised of the four main rivers in the Czech Republic (Vltava, Labe, Odra and Morava) and their major tributaries. The location of all main urban areas was compared with the network to ensure all rivers flowing through major towns and cities were included. Following the initial selection, a further 8 stations were selected to ensure a representative station was present for each reach of the network (Table I).

Another key data requirement for the project was a suitable scale digital terrain model (DTM). A number of options were considered with varying cost, resolution, and vertical accuracy. The selected DTM was purchased from Multi-Media Computer, Prague, and had a cell resolution of 100 m and a vertical accuracy of 1 m. This was considered a reasonable degree of accuracy for the scale of the modelling which was undertaken. The ultimate model output would be the average flood depth per postal code, which would be over an area typically between 1 and 20 km^2, depending on the population density.

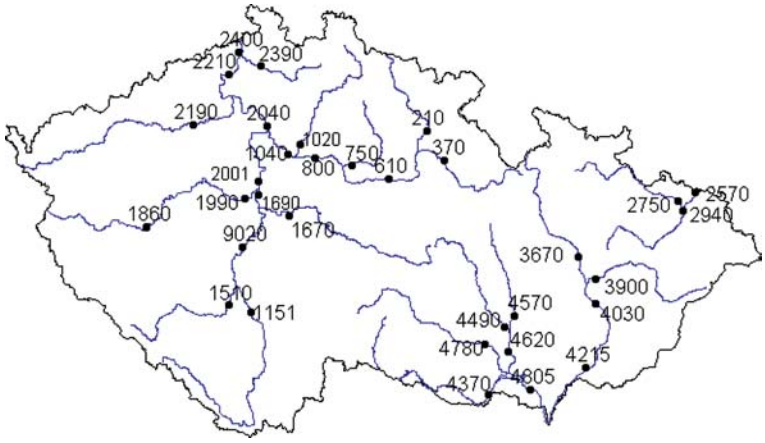

Figure 1. The river network used for the model. Station details are given in Table I.

3. Model Structure

The model consisted of two components, a hydrological component which provided a set of synthetic flood events and a hydrodynamic component to provide a flood depth and extent for each event. The predictions of flood depth were then averaged over a postcode basis and used with information on building stock and damage to define an insured loss.

3.1. GENERATION OF A FLOOD EVENT SET

A similar event-based flood risk model for the UK had used stochastic rainfall events to generate a set of flood events through rainfall runoff modelling (Rodda, 2001). In the current study however time and cost constraints did not allow such a detailed approach. Instead the flood event was generated directly from flow data through a judgement based approach using information from historical flood events and local knowledge.

An important distinction was that synthetic events were generated rather than stochastic events. Stochastic events require a sampling of the base data, which in the case of flooding is the peak flow at all the stations. This can then produce a set of events each with a specific probability, however the disadvantages are that large amounts of data are required and a large number of events have to be simulated (in the order of 1000). In addition the event set can in this way be defined purely by statistical analysis without a knowledge of the physical processes, and the magnitudes of flows used are defined by existing flood frequency curves rather than hydrological characteristics, giving rise to under-estimation.

This last point was particularly evident in the August 2002 floods where the existing flood frequency curve for the Vltava at Prague used 3700 m^3/s as the 1 in 100 year event. The peak observed flow during the floods was

Table I. Details of gauging stations used for the Czech flood model development

River	Station name	Station number	Catchment area (km^2)	Start of record
Metuje	Jaromer	210	607.2	1948
Orlice	Týniště nad Orlicí	370	1,591	1911
Labe	Přelouč	610	6,432	1971
Cidlina	Sány	750	1,156	1925
Labe	Nymburk	800	9,724	1931
Jizera	Tuřice-Předměřice	1020	2,159	1982
Labe	Brandýs nad Labem	1040	13,110	1911
Vltava	Ceske Budejovice	1151	2,848	1989
Otava	Písek	1510	2,913	1912
Sázava	Poříčí nad Sázavou	1670	4,000	1912
Vltava	Zbraslav	1690	17,820	1941
Berounka	Plzeň-Bílá Hora	1860	4,017	1931
Berounka	Dobřichovice	1990	8,720	1931
Vltava	Praha-Chuchle	2001	26,720	1986
Labe	Mělník	2040	41,820	1926
Ohøe	Louny I.	2190	4,983	1922
Labe	Usti na Labem	2210	48,560	1941
Ploučnice	Benešov nad Ploučnicí	2390	1,156	1926
Labe	Děčín	2400	51,100	1888
Odra	Svinov	2570	1,615	1923
Opava	Děhylov	2750	2,039	1926
Odra	Bohumín	2940	4,662	1920
Morava	Olomouc-Nové Sady	3670	3,322	1921
Bečva	Dluhonice	3900	1,599	1920
Morava	Kroměříž	4030	7,014	1916
Morava	Strážnice	4215	9,147	1921
Dyje	Trávní Dvůr	4370	3,449	1926
Svratka	Brno-Poříčí	4490	1,638	1919
Svitava	Bílovice nad Svitavou	4570	1,117	1918
Svratka	Židlochovice	4620	3,939	1921
Jihlava	Ivančice	4780	2,681	1924
Dyje	Breclav Ladnav	4805	12,280	1988
Vltava	No station*	9020	–	–

* No gauging station was present on this reach so flood flows were taken as the sum of 1151 and 1510 (the upstream stations).

5300 m^3/s. Taking this flow as a stochastic event based on sampling from the flood frequency curve would have given a return period of 3,500 years. Further calculations by Holicky and Sykora (2003) gave the return period as 350 years based on a log normal distribution.

A number of reports and articles (e.g. Buchtele, 1989; Hradek *et al.*, 1997; Buchtele *et al.*, 1999; Kundzewicz, 2000) were consulted to establish the worst 11 flood events since 1935, as listed in Table II. The most severe flood events were caused either by snow melt in the spring or by prolonged and intense summer rainfall commonly between May and September. Mean daily flow data was then obtained from the CHMI for the years when these events occurred for the full set of selected gauging stations. The flow data for a 10 day envelope around the date when the peak flow was recorded was then interrogated to find the maximum mean daily flow for each station for each flood event. A growth curve index using the ratio of maximum mean daily flow to the median annual flood was then established for each station to describe the severity of the flooding. The values were plotted on a thematic map using ArcView (Figure 2). This enabled a spatial correlation of the severity of the flooding for each event.

From comparing these maps for the different events and identifying the mechanism responsible for the flooding, three distinct event patterns were evident. These were summer rainfall events producing flooding in the west, summer rainfall events producing flooding in the east, and snow melt events producing less severe but more widespread flooding across the whole river network. A set of 30 synthetic events was then generated based on these three patterns. The set was determined largely through a qualitative analysis of the historical events and a knowledge of the hydrology of the river basins. The fact that summer rainfall flood events were confined to either the west or east of the country illustrated that the extreme amounts of rainfall required to produce this severe flooding were only possible when depressions became stationary over a part of the country and effectively rained out. The magnitude of the precipitation was also greatest in the mountains and depending on the relationship with the mountains and the circulation of the depression catchments could either be in the rain shadow or experience severe flooding. According to Hradek *et al.* (1997) the most severe flooding occurs when the depression or rain bearing clouds move in an upstream direction, bringing initially rain to the lowlands and later extreme rain in the mountains. In this instance the lowlands would be saturated and rivers at elevated flows when the flood waves from the mountains arrive producing severe flooding.

Snowmelt events were characterised by less extreme flows and the most severe flooding being on the downstream river reaches. This was assumed to be due to the snow melting at lower latitudes but remaining in the higher altitude headwater basins. The effect of ice jams was not considered in these scenarios as it involved a more complex hydrodynamic representation, which

Table II. Worst 11 flood events in the Czech Republic since 1935 (excluding August 2002)

Date	Rivers affected	Peak flow	Key cause	Notes
July 1997	Morava, Becva, Odra, and tributaries	1034 Morava at Kromeriz, approx 800 Becva at Dluhovice	Heavy rainfall (east)	50 deaths, 538 towns and cities affected, damage estimated at 2 billion US$
July 1981	Berounka, Otava, Vltava, Labe	1075 at Beroun (Berounka) 447 at Pisek (Otava) 1696 at Modrany (Vltava) 2377 at Usti (Labe)	Heavy rainfall (west)	30-year flood
March 1981	Labe, Ohre, Orlice, Morava	340 at Debrne (Labe) 490 at Karlovy Vary (Ohre) 318 Tyniste (Orlice) 1170 Brandys (Labe) 602 Straznice (Morava)	Snowmelt	100-year flood
August 1977	Odra	848 at Bohumin	Heavy rainfall (east)	7-year flood
July 1954	Vltava, Labe	2920 on Vltava, approx. 1740 on Labe	Heavy rainfall (east)	Newly completed Vltava cascade reservoirs stored the flood volume
March 1947	Vltava	2272 at Prague (Vltava)	Snowmelt	
February 1946	Morava, Cidlina, Labe	164 on Cidlina, 795 on Labe at Přelouč, 383 on Morava	Snowmelt	
March 1940	Vltava	3248 at Prague (Vltava)	Snowmelt	Largest winter flood on record since 1825
September 1938	Orlice	469 on Labe	Heavy rainfall (west)	20-year flood
September 1937	Svitava, Opava	64 on Svitava 208 on Opava	Heavy rainfall (east)	
March 1937	Morava, Svratka, Odra	150 on Svratka, 552 on Morava	Snowmelt	

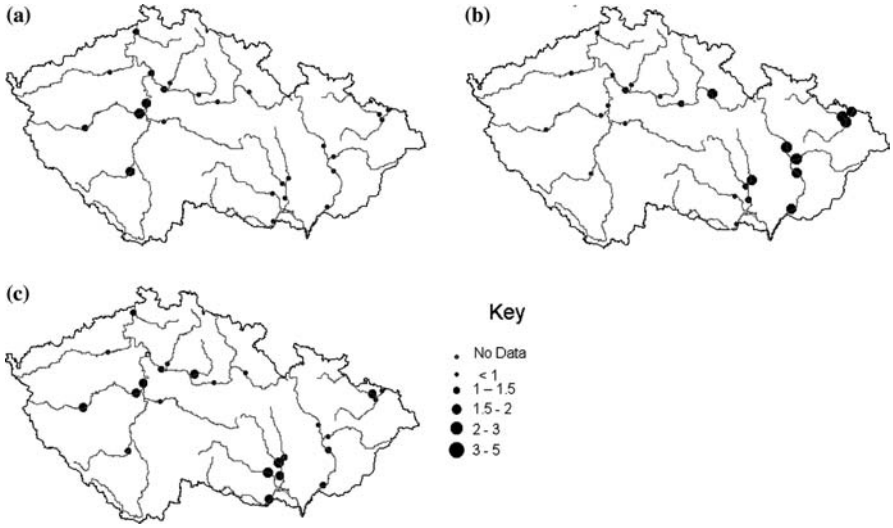

Figure 2. 77 Examples of western summer rainfall (A, July 1981), eastern summer rainfall (B, July 1997) and snow melt (C, March 1947) in terms of the ratio of the peak flood discharge to the median annual flood (Q/Q2) values.

was not appropriate for the resolution of the generalised modelling undertaken in this study.

The patterns of the synthetic events were described by the number of river basins which were affected, based on a zoning of basins by their headwater area (Figure 3).

- Zone 1 incorporated the Vltava, Otava, Berounka, and Ohře rivers which all have their sources in the Šumava, Český les and Krušné mountains on the western border, along with the lower Labe which is fed by these rivers.
- Zone 2 included the middle reaches of the Labe and the Jizera, Cidlina and Ploučnice, tributaries whose source is in the Krkonoše and Jizerské mountains in the north of the country.
- Zone 3 incorporated the Dyje and Jihlava rivers whose sources are in the Českomoravská vrchovina mountains in the south.
- Zone 4 incorporated the Sázava, Svitava and Svratka, draining the central Českomoravská vrchovina mountains.
- Zone 5 incorporated the upper reaches of the Labe, the Odra and Morava whose sources are all in the Jeseník, Moravskoslezské Beskydy and Bílé Karpaty mountains in the north-east.

In this way in a summer rainfall scenario flooding in the upper Labe and Odra would occur in the same event since the headwaters both originate

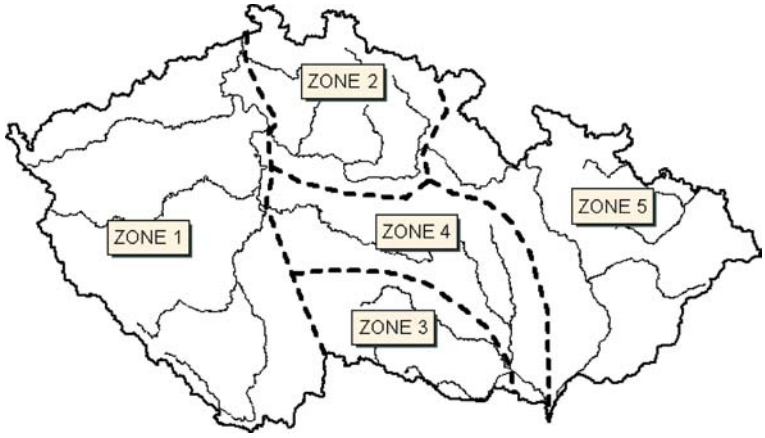

Figure 3. Delineation of zones used for the synthetic flood events.

nearby in the Jesenik Mountains. However it was not considered possible that severe flooding in the upper Labe and Odra (Zone 5) would be concurrent with severe flooding in the Ohre (Zone 1), due to the considerable distance between the respective headwaters. The flow magnitudes for the synthetic events were simply based on the growth curve index and using the rule of thumb that if one tributary was in flood but the other not, the downstream magnitude would be unchanged (Figure 4a). Whereas if two upstream tributaries were flooding at a similar magnitude (e.g. a growth factor of 2) then the downstream reach would have an increased magnitude (growth factor of 3), as shown in Figure 4b.

Initial flood magnitudes were taken as the growth factors and then multiplied by a random factor between + 10% and −10% to give a more realistic variation to the flows for different events. Further refinement was required to convert these flows which were based on the mean daily flow to a peak flow. Observed data from 1997 was used to define a conversion factor to change mean daily flow into peak flow for a number of the stations. For others and average value, commonly +15% was used. For very large catchments, over 10,000 km^2 there was only a very minor difference between the peak and mean daily flow so no refinements were required.

3.2. CALCULATION OF FLOOD DEPTH

The synthetic events gave a flood flow at each gauging station on the network. This had to be converted into a water level so that the flood depth could be modelled for the whole of the reach. In the first instance the water level was found by the use of rating curves provided by the CHMI. A number of stations in the east of the country had very good ratings at high flows since

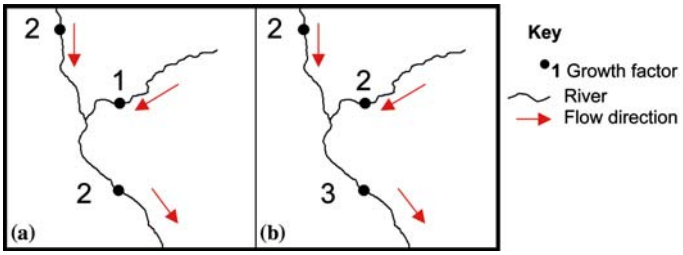

Figure 4. The procedure for assigning the Q/Q2 growth curve index at river confluences.

they made use of flow and level information from the 1997 floods. The rating equations were not as reliable at high flows for stations further west and in many cases new curves were plotted using the latest information from the flooding in 2002. Only a peak flow and level value were available at the time so a full revision of the rating curves was not possible and equations had to be estimated based on the best available data. The flood depth was then calculated as the flood level minus the bankfull flood level, which was assumed to be the level associated with a 1 in 2 year return period flood. At any station where the flow was less than the 2 year flood it was assumed that no flooding occurred. The other important assumption for the mapping of the flood depth was that the above bank flood level was maintained for the whole of the reach length.

In order to convert the flood depth at a point into a map showing the flood depth the application of GIS was required, and in particular the use of grid cell based modelling. Arc/Info was used for this project in preference to ArcView or other desktop systems, due to its stability, ease of programming and its ability to process very large datasets. An automated routine was developed to generate the maps of flood depth that relied on having a river network which was hydrologically consistent with the DTM. This meant that the rivers had to follow the DTM cells which were the lowest point in the valley and in addition always flow to downstream cells of lower altitude. A river network supplied by the CHMI was not consistent with the DTM, and in many places poorly digitised so a new network was produced based on the DTM. Routines are available in the Arc Info GRID option which allow the drainage network generation. Lakes could not be modelled so these were represented as river reaches. However the Czech Republic has no major lakes in densely populated areas so this was not considered an issue. Another problem was in places where the river actually defined the national border. Here the DTM derived drainage network could not be defined since the DTM was also clipped to the national boundaries. The river reaches in this case, the lower Dyje, had to use the CHMI river network.

The propagation of the flooded area was undertaken on a reach by reach basis. The individual reach relating to each station was identified and a buffer of maximum floodable area was defined as a polygon surrounding this reach. The width of the buffer was based on maps of maximum flood extent where available or otherwise taken as 5 km either side of the channel for tributaries and 10 km for the major rivers. The DTM was clipped to this polygon and a series of grid cell based operations were undertaken using this grid and a grid of the river reach at the same resolution (see Figure 5).

Firstly for each cell in the buffer, the corresponding destination cell in the river was determined by the path of the lowest cumulative altitude taken from the buffer cell to the river. The buffer cell was then given the corresponding river cell altitude. The depth of flooding was then added to all the buffer cells and these were then subtracted from the DTM to give an altitude based flood extent map.

This initial flood map had large areas of flooded cells which were unconnected to the river channel. It was likely that many of these were in tributary river valleys where no river reach was being modelled, however for the purpose of this study a continuous flooded extent was required otherwise the results and therefore the methodology would look questionable. To remove the unconnected areas further grid cell operations were undertaken.

All non-flooded cells were classified as null data, then the destination river cells were once more determined for all cells in the buffer. This operation required that all cells have a numeric value so when the path from a buffer cell met a null data cell the operation was halted and a null

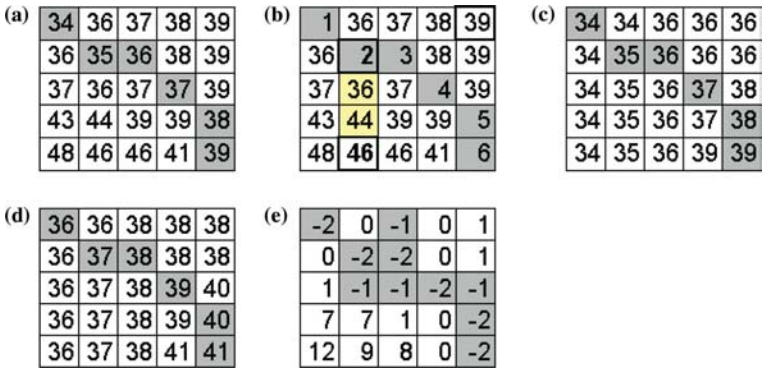

Figure 5. A simplified illustration of the grid cell based operations used to produce a flood extent map: River (grey) and land cells with altitude; Determining the lowest altitude path (light grey) from a source cell (bold) to the nearest river cell (2); Allocation of river cell altitude to all source cells; Flood depth of 2 m added to each cell; Grid (D) subtracted from DTM grid (A).

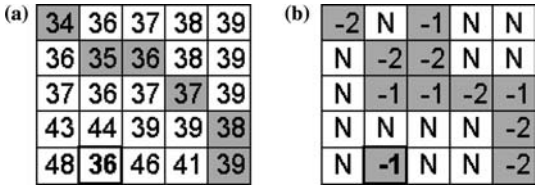

Figure 6. A simplified illustration of the removal of un-connected flooded cells: An unconnected flooded cell (bold) in (a) is surrounded by null cells (N) in (b) and therefore removed during the operation to determine its destination river cell.

data value was also returned for the buffer cell. In this way all unconnected flooded areas were removed since the path from any cell within this area would come across a null data cell on its way to the river (Figure 6).

The flooded extents for each of the individual reaches were then combined in an order so that the flood depth from particular river segments was given priority. In this way a main river in flood would always flood a tributary channel but not *vice versa*.

3.3. MODEL CALIBRATION

This method of flood depth propagation was tested using the actual measured flood levels at selected stations for 1997 and calibrated using published maps of flood extent. Some minor changes were made to the width of the maximum flood extent buffer, but the model generally produced a very good simulation of the flood extent (Figure 7). Most of the differences between the observed and predicted flood extents were due to the flooding from tributary rivers which were not modelled being mapped for 1997. Other difference could be attributed to the model not including defences within the hydrodynamic calculations, the mapping of surface water ponding and errors due to the resolution of the DTM.

3.4. MODEL APPLICATION

The prediction of flood extent for each of the events were then combined with maps of post code areas so that the average depth of flooding per post code could be calculated. One important aspect of the flood propagation which could not be explicitly included within the routine described above was the role of defences. This is because the typical flood defences – raised bunds, dykes or demountable flood walls are too narrow to be represented by the 100 m DTM. Instead, the defences were included in the post-processing. Information on the standard of protection for defences was obtained for particular municipalities within the major cities such as

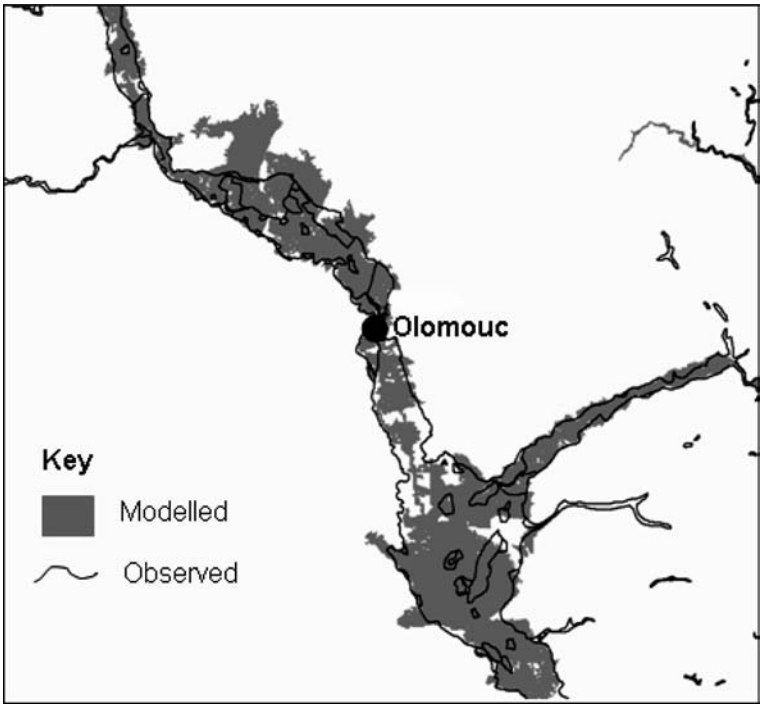

Figure 7. Comparison of the July 1997 modelled and observed flood extents around the city of Olomouc in Moravia.

Prague. The postcodes having this level of protection were then identified. During each flood event the return periods for every river segment were calculated. If this was higher than the design standard of the defences then all postcodes were assumed to be flooded. If not then defended postcodes were assumed not to have flooded. According to the CHMI no significant defence breeching occurred during the August 2002 flood.

Further calculations were undertaken using the average flood depth per post code, information on post code building stock and damage functions to calculate the insured losses for each event. The main disadvantage of the synthetic event set though was that although the losses from each event could be compared an actual return period of the loss was not generated. Since this is an important parameter for insurance purposes, a degree of stochastic analysis was undertaken.

4. The Floods of 2002

During the model development some of the worst flooding on record was recorded in the Czech Republic. This provided the project with valuable data

for both model development and calibration. It was particularly useful for defining the synthetic flood events since more extreme flows could be modelled from a knowledge of this event. An initial observed flood outline from Prague was also used to test the performance of the flood model.

5. Summary

This paper has described the development and application of a flood risk model for the Czech Republic. The model can predict the risk of flooding on a post code resolution for the main rivers in the country and in this respect it has served its purpose and been applied for a variety of insurance related studies. Due to a limited time period available for the production of the model a number of simplifying assumptions were used. Further development of the model will aim at providing a more rigorous representation of key aspects such as the role of defences and the routing of flows through the river network.

Acknowledgements

The author acknowledges the role of CHMI, in particular Mr J. Kubat and Mr. P. Sercl, for supplying the hydrological data; Martin Duris and Petr Muska (PBA Prague) for their general advice and assistance, and Benfield Ltd for providing the contract to undertake this work.

References

Buchtele, J.: 1989, Floods and droughts in the Labe River basin–the hydrograph shape. In: M. L. Kavvas (ed.), *New Directions for Surface Water Modelling*, IAHS Publ. No. 181. Wallingford, UK.

Buchtele, J., Buchtelova, M., Fortova, M., and Dubrovsky, M.: 1999, Runoff changes in Czech river basins – the outputs of rainfall-runoff simulations using different climate change scenarios. *J. Hydrol. Hydromech.* **47**(3), 180–194.

Buchtele, J., Dittrt, F., and Elias, V.: 1999, Practical experience gained from the evaluation of the July 1997 floods in the Czech Republic. *Proceedings of 34th MAF Conference on River and Coastal Engineering*, July 1999, Keele, UK, pp. 3.5.1–3.5.13.

Holicky, M. and Sykora, M.: 2003, Statistical evaluation of discharges on the Vltava River in Prague. *Proceedings* of the *International Conference – Flooding 2002*, Edinburgh, UK, November 2003, pp. 25–28.

Hradek, M., Kolejka, J., and Svehlik, R.: 1997, Czechia and Slovakia. In: C. Embleton, and C. Embleton-Haman (eds.), *Geomorpological Hazards of Europe*, Elsevier, Amsterdam.

Kundzewicz, Z. W.: 2000, The Odra flood of summer 1997 in perspective. In: A. Bronsert, C. Bismuth, and L. Menzel (eds.), *Proceedings of the European Conference on Advances in Flood Research*, November 2000, Postdam Institute for Climate Impact Research Report No. 65, Potsdam, Germany, pp. 592–690.

Morris, D. G., and Flavin, R. W.: 1995, *Flood Risk Map for England and Wales*. Institute of Hydrology Report No. 30, Wallingford, UK.

Rodda, H. J. E.: 2001. The development of a stochastic rainfall model for UK flood modelling. In: P. Krahe and D. Herpetz, (eds.), *Generation of Hydrometeorological Reference Conditions for the Assessment of Flood Hazard in Large River Basins*. CHR-Report No. I-20, Koblenz, Germany.

Natural Hazards (2005) 36: 221–235

Regional Rainfall Depth–Duration–Frequency Equations for an Alpine Region

MARCO BORGA*, CLAUDIA VEZZANI and GIANCARLO DALLA FONTANA
Department of Land and AgroForest Environments, University of Padova, via dell'Università, 16, Legnaro 35020, Italy

(Received: 22 November 2003; accepted: 30 June 2004)

Abstract. In this paper the scaling hypotheses are applied to annual maximum series of rainfall depth for different rainfall duration to derive the depth–duration–frequency (DDF) curve. It is shown that, based on the empirically observed scaling properties of rainfall and some general assumptions about the cumulative distribution function for the annual maximum of the rainfall depth, it is possible to derive a simple DDF relationship. This general framework provides a basis for the generation of maps that can be used to infer DDF curves at any point of a particular area. Data from a dense raingauge network in a mountainous region in north-eastern Italy (the Trentino Province) are used to clarify the methodology for the construction and regionalization of the DDF relationship. The geographical variation of short-duration (i.e., less than 60 min) rainfall extremes is also evaluated by using the same framework. It is found that depth–duration ratios, defined as the ratios of the t-min to the 60-min rainfall depths of the same return period, may be considered independent of return period and geographical location for any storm duration less than 60 min.

Key words: rainfall process, extreme rainfalls, statistical modelling, Gumbel distribution, scaling processes

1. Introduction

Design storms, defined as the rainfall intensity pattern for various probability of occurrences or return periods, are commonly required for designing hydraulic structures or for evaluating the effectiveness of a natural or man-made drainage system. The objective of rainfall frequency analyses is to estimate the amount of rainfall falling at a given point for a specified duration and return period. The frequency of the rainfall is usually defined by reference to the annual maximum series, which comprises the largest values observed in each year. An alternative data format for rainfall frequency studies is that based on the *peak-over-threshold* concept, which consist of all large precipitation amounts above certain thresholds selected for different

* Author for correspondence. E-mail: marco.borga@unipd.it

durations. Due to its simpler structure, the annual-maximum-series-based method is more popular in practice.

Design storms are generally based on models linking rainfall depth, duration and frequency (DDF models). Such models enable the estimation of rainfall frequency for any intermediate duration. A further reason for developing and using a DDF model is to reconcile rainfall estimates for different durations. If each duration is treated separately, it is possible that contradictions between rainfall estimates of different durations could occur, for example if the estimated 12-h 100-year rainfall were smaller than the 6-h 100-year rainfall at the same site. The DDF relationship for the return time T takes often the form of a power law relationship

$$h(d)_T = a_T d^{n_T} \tag{1}$$

where $h(d)_T$ is the rainfall depth at the specified return time T and duration d, and a_T and n_T are parameters. Power laws of this form are commonly used in Italy (Della Lucia *et al.*, 1976; Moisello, 1976; Burlando and Rosso, 1996; Ranzi *et al.*, 1999) and elsewhere (Chow *et al.*, 1988; Reed and Stewart, 1994; Koutsoyiannis *et al.*, 1998; IH, 1999). Note that these formulae are often expressed in terms of rainfall intensity rather than rainfall depth over a certain duration. The latter has been chosen here because it is cumulated rainfall depth, rather than instantaneous intensity, that is actually measured and that is of importance for flood estimation.

The traditional methodology to construct DDF curves has three main steps (Chow *et al.*, 1988). In the first step, raw data are examined to obtain annual maximum rainfall depth series for each time duration. Then, a statistical analysis is carried out for each duration to estimate the quantiles for different return periods. Lastly, the DDF curves are usually determined by fitting a specified parametric equation for each return period to the quantiles estimates, using regression techniques. Several parameters needs to be estimated in this procedure. Usually, at least two parameters need to be estimated for each time duration, and other two for each DDF curve.

In contrast to the above treatments, several models have been recently developed which attempt to statistically and simultaneously match various properties of the rainfall process at different levels of temporal aggregation (Burlando and Rosso, 1996; Benjoudi *et al.*, 1997; Kottegoda and Rosso, 1997; Menabde *et al.*, 1999; Ranzi *et al.*, 1999; Nguyen *et al.*, 2002; Veneziano and Furcolo, 2002). These procedures were based on the "scale invariance" (or "scaling") concept. The scale invariance implies that statistical properties of extreme rainfall processes for different time scales are related to each other by an operator involving only the scale ratio and the scaling exponent. Two important practical implications of the scaling models of DDF curves are: (i) from a higher aggregation level it is possible to infer the statistical properties of the process at the finer resolutions, that may not

have been observed; (ii) these models require a much smaller number of parameters with respect to the traditional heuristic methods used to derive DDF curves. However, note that a DDF model should not be expected to improve the accuracy of estimating rainfall for the primary durations at which data are available. Although a DDF model incorporates information from several durations, Buishand (1993) showed that the dependence between annual maxima over different durations is such that little or no improvement can be obtained.

In this paper, data from a dense raingauge network in a mountainous region in north-eastern Italy (the Trentino province; Figure 1) are used to show how it is possible to derive a simple DDF relationship in the form of (1) based on empirically observed scaling properties and some assumptions about the cumulative distribution for the annual maximum of rainfall depth. Moreover, it is shown how it is possible to use the above model to study the geographical variation of DDF curves and, more specifically, to estimate maps that can be used to infer DDF curves at any point of the study area. Specific attention is devoted to the analysis of short-duration (i.e., less than 60 min) rainfall extremes. It is shown that it is possible to identify two scaling exponents, one for rainfall duration shorter than 60 min and one for duration longer than this threshold. The scaling exponent for duration shorter than 60 min can be considered fairly constant over the study area. This

Figure 1. Study area location: the Trentino province and Trento.

finding, considered within the scaling approach, provides an explanation for the often-observed empirical result that the ratio of the t-min rainfall to 60-min rainfall for the same return period may be considered constant over a given geographical region (Hershfield, 1962; Bell, 1969; Ferreri and Ferro, 1990; Kothyari and Garde, 1992; Alila, 2000).

2. The Scaling Concept

Over the last two decades, concepts of scale invariance have come to the fore in both modelling and data analysis in hydrological precipitation research. Just a very limited account of this research is provided here.

Lovejoy and Schertzer (1985) introduced the ideas of scale invariance and fractals into rainfall modelling through evidence that rainfall may be scaling. Gupta and Waymire (1990) studied rainfall spatial variability by introducing the concepts of simple and multiple scaling to characterise the probabilistic structure of the precipitation process. These results were taken one-step further by Burlando and Rosso (1991, 1996) as they derived a general distribution-free formulation of DDF curves based on either scaling or multiscaling conjecture. Based on data from two stations in Italy, Burlando and Rosso (1996) showed that both the simple scaling and multiscaling log-normal models can be used to derive DDF curves of station precipitation. Building on the previous scaling work, Menabde *et al.* (1999) developed a simple scaling methodology to use daily rainfall statistics to infer the DDF curve for rainfall duration less than 1 day. The scaling hypothesis was verified by fitting the model to two different sets of data (from Australia and South Africa). Assuming a (temporal) simple scaling behaviour, Salvadori and De Michele (2001) used the theoretical relations linking the Generalized Pareto and Generalzed Extreme Value (GEV) distributions to derive the relations between the scaling exponents of the two distributions and to estimate the parameters of the two distributions at different temporal scales.

The distribution of a random variable (such as the one, identified as $H(D)$, representing the maximum rainfall depth of duration D observed in each year), satisfies the scaling relation when

$$H(\lambda D) \stackrel{d}{=} \lambda^n H(D) \tag{2}$$

where $\stackrel{d}{=}$ denotes equality in the probability distribution, λ denotes a scale factor and n is a scaling exponent, typically ranging from 0.3 to 0.5 (Burlando and Rosso, 1996; Menabde *et al.*, 1999) for the maximum annual rainfall depth distribution. This property is referred to as "*strict sense simple scaling*" by Gupta and Waymire (1990). This also implies that the raw moments of any order are scale-invariant, that is

$$E[H(\lambda D)^q] = \lambda^{qn} E[H(D)^q] \quad q = 1, 2, 3, \ldots \tag{3}$$

where q denotes the order of the moment and $E[\ ]$ is the expectation operator. The latter property is defined as "wide sense simple scaling" (Gupta and Waymire, 1990) since it is a weaker property than strict sense simple scaling. It must be stressed that in practical applications the scaling regime (when observed) usually holds only between an inner cutoff $\lambda_{\min}$ and an outer cutoff $\lambda_{\max}$; that is, for $\lambda_{\min} \leq \lambda \leq \lambda_{\max}$.

The only functional form of $E[H(D)^q]$ satisfying (3) is

$$E[H(D)^q] = f(q) D^{-qn} \tag{4}$$

where $f(q)$ is some function of q. Notice that if the exponent in (4) is not a linear function of q, in such cases the process is said to be "multiscaling" (Gupta and Waymire, 1990). In this last case, if $\partial^2 n/\partial q^2$ is negative there is a decrease in the temporal variability with increasing temporal scale. Conversely, a positive value of $\partial^2 n/\partial q^2$ indicates an increase in the temporal variability with increasing scale. The concave curve is typical for natural phenomena. Based on the literature on turbulence, this feature is explained by Gupta and Waymire (1990), among others, by the "cascading down" of some large-scale energy flux to successively smaller scales. In the multiscaling case, the scaling properties can be used for either scale magnification or scale contraction, but not for both. This is called the "irreversibility property" of the rainfall process. For concave growth curve of the scaling exponent, Gupta and Waymire (1990) have shown that only scale contraction or "downscaling" is possible.

We assume here that wide sense simple scaling holds for a certain considered range of durations. Based on the scaling property defined above, and taking $\lambda = d/D$, one obtains for the first two moments

$$\begin{aligned} &E[H(d)] = d^n E[H(D)] \\ &\mathrm{Var}[H(d)] = d^{2n} \mathrm{Var}[H(D)] \\ &\mathrm{CV} = \sqrt{\frac{\mathrm{Var}[H(d)]}{E^2[H(d)]}} = \mathrm{const} \end{aligned} \tag{5}$$

Based on (5), the coefficient of variation, as well as the coefficient of skewness and the coefficient of kurtosis, is independent of duration d.

If we denote with a_1 the mean of the annual maximum rainfall depth for the specified temporal duration assumed as reference duration D (e.g., the hourly duration, if d is measured in hours), Equation (5) can be written as

$$\begin{aligned} &E[H(d)] = a_1 d^n \\ &\mathrm{CV} = \mathrm{const} \end{aligned} \tag{6}$$

The values of a_1 and n can be estimated by linear regression of expectations of rainfall depth against duration, after log transformation, whereas the value of CV can be obtained as the average of coefficient of variation computed for the different durations, in the range of durations for which the scaling property holds.

The theory discussed above and the procedures derived from it were tested on a dataset provided from a dense raingauge network in a mountainous region in north-eastern Italy (the Trentino province; Figure 1). More specifically, in order to exemplify the scaling property, we analysed a set of annual maxima from the Trento precipitation station (Figure 1: latitude: 46°04′, longitude 11°8′, altitude: 320 m a.s.l.) where data are available for 22 years for short temporal aggregations (less than one hour, that is 15, 30 and 45 min) and for 57 years for the five canonical durations equal or larger than one hour (that is 1, 3, 6, 12 and 24 h). Figure 2 represents the scaling behaviour of the moments, defined by (4). It can be seen that this data set shows very good scaling behaviour in the range of durations considered. The scaling exponents were calculated by regression of the raw moments of order q against duration (after logarithmic transformation) and are shown in

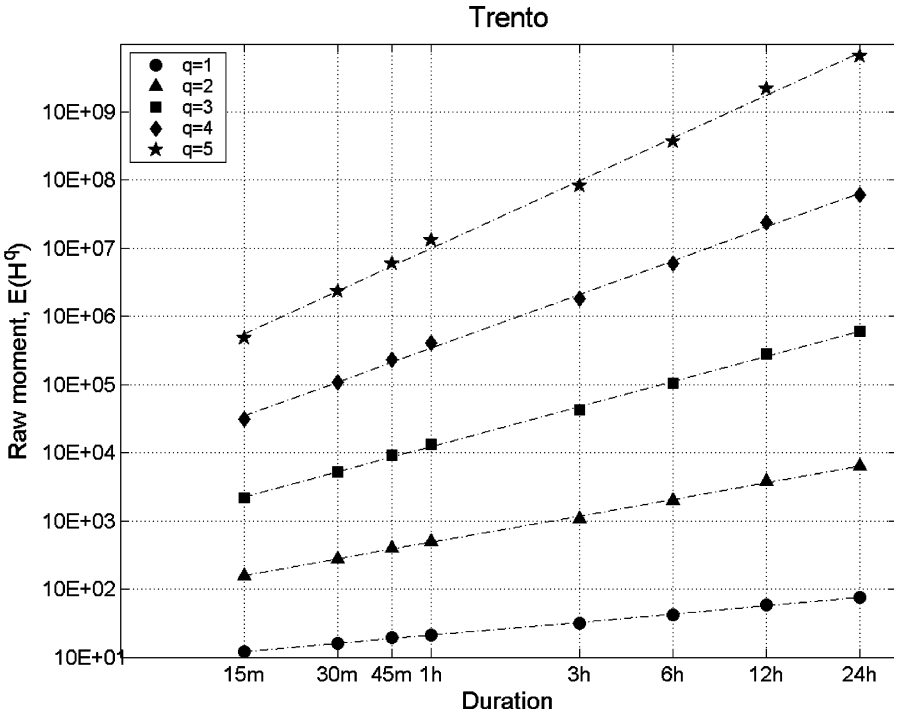

Figure 2. Scaling of the moments with durations for Trento station.

Figure 3. Their dependence on q is precisely linear, thereby confirming the hypothesis about wide sense simple scaling. For the Trento station, the scaling exponent n, computed in the range 15 min to 24 h, is equal to 0.399.

3. A Gumbel Scaling Model of DDF Relationship

The Gumbel or extreme value type 1 distribution has been used extensively in hydrology to model flood flows and extreme rainfall depths (Chow *et al.*, 1988; Stedinger *et al.*, 1993). The Gumbel cumulative distribution function can be easily inverted to provide the Tth quantile of Gumbel random variable for duration d in the following form

$$h_T(d) = \mu(d)\left\{1 - \frac{\mathrm{CV}(d)\sqrt{6}}{\pi}[\varepsilon + y_T]\right\} \tag{7}$$

where

$$y_T = \ln\left[\ln\left(\frac{T}{T-1}\right)\right]$$

where $\mu(d)$ is the mean and ε is Eulers constant, approximately 0.5772157. The relationships (6) can be substituted in (7) to obtain

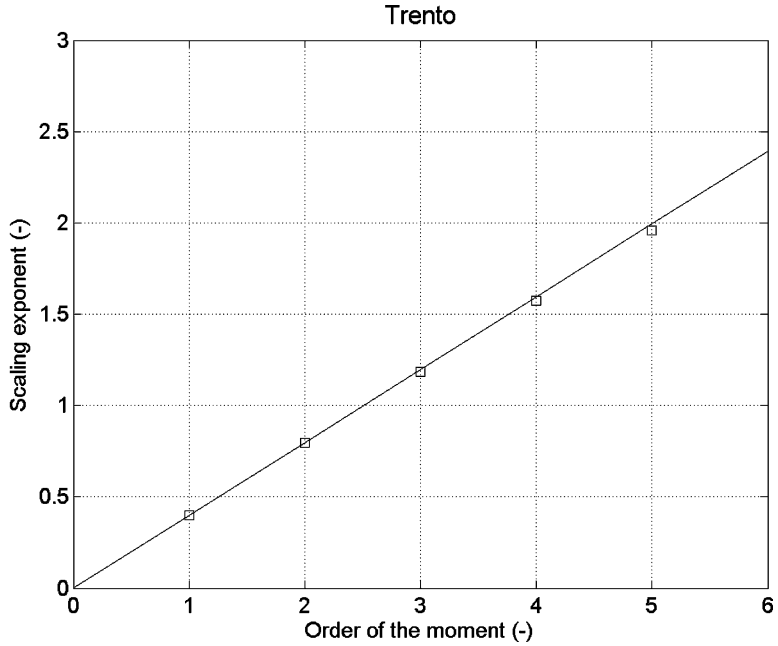

Figure 3. Scaling exponents for Trento station.

$$h_T(d) = a_1 \left\{ 1 - \frac{\mathrm{CV}\sqrt{6}}{\pi} [\varepsilon + y_T] \right\} d^n \tag{8}$$

which represents the Gumbel simple scaling model of DDF curves, in the form of Equation (1).

L-moments estimators have been proposed for the Gumbel distribution (Stedinger *et al.*, 1993). In this last case, the Gumbel simple scaling model of DDF curves can be written as follows:

$$h_T(d) = a_1 \left\{ 1 - \frac{\tau_2}{\ln(2)} [\varepsilon + y_T] \right\} d^n \tag{9}$$

where τ_2 denotes the *L*-moment coefficient of variation (Stedinger *et al.*, 1993), obtained as the average of *L*-moment coefficient of variations of the various durations.

The result of the application of the Gumbel simple scaling model to Trento rainfall depth data is shown in Figure 4, where the model estimated probability are compared with the sampling cumulated frequency of observed data. The Gumbel model was applied in this case with the product moment estimation procedure. As a general comment, we see that the agreement between the sample *cdfs* and the theoretical ones is indeed

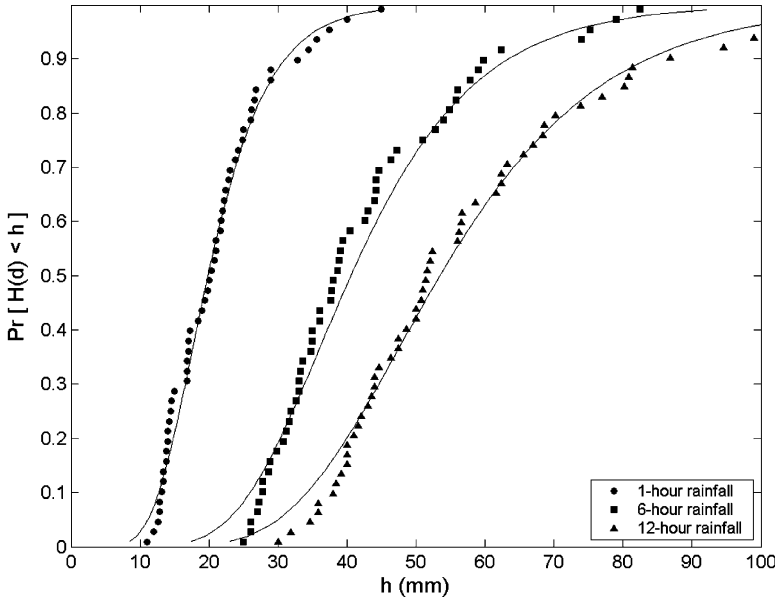

Figure 4. Cumulative distribution frequency (*cdf*) for the annual maximum rainfall depth for Trento station, by using the simple scaling Gumbel distribution.

empirically satisfactory. Moreover, thanks to the scaling relations, it would be possible to draw theoretical *cdfs* for any desired level of temporal aggregation, for which the scaling property holds.

4. Spatial Estimation of DDF Curves in the Study Area

The general framework described above provides a sound basis for evaluating the spatial variability of DDF curves in a given region. The idea is to study the variation of the DDF model parameters (a_1, n and CV), instead of the variation of the rainfall quantiles (as is usually done with the traditional approach).

The study area for the investigation is the Trentino province, with an area of around 6000 km^2. The area is characterised by a mountainous terrain, with altitudes ranging from 150 to 3600 m a.s.l. The area lies at the southern border of the "inner alpine province" with its own distinctive climatic characteristics (Fliri, 1975). The inner alpine province is characterised by low precipitation amounts, due to the dual sheltering effect of the ranges to both the north and south. The south-eastern part of the Trentino province is characterised by higher precipitation amounts, and commonly experiences showery precipitation, with thunderstorm and hail, particularly in summer and autumn. Thus the annual rainfall varies from about 1300 mm in the south-eastern part of the area to about 900 mm in the northern part.

Records of annual maximum rainfall depth at 91 recording stations were used. The durations examined were 15, 30, 45 min and 1, 3, 6, 12 and 24 h.

In the first stage, based on meteorological and climatic evidences as well as previous research findings (Willems, 2000), we considered the possibility to differentiate the scaling regimes for durations either shorter or longer than 1 h, associated with two different types of storms: storms associated with airmass thunderstorms, characteristic of the summer season, and storms associated with cyclonic and frontal storms, more frequent in autumn. More specifically, we made the assumption that it is possible to identify a scaling exponent for each of the two duration ranges, and that the scaling exponent for short-duration rainfall is independent of geographical location. We studied the relationship (by using linear regression) between the mean values of the annual maximum rainfall depth for duration equal to 15, 30, 45 min, and 1, 3, 6, 12, and 24 h to those of 60 min-duration, across 55 stations located in the Trentino province with at least 15 years of observations. Results are reported in Figures 5a–c for 30-, 45-min and 6-h duration, respectively. Results indicate that the 60-min mean rainfall depth value alone explain, on average, 86–94% of the spatial variability of the mean rainfall depth for duration less than 1 h. The high coefficient of determination and low standard error of estimates lend support to the argument that the need

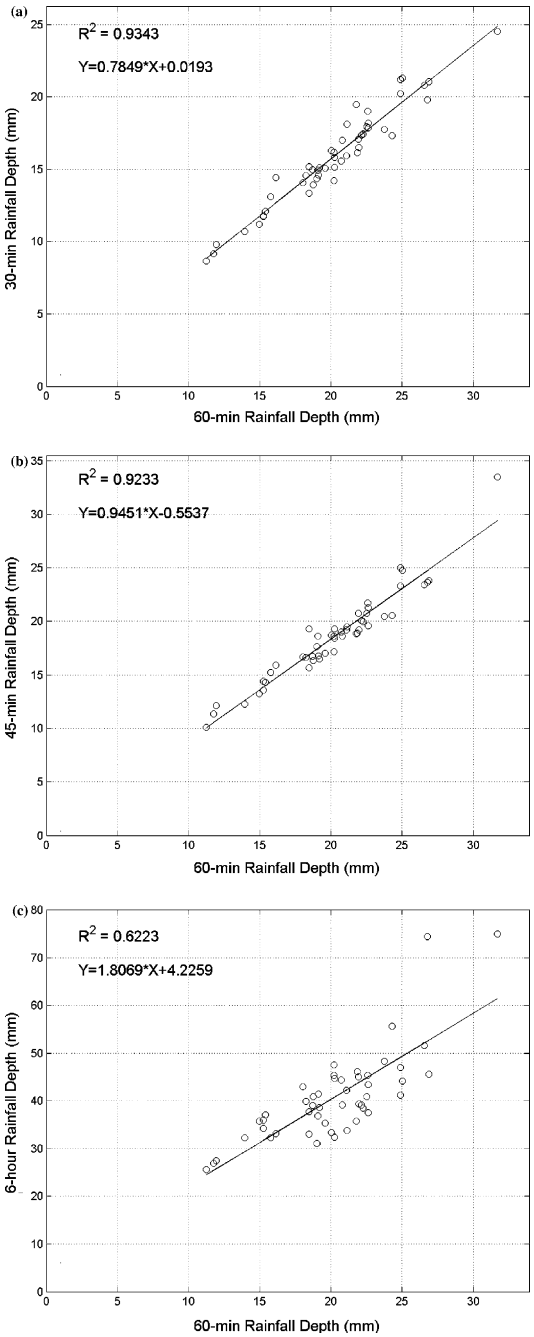

Figure 5. Depth–duration linear relationship for (a) 30-min and (b) 45-min, (c) 6-h mean values with 60 min as base duration.

for more geographic information is unnecessary, for duration less than 60 min. On the contrary, results reported for duration longer than 60 min show that the fraction of variance explained by 60-min rainfall depth alone reduces progressively going from 3- to 24-h duration. This suggests that, while the scaling exponent for short-term rainfall can be considered fairly homogeneous across the study area (with a value equal to 0.366), the exponent for the durations comprised between 1 and 24 h needs to be considered geographically variable. This high degree of consistency in short-duration rainfall frequency implies that local convective cells have similar physical properties irrespective of geographical location. While this hypothesis has never been verified before in the study area, it has been advocated in other studies (Hershfield, 1962; Bell, 1969; Ferreri and Ferro, 1990; Alila, 2000), as detailed below. Incidentally, no break in scaling could be observed for the data from the Trento station (Figure 2), because the overall scaling exponent (0.399, computed for Trento station on the range from 15 min to 24 h) was pretty close to the constant value computed for the whole area for short durations rainfalls (0.366).

In the second step, we fitted the Gumbel simple scaling DDF model to the data. This model was considered suitable, since the Gumbel distribution was found to be appropriate for almost all the stations, using Kolmogorov and Filliben test. However, it is well known that small sizes of record may hide the appropriateness of more general distributions, such as the GEV (Generalized Extreme Value) distribution (Jenkinson, 1955). We are going to apply to these data a GEV distribution, which embodies the scaling behaviour and a regional approach for the estimation of the shape parameter k. Results will be reported soon on this study extension and on the comparison between the corresponding results.

Tests were carried out to check the validity of the simple scaling assumption (Ranzi *et al.*, 1999), which was not rejected on most of the stations. Two parameters of the DDF model (a_1 and n) were estimated, for durations longer than 1 h, based on stations with at least 15 observations for each duration (55 stations), whereas the third model parameter (CV) was estimated based on stations with at least 25 years for each duration (43 stations), in order to reduce sampling uncertainty.

A kriging procedure (Borga and Vizzaccaro, 1997) was used to estimate the spatial distribution of the three parameters across the area (the spatial distribution of two parameters, a_1 and n, is represented in Figures 6a and b, respectively). These estimates were then used to generate DDF curves at any point in the region. On the basis of data from a wider region, research is under way to establish relationships between the scaling parameters and geographical information, such as the altitude, and climatic information, such as the mean annual precipitation amount.

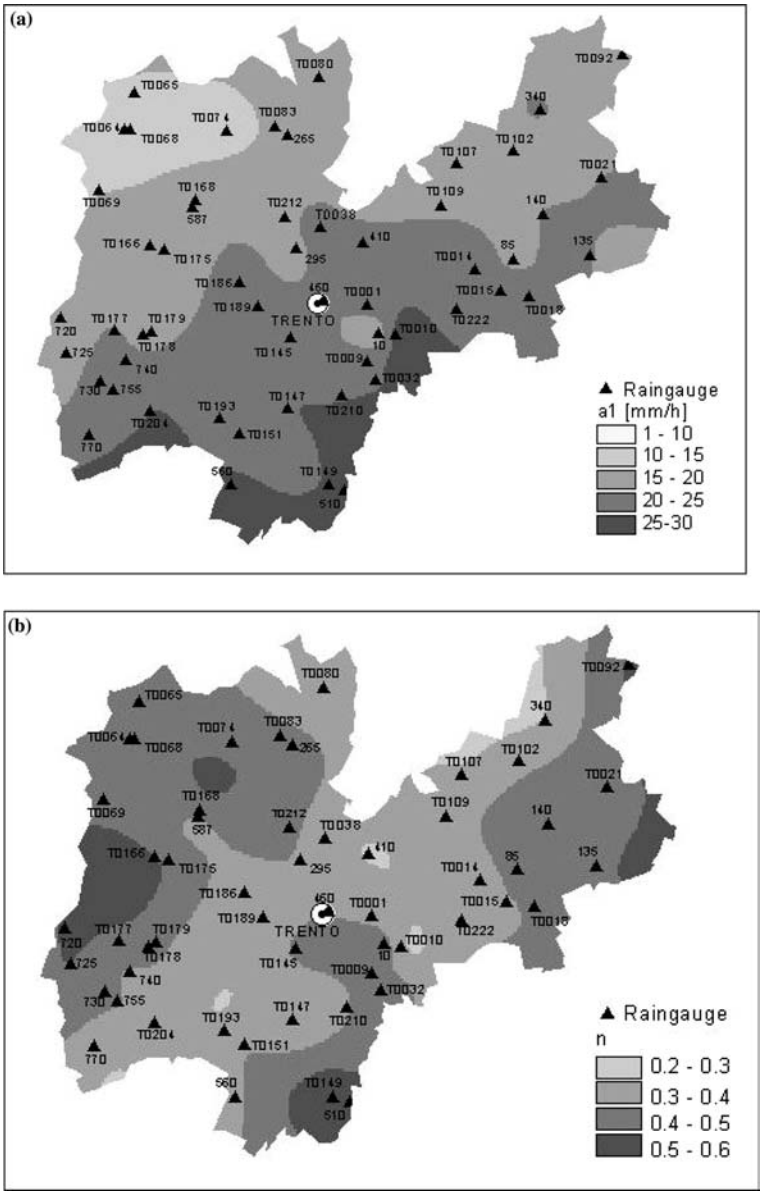

Figure 6. Spatial variation of (a) parameter a_1 and (b) parameter n.

It is interesting to note that the approach used here concerning short duration rainfalls (based on adopting a spatially constant scaling exponent) leads the ratio of the t-min rainfall to 60-min rainfall (for the same return period) to be independent of the geographical location. This is an often-observed features of short-duration rainfall, noted and

reported, among others, by Hershfield (1962) and Bell (1969) for the United States, by Ferreri and Ferro (1990) for Italy, by Kothyari and Garde (1992) for India and by Alila (2000) for Canada. Moreover, the difference in the values reported for the scaling exponent in these studies is rather small, with a value of 0.393 for Canada (Alila, 2000), 0.386 and 0.345 in Sicily and Sardinia, respectively (Ferreri and Ferro, 1990) and 0.290 for India (Kothyari and Garde, 1992).

The overall performance of the procedure used to estimate DDF curves across the region was assessed by counting the exceedances of certain quantiles and comparing observed and expected exceedances (Buishand, 1991). DDF curves were estimated at each station of the network (without using the local data); then, the number of exceedances of rainfall depths with various rarities was counted. This test was carried out for $T = 50$, 100, and 200 years. The expected number of exceedances is obtained by dividing the total number of station years by T. This is based on the fact that for the annual maximum $H(d)$ at a certain site

$$\Pr[H(d) > h_T] = \frac{1}{T} \tag{10}$$

For example, for $T = 100$ years, the observed number of exceedances (over all the durations) is equal to 113, while the expected number is equal to 126 (since the total station years are 12579). This result shows that there is a small bias, with 11% fewer exceedances observed than expected according to the method. However, the difference is only slightly more than the binomial standard deviation (equal to 11.2), given by $[M(1-1/T)]^{0.5}$, where M is the expected number of exceedances.

5. Conclusions

The traditional framework of DDF estimation is not free of empirical considerations, which may be inconsistent with the probabilistic foundation of DDF relationships. The use of the scale invariance concept on the DDF derivation represents an attempt to cast the DDF relationship within a general mathematical and physical framework. The simple scaling framework also yields a more parsimonious model parametrisation for DDF relationship with respect to the traditional one, based on regression of quantile estimates against duration.

The simple scaling hypothesis has been found to describe reasonably well the DDF characteristics of rainfall depth annual maxima from a network of raingauges in an alpine region. The assumption of wide sense simple scaling lead to a simple form of the DDF relationship, based on the Gumbel distribution. The efficient parametrisation of the model (based on only three parameters) allowed the study of the geographical variation of DDF curves,

based on the analysis of the parameters of the DDF curves, instead of the variation of rainfall depths. The results obtained show that the scaling framework offers a good basis for the regionalisation of DDF curves. Furthermore, this methodology allows the incorporation of data from the more dense network of non-recording stations in the process of DDF relationship construction. This results potentially in a more detailed information on the geographical variation of DDF curves.

It has also been shown that it is possible to derive separate scaling regimes for short duration rainfall (with duration less than 1 h) and for longer temporal aggregations. The scaling exponent for short duration rainfall may be considered fairly independent of the geographical location, thus implying a high degree of consistency for this kind of rainfall.

Acknowledgments

This research was jointly funded by Sixth Framework Program of the European Commission (FLOODsite project, EC Contract number: GOCE-CT-2004-505420) and by Provincia Autonoma di Trento (Italy). The authors thank two anonymous reviewers for contributing to the clarity of this work.

References

Alila, Y.: 2000, Regional rainfall depth–duration–frequency equations for Canada, *Water Resour. Res.* **36**(7), 1767–1778.

Bell, F. C.: 1969, Generalised rainfall depth–duration–frequency relationships, *J. Hydraul. Div. Am. Soc. Civ. Eng.* **95**(1), 331–327.

Benjoudi, H., Hubert, P., Schertzer, D., and Lovejoy, S.: 1997, Interpretation multifractale des courbes intensité-duree-frequance des precipitations, *Geosci. Surface Hydrol. Surf. Geosci. Hydrol.* **325**, 323–336.

Borga, M., and Vizzaccaro, A.: 1997, On the interpolation of hydrologic variables: formal equivalence of multiquadratic surface fitting and kriging, *J. Hydrol.* **195**, 160–171.

Buishand, T. A.: 1991, Extreme rainfall estimation by combining data from several sites, *Hydrol. Sci. J.* **36**, 345–365.

Buishand, T. A.: 1993, Rainfall depth–duration–frequency curves; a problem of dependent extremes, In: V. Barnett and Turkman, K. F. (eds), *Statistics for the Environment*, Wiley, pp. 183–197.

Burlando, P., and Rosso, R.: 1991, Statistical models for design storm prediction, In: U. Maione (ed.), *Modelli idrologici superficiali nella pianificazione di bacino*, Città Studi, Milano, pp. 367–421 (in Italian).

Burlando, P., and Rosso, R.: 1996, Scaling and multiscaling models of depth–duration–frequency curves for storm precipitation, *J. Hydrol.* **187**, 45–64.

Chow, V. T., Maidment, D. R., and Mays, L. W.: 1988, *Applied Hydrology*, McGraw-Hill, New York.

Della Lucia, D., Fattorelli, S., and Provasi, S.: 1976, Determinazione delle zone omogenee per le piogge intense nel Trentino, *Memorie del Museo Trentino di Scienze Naturali*, **21**(2).

Ferreri, G. B., and Ferro, V.: 1990, Short duration rainfalls in Sicily, *J. Hydraul. Eng.* **116**(3), 430–435.

Fliri, F.: 1975, *Das Klima der Alpen im Raume Tirol*, Universitäts-Verlag Wagner, Innsbruck.

Gupta, V. K., and Waymire, E.: 1990, Multiscaling properties of spatial rainfall and river flow distributions, *J. Geophys. Res.* **95**(D3), 1999–2009.

Hershfield, D. M.: 1962, Extreme rainfall relationships, *J. Hydraul. Div. Am. Soc. Civ. Eng.* **88**(6), 73–92.

Hosking, J. R. M., Wallis, J. M., and Wood, E. F.: 1985, Estimation of the generalized extreme value distribution by the method of probability weighted moments, *Technometrics* **27**(3), 251–261.

IH (Institute of Hydrology): 1999, *Flood Estimation Handbook*, Institute of Hydrology.

Jenkinson, A. F.: 1955, The frequency distribution of the annual maximum (or minimum) value of meteorological elements, *Q. J. Royal Meteorol. Soc.* **81**, 158–171.

Kothyari, U. C., and Garde, R. J.: 1992, Rainfall intensity–duration–frequency formula for India, *J. Hydraul. Eng.* **118**(2), 323–336.

Kottegoda, N. T., and Rosso, R.: 1997, *Statistics, Probability and Reliability for Civil and Environmental Engineers*, McGraw-Hill, 735 pp.

Koutsoyiannis, D., and Baloutsos, G.: 2000, Analysis of long record of annual maximum rainfall in Athens, Greece, and design rainfall inferences. *Natural Hazards* **29**, 29–48.

Koutsoyiannis, D., Kozonis, D., and Manetas, A.: 1998, A mathematical framework for studying intensity–duration–frequency relationships, *J. Hydrol.* **206**, 118–135.

Lovejoy, S., and Schertzer, D.: 1985, Generalized scale invariance and fractal models of rain, *Water Resour. Res.* **21**, 1233–1250.

Menabde, M., Seed, A., and Pegram, G.: 1999, A simple scaling model for extreme rainfall. *Water Resour. Res.* **33**(12), 2823–2830.

Moisello, U.: 1976, Il regime delle piogge intense di Milano, *Ingegneria Ambientale* **5**, 545–561.

Nguyen, V.-T.-V., Nguyen, T.-D., and Ashkar, F.: 2002, Regional frequency analysis of extreme rainfalls, *Water Sci. Technol.* **45**(2), 75–81.

Ranzi, R., Mariani, M., Rossini, E., Armanelli, B., and Bacchi, B.: 1999, *Analisi e sintesi delle piogge intense del territorio bresciano*, Technical Report N. 12, University of Brescia, 94 pp.

Reed, D. W., and Stewart, E. J.: 1994, Inter-site and inter-duration dependence in rainfall extremes. In: V. Barnett and K. F. Turkman (eds), *Statistics for the Environment 2: Water-Related Issues*, Wiley, pp. 125–143.

Salvadori, G., and De Michele, C.: 2001, From generalized Pareto to extreme values law: Scaling properties and derived features, *J. Geophys. Res.* **106**(D20), 24063–24070.

Stedinger, J. R., Vogel, R. M., and Foufoula-Georgiu, E.: 1993, Frequency analysis of extreme events, In: D. R. Maidment (ed.), *Handbook of Hydrology*, McGraw-Hill, New York, pp. 18.1–18.66.

Veneziano, D., and Furcolo, P.: 2002, Multifractality of rainfall and scaling of intensity–duration–frequency curves, *Water Resour. Res.* **38**(12), 1306, DOI:10.1029/2001WR000372.

Willems, P.: 2000, Compound intensity/duration/frequency-relationships of extreme precipitation for two seasons and two storm types, *J. Hydrol.* **233**, 189–205.

Natural Hazards (2005) 36: 237–256

An Integrated Approach for Realtime Floodmap Forecasting on the Belgian Meuse River

C. DAL CIN[1,★], L. MOENS[2], PH. DIERICKX[3], G. BASTIN[2] and Y. ZECH[1]

[1]*Department of Civil and Environmental Engineering, Université Catholique de Louvain (UCL), Place du Levant 1, 1348 Louvain-la-Neuve, Belgium;* [2]*Centre for Systems Engineering and Applied Mechanics (CESAME UCL), Avenue Georges Lemaître 4, 1348 Louvain-la-Neuve, Belgium;* [3]*Direction générale des Voies Hydrauliques, Walloon Ministry of Equipment and Transport, Boulevard du Nord 8, 5000 Namur, Belgium*

(Received: 17 October 2003; accepted: 30 June 2004)

Abstract. The last important floods of the Meuse river have shown the need to design powerful and real-time forecasting tools. With the support of CESAME and the department of Civil and Environmental Engineering at UCL, the Service of Hydrologic Studies (SETHY) of the Walloon Ministry of Equipment and Transport developed two models: Hydromax and Hydroaxe. These two complementary and user-friendly applications work with the data provided by the measurement network of SETHY (raingauges, water levels, discharge measurements, weir-gate positions). Hydromax produces local river flow forecasting for the main natural tributaries of the Meuse. These predictions are used by Hydroaxe to compute discharge propagation and water levels all along the Meuse. In Hydromax, the predictions are produced by a grey box model which involves two main parts. A nonlinear production function computes the effective rainfall from the mean areal rainfall. This part is based on a conceptual approach, the river basin being modelled as a reservoir. In the second part, a linear ARX (AutoRegressive model with eXtra input) transfer function (black box), describes the superficial runoff of the effective rainfall towards the watershed outlet. This transfer function is used to compute short term river flow predictions. Hydroaxe uses a Preissmann finite difference scheme to solve the Saint-Venant equations of shallow-water, completed with the Exchange Discharge Model describing the momentum exchanges between the main channel and the floodplains. The optimisation of the computation time requires a one-dimensional approach, based on a dense (1 point/m^2) and accurate (15 cm in x, y, z) topography provided by SETHY and carried out through an original combination of technologies: swath bathymetry and airborne laser (Lidar). With the help of a GIS (Geographic Information System) and the DTM (Digital Terrain Model), the water levels calculated by Hydroaxe are transformed in flooded areas, fitted for an easy and fast overview of the extent of the flood event.

Key words: Meuse river, flood, forecasting, real-time, GIS, DTM

★ Author for correspondence. E-mail: dalcin@gce.ucl.ac.be

1. Introduction

The early warning of extreme hydrological situations, all over the Meuse river basin, is one of the main missions of the Service of Hydrologic Studies (SETHY) of the Walloon Ministry of Equipment and Transport. The Meuse is a navigable river, which flows through France, Belgium and the Netherlands. Its catchment has an area of 12,220 km^2 in Wallonia (southern Belgium), i.e. 73.3% of the Walloon territory (see Figure 1). The tributaries of the Meuse are notable for their very varied characteristics, with very high flows in winter and extremely low waters in summer.

The big floods in 1993 and 1995 have shown the need to perform real-time forecasting of water levels and flooded areas. With the technical support of CESAME and the department of Civil and Environmental Engineering of UCL, SETHY has started the development of two applications: Hydromax (Moens and Bastin, 1995) and Hydroaxe (Scherer, 1999; Adriaensen, 2001; Dal Cin, 2002).

Since 1995, Hydromax produces real-time local river flow forecasting for the main natural tributaries of the Meuse river. For 6 years, Hydromax can also forecast high river flow at three stations on the Meuse river. Several predictions of Hydromax are used by Hydroaxe to compute discharge propagation and water levels all along the Meuse river. Hydroaxe is based on 1D shallow water equations according with the river profiles and including the effect of the floodplains. Hydroaxe is currently operational on the Walloon Meuse. As Hydromax, Hydroaxe was developed to meet the

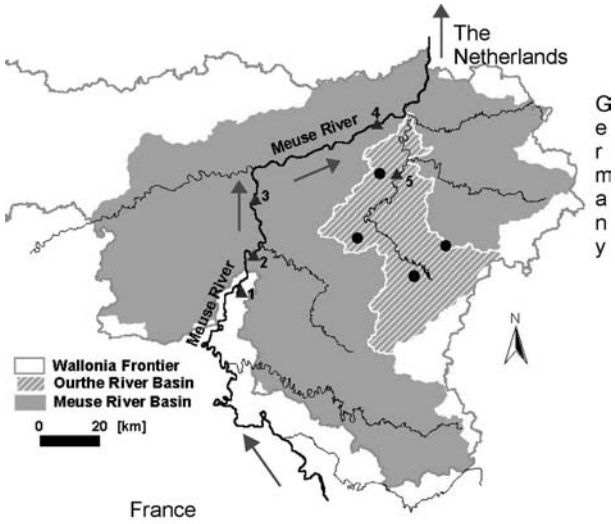

Figure 1. The Walloon Meuse river basin and its main tributaries. (Locations: 1 = Chooz, 2 = Waulsort, 3 = Lustin, 4 = Ivoz, 5 = Tabreux. The dots are the raingauges used by Hydromax for the forecasting of Tabreux.)

requirements of an efficient real-time forecasting. These two applications are connected in real-time to the measurement network of SETHY.

Thanks to a dense and accurate Digital Terrain Model (DTM) obtained through laser scanning and swath bathymetry, the water levels produced by Hydroaxe are then used by a Geographic Information System (GIS) to draw flood maps.

The flood maps produced at the crisis centre of SETHY can be used as a support for the real-time management of an incoming flood, as well as a tool to develop a long-term water management policy.

The present paper will first give a short description of the major functions of SETHY. The paper will then focus on the three parts of the forecasting tool: Hydromax, Hydroaxe and the computation of flood maps with ArcView GIS.

2. The Service of Hydrologic Studies: SETHY

2.1. MISSIONS

SETHY has many missions about the water flows in the rivers and canals throughout the South of Belgium. Figure 2 shows its primary objectives and the interconnected means necessary to reach them.

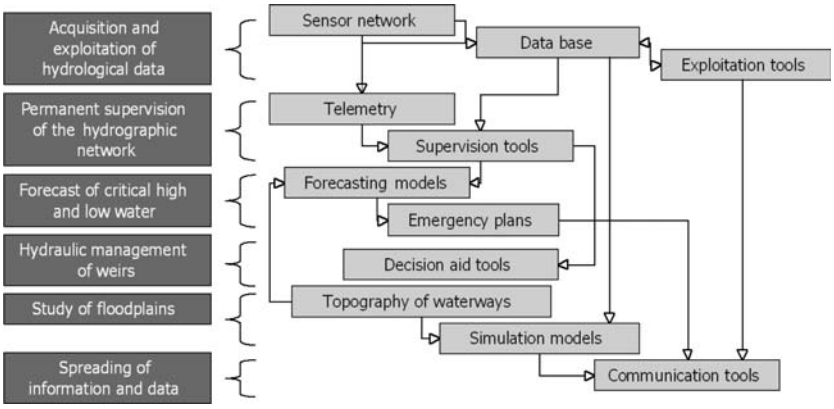

Figure 2. Missions and means of SETHY.

Many hydraulic structures are located in the Walloon hydrographic network: dams, weirs, reservoirs, locks, hydropower plants, pumped storage plants. They have numerous and sometimes conflicting interests: navigation, drinking water reserve, flooding mitigation, tourism, power production. SETHY has permanent contacts with the public and private organisations in charge of these structures, in order to guarantee a comprehensive and coherent management of the water resource.

2.2. MEASUREMENT NETWORK AND PREDICTION MODELS

The measurement network is the cornerstone of applied hydrology. A dense, complete, coherent and integrated network, all over the Walloon region was developed and managed for many years. Today, more than 230 hydrologic stations are working on this territory of approximately 18,000 km^2. The real-time network records accurately the rainfall, the water levels and the discharge of rivers and lakes, together with the positions of weirs across waterways. SETHY's network incorporates state of the art techniques: weather radar, ultrasonic flowmeters, laser sensors, etc. All measurements are stored directly in a huge database with specific management tools integrated: quality control, supervision, exploitation, internet dissemination, warnings, etc.

One of the main missions of SETHY is the early warning for extreme hydrological situations. For the prediction of discharge, Hydromax (see Section 3) was developed and, on another hand, Hydroaxe (see Section 4) for the water levels and flooded areas. These two relevant applications for real-time flood forecasting are handled as shown in Figure 3.

2.3. INVESTIGATION OF FLOODPLAIN AREAS

The knowledge of floodplains is a complex task but definitely necessary to draw flood-map forecasting (see Section 5). SETHY organises aerial photograph surveys during flooding and field surveys after flooding. However these actions only show the extension of flooded zones and are not sufficient to compute occurrence or risk probabilities. Hydraulic models must be used, but in many cases the topography of floodplains areas and the bathymetry of rivers are not known with adequate accuracy. Conventional techniques (land survey, photogrammetry, remote sensing) are either too slow, or too expensive, or too inaccurate. In order to obtain the best information for the hydraulic models, SETHY has set an ambitious objective at the end of the nineties: the creation of a DTM with very stringent criteria (density of 1 measured point per m^2 and an accuracy of 15 cm in x, y, z). The 15 cm in altitude is required in Belgium due to the topography of the floodplain. A water-level small difference could highly affect the inundation extension. To achieve these objectives, SETHY has carried out surveys using an innovative combination of state of the art techniques: swath bathymetry and airborne laser (also known as Lidar). The surveys have been conducted on 450 km of waterways and 1500 km of smaller rivers.

2.3.1. *River Bathymetry*

For the bathymetric survey of waterways, SETHY implemented swath bathymetry (see Figure 4). This technique is frequently used offshore. But on

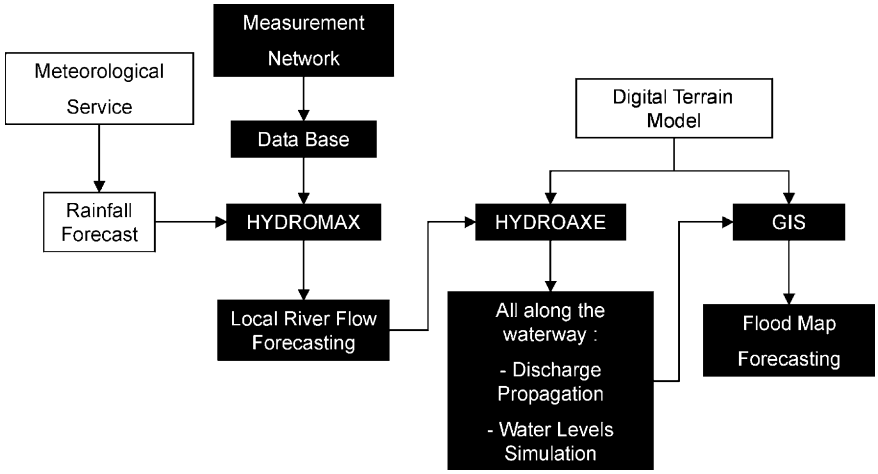

Figure 3. From the measurement network to the real-time flood forecasting.

rivers, specific problems had to be taken into account: shallow depth, obstacles (bridges, trees along the banks, narrow valleys, meanders) for DGPS (Differential Global Positioning System). Swath bathymetry records depth profiles across tracks. Acquisition rates of several profiles per second are achieved. Motion sensors measure the roll, pitch and heave. A gyro gives the heading and RTK (Real-Time Kinematic) DGPS positioning gives a centimetre accuracy. The GPS positioning is combined with inertial navigation or with land survey in areas where obstacles preclude a good reception of GPS signals. The unprocessed profiles are displayed onboard.

The DTM was originally built for hydraulic modelling, but it is also very useful for navigation and dredging operations. The technique is very fast and generates no obstacles for the navigation since the measurements are realised along length tracks.

2.3.2. *Survey of the Valleys*

For the survey of valleys and floodplains (see Figure 5), SETHY implemented airborne laser (LIDAR) which provides a high frequency scanning of the ground (more than five point by square meters). The aircraft is positioned by DGPS and an inertial system records the heading and the movements. In addition to the high acquisition rate and the fairly low cost of this technique, the laser gives a possibility to record several echoes. Frequently, the first and the last echo are recorded (see Figure 5).

This is a major benefit of the technique since it gives a possibility to generate an "envelope" DTM and a "soil" DTM which correspond to the top and the base of the vegetation respectively. The last one will be used in the hydraulic models. No other teledetection system offers this result.

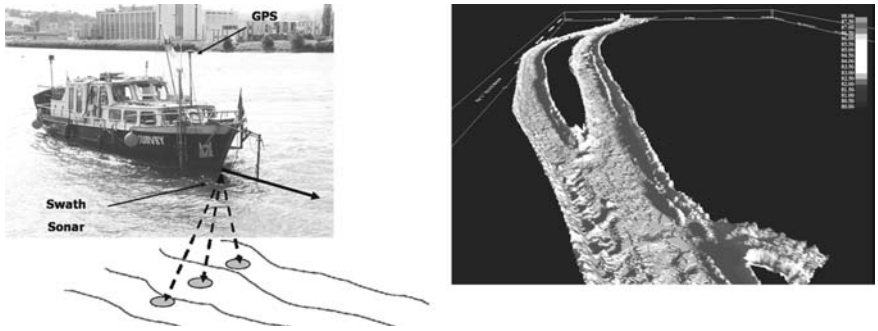

Figure 4. Bathymetric survey with swath sonar.

2.3.3. *Combination of DTM*

The river DTM created by sonar (see Section 2.3.1) and the laser DTM (see Section 2.3.2) can be combined to describe exactly the actual topography of the river with 15 cm of accuracy. SETHY has now the best DTM for any kind of hydraulic models.

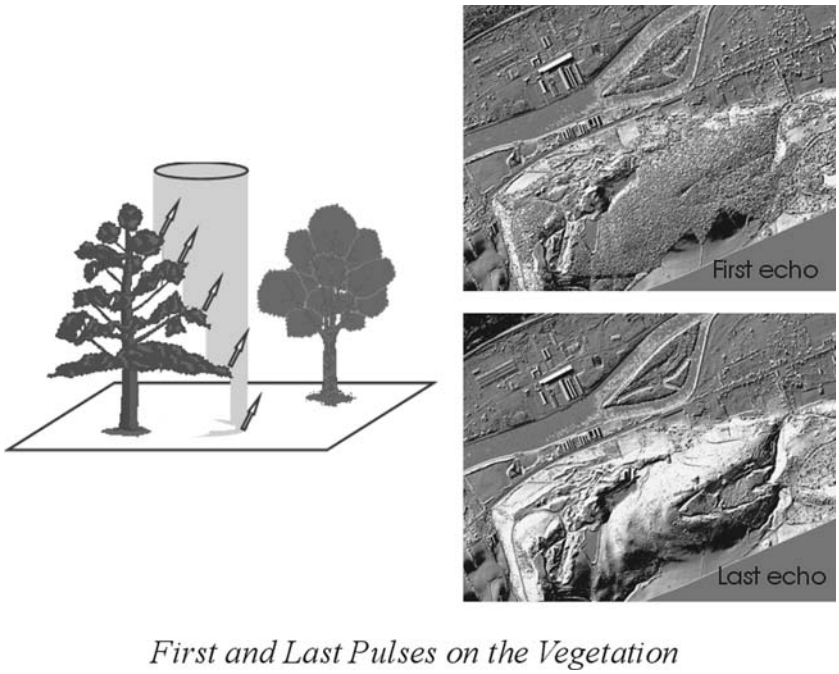

Figure 5. Survey of valleys and floodplains with an airborne laser (LIDAR).

3. Local River Flow Forecasting in Real-Time: HYDROMAX

3.1. INTRODUCTION

The purpose of this section is to give a general description of Hydromax and to demonstrate its performance with a typical example and statistical assessments. Hydromax provides in real-time local river flow forecasting, which is produced by a mathematical model. This model involves four parts.

(1) An optimal minimum variance interpolator which computes the mean areal rainfall on the watershed.
(2) A non-linear conceptual production function which describes the whole watershed as a single macroscopic reservoir. This function computes the effective rainfall from the mean areal rainfall.
(3) A linear ARX transfer function which describes the superficial runoff of the effective rainfall towards the watershed outlet and computes the short term river flow forecasting.
(4) A simulation model which produces long term river flow forecasts from meteorological data.

The identification of the model is quite data saving because only rainfall and river flow measurements are required while a detailed physical description of the basin is not needed. Hydromax has been developed to be user friendly and to fulfil the real-time forecasting requirements. It is successfully in routine operation since January 1995 for the main tributaries of the Meuse river.

Hydromax is directly connected to the hydrological data base of SETHY (see Figure 3). In real-time, about 100 stations of the measurements network scattered in the Meuse basin can be used by Hydromax. The data are collected with a basic time-step of 1 h ($\Delta t = 1$ h). Hourly rainfall and river flow measurements over a period of several years (including big floods) were thus available for the model development. Obviously, the basic time-step Δt must be much smaller than the concentration time of the considered river basins.

3.2. ESTIMATION OF THE MEAN AREAL RAINFALL

The input of the model is the mean areal rainfall over the considered watershed. The possible spatial heterogeneity of the rainfall is thus not taken into account here. The point rainfall depth is denoted $P(z)$ with $z = (x,\ y) \in \mathbb{R}^2$, the Cartesian coordinates. It is assumed to be a realisation of a two-dimensional random field with constant mean and linear variogram. The rainfall measurements are available at n measurement stations. The average areal rainfall PB over a catchment area $\Omega \in \mathbb{R}^2$ is then defined as:

$$\mathrm{PB} = \frac{1}{|\Omega|}\int_{\Omega} P(z)\mathrm{dz} \tag{3.1}$$

As is well known, an optimal (linear, unbiased, minimum variance) estimation of PB can be computed from the set of rainfall observation $\{p_{i,i=1,\ldots,n}\}$ as:

$$\mathrm{PB} = \sum_{i=1}^{n} \lambda_i P_i \tag{3.2}$$

with the λ_i solutions of the so-called "kriging" system (see Bastin *et al.*, 1984, for further details).

3.3. COMPUTATION OF THE EFFECTIVE RAINFALL WITH THE PRODUCTION FUNCTION

The role of the production function is to transform the mean areal rainfall PB into an effective rainfall PN which is supposed to reach the basin outlet as surface runoff. The model describes the balance of water volumes during time intervals Δt. During each time interval the amount of precipitated water is decomposed as follows:

$$\mathrm{PB}(t) = \mathrm{PN}(t) + E_1(t) + W(t) \tag{3.3}$$

with t the discrete time index. $E_1(t)$ represents the part of the rainfall PB(t) that directly evaporates during the current time interval. $W(t)$ represents the amount of water that will not participate in the runoff but will be stored in the basin under various forms (vegetation interception, superficial depressions, soil moisture). The storage of the water in the river basin is then represented by a linear reservoir with inflow $W(t)$ described by the difference equation:

$$S(t) = S(t-1) + W(t) - E_2(t) - I(t) \tag{3.4}$$

where $S(t)$ denotes the stock of water in the river basin, $I(t)$ is the amount of water drained by percolation and $E_2(t)$ is the part of stored water evapotranspirating during the current time interval. The percolation term $I(t)$ is represented by a linear function of the available water stock:

$$I(t) = \alpha(S(t-1) + W(t)) \tag{3.5}$$

with α a specific percolation parameter. The evapotranspiration terms $E_1(t)$ and $E_2(t)$ are computed as:

$$\begin{aligned} E_1(t) &= \min(\mathrm{PB}(t), \mathrm{ETP}(t)) \\ E_2(t) &= \max(0, \min(\mathrm{ETP}(t) - \mathrm{PB}(t), S(t-1) + W(t) - I(t))) \end{aligned} \tag{3.6}$$

where ETP(t) represents an estimate of the seasonal potential evapotranspiration for the considered basin. It is furthermore assumed that there is a physical upper limit $S_{\max}$ of the amount of stored water $S(t)$ in the river basin. The water storage $W(t)$ is then expressed as a function of $S(t)$ and PB(t) in order to:

- guarantee the condition $0 \leq S_{\max}$ for all t,
- verify the hydrological principle that the effective rainfall $\mathrm{PN}(t)$ increases with both rainfall intensity $\mathrm{PB}(t)$ and soil moisture $S(t)$. The following function satisfies these requirements:

$$W(t) = [S_{\max} - S(t-1)]\left[1 - \exp\left(-\beta \frac{\mathrm{PB}(t) - E_1(t)}{S_{\max} - S(t)}\right)\right] \tag{3.7}$$

with β a specific runoff coefficient.

The production function model then involves three parameters (α,β, $S_{\max}$) that have to be calibrated from experimental data for each considered river basin (Wéry, 1990).

3.4. COMPUTATION OF THE SHORT TERM RIVER FLOW FORECASTING WITH A LINEAR TRANSFER FUNCTION

At each time t, a forecasting $\hat{Q}(t+h)$ is computed for the future time instant $(t+h)$ (i.e., with a prediction horizon of h measurement time steps) as a linear combination of past river flow measurements and past effective rainfall values, with a linear regression model (ARX model) of the form (Ljung, 1999):

$$\hat{Q}(t+h) = \sum_{i=1}^{n} a_i Q(t-(i-1)h) + \sum_{j=1}^{m} b_j \mathrm{PN}(t-(j-1)h) \tag{3.8}$$

where $Q(t-(i-1)h)$ denotes the riverflow measurements at the past time instants $(t-(i-1)h)$ while $\mathrm{PN}(t-(j-1)h)$ represents the effective rainfall cumulated over h successive time steps and computed with the production function.

For each river basin, the values of the prediction horizon h and the coefficients a_i, b_j are determined from experimental data. To get accurate forecasts, the prediction horizon h must obviously be smaller than the natural response time of the river basin. As a rule of thumb, it is selected between the one fifth and the one third of the peak time of the unit hydrograph. The dimensions n and m of the regression terms in the model are selected using classical statistical tools of system identification theory (correlogram of prediction errors, Bayesian Information Criterion, etc...) (Ljung, 1999) according to a parsimony principle. The parameters a_i and b_j are calibrated by linear regression.

3.5. COMPUTATION OF LONG TERM RIVER FLOW FORECASTS FROM METEOROLOGICAL DATA

The goal here is to compute river flow forecasts over prediction horizons that are significantly larger than the natural response time of the river basin. This obviously requires to anticipate the future mean rainfall ($\hat{\mathrm{PB}}(t+kh)$). In this

case, it is provided by weather forecast and transformed by the production function (see Section 3.3) in future effective rainfall ($\hat{\mathrm{PB}}(t+kh)$). The long-term river flow forecasts may be then computed by iterating the short-term prediction model (see Section 3.4, equation 3.8).

3.6. MODEL IDENTIFICATION PROCEDURE AND PARAMETER CALIBRATION

In order to identify a forecasting model for a given river basin, a set of rainfall – riverflow data must be available for a significant period of time involving floods as well as low water periods. The identification procedure can then be summarized in seven steps as follows:

(1) Computation of the mean areal rainfall PB(t) by kriging for each time step t.
(2) Computation of the unit hydrograph by spectral analysis of the data.
(3) Selection of the short term prediction horizon (see Section 3.4).
(4) Resampling of the data according to the selected short term prediction horizon.
(5) Using the data from flood periods only, identification of the dimensions n and m of the transfer function under the assumption that the effective rainfall PN is (almost) equal to the total rainfall PB.
(6) From the whole set of data, calibration of the parameters ($\alpha, \beta, S_{\max}$) by non-linear optimization and (a_i, b_j) by linear estimation, in order to minimize the mean square prediction error.
(7) Validation of the model with a new set of data that were not used in the previous steps.

3.7. AN EXAMPLE: THE FLOOD OF FEBRUARY 2002

In this section, the Hydromax performance is illustrated with a typical forecasting example in the Ourthe River basin (see Figure 1). The outlet of the river basin is located at Tabreux (1607 km^2) and four raingauges are available. Hourly rainfall-discharge data during 2 years (1992–1993) have been used to calibrate the model. The estimated model parameters are given in Table I. The selected predicted horizon is $h = 6$ h.

The predictive capability of the model is here illustrated with the flood of February 2002 (which is not in the data set used for model calibration). In Figure 6, a typical example of on-line forecasting with Hydromax is shown. We can see that Hydromax computes a short term prediction for 10 a.m. of 233 m^3/s (* in Figure 7), which is to be compared to the actual value of 160 m^3/s. Hydromax also computes a long term prediction over an horizon of 42 h (+ line) for the given scenario of future rainfalls and an "optimistic" prediction (o line) under the assumption that the rainfall will definitely stop.

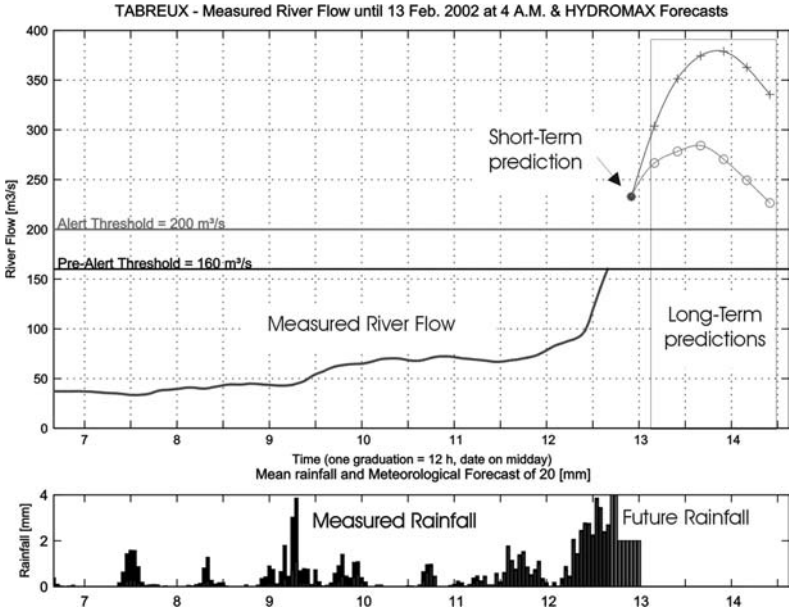

Figure 6. Example of Hydromax window: forecasting of Ourthe river (a Meuse river Tributary). Flow rate during the big flood of February 2002 (from 7 to 14 February).

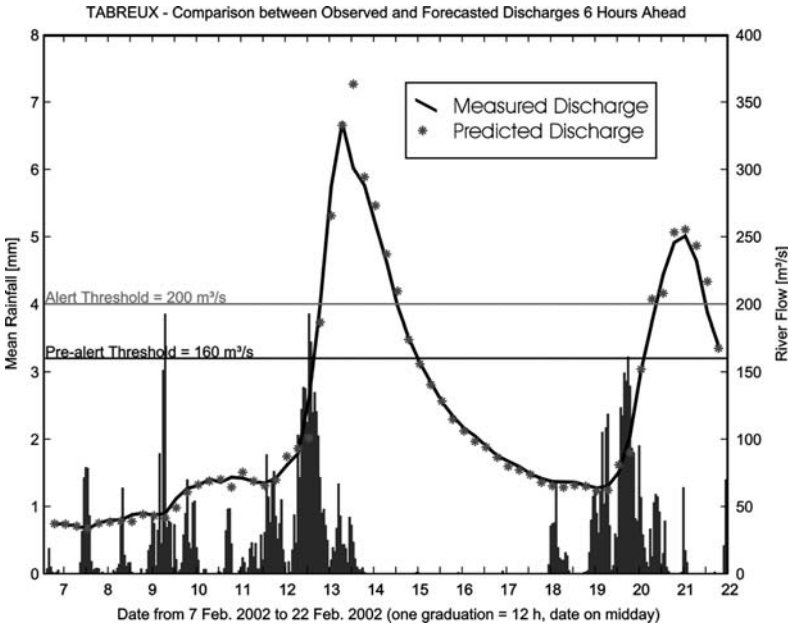

Figure 7. Tabreux-comparison between observed and forecasted discharges during the big flood of February 2002.

Table I. Tabreux-parameters of the model

α	β	$S_{\max}$ *[mm]*	a_1	a_2	b_1	b_2	b_3	b_4
0.00065	0.86	76	1.353	−0.41	2.382	0.896	0.202	0.993

Table II. Upper bound of the forecasting relative error at a level of 90%

Horizon	6 h ahead	12 h ahead	18 h ahead	24 h ahead	30 h ahead
$\left\|1-\frac{\hat{Q}}{Q}\right\| \leq$	0.07	0.13	0.18	0.22	0.32

In Figure 7, a comparison between the observed river flow discharges and the short-term predictions all along this flood of February 2002 is presented. Finally the statistical accuracy of Hydromax at a level of 90% is illustrated in Table II.

4. Real-Time Computation of Discharge Propagation and Water Levels: HYDROAXE

4.1. MATHEMATICAL MODEL

Hydroaxe is designed for real-time utilisation and flood forecasting. The mathematical model is thus a one-dimensional model, based on the Saint-Venant shallow-water Equations (4.1) and (4.2), in order to meet the short computation time requirements.

Mass conservation:

$$\frac{\partial A}{\partial t}+\frac{\partial Q}{\partial x}=L\frac{\partial h}{\partial t}+\frac{\partial Q}{\partial x}=L\frac{\partial z}{\partial t}+\frac{\partial Q}{\partial x}=0 \tag{4.1}$$

Momentum conservation :

$$\frac{\partial Q}{\partial t}+\frac{2Q}{A}\frac{\partial Q}{\partial x}-L\frac{Q^2}{A^2}\frac{\partial h}{\partial x}-\left.\frac{Q^2}{A^2}\frac{\partial A}{\partial x}\right|_{h=cst}+gA\frac{\partial z}{\partial x}+gAs_f=0 \tag{4.2}$$

where Q = discharge, A = cross section area, h = water depth, L = width of the section at the water level, z = level of the bottom, g = gravity constant and s_{f} = the friction slope.

The Saint-Venant equations are completed by the Exchange Discharge Model (Bousmar and Zech, 1999), which includes the effects of the momentum exchanges between the river and the floodplains:

Mass conservation:

$$\frac{\partial A}{\partial t}+\frac{\partial Q}{\partial x}=q_{\mathrm{l}}=q_{\mathrm{in}}-q_{\mathrm{out}} \tag{4.3}$$

Momentum conservation:

$$\frac{\partial}{\partial t}(\rho AU) = -\frac{\partial}{\partial x}\left(\rho AU^2\right) - \rho gA\frac{\partial z}{\partial x} + \rho q_{\text{in}} u_{\text{l}} - \rho q_{\text{out}} U - \rho gAs_{\text{f}} \quad (4.4)$$

where q_{l} = lateral discharge, q_{in} = inflow component of the lateral discharge, q_{out} = outflow component, ρ = density of water, $U = Q/A$ = mean velocity, u_{l} = velocity component of the lateral inflow in the direction of the main flow. These two equations are solved with an implicit Preissmann scheme allowing rather large time steps.

4.2. GEOMETRICAL MODEL

The Meuse is considered as a network composed of elements such as ''elementary reaches'', ''weirs'', ''junctions'', ''hydrographs'' and ''limnigraphs''. Each element is represented by equations describing the relation between the water-level and the discharge evolution between two cross-sections, such as Equations (3) and (4) for the ''elementary reach'' elements (see Figure 8).

4.3. HYDROAXE DATA

First of all, Hydroaxe needs data describing the geometrical aspects of the problem. The 1D formulation of the model requires 1D data, i.e., cross-section profiles, derived from a DTM. This DTM is elaborated with a GIS (ArcView 3.2a GIS), and from the dense and accurate laser and sonar measurements of the topography (see Section 2.3). It is completed by delineating the bank limits and the flow limits, to separate the minor bed from the floodplains. Cross-sections are then computed. One cross-section profile every hundred metres seems enough to yield an accurate forecasting.

The cross-sections derived from the DTM are corrected: obstacles like the trees eventually detected by the laser are erased, and the gaps/bumps above the water level are filled/cut to avoid too many flow separations (see Figure 9a). They are also simplified: the number of points is decreased to allow a faster computation and to satisfy the real-time requirements of the model (see Figure 9b).

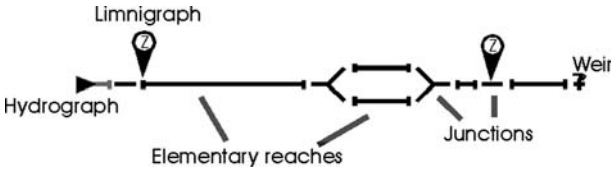

Figure 8. Geometrical network of a reach.

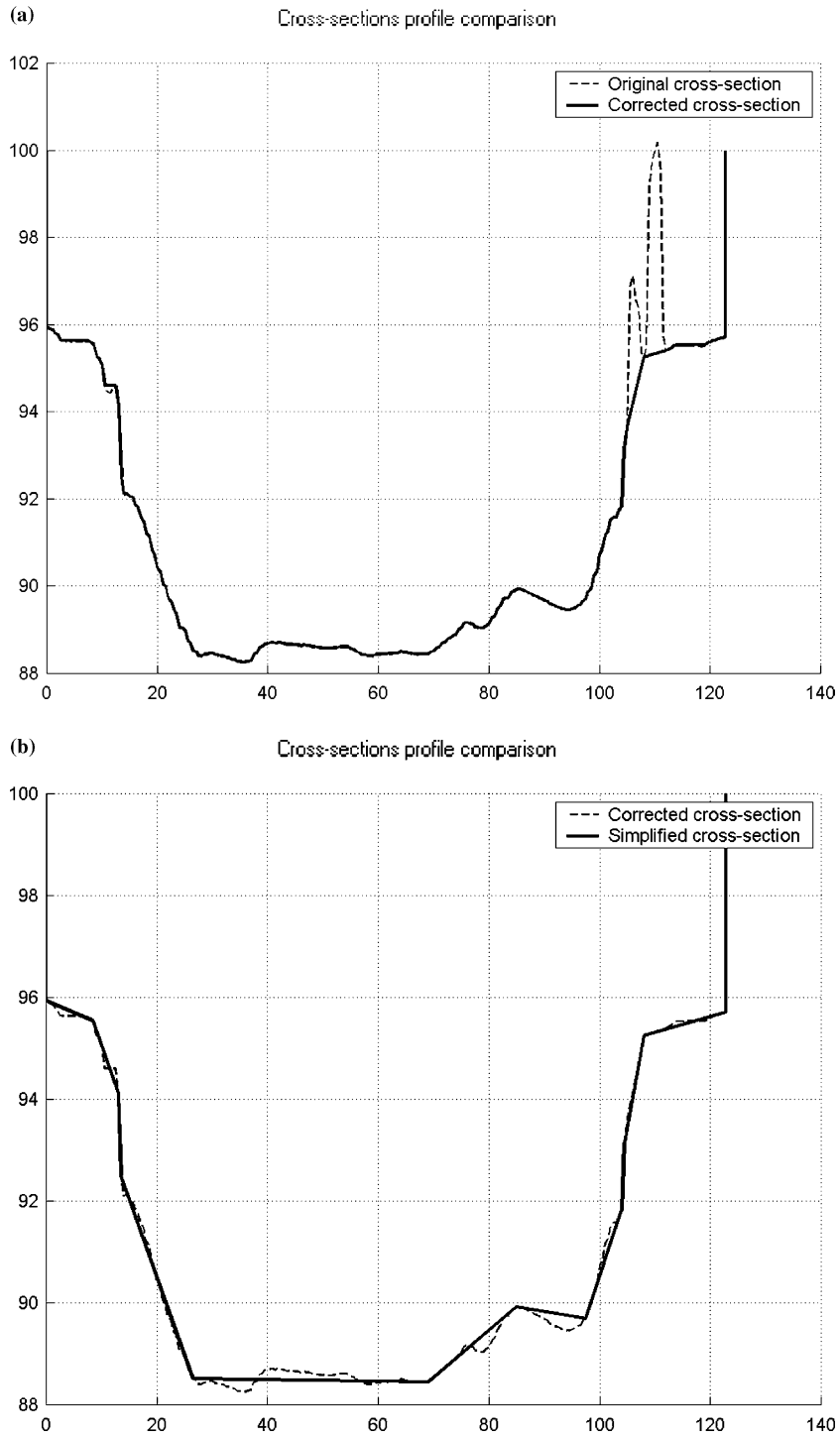

Figure 9. (a) Corrected cross-section. (b) Simplified cross-section.

Hydroaxe needs a set of discharges as upstream condition (measured in Chooz, see Figure 1) at the start of the Belgian Meuse network (French-Belgian border), and for its eight major tributaries. These discharges are produced by Hydromax, as explained in Section 3. The historic (= measured) part of these discharges covers 48 h, and the forecasting spreads on 18 h more. The discharges are injected in the model with some delay, corresponding to the flow time between the available hydrologic stations and the confluences of the tributaries (see Figure 1).

The downstream condition of Hydroaxe, i.e. the downstream water level, is given by the 48 last hourly level measurements at the downstream limit of the network (Ivoz; see Figure 1). The 18 next hourly levels needed by Hydroaxe are an average of the last 5 hourly measurements in Ivoz. Actually, simulations have shown that the downstream water level has little influence on the computed water levels except for the last downstream kilometres.

Several water-level stations are available along the Meuse river. The measured levels are introduced in Hydroaxe as controls and comparison tools for the user. This set of data is transmitted to Hydroaxe by Hydromax.

4.4. CALIBRATION

The major difficulty of practical use of Hydroaxe is the determination of the Manning's roughness coefficients for the main channel and the floodplains. This calibration requires three sets of data: an accurate measurement of the upstream discharge, the limnigraphs of the downstream and upstream water levels, for the concerned reaches. The first step consists in calibrating the roughness coefficient $n_{\min}$ of the main channel: the upstream discharge and the downstream water level are used by Hydroaxe to compute the upstream water level. The coefficient $n_{\min}$ is adapted until the difference between the computed and measured upstream water levels is minimised.

Once the roughness of the main channel is calibrated, the same process is applied to find a value n_{maj} for the floodplains. But this requires of course a flood event causing significant overflows. These operations have to be repeated each time that the minor bed geometry is changed (natural changes or dredgings).

4.5. THE HYDROAXE PROGRAM AND ITS RESULTS

The Hydroaxe user interface has been developed on a Unix platform using Matlab. Nevertheless, its computation kernel, named CatRiv (*CAlculation of Transients in RIVers*), is implemented in C++ language. Hydroaxe allows the user to choose the results he wants to produce with CatRiv, to visualize these results, and to store the water levels required for the computation of flooded areas with ArcView GIS.

Figure 10 represents a typical result window of Hydroaxe. For each selected cross-section (like Waulsort and Lustin in Figure 10), the user can observe the evolution of the water level and of the discharge for the 66 h of simulation. If water level and/or discharge measurements are available in this cross-section, it can also be displayed and compared with the model results. The 18 last hours of computation are the forecasted part of the results. It is of course the most useful information for SETHY to manage the flood event. Hydroaxe offers also the possibility to visualize the evolution of a water profile in a chosen reach. This evolution is illustrated by a movie of 66 images (1 per h), showing the bed of the river and the water level evolution.

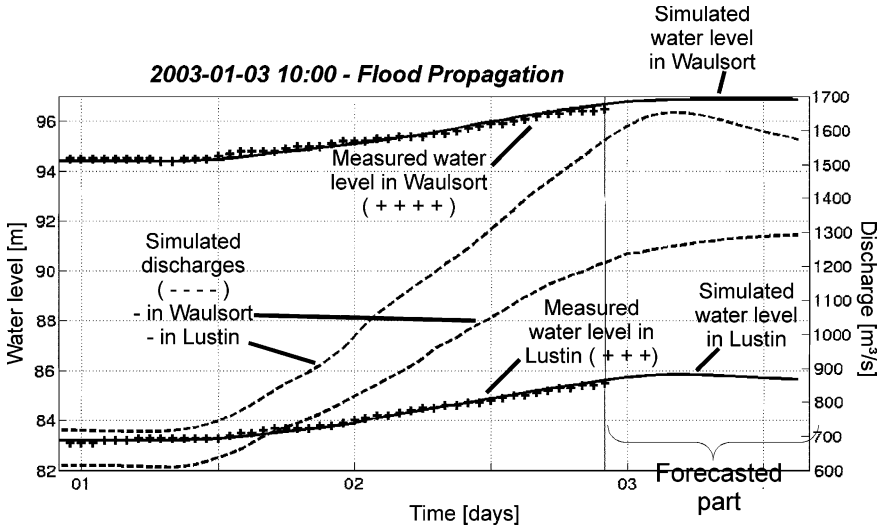

Figure 10. Hydroaxe result window: measured and simulated water levels in Waulsort and Lustin (2003-01-03).

5. Real-Time Computation of Flooded Areas with a GIS

5.1. INTERPOLATION OF WATER LEVELS

When the user works with Hydroaxe, he has the possibility to choose the moment and the reaches for which he wants to visualize the flooded areas. Hydroaxe can therefore transmit the needed water levels on the appropriate directory on the network. A separate computer can then carry out the treatment of these data with ArcView GIS.

The water level of each cross-section is extrapolated to five points of the sections: the intersection of the cross-section with the middle axis, with the bank limits and with the flow limit of the floodplains (see Figure 11). Then, these levels are interpolated and extrapolated to produce a water table. The interpolation is executed reach by reach, with the ArcView interpolation

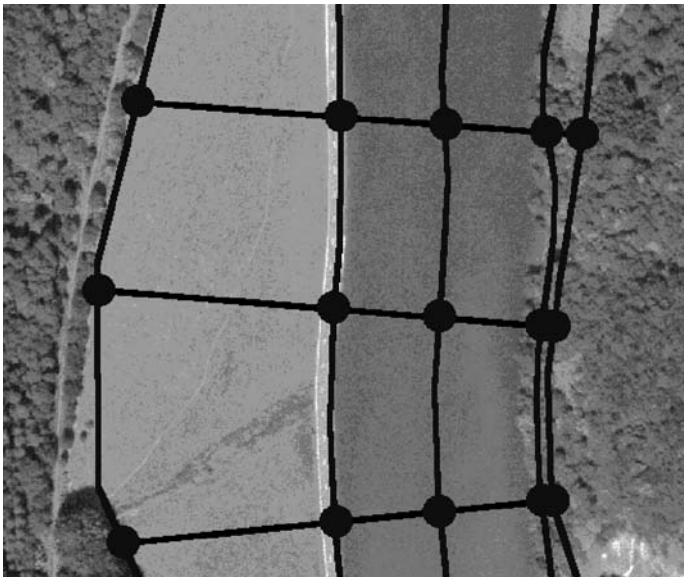

Figure 11. Five points of interpolation per cross-section.

procedures. A ''tension spline'' method of interpolation has been chosen, in order to minimize the curvatures and the slopes of the water surface.

5.2. COMPARISON WITH THE DIGITAL TERRAIN MODEL

Each reach of the model is represented by a digital model, based on sonar and laser surveys. These DTMs are grids of square cells, as well as the water tables. It is thus easy to produce the grid of the flooded areas of a reach: the DTM levels are subtracted from the water levels. Figure 12 shows a part of a DTM, i.e., the combination of the laser measurements (floodplains) and of the sonar measurements (main channel).

The map of flooded areas (see Figure 13) is corrected by the pointing of potentially flooded zones, i.e., the zones which are below the level of the water but separated from the river by natural or artificial obstacles.

5.3. VISUALIZATION

Besides the grid of the flooded areas, the user can display other useful information (ortho-images, the DTM and geographical maps) for a better identification of the location of risk. The flood map is accompanied by an adequate legend of the water depth.

This ArcView procedure has been designed to allow different resolutions of the final interpolated grid: cells from 2 to 10 m. The bigger cells require less computation time and are appropriate in crisis situations and very short-

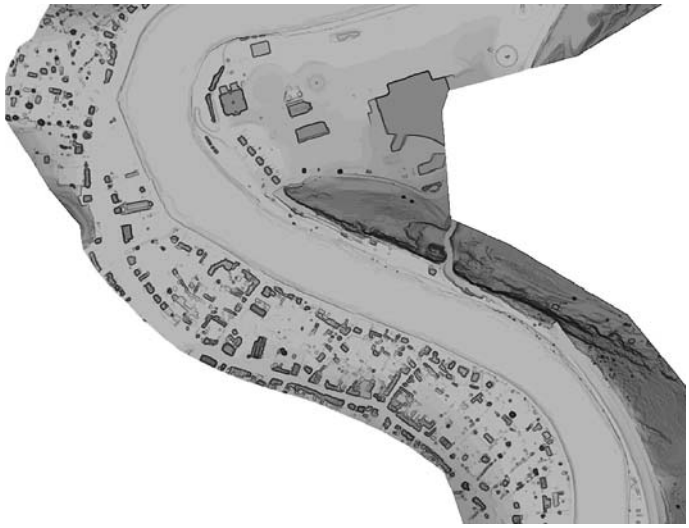

Figure 12. DTM example.

Figure 13. Flooded areas – typical results with ArcView GIS.

term forecasting. But the smallest cells are useful to produce more accurate flood maps for long-term projects.

6. Conclusion and Perspectives

Since their implementations at the crisis centre of SETHY, Hydromax and Hydroaxe have been successfully used to produce respectively, local river

flow forecasts and simulations of discharge propagation and water levels all along the Meuse river.

The integration of these two real-time applications with an accurate DTM used by a GIS, forms an integrated tool to provide real-time flood-map on the Belgian Meuse. With this decision aid tool, SETHY is able to predict and to manage efficiently the consequences of a flood event. The coupled Hydromax and Hydroaxe models were used during the last two significant floods of the Meuse river, in February 2002 and January 2003. The water levels computed in January 2003 for the cities of Waulsort and Lustin are shown in Figure 10, illustrating the satisfactory behaviour of the models concerning the dynamics of the flood. The accuracy of the water levels could be improved, but is quite acceptable.

At the moment, one of the major limitations of the model application is the lack of accuracy on the upstream boundary condition (discharge at the French-Belgian border), which will be soon filled up with the setting up of a new flowmeter in Waulsort (see Figure 1). These new data should also allow a calibration of the Manning's coefficients, in order to improve the water level forecasting.

A next development will be the integration of automatic weather forecast in Hydromax, and the use of real-time rain data provided by weather radars. In fact, the rainfall, on a basin base, predicted by the Aladin-Belgium meteorological model (IRM – Belgian Royal Meteorological Institute) will soon be automatically full-integrated in the data base of SETHY.

Recently, all the weirs of the Meuse have been provided with sensors, giving in real-time the positions of the gates and the flapgates. These data are transmitted to SETHY and integrated in the database. Hydroaxe is then able to calculate the water level and the discharge passing through each weir. The next challenge is to take into account the programming of the controllers governing the moves of the gates. This will improve the efficiency of the model for the 18 h of prediction.

References

Adriaensen, C.: 2001, Modèle de prévision d'axes hydrauliques de crue sur la Meuse wallonne et la Haute Sambre. Université Catholique de Louvain.

Bastin, G. and Moens, L.: 2000, Hydromax: A real-time application for river flow forecasting. *Int. Symp. River Flood Defence, Kassel* **1**, D-33–D-40.

Bastin, G., Lorent, B., Duqué, C., and Gevers, M.: 1984, Optimal estimation of the average areal rainfall and optimal selection of raingauge locations, *Water Resour. Res.* **20**(4), 463–470.

Bousmar, D. and Zech, Y.: 1999, Momentum transfer for practical flow computation in compound channels, *J. Hydraul. Eng.* **125**, 696–706.

Dal Cin, C.: 2002, Marché de services pour l'étude de l'implantation d'un système de visualisation des prévisions de zones inondables de la Meuse en cas de crue. Université Catholique de Louvain.

Ljung, L.: 1999, *System Identification – Theory for the User*, 2nd edn, Prentice Hall, Upper Saddle River, NJ.

Moens, L. and Bastin, G.: 1995, Rapport final dans le cadre de la convention de recherche et d'étude pour l'application de modèles mathématiques prévisionnels des débits de crue et leur mise en oeuvre informatique. Université Catholique de Louvain.

Scherer, R.: 1999, Réalisation d'un modèle de prévision d'axes hydrauliques de crue sur la Haute Meuse wallonne. Université Catholique de Louvain.

Wéry, B.: 1990, Identification des systèmes hydrologiques – Application à la prévision des crues. PhD thesis, University of Louvain-la-Neuve.

Natural Hazards (2005) 36: 257–271

Flood Forecasting and Flood Warning in the Firth of Clyde, UK

YUSUF KAYA*, MICHAEL STEWART and MARC BECKER
16 Carrick Drive, Mount Vernon, Glasgow G32 0RW, UK

(Received: 18 November 2003; accepted: 30 June 2004)

Abstract. Coastal flooding has caused significant damage to a number of communities around the Firth of Clyde in south-west Scotland, UK. The Firth of Clyde is an enclosed embayment affected by storm surge generated in the Northern Atlantic and propagated through the Irish Channel. In recent years, the worst flooding occurred on 5th January 1991 with the estimated damage of approximately £7M. On average, some £0.5M damage is caused each year by coastal flooding. With the latest climate change predictions suggesting increased storm activity and the expected increase in mean sea levels, these damages are likely to increase. In line with the expansion of flood warning provision in Scotland, the Scottish Environment Protection Agency (SEPA) has developed a flood warning system to provide local authorities and emergency services with up to 24 h warning of coastal flooding within the Firth of Clyde and River Clyde Estuary up to Glasgow City Centre. The Firth of Clyde flood warning system consists of linked 1-D and 2-D mathematical models of the Firth of Clyde and Clyde Estuary, and other software tools for data processing, viewing and generating warning messages. The general methodology adopted in its implementation was developed following extensive consultation with the relevant authorities, including local councils and police. The warning system was launched in October 1999 and has performed well during four winter flood seasons. The system currently makes forecasts four times a day and is the only operational coastal flood warning system in Scotland.

This paper summarises the development of the warning system, gives a review of its operation since its launch in 1999 and discusses future developments in flood warning in Scotland.

Key words: flood forecasting, flood warning, tides, surges, numerical modelling

1. Introduction

Following the flooding in January 1991 SEPA, (the then Clyde River Purification Board) immediately commissioned an initial study (Townson and Collar, 1993) to assess the frequency of flooding and associated cost of damage at several sites within the Firth of Clyde area.

The initial study (Townson and Collar, 1993) investigated the damage caused by flooding in four locations: Tarbert, Rothesay, Dumbarton, and Saltcoats (see Figure 1). The study estimated an average annual flood damage

* Author for correspondence. E-mail: yusuf_kaya@msn.com

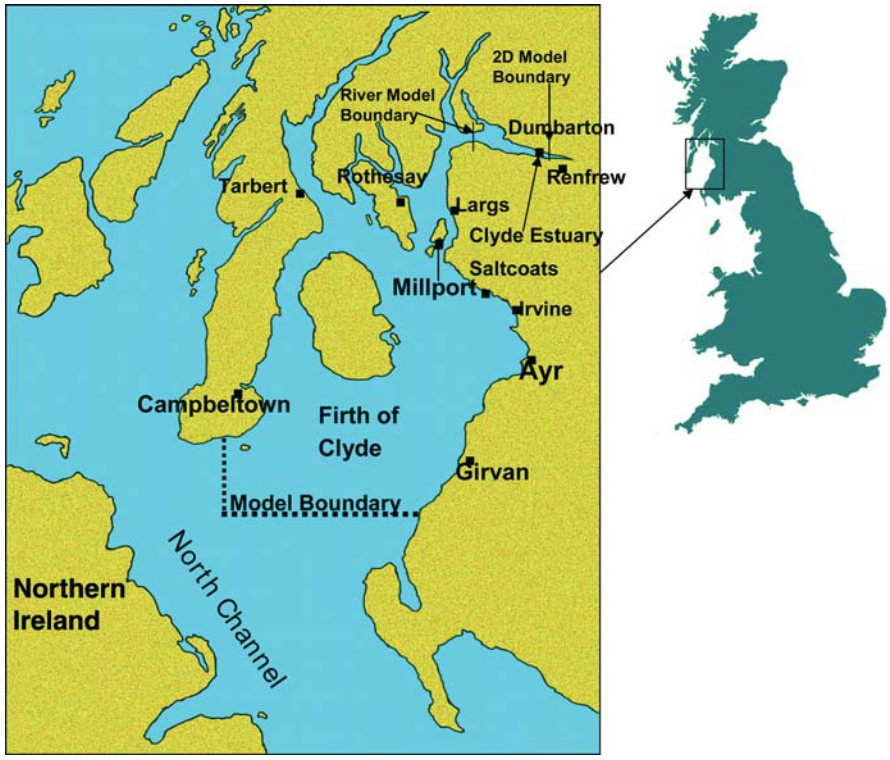

Figure 1. Location plan.

cost to property around the Firth of Clyde to be in excess of £0.45M (Townson and Collar, 1993) (based on 1999 costs). This was based on using published data on flood damage costs per unit area of property affected (FLAIR, 1990).

It was estimated that the average benefit that would be gained by the provision of a Flood Warning System, for the above locations alone would be in the order of £158,000 per annum (based on 1993 figures). The conclusion of the study was that a significant proportion of the flood damage cost could be saved by the provision of a flood warning system. This prompted SEPA to proceed with a further study (Firth of Clyde Modelling Study, 1996) to assess the practicalities of storm surge modelling in the Firth of Clyde. Although the UK Continental Shelf model covers the Firth of Clyde area, its representation of the upper parts of the Firth is crude due to its large grid size. Following the successful outcome of the initial modelling work, SEPA decided to set up a coastal flood warning system covering the entire Firth of Clyde and part of Clyde Estuary up to Glasgow City Centre which is about 15 km east of Renfrew. The system was developed in 1999 and has been operational since 1 October 1999.

The earlier work relating to the development and operation of the scheme was reported elsewhere (Townson *et al.*, 1994; Collar *et al.*, 1995; Becker and Kaya, 2000; Becker *et al.*, 2000; Burns *et al.*, 2000).

2. SEPA's Role in Flood Warning

In Scotland the provision of flood warnings is a discretionary function of SEPA. In recognition that other organizations, including local authorities and the various emergency services, also have key roles to play during flood events SEPA developed a Flood Warning Strategy (Policy No. 34) which sets out the levels of service offered by SEPA (sepa.org.uk).

In November 2001, SEPA extended the successful 'Floodline' service from England and Wales to Scotland. Although not a statutory duty, flood warning is a high profile activity for SEPA and over the years an increasing number of local authorities and the public have come to rely upon the service provided.

Floodline allows users access, via the telephone (0845 988 1188) or web site (sepa.org.uk), to general flood alerts, 'Flood Watch', or any locally specific flood warnings that may be in force. Floodline also provides information and advice on how to prepare for flooding.

The introduction of Floodline in Scotland, the setting up of the National Flood Warning Development Team and the appointment of a full time Flood Awareness Public Relation (PR) Officer shows SEPA's commitment to improving flood warning in Scotland.

3. Flood Forecasting System Development

3.1. WARNING SYSTEM

The Firth of Clyde flood warning system was developed after extensive consultation with various parties including the relevant Local Authorities, Police, Fire Brigade and the Maritime and Coastguard Agency. The coastal area covered by the scheme falls within seven local authorities. These are Argyll and Bute, North Ayrshire, South Ayrshire, Inverclyde, West Dunbartonshire, Renfrewshire, and Glasgow City.

At SEPA's request, local Councils provided threshold levels at 42 critical locations where flooding were known to occur. These included those areas with a known history of flooding such as Tarbert, Rothesay, Saltcoats, and Dumbarton. The threshold levels were the current defence levels when overtopped flooding of properties or public services would occur. All 42 locations were included in the warning system. However, other areas, not identified at present, maybe at risk from higher surges could be added to the system in future if required.

A schematic overview of the Firth of Clyde Flood Warning System is shown in Figure 2. The main elements of the Flood Warning Scheme are:

- receipt of forcing data from Met Office (predicted surge and wind),
- a linked mathematical modelling system of Firth of Clyde and Clyde Estuary,
- data visualisation,
- pager alarm,
- fax generation.

The predicted surge data at the North Channel and predicted wind data representing the Firth of Clyde area (speed and direction) is automatically received from the Met Office through MIST (Meteorological Information Self Briefing Terminal), for a fixed period of 36 h commencing at 00.00 GMT and 12:00 GMT each day. This data is produced by the UK Continental Shelf model and Met Office atmospheric model respectively. The forecast data, in the form of hourly values, is received by SEPA at 03:00, 09:00, 15:00 and 21:00 GMT each day respectively.

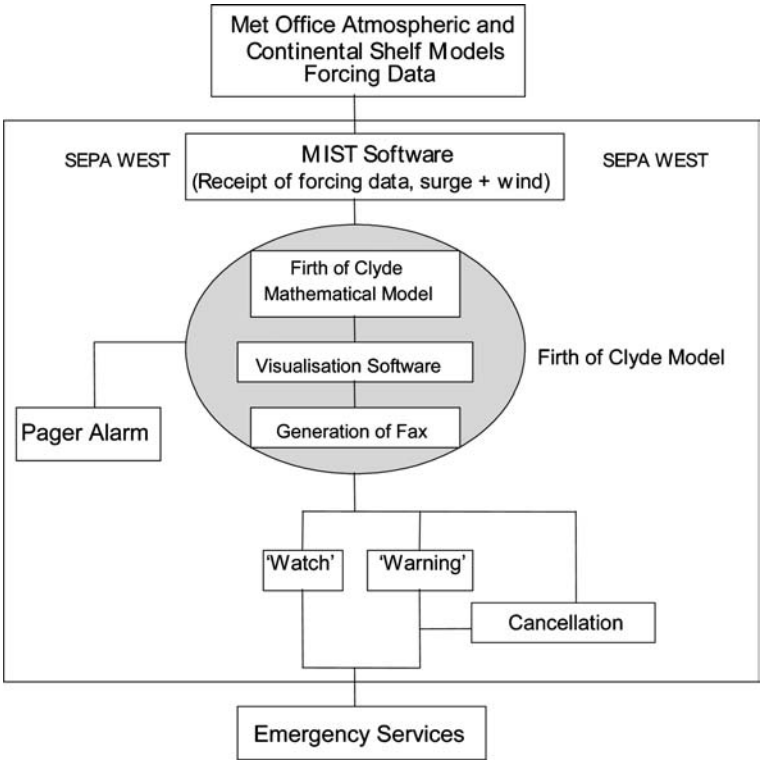

Figure 2. Schematic overview of Firth of Clyde flood warning scheme.

The surge and wind data received is then automatically passed to the mathematical model for forecasting of tide levels within the model boundaries. The process is described below.

3.2. HYDRODYNAMIC MODELLING SYSTEM

The entire Firth of Clyde has been modelled using the FLOFIELD two-dimensional modelling system (a derivative of the DIVAST (Falconer, 1986) software package). DIVAST (Depth Integrated Velocity And Solute Transport) is widely used for modelling coastal waters where stratification is insignificant. FLOFIELD is the hydrodynamic part of DIVAST. The two-dimensional model covers the entire Firth of Clyde and lower parts of the Clyde Estuary and is based on uniform 500 m grid spacing.

A one-dimensional numerical model of the Clyde Estuary was previously set up for another study. The model was based on in-house river modelling software package FLOODTIDE which is based on the solution of Saint-Venant equations for shallow water waves using finite difference techniques. The average cross section spacing is 300 m.

The two models were linked together to form a single modelling system covering the entire Firth of Clyde and Clyde Estuary up to Glasgow (i.e. from the North Channel in the Irish Sea to Glasgow City Centre, including the sea lochs/fjords). The linking of the two models eliminated the need for a physical boundary between the two models in the Greenock area.

The models overlap over a distance of about 24 km as shown in Figure 1 (distance between the river model and 2-D model boundaries). This was necessary to allow smooth transition of water level predictions from one model to the other at their boundaries at each time step. Boundary conditions at the furthest downstream section of the river model are based on the predicted water levels from the two-dimensional model at that point. Similarly, boundary conditions at the eastern open boundary of the two-dimensional model are based on the predicted water levels from the river model. At the start of each time step this information is exchanged between the two models and the models are run consecutively.

The linked model is driven by tidal variations (astronomical tide and surge) at the boundary in the North Channel, fluvial flow input at the tidal limit of the Clyde Estuary, and wind data (speed and direction) representing the Firth of Clyde area.

An L-shaped open boundary was chosen at the North Channel to allow flexibility during model calibration in adjusting water level variations along both boundaries and also allowing small phase differences between the two boundaries. Test runs were carried out using a number of phase differences and water surface slopes along both boundaries. Although no phase difference was introduced between the two boundaries in the final calibrated

model, water surface elevation was adjusted along each boundary to take Coriolis effects into account (Falconer, 1986).

The astronomical component of the tide in the North Channel is calculated automatically within the modelling software using 97 harmonic constants representing astronomical tides in Campbeltown and Girvan (i.e. at the two ends of the model boundary shown in Figure 1). The forecast surge levels in the North Channel and corresponding representative wind speed and direction data are provided by the Met Office for a 36 h period and received through MIST. The surge data is then combined with astronomical tide and the combined level is used as open boundary conditions along the L-shaped boundary at the North Channel. Wind data is used to calculate shear stress on the free surface.

At present the fluvial data at the tidal limit upstream of Glasgow is set to a constant average flow. There are two reasons for this: firstly there is no forecast fluvial flow data available at the tidal limit, and secondly variation in fluvial flows in this location would not significantly affect the model predictions within the area of interest (i.e. Glasgow city centre and downstream). However, the system has been designed in a modular way, which makes it suitable for the inclusion of any number of forecast river flow data if such information becomes available in future.

The model bathymetry was obtained from relevant Admiralty charts. Model test runs carried out subsequently indicated that model predictions are not sensitive to bathymetry.

In order to provide data for model calibration and verification and also for assessing model performance, a number of tide gauges were installed in the Firth of Clyde by SEPA. These are located at Tarbert, Rothesay, Campbeltown and Girvan. These gauges, together with the existing tide gauges at Millport, Ayr Harbour, and subsequently installed Renfrew tide gauge, provide a good coverage of water level and tidal propagation within the Firth of Clyde area. The gauge data at Campbeltown and Girvan allows comparison to be made with the forecast surge data at the model boundary in the North Channel received from the Continental Shelf Model.

Model calibration and verification was carried out against a number of recent surge events for which relevant data was readily available. Some of the model results are given in Tables I and II. At all locations the average difference between the predicted and recorded tide levels was well within the target value of ± 0.1 m if there were no gross errors in the boundary surge forecast received from the Met Office.

The model results indicated that the accuracy of model predictions is strongly dependent on the accuracy of the surge data applied at the open boundary in the North Channel. Using recorded surge levels at Campbeltown and Girvan as boundary data produces very good match with recorded data at other tide gauge locations within the Firth, as shown in Table I and

Table I. Difference between model predicted and recorded peak water levels and their timings at a number of locations within Firth of Clyde for the 22 February–1 March 1997 event (boundary conditions were based on recorded tide levels at Girvan and Campbeltown)

Location	Difference in	
	Water level (m)	Timing (min)
Ayr	±0.04	±15
Millport	±0.06	±15
Rothesay	±0.05	±15
Tarbert	±0.05	±15

Table II. Difference between model predicted and recorded peak water levels and their timings at a number of locations within Firth of Clyde for three surge events (boundary conditions were based on Met Office forecast surge levels combined with astronomical tides)

Event	Location	Difference in	
		Water Level (m)	Timing (minutes)
January 1995	Millport	±0.2	±15
	Rothesay	±0.2	±15
	Tarbert	−0.3	±15
December 1994	Millport	−0.15	±15
	Rothesay	±0.1	±15
8–12 February 1997	Girvan	±0.05	±15
	Rothesay	±0.1	±15

Figure 3a. Larger differences were predicted when the Met Office predicted surge data was used to determine the conditions along the southern open boundaries as shown in Table II.

A discrepancy was observed at Renfrew between the model predictions and recorded tide levels for some tidal events as shown in Figure 3b for the December 1998 event. In these limited number of cases the recorded data showed a double peak which the model has failed to reproduce.

Further investigations were carried out and the model was subsequently refined. This involved the extension of the two-dimensional model further into the Clyde Estuary, and also increasing the resolution of the river model over the area where the two models overlap to better represent the complex nature of the flooding and drying processes in this area. The refined model appears to reproduce the double peak at Renfrew as shown in Figure 4.

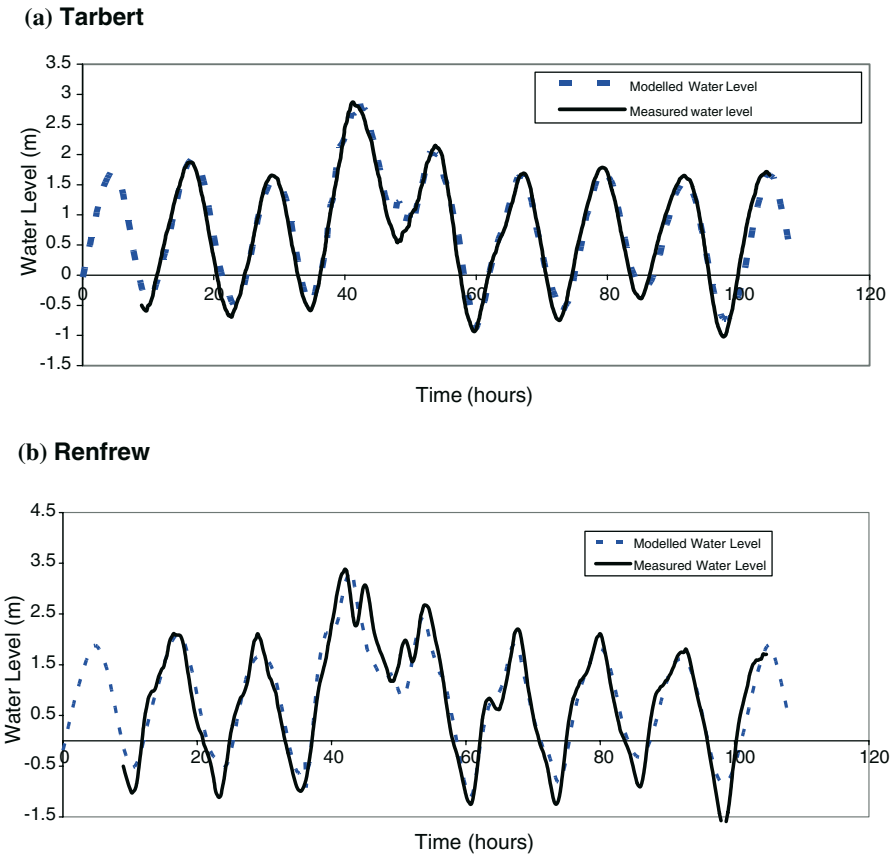

Figure 3. Comparison of predicted and observed water levels at Tarbert and Renfrew for the December 1998 surge event (a) Tarbert; (b) Renfrew.

Recent studies of surges within the Firth of Clyde indicate that up to one third of the surge arriving at the upper parts of the Clyde could be generated within the Firth itself. This indicates the importance of a detailed model to represent local conditions accurately, particularly within the inner Firth, where the topography of seabed is more complex. The current model appears to represent local hydrodynamic conditions well.

3.3. SYSTEM OPERATION

The warning system is online at all times and regularly checks the arrival of new surge and wind data. This is done by checking the last update date and time of two text files containing forecast surge and wind data. As soon as the arrival of new data is detected the system automatically reads this data, prepares all the appropriate data files and triggers the linked modelling

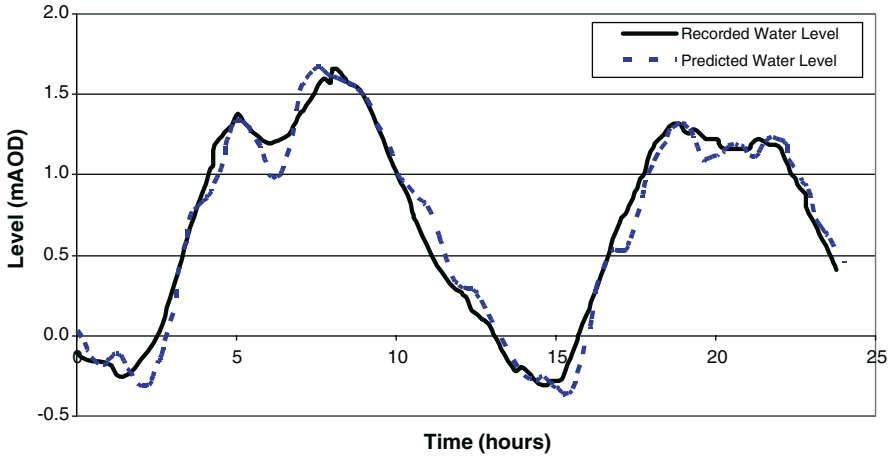

Figure 4. Comparison of predicted and observed water levels at Renfrew for the February 2000 surge event (refined model).

system to run for a 36 h simulation period representing the surge forecast period. The results for the first 6 h of the run are ignored by the warning system as they mostly correspond to the time already elapsed (due to data being received three hours late and time spent for data processing and model run, etc.). Once the run is complete a pager message is automatically issued to SEPA duty officers if any flooding or risk of flooding is predicted. The duty officer, having received the message on his pager, can then access the warning system through his portable computer and interrogate the model results. If no risk of flooding is predicted no pager messages are issued and the system awaits the arrival of next set of data from the Met Office.

The main controlling software of the warning system has been developed using Microsoft Excel, combining Visual Basic applications, DOS Windows, and Microsoft-Word word processing package for the preparation of warning messages. A facility exists within the system for displaying a general map of the Firth of Clyde area showing the colour coded model predictions at all critical locations. The locations where no flood risk is predicted are shown in *green*, locations where direct flooding is predicted are shown in *red*, and locations where the predicted level is approaching the predefined critical level for flooding (usually within 0.3 m) is shown in *amber*.

Having seen the overall map of the Firth to determine if any risk of flooding is predicted, the duty officer, if he wishes, can then access more detailed information for each of the affected areas. This includes plots showing predicted water level and critical level for flooding at each location. The plots for critical locations falling within the same Council boundaries are grouped together. Once the duty officer is satisfied with the model

predictions, he can then send out to each affected authority the facsimile message prepared automatically by the warning system.

The facsimile message includes the basic information such as type of warning ('Flood Watch' for predicted level approaching threshold level or 'Flood Warning' or 'Severe Flood Warning' for predicted level exceeding threshold level), the predicted peak water level, threshold level for flooding, time of predicted flooding, and duration of flooding.

The next model run is carried out 6 h later, and following the run, the previously issued warning messages are updated. If no flood risk is predicted for the areas for which a previous warning was issued, a cancellation message is issued.

The system is robust, fully automated and user friendly. It can easily be modified to alter threshold levels for flooding should any flood alleviation measures be implemented or existing defences deteriorated in future, and would allow inclusion of other critical areas if required. The system is portable and can be operated on a standard PC with access to Microsoft Excel and Word.

4. System Performance

4.1. PERFORMANCE DURING THE FIRST FOUR SURGE SEASONS

The Firth of Clyde Flood Warning scheme was formally launched in October 1999, at the start of the 1999/2000 storm surge season. During the course of the 1999/2000 winter season some 20 'Flood Watch' and 14 'Flood Warning' messages were issued, for five separate storm surge episodes. Of the four complete surge seasons since the system has been operational, the 1999/2000 season was the most active in terms of surge activity in the Firth and the 2002/2003 season was the least active with no warnings having been issued.

A review of the performance of the flood forecasting system over the first four seasons of operation is given below, especially in relation to the flood event in the early hours of Christmas morning 1999, and the storm surge event of January 2002.

The performance of the forecasting system, like any other modelling tool, is a reflection of the input data as well as how the model itself performs. For the Firth of Clyde system these can be summarised as;

(a) the performance of the boundary surge data received from the Continental Shelf Model (CSM), and to a lesser extent wind data at 10 m above sea level via the Met Office,
(b) and the propagation of tides (astronomical and surge) within the model domain.

The following section highlights the performance of the system in relation to the above.

Over the Christmas 1999 period some of the highest tides of the year occurred, and these, combined with the generation of a significant surge (of up to 1 m) along the western seaboard of the UK, resulted in some minor flooding along the Firth of Clyde coast and more significant flooding in the Clyde Estuary. The meteorological conditions which generated the surge resulted from the rapid development and movement of a depression which formed off south west Ireland on the 24th December and had moved into the northern North Sea by midday 25th December.

Figure 5 illustrates the difference between the average surge forecast provided from the UK Continental Shelf Model and the actual recorded surge (residual) at the model boundary, which at the time of the high tide on Christmas morning was in excess of 1.0 m at the model boundary, some 0.3 m above the forecasted surge.

This under-prediction of the boundary surge on the Christmas morning high tide inevitably resulted in under-prediction of the peak water levels within the Firth for this event. The extent of this is illustrated below in Table III (italicised), along with the difference in observed and predicted tides over the Christmas period as a whole, for those tides where either a Flood Watch or Flood Warning was issued.

The most significant errors in the Firth of Clyde model predictions occurred in the Clyde Estuary where the propagation of the surge/tide into the upper estuary of the Clyde produced a double peak on the early morning of the 25th December 1999 tide (Figure 6). This was also associated with a

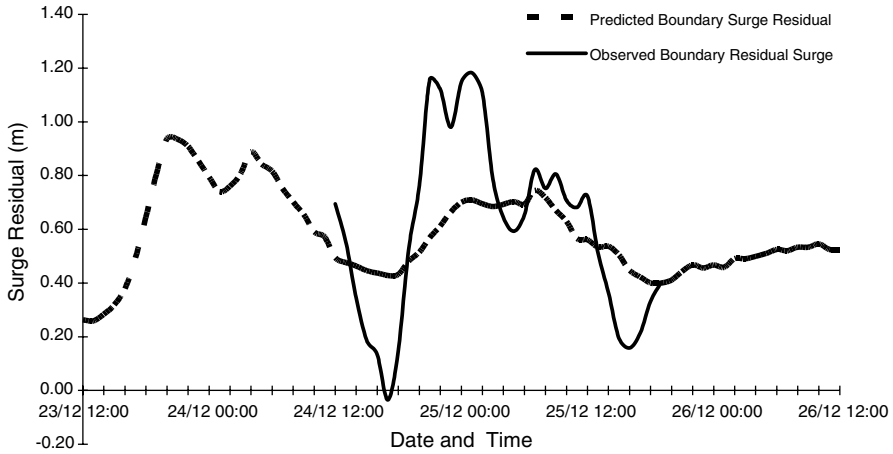

Figure 5. Comparison of observed and predicted surge residuals at southern model boundary.

Table III. Error in predicted peak water levels for high tides on 24–25 December 1999

	24/12/99 A.M.	24/12/99 P.M.	25/12/99 A.M.	25/12/99 P.M.
Campbeltown	−0.11	+0.01	−0.26	+0.24
Tarbert	0.00	+0.06	−0.12	+0.35
Rothesay	0.00	+0.12	−0.27	+0.33
Renfrew	+0.01	−0.13	−1.13	+0.14

(negative/positive values refer to underprediction/overprediction respectively as compared to

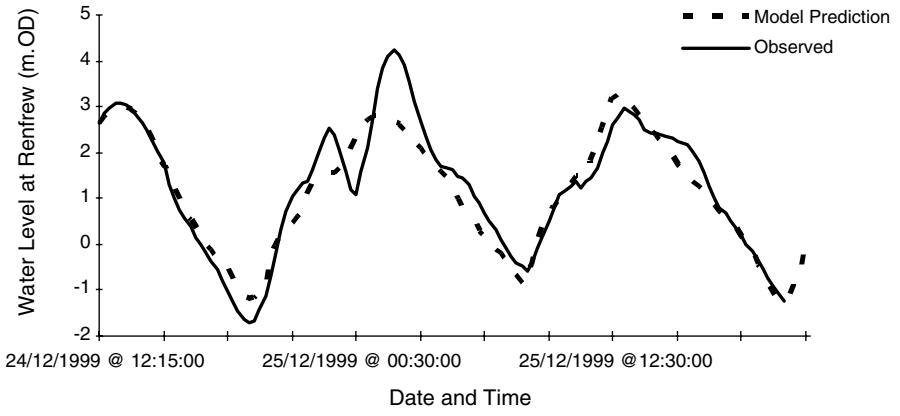

Figure 6. Observed and predicted tide levels (astronomical + surge) at Renfrew.

considerably elevated peak water level, resulting in the surge at Renfrew being in the order of 2 m, and causing extensive flooding to parts of Renfrew. The modelling system was unable to replicate this phenomenon, which resulted in a significant underestimate of the Christmas morning total water levels at Renfrew and Glasgow. Clearly this magnitude of error could not be entirely accounted for by errors in the boundary surge data (see Figure 3b). The refinements made to the model as previously discussed have significantly reduced the error introduced by coarse representation of this area in the original model.

In terms of predicted water levels within the Firth of Clyde, although significant errors occurred on the 25th December, in all other events during the 1999/2000 season, for all locations, predicted total water levels were well within ±0.2 m of the observed and mostly considerably better. In addition both the timing of events (in terms of timing of peak levels and levels at which inundation commenced) was well within acceptable limits (within 0.5 h), given the lead times (generally in excess of 12 h) available.

Whilst the event of Christmas morning 1999 was the most severe in the Clyde Estuary (upstream of Greenock), the storm surge of the 28th January 2002 was the most severe for the Firth of Clyde, during the period of operation of the forecasting system. This event was associated with a major Atlantic depression moving to the north of Scotland, with a very low atmospheric pressure (986 mbar) with winds exceeding 110 km/h widely. These were classic conditions for the generation of a large surge along the West coast of Scotland, with a surge of 1.2 m occurring at the model boundary. The event was well forecasted by the Met Office which produced accurate boundary data for the model. Peak water levels observed at SEPA tide gauges within the Firth of Clyde were within 5 cm of the predicted water levels. However, again there was an under-prediction in peak water levels through the Clyde Estuary.

Another surge event 5 days later on the 1st February 2002 again produced high water levels in the Clyde Estuary. Indeed, early indications from initial model runs indicated that this event may equal the severity of the 1991 storm surge event, due to the coincidence of high tide and storm surge. However, subsequent model runs downgraded the event severity as the coincidence of surge peak moved away from the peak of the high tide.

Subsequently, the modelling system has been refined in the Greenock area as described in Section 3.2 above. The refined system now appears to adequately predict the double-peaks at Renfrew (see Figure 4). It is expected that this will improve future model predictions at this location.

4.2. DISSEMINATION OF WARNINGS

It was recognised at the implementation stage of the project that a proces of continual review and feedback was needed to ensure that the warnings provided by SEPA remain accurate, timely and comprehensible by those who act upon the information, whilst adhering to SEPA flood warning policies.

To achieve this, a formal review of the previous seasons operations take place each year, involving all those agencies involved in the flood warning scheme. The key findings from this review were:

(a) warnings received by Fax are clear and legible, although alternative methods (SMS messaging, e-mail) should also be investigated,
(b) further guidance is required to enable the emergency services to interpret what a predicted water level means in terms of flood extent,
(c) related to item (b), above, was the need to collect more detailed coastal topographic information to model and predict flood extents, and to identify other areas at risk, but not currently included in the warning scheme,
(d) raising awareness of those living or working in areas of flood risk.

These issues are currently being progressed further by representatives of all agencies involved in the scheme to develop improved guidance with regard to appropriate response to a warning issued by SEPA. The implementation of a new flood warning and awareness service in Scotland ('Floodline') is contributing to the achievement of this objective.

5. Future System Developments

At present, the warning system does not consider the effect of wind generated waves on flood risk. A wave recorder has been installed off the North Ayrshire coast, where wave effects are considered to be significant. The data collected will be used to set up wave look-up tables, which will then be incorporated into the warning system. This will allow a combination of tide, surge and wind wave data in assessing the flood risk.

The Met Office now provide the output from the Continental Shelf Model runs at six hourly intervals, which has been implemented for the Firth of Clyde system. This has improved the forecasts, especially where rapidly developing small-scale storm systems are involved in surge generation, such as that which occurred on the 25th December 1999.

Performance of the system is continually reviewed and any development needs will be identified and assessed during these reviews.

6. Summary and Conclusions

The flood forecasting tool and dissemination during its first four seasons of operation provided generally accurate and timely warnings. The expected problem of rapidly developing Atlantic depressions and the accurate forecasting of these, in relation to surge generation over a relatively small area, was recognised as a problem at an early stage, and the impact of this has been demonstrated by the event on the 25th December. However, continued improvements in the Continental Shelf and Met Office atmospheric models and especially the increased frequency of model simulations have improved forecasts during such events.

Further refinements to the forecasting system, including the incorporation and validation of a wave model, and improved guidance for the emergency services are all being undertaken to ensure the forecasting system continues to provide timely, accurate and useful warnings.

Acknowledgements

The authors are grateful to SEPA for permission to publish this paper. They also wish to acknowledge the significant contribution made by Dr James

Curran, Dr John Townson, Dick Collar and their colleagues in the development and implementation of the scheme. The views expressed in this paper are those of the authors and do not necessarily reflect the views of their employers.

References

Becker, M., and Kaya, Y.: 2000, Firth of Clyde flood warning scheme, The Institution of Civil Engineers, Scottish Hydraulic Study Group, Glasgow, UK.

Becker, M., Burns, J., and Kaya, Y.: 2000, Coastal Flood Warning in the Firth of Clyde, Joint CIWEM and ICE seminar on Flooding: Risk and Reactions, October 2000.

Burns, J., Becker, M., and Kaya, Y.: 2000, Firth of Clyde flood warning scheme, 35th MAFF Conference of River and Coastal Engineers, Keele University, July 2000.

Collar, R. H. F, Townson, J. M, Kaya, Y, Wark, J., and Curran, J.: 1995, Coastal flood warning and surge modelling for the Firth of Clyde, 30th MAFF Conference of River and Coastal Engineers, Keele University, July 1995.

Falconer, R. A.: 1986, A two-dimensional mathematical model study of the nitrate levels in an inland natural basin. *Proceedings of the International Conference on Water Quality Modelling in the Inland Natural Environment*, BHRA Fluid Engineering, Bournemouth, Paper J1, pp. 325–344.

Firth of Clyde Modelling Study: 1996, Scottish Environment Protection Agency (SEPA). Report by Babtie Group (unpublished).

FLAIR: 1990, Floof Loss Assessment Information Report. Flood Hazard Research Centre, Middlesex Polytechnic, December 1990.

Townson, J. M., and Collar, R. H. F.: 1993, Assessment of the potential of a coastal flood warning scheme for the Firth of Clyde. Report to Clyde River Purification Board, May 1993.

Townson, J. M., Collar R. H. F., and Kaya, Y.: 1994, Coastal flooding in the Clyde Estuary. Paper presented to ICE Scottish Hydrological and Hydraulics Study Groups.

Natural Hazards (2005) 36: 273–295

Flood Management Strategy for the Upper and Middle Odra River Basin: Feasibility Study of Raciborz Reservoir

EDOARDO FAGANELLO[1,★] and LAURENCE ATTEWILL[2]
[1]*5D Coley Hill, Reading, Berkshire, RG1 6AE, UK;* [2]*19 The Green, Marsh Baldon (Oxford), OX44 9LJ, UK*

(Received: 1 November 2003; accepted: 30 June 2004)

Abstract. The river Odra, which rises in the Czech Republic and disgorges into the Baltic, suffered an extreme flood in July 1997 which was responsible for the loss of 55 lives and over a billion dollars worth of damage in southern Poland. The return period of the flood is variously estimated between 250 and 1000 years. The paper describes the hydrological and hydraulic studies undertaken for a flood reservoir (storage capacity is approximately 180,000,000 m^3) to be constructed on the River Odra just upstream the ancient town of Raciborz, on the border between Poland and Czech Republic. These studies included the hydrodynamic modelling of a 220 km stretch of the river down to the city of Wroclaw where most of the damage occurred, flood damage analysis with and without the proposed reservoir, sensitivity analysis of operating rules for Nysa reservoirs and improvement of flood control capacity of existing channels and polders. Cost-benefits analysis, environmental impact assessments and resettlement plans, in addition to the engineering studies of the dam itself, were also carried out during the project stage but have not been included in the present paper.

Key words: dam, flood, modelling, reservoir operations

1. Introduction

The river Odra, which is the second largest river of Poland, rises in the Sudety mountains in the Czech Republic and flows north to the Baltic Sea. The river is prone to flooding, as is shown by the 13 serious floods that have occurred since 1880. The last of these floods, known in Poland as the Great Flood, occurred in July 1997 and resulted in the loss of 55 lives, the flooding of some 680,000 households and damage the direct cost of which is estimated at US$4 billion (Figure 1). The flood started in the Czech stretch of the Odra where the severity of the flood was the worst of the 20th century.

Water levels in the Polish stretch of the Odra started to rise on the 5th July and reached its peak at Raciborz on 9th July, when the flow was estimated by

★ Author for correspondence: E-mail: edoardo.faganello@mouchelparkman.com; edofaganello@hotmail.com

the Polish Meteorology and Water Management Institute to be 3260 m^3/s. A peak flow of 3640 m^3/s was recorded approximately 200 km downstream at Trestno, Wrocław on 12th July. All towns and villages in the floodplain of the Upper Odra basin, including Raciborz, Opole and Wrocław, were inundated (Figure 2).

The flood wave broke or overtopped embankments in many places and flooded old polder territories on which settlements, city districts and farms were built post-war.

Since the latter part of the 19th century a flood protection system was developed to protect the basin from flooding. At the time of the 1997 flood this system comprised:

- 19 impounding reservoirs with a flood storage capacity of 150 Mm^3,
- 12 dry flood prevention reservoirs with a total capacity of 28.6 Mm^3,
- 13 polders with a total capacity of 178.4 Mm^3,
- 800 km of protection dikes,
- Three diversion channels around the major towns of Raciborz, Opole and Wrocław.

However this system, thought to be one of the most comprehensive in Europe, failed to contain the Great Flood.

The possibility of the construction of a flood reservoir at Raciborz was first proposed after the 1880 flood and by 1906 a scheme with a storage capacity of 640 Mm^3 had been designed. Over the course of the century the scheme characteristics evolved with a gradual reduction in the storage capacity due to the expansion of towns and villages. The present project, the conceptual design of which was prepared by Hydroprojekt Warszawa (1998), comprises three stages:

Figure 1. The River Odra during the 1997 flood event.

Figure 2. Study area.

- The construction of the Bukow Polder close to the Czech border.
- The construction of a dry reservoir at Raciborz.
- Channel improvements, and the construction of a new polder and bypass for the city of Wrocław.

Stage I, the Bukow polder, was completed in 2001. The results of the study of the operation and benefits of the second stage of these flood mitigation measures, Raciborz reservoir, are presented in this paper.

2. Historical Floods

Floods are a common natural catastrophe. Because they cause losses of life and damage to property, information is available from historical observations and chronicles. There are credible observations from the beginning of the 19th century, when river water levels began to be measured. Large floods on the Odra and its tributaries have been frequent and occurred in: 1813, 1829, 1854, 1880, 1902, 1903 and also in the last 50 years of the 20th century: 1958, 1965, 1970, 1972, 1975, 1977, 1978, 1981, 1985 and 1997 (Figure 3).

The 1997 flood was the largest in the whole history (Kundzewicz et al., 1999) and revealed the need for improvement in hydraulic structures (reservoirs) and embankments, modernised hydro-meteorological services, creation of infrastructure and rationalisation of organisation of direct flood defence systems. It also led to renewed interest in the projected reservoirs at Raciborz and Kamieniec Zabkowicki (on the tributary Nysa Kłodzka).

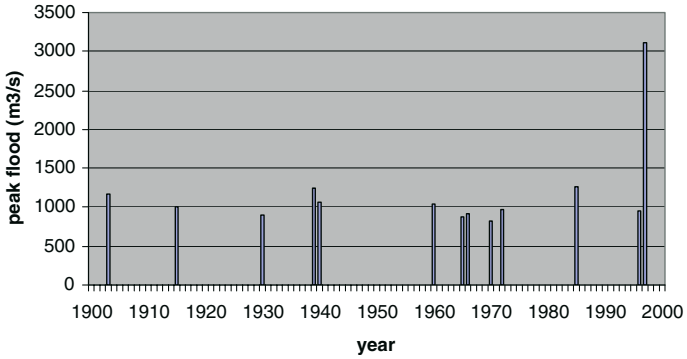

Figure 3. Historical floods exceeding the river Odra in-bank capacity at Miedonia.

3. Meteorology

The average rainfall over the upper Odra basin and the surrounding region is influenced by the topography as well as the cyclonic circulation. Thus the isohyetal maps show high values along the Odra water divide with median annual totals of up to 1000 mm/year over the border area (an isohyet is a contour of constant rainfall). The seasonal distribution is dominated by summer maximum precipitation, and by significant snow storage in winter resulting in spring snowmelt. The precipitation results in an average runoff of 314 mm/year for the basin above Racibórz-Miedonia, but the high flood peaks occur largely in summer.

The July 1997 flood event was caused by extremely heavy rains which occurred on 3–10 July and in two subsequent waves. The distribution of rainfall over 4–8 July in Poland is illustrated by Figure 4.

A wide area received rainfall over 200 mm in 4 days, while during the same period the rainfall at Czech stations within the basin reached over 400 mm. In terms of long-term July averages, the rainfall in July 1997 reached over 400% over wide areas along the Czech-Polish boundary.

4. Catchment Characteristics

The River Odra, along its course from the Czech/Polish border, from Bohumin to Wrocław and below, is flanked in the southwest by the mountainous area of the Sudety. Part of this area is within the Czech Republic, but the lower tributaries like the Nysa Kłodzka have their catchments largely within Polish territory. The relief of the upper catchments is steep, with elevations up to 1400 m, and the geology is relatively impermeable; the drainage network is therefore dense and the runoff potentially rapid.

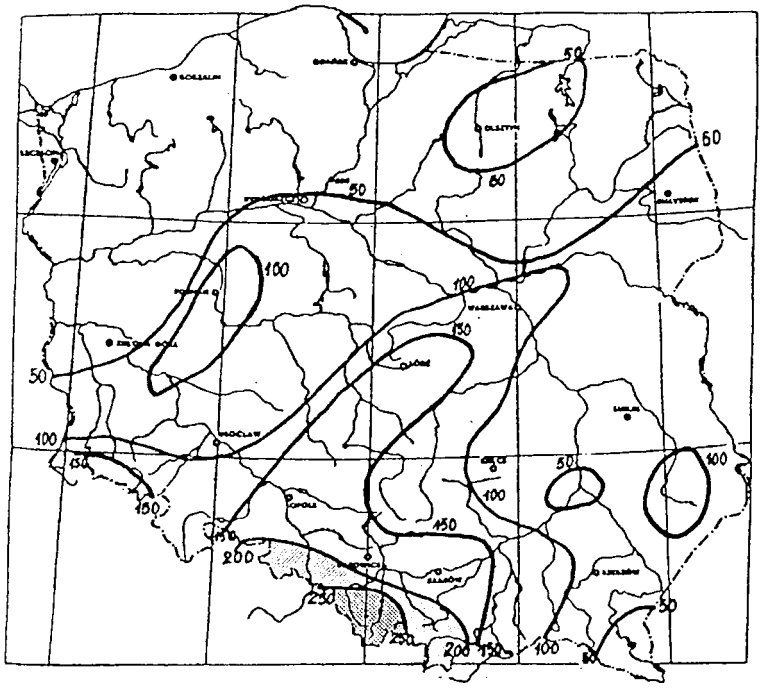

Figure 4. Distribution of rainfall in Poland, 4–8 July 1997: isohyets are in millimeter depth of total rainfall in the event.

The main Czech tributaries are the Opawa (catchment area = 2039 km^2), Ostrawica (822 km^2) and Olza (1118 km^2). The Czech Odra basin is 4665 km^2 in area with a length of 92.4 km. Within Poland the Odra flows in two arms from the river Psina outlet to Raciborz (44 km from Opawa outlet) and to Kozle (92 km); below Krapkowice the Odra flows over chalk overlain by sand. The Odra divides above Opole (148 km) into a diversion channel; there is dense urban development on the island between these arms. Diversion channels are also located at Brzeg (197 km) and Olawa (213 km). Downstream Kozle the Odra River is canalised; the gradient from the Olza confluence to Kozle is 0.045% or 1:2220.

The right bank tributaries such as Ruda, Kłodnica, Mala Panew and Stobrawa do not have the character of mountain rivers, and their contribution to floods are much lower than the left bank tributaries (Osobloga and Nysa Kłodzka). The catchment of the upper Odra is shown in Figure 5.

5. Description of Raciborz Reservoir

The role of Raciborz reservoir is to reduce the frequency and severity of flooding in the Upper Odra river. This will be achieved in two ways:

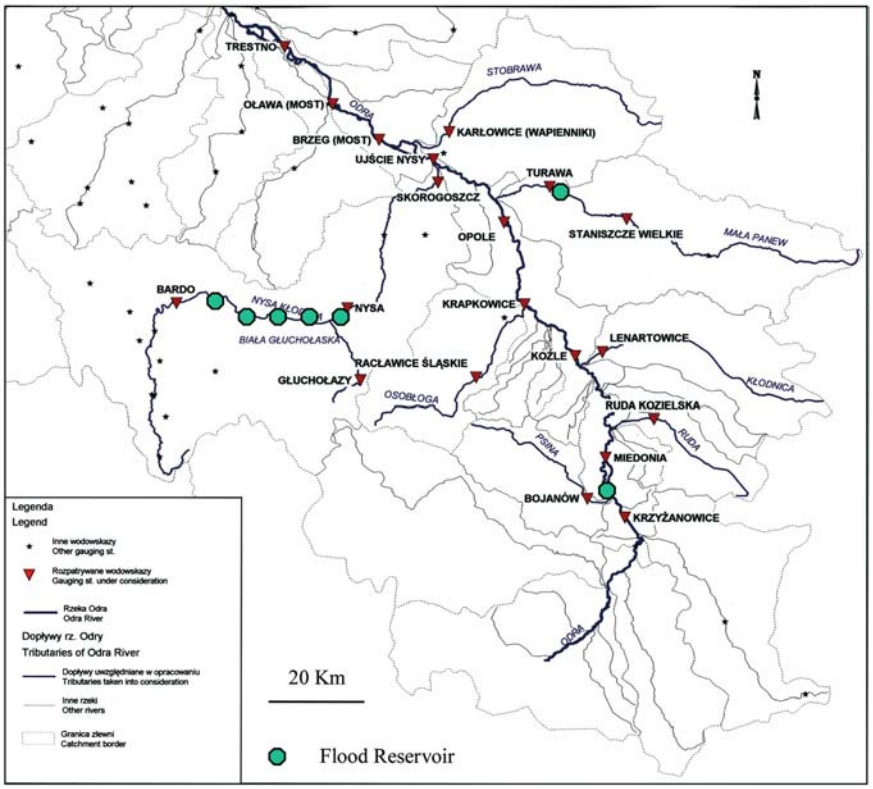

Figure 5. Catchment of the upper Odra.

- Firstly, the reservoir will provide flood storage so that the flow rate downstream of the reservoir will be greatly reduced and the effectiveness of the existing flood defence system in containing the flows will be improved.
- Secondly the reservoir will delay the timing of the flood peak at the confluence of the important left-bank tributary Nysa Kłodzka with the Odra so that the adverse combination of the two flood waves that was so damaging in 1997 is very much less likely.

The location of the reservoir was selected to be upstream of the town of Raciborz and within Polish territory: the maximum flood level is constrained by a Czech/Polish protocol.

The reservoir is formed by an earth embankment dam, 22.5 km long and with a maximum height of 10 m. The storage volume of the reservoir will be 185 Mm^3. In normal operation the reservoir will be dry with the river flowing through a main gated outlet structure into the bypass channel. Releases will

also be made through a subsidiary outlet into the old river that flows through the town.

In times of flood the outflow through the outlet structure will be controlled by operating the gates so that excess water is stored within the reservoir. The outflow is varied according to the magnitude of the expected flood and therefore a flood warning system is essential. The strategy of the operation rules is that for any flood, irrespective of return period, the flood storage is used to its maximum extent and the reservoir outflow is selected to achieve this.

The construction of the reservoir will necessitate the resettlement of 240 families. The layout of the reservoir is shown in Figure 6.

The Raciborz dam is designed, in accordance with Polish law, to pass a probable maximum flood (PMF) without overtopping. The peak flow of the PMF is estimated at 3700 m^3/s. Preliminary flood routing analysis shows that this inflow would be attenuated by the reservoir and the maximum outflow would be approximately 2800 m^3/s which is within the capacity of the outlet structure if all the gates are raised to their maximum extent. However, in the very unlikely event of a mechanical malfunction of two or more of the six gates this outlet capacity is not assured and in an extreme case of malfunction

Figure 6. Location and layout of Raciborz reservoir.

of all gates the outflow capacity could be limited to about 2000 m^3/s. In order to assure the safety of the dam under these conditions it may be considered desirable to provide additional spilling capacity.

A decision on whether to incorporate an auxiliary spillway will be taken at the detailed design stage.

6. Objective of Hydrodynamic Modelling

The principal objective of the flood modelling was to evaluate the flood damage reduction attributable to the proposed reservoir. This has been assessed by the use of a hydrodynamic flood wave model which simulates the extent of flood inundation that may occur for a range of floods of different return periods, both for the case with the reservoir and the case without the reservoir. The sequence of tasks was as follows:

- Hydrological analysis of the study catchment and preparation of hydrological input data for hydrodynamic model;
- Construction of a hydrodynamic flood-wave model of the upper Odra river;
- Calibration and verification of the model using historic flood events of 1997 and 1977;
- Evaluation of alternative flood scenarios, for a range of return periods, with and without Raciborz reservoir;
- Preparation of flood inundation mapping for each flood scenario by overlaying the flood envelopes, produced by the flood-wave model, over the digital elevation model of the Odra valley;
- Analysis of the inundation mapping to assess the predicted inundation cost for each of the alternative scenarios, at the range of return periods, with and without Raciborz reservoir.

7. Hydrology

The objective of the hydrological analyses was to produce synthetic input hydrographs for the model for a range of return periods.

This was achieved by an analysis of the historic flow data from the gauging stations shown in Figure 5 and a prediction of the peak flows for a range of return periods computed according to Polish standards by the Institute of Meteorological and Water Management. The hydrograph of the 1997 flood at Miedonia, which is estimated by the Institute to be close to a 1000-year event, is shown in Figure 7.

The estimation of the frequency or the return period of rare floods is not easy, as extrapolation from the record at a single station involves uncertainty about the choice of statistical distribution to represent the extreme floods,

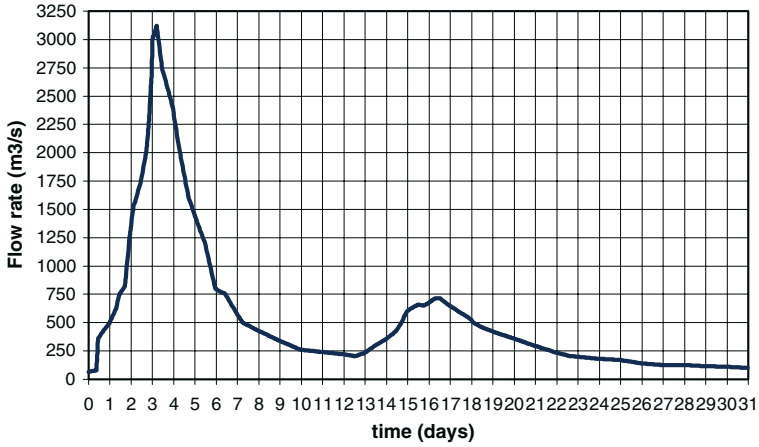

Figure 7. 1997 flood hydrograph at Miedonia.

and also the choice of method of fitting the curve to the records (see Figure 8). This procedure is particularly hazardous and sensitive to choice when one flood is a marked outlier to the other flood records. It was therefore decided to test the sensitivity of the estimation of return period by considering

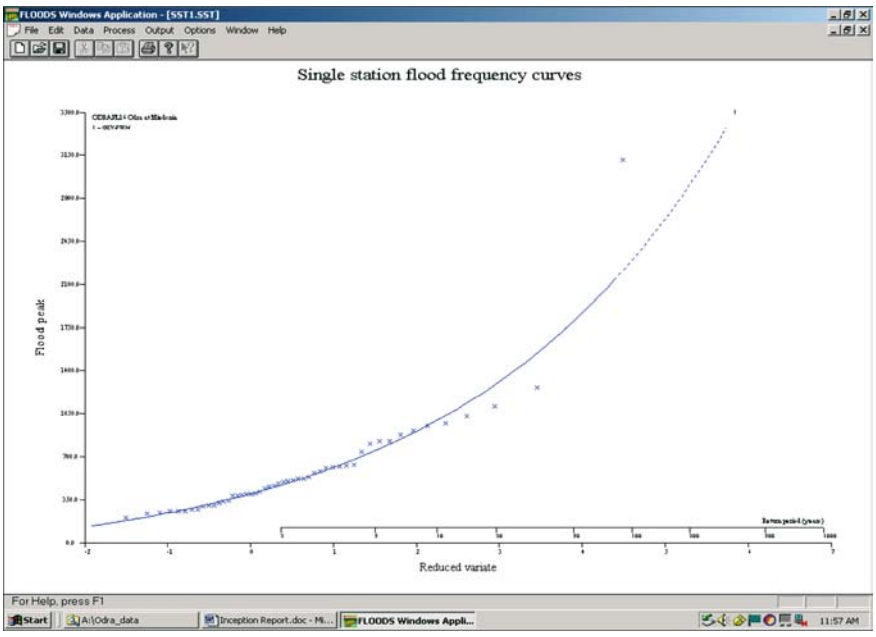

Figure 8. Single station flood frequency curve (river Odra at Miedonia), from FLOODS software package (CEH, United Kingdom).

an alternative approach. The peak flows of the 1997 event were well over double the maximum previously recorded at a large number of stations in the upper Odra basin. Although measured records cover a period of about 50 years, there is additional evidence in terms of flood marks that the 1997 flood greatly exceeded previous floods from 1880, while other historical evidence suggests that this also applies to a much longer period.

A range of approaches is possible. One could assess the frequency of the 1997 event from historical evidence or from the measured record giving limited weight to the exceptional outlier, which would provide an estimated return period of the order of 1000 years or 0.1% frequency and fit a curve on this basis. At the other extreme one could assume that the 50-year period of measured record is a random sample, and fit a distribution by a method which gives reasonable weight to the outlier as the highest in 50 years.

This approach tends to ignore the historical evidence and clearly gives a lower return period or higher frequency to the 1997 event. A further refinement of the latter approach would be to adopt the regional flood frequency approach, which is described in the next section.

The regional approach to flood frequency analysis has been found to give consistent estimates of the relation between flood magnitude and return period or frequency of occurrence when applied to areas of reasonable hydrological homogeneity. It was therefore decided to apply the approach to flood records in the Odra basin as a supplement to the analysis of single station records.

The method depends on the collection of annual maximum flood series from the gauging stations within a region. The method derives from the approach developed during investigation of floods in the British Isles (Natural Environment Research Council, 1975) and its application to many different regions of the world has been described in a number of papers (Meigh *et al.*, 1997; Sutcliffe and Farquharson, 1995).

The annual maximum flood series for individual stations are preferably based on peak flows but where basins are large may be based on daily mean flows. The maximum flows in each hydrological year at each station are reduced to non-dimensional form by division by the mean annual flood (MAF) estimated from the whole period of record at the station. Each non-dimensional record can be analysed as a single-station record. The software used in this study (FLOODS), which was developed by the Centre for Ecology and Hydrology, Wallingford, provides alternative methods of standardization, alternative frequency distributions and methods of fitting. The most common choice is standardization by the mean, the generalised extreme value distribution (GEV) and fitting by probability weighted moments (PWM) which has been found to give reasonable estimates for flood records.

The software enables flood records from a number of stations to be combined in analyses to give a dimensionless flood frequency curve for stations, for example, from individual tributaries or whole basins. Stations may of course be grouped in other ways, either geographically (by latitude and longitude) or by one or more basin characteristics (e.g. size or climate). It is usual to test different groupings before deciding how to combine individual stations. In a previous study of flood records in the upper Vistula basin it was found that the flood frequency curves for individual tributaries and the whole upper basin were virtually identical (Gibb Ltd and Safege, 1995).

To apply this approach, annual maximum flood records were obtained for six stations on the upper Odra within the Czech Republic, and ten stations within Poland on the upper Odra and the Nysa Kłodzka. Another six records were obtained from lowland tributaries below Raciborz, five on the right bank and one on the left; these appear to have a quite different flood regime to the upper Odra. The dates of the annual maximum floods in each year were available for a number of stations. Although the majority are in the summer months, they have been observed in all months. This has been noted elsewhere to indicate variable flood regimes.

After inspection of the results, the stations were grouped as follows:

- the 6 stations on the upper Odra in the Czech Republic (ODRACZ),
- the 6 stations on the main Odra below Raciborz (ODRAMAIN),
- the 4 stations on the Nysa Kłodzka (NYSAALL),
- the remaining 6 stations on the Odra.

The 16 stations included in the first three sets were also combined to represent the mountainous part of the upper Odra (ODRANYSA). The curves for these regions are illustrated in Figure 9.

It will be seen that the curves for the upper Odra groupings are very similar up to 50–100 years, but the Nysa curve is higher at longer return periods. The curve for the lower basins is different and is treated separately. The curve for the whole upper Odra is considered as reasonably representative of the whole area. Because the individual records all contain the 1997 flood, this approach does not avoid the problem of the extreme outlier; however, the PWM fitting procedure has been shown to be reasonably robust in the face of this problem. It is noteworthy that the regional curve is very similar to that derived in 1995 during a previous study of flood records for the upper Vistula basin (Gibb Ltd and Safege, 1995), though it diverges moderately at return periods of 200 years or higher.

Comparison of the 1997 flood at individual stations, expressed as Q/MAF, with the regional curve derived from the 16 stations in the upper Odra basin, indicates a lower limit of the range of return periods which could be allocated to this event. This implies that the whole set of records is typical of the region, but it has been shown that the group curves are similar to each other

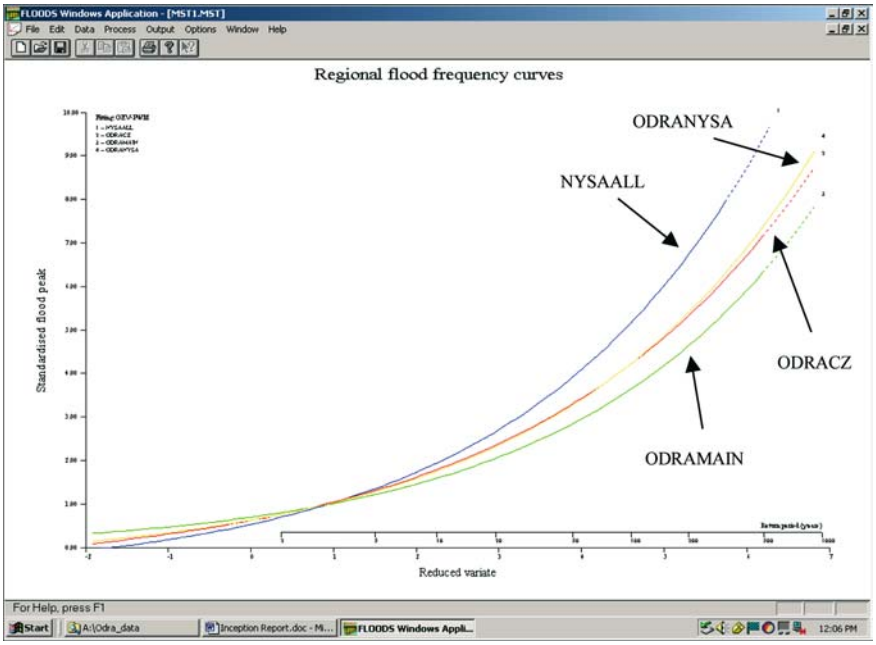

Figure 9. Regional flood frequency curves, from FLOODS software package.

and that the regional curve is similar to that of the upper Vistula. The lower limit for the return period of the 1997 event, on this basis, is about 200 years for the Odra stations from Bohumin down, but rather higher at about 300 years for the Nysa stations.

8. Hydrodynamic Model Description

The Upper Odra hydrodynamic model has been built using MIKE 11, a widely used software package developed by the Danish Hydraulic Institute (DHI). MIKE 11 solves the vertically integrated equations of conservation of mass and momentum (the 'Saint Venant' equations) by using a finite difference scheme (the 6-point Abbott-scheme) (Danish Hydraulic Institute, 2001).

The model covers approximately 204 km of the main river channel (between the village of Olza, situated near the Czech border and the village of Trestno, immediately upstream of Wrocław) and includes the floodplain on the right and left bank as well as the two main tributaries: the Nysa Kłodzka and the Mala Panew (63.5 and 18 km respectively). A total of 342 cross sections have been included in the model. The cross sections used in the hydrodynamic model are the result of a recent survey carried out after the 1997 flood event.

The MIKE 11 model does not cover the six relevant reservoirs (Kamienec, Topola, Kozielno, Otmuchow, Nysa and Turawa) situated on these two tributaries. The effect of these reservoirs has however been considered in separate flood routing calculations and the resulting outflows included in the model as input hydrographs.

The methodology adopted for modelling the floodplain of the Odra has involved three different techniques:

- Extension of the in-bank river cross sections into the floodplain;
- Introduction of flood cells (static storage) so that when the bankfull capacity of the main channel is exceeded water spills into them (this technique has been used in particular to model some of the polders);
- Simulation of the adjacent floodplain as a 'separate river' using parallel river branches attached to the main channel by lateral spill units (link channels).

The bed level of the link channels has been set to the embankment level at these points, while the width has generally been set to between 200 and 500 m. However, a certain level of approximation is always expected in schematising complex flow patterns using a one-dimensional model.

An initial global value of 0.05 of Manning's roughness has been considered in the computations although different values in the range of 0.03–0.100 have been used locally to reflect the land use and adjust model calibration.

The Odra river is maintained as a navigable river. A large number of sluices and lock structures have been constructed along its watercourse as well as bypass and diversion channels in order to improve and increase the capacity of the system during a flood event.

There are two main types of hydraulic structure which have been incorporated in the hydraulic model by using the recently surveyed river cross-sections and the inventory of the existing hydraulic structures between the Polish-Czech boundary and Trestno compiled during the study:

- weir complexes, which may consist of a variety of broad and sharp crested weirs, barrages, sluice and radial gates associated with culverts and/or bridges,
- polders.

Only permanent structures have been taken into account and modelled as fixed (without operation rules). Removable gates have not been included in the model because they are usually removed from the watercourse during flood events. Navigation locks have been simulated with the gates open. The existing flood protection scheme of the upper Odra valley also comprises the use of several polders for flood mitigation during high rivers stages. Table I shows the polders, which have been included in MIKE 11 model and how they have been simulated.

Table I. Summary of polders in the upper Odra valley

Polder name	Flood storage volume (m^3)	Max area (ha)	Modelled as
Bukow (right and left bank)	39,000,000	831	Flood cell
Obrowiec	3,600,000	277	Flood cell
Zelazna	1,700,000	200	Floodplain
Czarnowasy-Dobrzen	3,200,000	220	Floodplain
Rybna-Stobrawa	13,000,000	825	Floodplain
Zwanowice	2,000,000	160	Flood cell
Brzezina-Lipki	3,500,000	257	Floodplain
Lipki-Olawa	30,000,000	3000	Floodplain
Blizanowice-Trestno	3,800,000	210	Flood cell
Olawka	12,000,000	1070	Flood cell

These areas are generally embanked and incorporate a mixture of both fixed and moveable structures regulating both the inflow to, and the outflow from, storage. These control structures have also become part of the model.

The input hydrographs (derived from the hydrological analysis and reservoirs flood routing calculations) and the downstream water level (in Wrocław) form the necessary boundary conditions for the model simulation (Figure 10).

9. Model Calibration and Verification

Once the hydrodynamic model for the upper Odra, Mala Panew and Nysa Kłodzka river was completed, it was calibrated progressively from upstream to downstream using the 1997 flood event and verified using the 1977 event.

The model was calibrated by adjusting the following parameters:

- roughness;
- hydraulic structures discharge coefficients;
- link-channels (out-of-bank) coefficients.

During a flood event there is great uncertainty about recorded flows. Rating curves are very often unreliable especially when the flow becomes out-of-bank. For each gauging station two separate rating curves should be considered: one for the rising limb and one for the falling limb. In addition peak water levels never coincide with peak flows because of unsteady flow conditions and hydrologic routing.

The 1997 event exceeded all recorded measures by far. The existing rating curves proved to be so unrealistic that high flow values had to be extrapolated. Therefore due to uncertainty in the measured flows the model

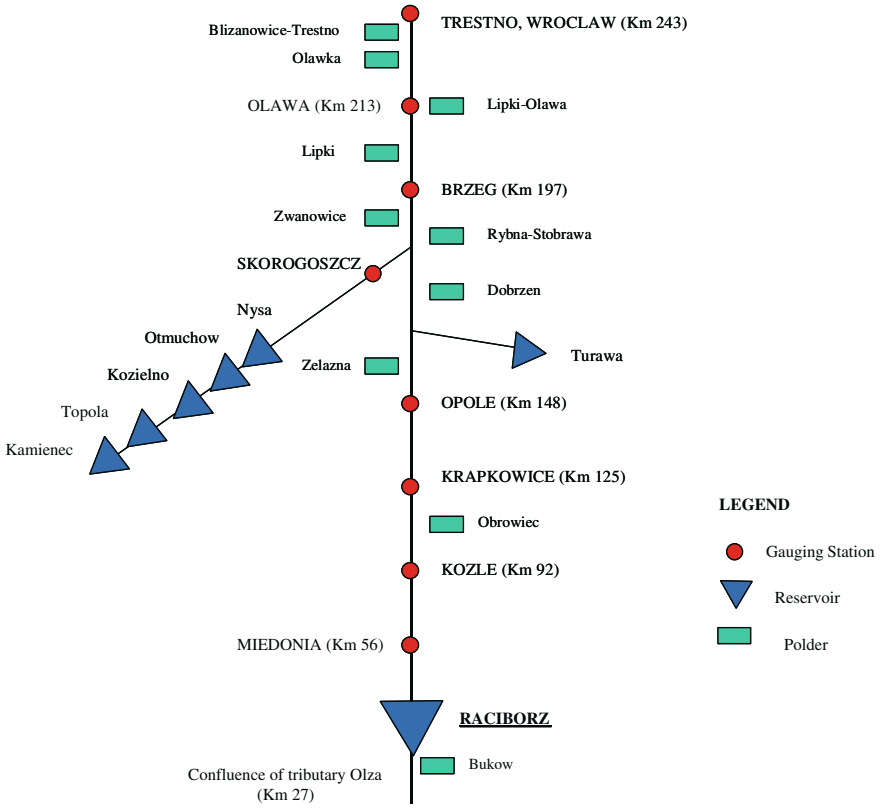

Figure 10. Model schematisation.

calibration focussed mainly on reproducing the observed water levels (reliable water levels are the key parameter in the flood mapping process).

The timing of the measured and modelled peak flows (see Figure 11 and Table II) generally showed a very good agreement (margin of error within ± 6 h).

The model calibration with the 1997 flood was verified with the less extreme 1977 flood (peak flows of 975 m^3/s at Miedonia and 1560 m^3/s at Trestno), and the comparison of measured and modelled water levels are included in Figure 12 and presented in Table III.

10. Flood Scenarios and Model Results

Once the model was calibrated and verified, the Raciborz reservoir cross-sections and related outlet structures were included in the model.

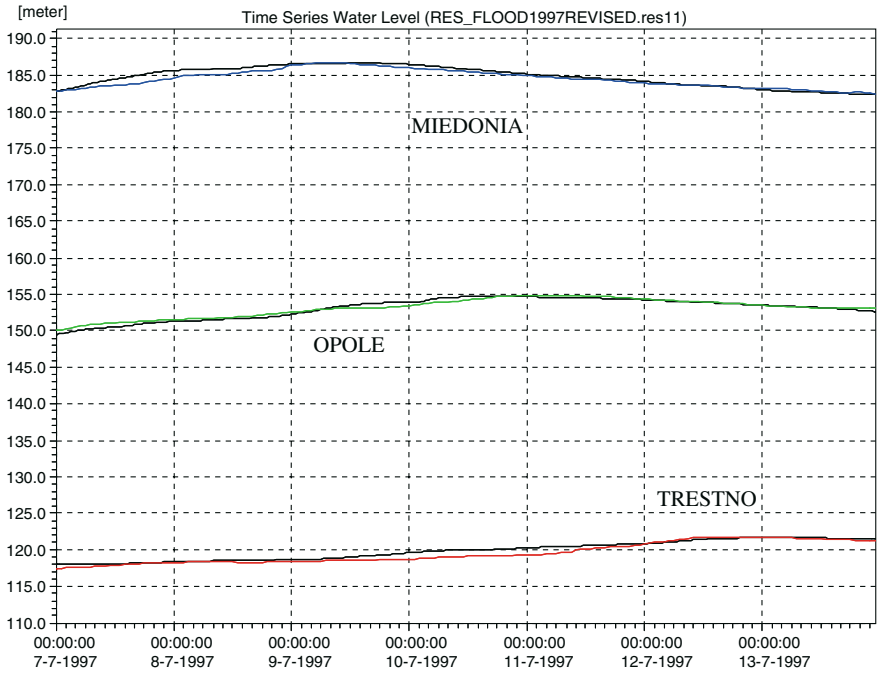

Figure 11. Comparison of measured and modelled 1997 water levels at Miedonia, Opole and Trestno (from Mike 11 software package).

Table II. Results from 1997 model calibration

Gauging stations	Recorded peak level (m OD)	Modelled peak level (m OD)	Recorded peak flow (m^3/s)	Modelled peak flow (m^3/s)
Miedonia	186.73	186.67	3120	2611
Kozle	171.98	172.02	3060	2690
Krapkowice	165.83	165.88	3170	2717
Opole	154.89	154.70	3170	2673
Skorogoszcz	145.12	145.37	1200	1244
Brzeg	136.50	136.55	3530	3827
Olawa	129.64	129.66	3550	3441
Trestno	121.76	121.71	3640	3301

A wide range of synthetically generated flood scenarios (including the 1997 event) was carried out to define the reservoir operating rules.

In order to optimise the flood attenuation process, Raciborz reservoir outflow is varied according to the magnitude of the expected flood with the support of a flood forecast system (see Table IV). The strategy of the reservoir

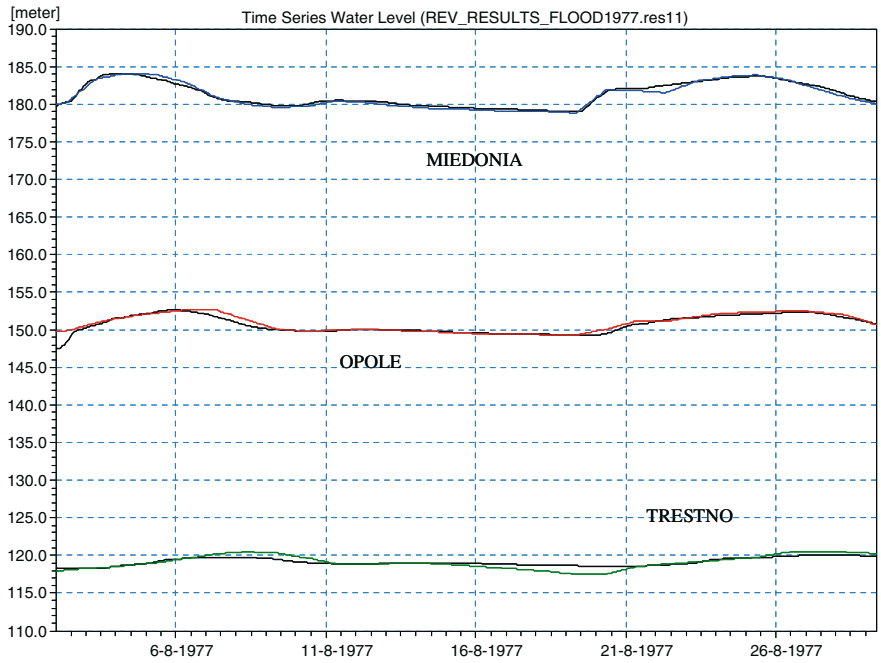

Figure 12. Comparison of measured and modelled 1977 water levels at Miedonia, Opole and Trestno (from Mike 11 software package).

is that for any flood, irrespective of return period, the flood storage is used to its maximum extent and the reservoir outflow is selected to achieve this (Figure 13).

Tables V and VI show the water level and flow reduction with Raciborz reservoir in place under different flood conditions.

Table III. Results from 1977 model verification

Gauging stations	Recorded peak level (m OD)	Modelled peak level (m OD)
Miedonia	184.09	184.06
Kozle	169.41	169.41
Krapkowice	161.84	161.83
Opole	152.68	152.62
Skorogoszcz	144.26	144.12
Brzeg	135.49	135.30
Olawa	129.10	129.32
Trestno	120.46	120.21

Table IV. Inflows and outflows from Raciborz reservoir and correlation of return periods

River Odra reservoir peak inflow (m^3/s)	River Odra reservoir peak outflow (m^3/s)	Return period (years)	
		Conventional method	Regional method
1000	300	10	11
1510	590	50	31
1735	800	100	45
2129	1042	333	79
2260	1150	500	94
2485	1300	1000	123
3008	1710	5000	211

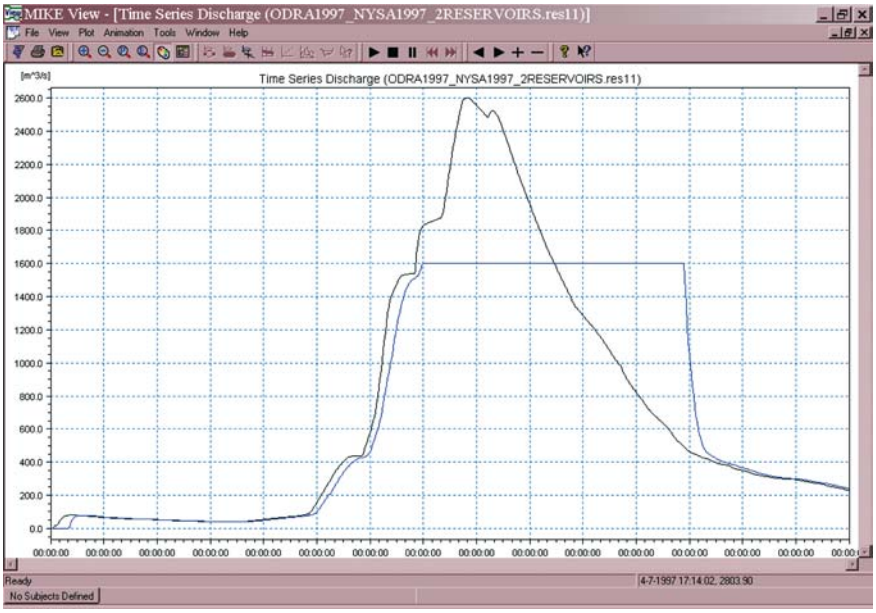

Figure 13. The simulation of the 1997 event: inflow and outflow from Raciborz dam (from Mike 11 software package).

11. Sensitivity

The sensitivity of the model results has been examined for the following changes:

- reservoir volume,
- storm timing,
- Nysa Kłodzka reservoirs operation.

Table V. Water level reduction with Raciborz reservoir in place under different flood conditions

Gauging stations	River Odra chainage (km)	Water level reduction with Raciborz reservoir in place (m)					
		10 year	100 year	500 year	1000 year	1997 event	5000 year
Miedonia	56	2.44	1.32	1.30	1.23	1.15	0.84
Kozle	92	2.22	1.20	1.26	1.19	0.95	0.74
Krapkowice	125	1.96	1.54	1.24	1.07	0.85	0.76
Opole	148	1.53	0.94	0.91	0.94	0.64	0.42
Brzeg	197	0.91	0.32	0.16	0.30	0.42	0.39
Olawa	213	1.29	0.26	0.41	0.61	0.28	0.28
Trestno	243	0.76	0.10	0.32	0.38	0.26	0.38

The model was run with a reservoir of 154 Mm^3 (16% reduction on the base case), representing an option which minimised resettlement, and with a reservoir of 290 Mm^3 (50% increase on base case) representing a possible future condition in which gravel deposits within the reservoir are extracted. The modelling showed that on average the effectiveness of the reservoir would decrease and increase by approximately 5% and 15% for the reduction and the increase in volume respectively.

The modelling also showed that the water level is not very sensitive to the relative timing of the main river and tributary flood peaks: a delay of 12 h in the time to peak of the Nysa result in a small water levels increase

Table VI. Flow reduction with Raciborz reservoir in place under different flood conditions

Gauging stations	River Odra chainage (km)	Flow reduction with Raciborz reservoir in place (m^3/s)					
		10 year	100 year	500 year	1000 year	1997 event	5000 year
Miedonia	56	657	777	964	974	911	850
Kozle	92	623	744	914	957	900	845
Krapkowice	125	556	644	792	843	850	776
Opole	148	539	508	672	814	851	784
Brzeg	197	651	508	382	628	1203	807
Olawa	213	542	134	470	649	820	883
Trestno	243	504	116	468	612	705	797

downstream the confluence: the high stage in the Odra controls the inflow from the Nysa Klodzka.

The sensitivity of the effect of the Raciborz reservoir to an alternative operating rule for the existing Nysa reservoirs, with and without the future Kamieniec Zabkowicki reservoir (with a 62,000,000 Mm^3 flood storage capacity) shows:

- The revised reservoirs operational rules significantly reduce the flood levels on the Nysa Kłodzka system and, to a lesser extent, those on the Odra downstream of the confluence;
- The effect of Kamieniec Ząbkowicki reduces as the Nysa peak flow coincides with the Odra peak flow;
- A flood forecast system for the Nysa catchment is necessary to optimise the flood attenuation process;
- Additional flood mitigation measures are necessary for the City of Wrocław in order to improve the current capacity of the flood protection scheme (approximately 2400 m^3/s).

12. Inundation Mapping

The effect of the reservoir in terms of inundated area was determined by compiling flood maps. The reduction in inundated area for the range of floods studied is illustrated in Table VII.

It can be seen that the level of protection given by the reservoir depends on the severity of the flood, and ranges from a 40% reduction in the gross area (which includes polders and the flood channels) for a 1 in 50 year flood to 29% reduction for a 1000 year flood (Figure 14).

Table VII. Flood mapping process results: inundated areas

Flood return period (conventional method)	River Odra reservoir peak inflow (m^3/s)	Inundated area with Raciborz (km^2)	Inundated area without Raciborz (km^2)	Inundated area reduction (km^2)
10 year	1000	153.14	259.17	106.02
100 year	1735	312.86	429.79	116.93
500 year	2260	466.13	632.60	166.47
1000 year	2485	472.85	666.79	193.94
5000 year	3008	622.11	761.87	139.76

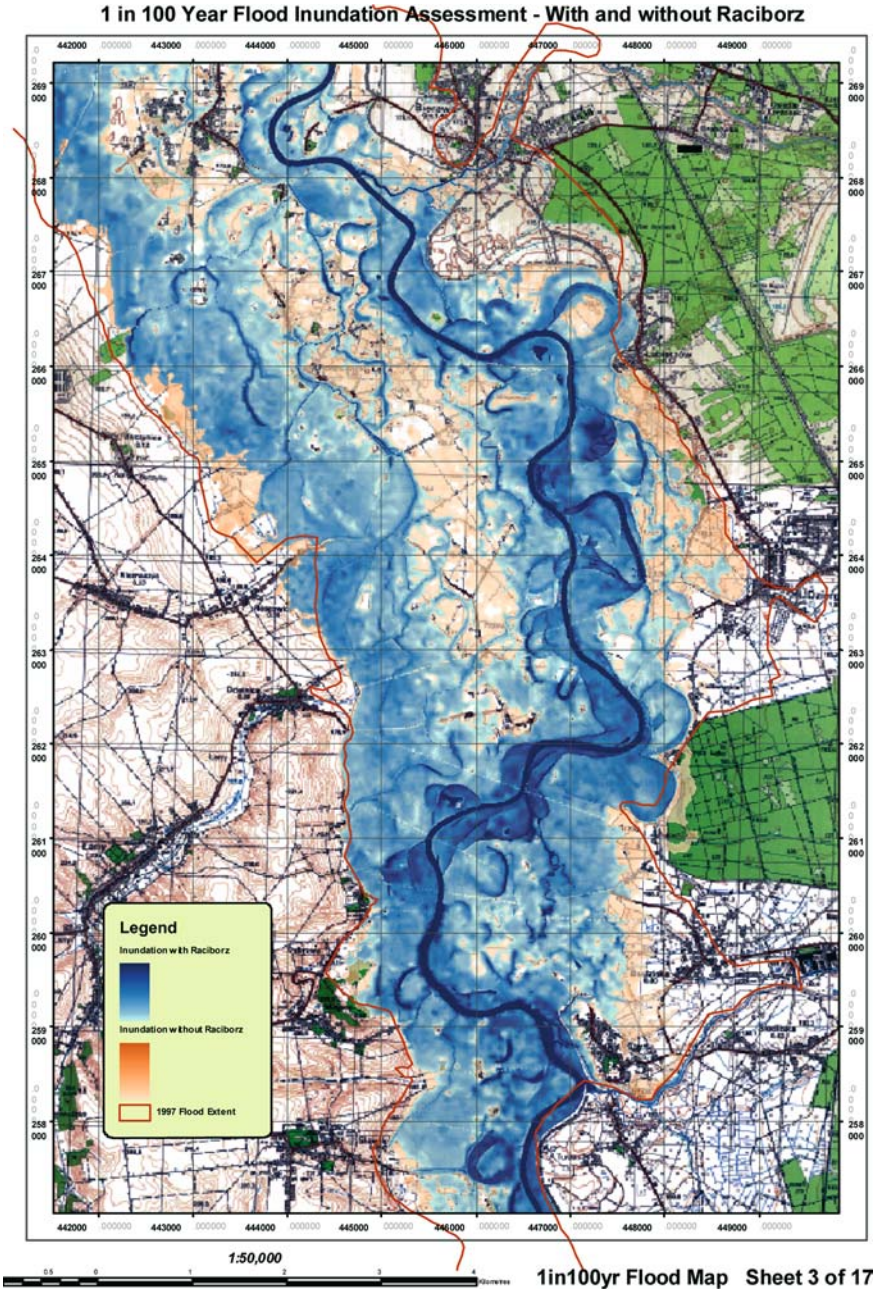

Figure 14. Example of 1 in 100 year water-depth Flood Map of the area between Turze and Cisek (approximately 25 km downstream the village of Raciborz) with and without the proposed reservoir.

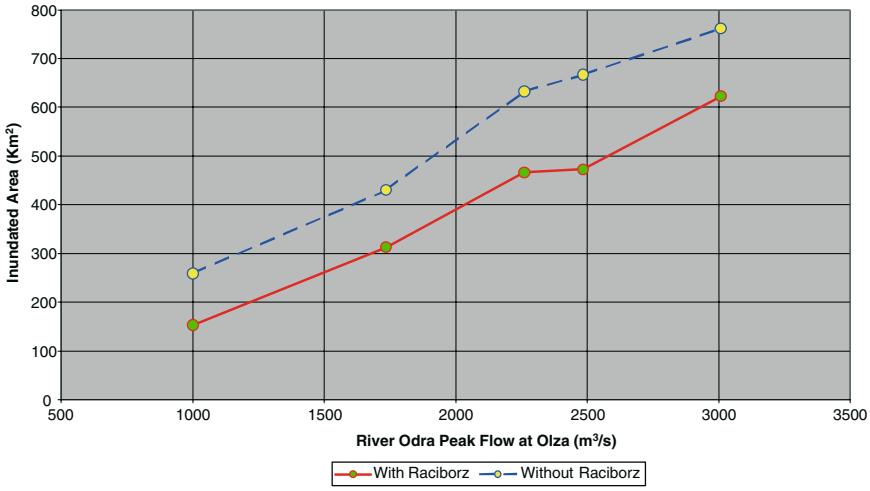

Figure 15. Odra river Flood Inundation Curve with/without Raciborz reservoir.

13. Reduction of Flood Damage

The reductions in flooded area were itemised into 18 different land use categories to enable reductions in flood damages to be costed using data derived from the 1997 flood. The reduction in flood damage attributable to the reservoir, is represented by the area between the with and without reservoir curves in Figure 15.

14. Conclusions

The conclusions of the study are that the Raciborz reservoir offers substantial but not complete protection against inundation of the upper Odra against severe floods. The effectiveness of the reservoir is sensitive to reservoir volume and it must be accepted that the proposed reservoir is at the small end of the range of useful volumes: a larger reservoir would be considerably more effective. The level of protection provided by the reservoir is naturally greatest immediately downstream and decreases, especially downstream of the Nysa confluence. However it is likely that Raciborz reservoir together with the implementation of the various channel improvements mitigation measures proposed for Wrocław will provide adequate protection to that city. The effectiveness of the reservoir will depend on careful operation in which a reliable flood warning and conjunctive use with the Nysa reservoirs are vital.

Acknowledgement

The authors are indebted to their Polish and British colleagues for their help in its preparation.

References

Hydroprojekt Warszawa: 1998, Conceptual Design of the Raciborz Dolny Reservoir, Warsaw, Technical Report.

Kundzewicz, Z. W., Szamalek K., and KoKowalczak P.: (1999) The Great Flood of 1997 in Poland, *Hydrol. Sci. J.* **44**, 855–870.

Meigh, J. R., Farquharson, F. A. K. and Sutcliffe, J. V.: (1997), A worldwide comparison of regional flood estimation methods and climate, *Hydrology. Sci. J.* **42**, 225–244.

Sutcliffe, J. V. and Farquharson, F. A. K.: (1995), Flood frequency studies using regional methods, Proc: Bernier Conference, UNESCO.

Gibb Ltd and Safege, (1995), Swinna Poreba Dam Feasibility Study, Final Report, Cracow, Technical Report.

Danish Hydraulic Institute (2001), MIKE 11, *A Modelling System for Rivers and Channels*, Denmark, Technical Manual.